Task II.5 – Integrative Approach to Understanding the Causes of Salt Marsh Dieback: Analysis of Climatic Drivers

Final Report

By:

Erick M. Swenson
Coastal Ecology Institute
Louisiana State University

E. Elaine Evers
Coastal Ecology Institute
Louisiana State University

John M. Grymes, III
Department of Geography
Louisiana State University

Submitted to:

Greg Grandy
Coastal Restoration Division
Louisiana Department of Natural Resources
LaSalle Building
617 N 3rd Street, 10th Floor
Baton Rouge, LA 70802

In Partial Fulfillment of:
DNR Interagency Agreement No. 2512-01-14

June 30, 2004

ACKNOWLEDGEMENTS

The data used in this report were supplied by the following Federal and State agencies, and we thank them for supplying us with the data in the form of digital data files:

The Louisiana Department of Wildlife and Fisheries (LDWF)
The United States Fish and Wildlife Service (USFWS)
The United States Geologic Survey (USGS)
The United States Army Corps of Engineers (USACOE)
The National Oceanic and Atmospheric Administration (NOAA)
The National Ocean Survey (NOS)
The Louisiana State Office of Climatology at Louisiana State University

This work was funded through with a contract (2512-01-14) from the Louisiana Department of Natural Resources, through a grant from the U. S. Department of Commerce, NOAA National Ocean Service.

TABLE OF CONTENTS

ACKNOWLEDGEMENTS 2
LIST OF TABLES 4
LIST OF FIGURES 5
INTRODUCTION 9
General Task Description 9
METHODS 10
Data Sources 10
Data Base Development 11
Data Analysis Techniques 12
Water Budget Calculations 12
Time Series Analysis 13
Statistical Analysis 13
RESULTS AND DISCUSSION 14
Gulf of Mexico Estuarine Forcing Functions 14
Coastal Water Levels, and River Discharge 16
Climatic Characterization 17
Open Water Salinities 18
Climate Driver – Salinity Statistical Model Results 19
The Role of ENSO for South Louisiana 20
CLIMATOLOGICAL OVERVIEW: 1998 - 2000 22
SUMMARY 27
LITERATURE CITED 31
DATA APPENDICES 70
Appendix A: Gulf of Mexico Water Level Plots. 71
Appendix B: Grand Isle Water Level Plots. 78
Appendix C: Daily river discharge plots. 81
Appendix D: Mean Monthly Water Level Plots. 108
Appendix E: Palmer Drought Severity Index (PDSI) data plots. 135
Appendix F: Precipitation data plots. 146
Appendix G: Temperature data plots. 157
Appendix H: Potential Evaporation (PE) data plots. 168
Appendix I: Precipitation surplus data plots. 179
Appendix J: Coastal Winds data plots. 190

LIST OF TABLES

Table 1. Summary of the major and secondary freshwater sources influencing salinities in the 26 northern Gulf of Mexico estuaries presented in Figure 2. 33

Table 2. Correlation matrix for weekly average water levels for ten stations around the Gulf of Mexico (Figure 8). 34

Table 3. Ranking of observed water levels for the NOS Grand Isle station for June, 1999 through July 2000. 35

Table 4. Classification matrix for the Barataria estuarine system based upon the Palmer Drought Severity Index (PDSI) and Mississippi River discharge. 36

Table 5. Climatic classification for the Barataria Estuarine System based upon the Palmer Drought Severity Index (PDSI) and Mississippi River discharge. 37

Table 6. Consecutive number of months that the monthly mean salinity equals (or exceeds) the listed salinity level for LDWF salinity stations in the Barataria system. 38

Table 7. Summary of regression results to predict salinity in the Barataria system using Mississippi River discharge, Precipitation at Louisiana climate region 9, and de-trended coastal water levels. 39

Table 8. Summary of Gulf of Mexico salinity forcing functions over the time period from 1950 though 2002. 40

LIST OF FIGURES

Figure 1. Diagram illustrating the connections among the various Sub-tasks on the overall causes Task for the Brown Marsh studies. 41

Figure 2. Conceptual model detailing the role of the major environmental forcing functions in controlling open water salinity and marsh soil salinity. 41

Figure 3. NCDC Climate Divisions for the states around the Gulf of Mexico. Monthly summary data from the sites numbered in red was used for this study. 42

Figure 4. Map showing the climate stations from which daily data was obtained. 42

Figure 5. Map showing the LDWF-USGS continuous salinity stations. 43

Figure 6. Map showing discrete salinity stations. 43

Figure 7. Map showing the USCE and USGS stream discharge stations. 44

Figure 8. Map of the Gulf of Mexico showing the National Ocean Survey (NOS) stations and the National Data Buoy Center (NDBC) stations from which hourly water level and meteorological observations were obtained. 44

Figure 9. Map of the Gulf of Mexico showing the estuaries characterized by Orlando, et. al., (1993). 45

Figure 10. Schematic of an estuarine system illustrating the major pathways of fresh water and coastal ocean water inputs to the system. 46

Figure 11. Distribution of river input into the Northern Gulf of Mexico. Modified from Orlando et. al., (1993). 47

Figure 12. Monthly average patterns of (top to bottom) precipitation, potential evapotranspiration, and surplus for the NCDC Climatic Divisions (Figure 3) around the Gulf of Mexico. 48

Figure 13. Distribution of surface salinity for 26 estuaries around the Gulf of Mexico.....49

Figure 14. Changes in surface salinity (in ppt) for 26 estuaries around the Gulf of Mexico resulting from either a high freshwater input year (filled circles) or a low freshwater input year (open circles). 50

Figure 15. Plot of weekly average water levels for stations around the Gulf of Mexico (Figure 8). 51

Figure 16. Plot of monthly mean water levels for Grand Isle, Louisiana, in centimeters relative to the station datum. 52

Figure 17. Plot of de-trended monthly mean water levels for Grand Isle, Louisiana, in centimeters relative to the station datum. 52

Figure 18. Plot of mean monthly water level at Grand Isle. 53

Figure 19. Plot of long-term (1955-2002) average monthly water level at Grand Terre (light blue) versus average monthly water levels for 1999 (red), 2000 (green), 2001 (dark blue), and 2002 (beige). 53

Figure 20. Monthly changes in freshwater input for rivers around the Gulf of Mexico (Figure 7.). 54

Figure 21. Time series plot of monthly mean Mississippi River discharge at Tarberts Landing. 55

Figure 22. Plot of mean monthly Mississippi River discharge at Tarberts Landing. 55

Figure 23. Plot of long-term (1955-2002) average monthly Mississippi River discharge (light blue) versus average monthly discharge for 1999 (red), 2000 (green), 2001 (dark blue), and 2002 (beige). 56

Figure 24. Contour plot of monthly surplus (rainfall-evapotranspiration), in millimeters, for the NCDC Climate divisions around the Gulf of Mexico. 57

Figure 25. Contour plot of monthly Palmer Drought Severity Index for the NCDC Climate divisions around the Gulf of Mexico. 58

Figure 26. Plot of long-term (1955-2002) monthly total precipitation (light blue) versus monthly total precipitation for 1999 (red), 2000 (green), 2001 (dark blue), and 2002 (beige). 59

Figure 27. Plot of long-term (1955-2002) monthly total evapotranspiration (light blue) versus monthly total evapotranspiration for 1999 (red), 2000 (green), 2001 (dark blue), and 2002 (beige). 59

Figure 28. Plot of long-term (1955-2002) monthly total surplus (light blue) versus monthly total surplus for 1999 (red), 2000 (green), 2001 (dark blue), and 2002 (beige). 60

Figure 29. Plot of long-term (1955-2002) monthly Palmer Drought Severity Index (light blue) versus monthly Palmer Drought Severity Index for 1999 (red), 2000 (green), 2001 (dark blue), and 2002 (beige). 60

Figure 30. Time series plot of daily mean salinity from the Louisiana Department of Wildlife and Fisheries continuous monitoring station at Grand Terre, Louisiana (Station 315). 61

Figure 31. Time series plot of daily mean salinity from the Louisiana Department of Wildlife and Fisheries continuous monitoring station at St. Mary's Point, Louisiana (Station 317).....61

Figure 32. Time series plot of daily mean salinity from the Louisiana Department of Wildlife and Fisheries continuous monitoring station in Little Lake, Louisiana (Station 326). 62

Figure 33. Time series plot of daily mean salinity from the Louisiana Department of Wildlife and Fisheries continuous monitoring station in Caillou lake, Louisiana (Station 518). 62

Figure 34. Time series plot of mean daily salinity from the Louisiana Department of Wildlife and Fisheries continuous monitoring station at Cypremort Point, Louisiana (Station 619).....63

Figure 35. Time series plot of mean daily salinity from the Louisiana Department of Wildlife and Fisheries continuous monitoring station at Cameron Louisiana (Station 719)...63

Figure 36. Time series plot of discrete salinity data from DEQ station 0138, Lake Pontchartrain Causeway at crossover number 4. 64

Figure 37. Time series plot of discrete salinity data from the Jefferson Parish EMPACT project (EPA funded) jointly conducted by the Coastal Ecology Institute at LSU and the USGS Baton Rouge office. 65

Figure 38. Time series plot of discrete salinity data from DEQ station 0084, Bayou Chevreuil at Chegby. 66

Figure 39. Time series plot of discrete salinity data from DEQ station 0113, Bayou Grand Caillou at Dulac. 66

Figure 40. Time series plot of discrete salinity data from Louisiana Department of Wildlife and Fishereis Station 407 in Vermillion Bay.....67

Figure 41. Time series plot of discrete salinity data from the United States Fish and Wildlife Service in the Sabine National Wildlife Refuge(Station BUS). 67

Figure 42. Plots of measured monthly mean salinity (solid line) and predicted monthly salinity (dashed line) for LDWF Station 315 (Top), LDWF Station 317 (middle) and LDWF Station 326 (bottom) in the Barataria system. 68

Figure 43. Summary of forcing function patters over the time period from 1950 through 2001.....69

INTRODUCTION

General Task Description

This report summarizes Task II.5, which was the development of an estuarine salinity and climate driver data base to investigate the effects of extreme changes in climate (temperature, evapotranspiration, precipitation, drought), Mississippi River discharge, local river discharge, and coastal sea levels on the salinities in Louisiana estuaries with emphasis on the Barataria-Terrebonne system. Of particular concern was the possible linkages between extreme events and the areas of "Brown Marsh" observed along the Louisiana coast during the spring and summer of 2000. This Task (II.5) was one of six collaborative tasks that used an integrative approach to understanding the causes of the Year 2000 marsh dieback. Each of the six causation tasks and their linkages to each other are presented in Figure 1.

The overall goal of this Task was to determine the degree to which the larger scale environmental drivers of climate, riverine discharge, coastal water levels and salinities were anomalous in the time leading up to and during the 2000 marsh dieback. This overall goal was divided into three tasks:

1. Develop a climatic driver and salinity data base specific to the Barataria-Terrebonne estuary that can be used by the modeling efforts (Task II.6) to both hindcast and forecast the specific environmental conditions responsible for brown marsh events.

2. Develop a climatic driver data base that has sufficient spatial distribution in the northern Gulf of Mexico to assess whether or not the conditions observed in 2000 were specific to Louisiana or was this a gulf wide phenomena.

3. Develop a climatic driver data base that has sufficient temporal distribution to be able to classify how unique the conditions observed in 2000 were.

The study focused on the Barataria-Terrebonne Bay system, to develop time series statistical models that explain the observed open water salinity as a function of precipitation, Mississippi River flow, and coastal water levels. Soil salinity modeling developed by Morris (1995) demonstrated that the salinity of the open water that is recharging the marsh substrate is a major factor controlling the soil salinity level. A conceptual model of the influence of the forcing functions analyzed in this report to soil salinity is shown in Figure 2.

METHODS

Data Sources

The data used in this Task analyzed came from the following sources :

1. **Climatic Data**
   Climatic data came from the Louisiana Office of Climatology at Louisiana State University, The Southern Regional Climate Center (SRCC) and from the National Climatic Data Center (NCDC). These data were used in the development of empirically derived climatic indicators to represent the full array of water-balance elements. The data included the Palmer Drought Severity Index (PDSI), Precipitation, and Temperature. The data were obtained for two sampling levels: (1) monthly summaries for the NCDC climate divisions shown in red in Figure 3), and (2) daily values for the stations shown in Figure 4.

2. **Continuous Salinity Data from Louisiana Estuaries**
   The Louisiana Department of Wildlife and Fisheries (LDWF) in conjunction with the United States Geologic Survey (USGS) and the Louisiana Department of Natural Resources (DNR) have Continuous data recorders at several locations in the coastal marshes. The stations used were those that had data records of 15 (or more) years in length. These stations are shown in Figure 5.

3. **Discrete Salinity Data from Louisiana Estuaries**
   The Louisiana Department of Wildlife and Fisheries (LDWF), the Louisiana Department of Natural Resources (DNR), The Louisiana Department of Health and Hospitals (DHH), The Louisiana Department of Environmental Quality (DEQ), the United States Army Corps of Engineers (USCE), and the United States Fish and Wildlife Service (USFWS) have discrete sampling at numerous locations in the Louisiana estuaries. Although this discrete data had limited value in a temporal sense (it is usually monthly or even bi-monthly samples) it was used to aid in assess spatial salinity patterns as well as documenting large-scale events. The stations used are shown in Figure 6.

4. **River discharge, coastal water levels, and coastal wind data**
   Daily stage and discharge of the Atchafalaya and Mississippi Rivers was obtained through the United States Army Corps of Engineers (USCE). Daily discharge data for various rivers around the Gulf of Mexico was obtained from the United States Geological Survey (USGS). The river discharge stations are shown in Figure 7. Hourly coastal water level data was obtained from the National Ocean Survey (NOS) and hourly meteorological data was obtained from the National Data Buoy Center (NDBC) from several stations around the Gulf of Mexico (Figure 8).

5. **Salinity data from other Northern Gulf of Mexico Estuaries**
   The relationship between climate drivers and estuarine salinities at several estuaries in the Gulf of Mexico was assessed based upon the literature. The data from 25 estuaries in the Gulf (Figure 9) documented by Orlando et al (1993) was used in this analysis.

Data Base Development

The data files were obtained in digital form in all cases either by downloading through the internet or in the form of a data CD. The data files were transferred to a desktop computer for analysis using "Statistical Analysis System" (SAS 1990 a, b, c, d, e). Because all the data were in time series format (either hourly, daily, or monthly) the same basic techniques were used for all sites. The levels of QC/QA were variable and inconsistent among the various data sets. Therefore, the data sets were inventoried and checked for data quality, and consistency. The following general procedures were used in the analysis:

a. Data Inventories
   - Total Observations in data set
   - Sampling Frequency
   - Spatial distribution of stations

b. Data Conversion
   - Convert to metric units
   - Calculation of salinity from conductivity or chloride

c. QA/QC Information
   - Investigate potential outliers
   - Plots of data distribution

d. Descriptive Statistics
   - Mean
   - Standard Deviation
   - Minimum
   - Maximum

e. Compute new parameters
   - Evapotranspiration (ET)
   - Water balance elements

f. Time series plots and analysis
   - Averaging and filtering of hourly and/or daily observations
   - Plots of daily and monthly observed and filtered data

g. Summarize the data
   Monthly averages and extremes
   Spatial patterns of climate drivers

h. Statistical modeling
   Salinity as a function of the various climate drivers
   Linear and auto-regressive models
   Determine importance of climatic drivers

Data analysis was conducted using "Statistical Analysis System" (SAS 1990 a, b, c, d, e) or Microsoft EXCEL. Once appropriate estimate(s) of ET were available, water-balance assessments were prepared to assess historical trends and variability of precipitation-driven freshwater resources The final analysis consisted of the classification of extreme events (magnitude, duration, frequency of occurrence) and the development of statistical models to explain the observed estuarine salinity using the climatic drivers.

Data Analysis Techniques

Water Budget Calculations

The sum of the water that vaporizes from the soil (evaporation) plus the moisture that flows through plant vascular system to the atmosphere (transpiration) is evapotranspiration (Mitsch and Gosselink, 1993). The overall precipitation surplus was calculated, on a monthly basis, using the precipitation and temperature data. The precipitation surplus (S) is calculated as the difference between the precipitation input (P) and the evapotranspiration loss (ET). The water budget parameters were calculated for the NCDC Climate Divisions presented in Figure 3.

The evapotranspiration loss was calculated using the Thorntwaite Equation as presented in Mitsch and Gosselink (1993).

$$ET_i = 16\,(10\,T_i / I)\,a$$

Where:

ET_i = potential evapotranspiration for month I (mm month-10)
T_i = mean monthly temperature (^oC)

I = local heat index $\sum_{i=1}^{12} (T_i / 5)^{1.514}$

$$a = (0.675\,I^3 - 77.1\,I^2 + 17{,}920\,I + 492{,}390) \times 10^{-6}$$

This equation is empirically based and is mainly used for terrestrial systems but has been successfully applied to wetland systems (Mitsch and Gosselink, 1993). The equation does not give completely reliable estimates since there many meteorological and biological factors affecting evapotranspiration. However, the equation does serves as a cost effective first approximation to the water balance for a wetland system (Mitsch and Gosselink, 1993).

Time Series Analysis

The observed hourly water level data from coastal stations around the Gulf of Mexico (Figure 8) for the time period from January 1, 1999 through June 30, 2000 was obtained from the NOS. The data was analyzed by removing the mean (to remove any long term trend) then smoothed (using a 25-hour running mean) to remove the astronomical tides. This allowed for the comparison of the overall water level patterns at the stations. Time series plots of the data are in Appendix F. The main interest is in the large-scale synoptic patterns. The period of record (1955-2001) hourly water level data was obtained from Grand Isle, Louisiana for use as an index station. This data was treated using the same techniques. The monthly average water levels for the Grand Isle station were also computed. The daily observations of river stage from the USGS and USCE stations around the gulf were used to compute monthly average river discharge.

Statistical Analysis

Regression models (SAS, 1990) were used to look at the importance of Mississippi River discharge, the Palmer Drought Severity Index, rainfall, and coastal water levels. Coastal water levels (as defined by the water levels at Grand Isle) were included to account for the possibility of the "stacking up" of water at the coast which could influence the transport of water in and out of the Barataria system. Several models were run, using various lags for river flow, rainfall, and coastal water levels, in an approach that was similar to that of Gagliano et al. (1973). Stepwise linear regression and Autoregressive models (SAS, 1990) were also used to produce a series of models using various combinations of variables (up to 9 variables). The results indicated that very little improvement in the model (5-7% improvement) was obtained by using more than three or four variables. In addition, any model used should be physically reasonable. A model using 1 month lag of the variables would be a physically reasonable model, whereas a model that used the 1 month lag and the 3 month lag, skipping the 2 month lag, would not be physically reasonable, although it might be statistically valid. Similar results were obtained by Wiseman, et al. (1990) in their analysis of Mississippi River flow and salinity. Because the overall goal is to obtain a model that is both parsimonious and physically reasonable, it was decided to limit the models to three or four variables.

RESULTS AND DISCUSSION

Gulf of Mexico Estuarine Forcing Functions

Water levels and open water salinity in coastal estuaries are generally controlled by a balance between the freshwater input generated from precipitation and runoff, and the saltwater mixing into the estuaries at the coast through the coastal boundary layer. The coastal boundary is in turn influenced by exchange with the deeper shelf and Gulf of Mexico waters, as well as the freshwater plume from the Mississippi River. These exchanges are bi-directional with significant transfers of mass and momentum as well as chemical and geological constituents also occurring between the shelf and the estuary (Wisemann, 1986).

Meteorological forcing in estuaries along the northern Gulf of Mexico can be considered in terms of: (1) exchange between the estuarine waters and the waters in the coastal zone; and (2) local forcing occurring within the estuary proper. Baumann (1987) attributed the changes in the spatial and temporal salinity patterns in the Barataria estuary to be due to three basic factors:

1. The seasonal evapotranspiration and precipitation regime,
2. Mississippi River discharge,
3. Seasonal water level cycle.

At time scales of a few days, the along-estuary wind stress drives an estuarine-shelf exchange; at longer time scales Ekman convergence/divergence driven by the alongshore wind stress drives the estuarine-shelf exchanges (Schroeder and Wiseman, 1986). Work by Kjerfve (1975) in Caminada Bay, Louisiana, demonstrated that the diurnal tidal influence, in addition to the wind forcing, can be important in controlling the internal dynamics of these systems. The most pronounced effect of wind forcing on the central Northern Gulf of Mexico systems is the difference between a northerly and a southerly wind. Strong winds from the south "push" water towards the coast forcing water into the estuaries, raising water levels about 0.3 - 0.5 m above normal. Conversely, winds from the north force water out of the estuaries depressing the water levels 0.3 - 0.5 m below normal. The "set up" of water usually occurs as a front approaches the area from the west and the southerly winds pile water along the coast, then after the front passes the winds shift to a more northerly direction. This situation results in a rapid drop in the estuarine water levels. Hart and Murray (1978) describe this type of situation occurring in Chandeleur-Breton Sound. These events result in substantial fluxes of water into, and out of, estuarine systems, and can have dramatic effects on the salinity distribution within the system. Thus, the salinity signal in these estuarine systems is fairly complex. A schematic detailing the major forcing functions discussed above is shown in Figure 10.

Orlando et. al., (1993) described the factors influencing salinity in 26 estuarine systems in the northern Gulf of Mexico (Figure 8). The distribution of freshwater input into these Northern Gulf of Mexico estuaries is presented in Figure 11. The Mississippi-Atchafalaya discharge dominates the input in the central portion of the Gulf, while the western (Texas) and eastern (Mississippi to Florida) portions of the Gulf are more heavily influence by local river flow . The overall precipitation, potential evapotranspiration, and surplus patterns, based on the monthly

NCDC Climate Division (Figure 3) data from 1950 through 2002, for the Gulf of Mexico is presented in Figure 12. In general, the Gulf of Mexico is characterized by low precipitation in Texas, higher and uniform precipitation in the central Gulf, and a distinct wet-dry season for Florida. Evapotranspiration exhibits a fairly uniform pattern across the central and eastern Gulf. Texas and southern Florida are characterized by high evapotraspiration. The surplus shows an overall pattern in which there is a rainfall deficit (evaporation exceeds precipitation) in the western part of the Gulf (and southern Florida) and a rainfall surplus (precipitation exceeds evaporation) in the central portion of the Gulf. The overall result is that some of the estuaries in the northern Gulf have the highest freshwater input per unit estuarine volume (Ward, 1980). Orlando et. al., (1993) concluded that high Mississippi River flows reduced the salinities in the lower portion of the estuaries in the central gulf (Louisiana) due to advection of Mississippi River water into the estuaries. During times of high river flow the local precipitation is unimportant. Conversely, at times of low Mississippi River flow, the salinities in the lower bays increase, and local precipitation becomes more important. The major freshwater sources for the 26 Gulf of Mexico estuaries described by Orlando et. al., (1993) are presented in Table 1. The Mississippi-Atchafalaya River flow serves as a primary or secondary source of freshwater to a large proportion of the Louisiana Estuaries.

The salinity of the estuaries around the Gulf of Mexico shows a fairly large range of values as a result of the freshwater input distribution. The average surface salinity for the 26 Gulf of Mexico estuaries studied by Orlando et. al. (1993) is presented in Figure 13 (the data for Barataria and Terrebonne-Timbalier was updated as part of this study). In general the central Louisiana estuaries exhibit lower salinities due to the effect of the Mississippi River discharge. The south Texas estuaries and the south Florida estuaries exhibit the highest salinities due to the general pattern of rainfall deficits in these locations. The data from Orlando et. al., (1993) were analyzed to look at salinity changes that occur in the Gulf of Mexico estuaries with changes in freshwater input for high and low freshwater input years. Figure 14 presents the changes in surface salinity (from average conditions) for high and low freshwater input years. The data show a general trend of salinity decreases of 2 to 5 ppt for high freshwater input years and increases of 5 to 7 ppt for low freshwater input years. There are a few exceptions to the overall pattern which is to be expected since this is a very limited data set

The inverse relationship between Mississippi river discharge and Louisiana coastal salinities was first mentioned by Geyer (1950). Barrett (1971) and Gagliano et al. (1973) further described this inverse relationship using linear statistics. Wiseman et al. (1990) used Auto-Regressive Moving Average (ARMA) models to analyze the relationship between weekly discharge of the Mississippi River and Louisiana coastal salinities. The river discharge portion of the models accounted for 30 to 50% of the variance of the observed salinity data along the coast. The results were consistent with a conceptual model in which Mississippi River discharge alters coastal salinities, which in turn propagates up-estuary and westward along the coast (Wiseman et al, 1990). Swenson and Turner (1998) developed empirical statistical models to explain the seasonal isohalines in the Barataria Estuarine System (BES) using coastal water levels, Mississippi River discharge, and local (New Orleans) precipitation from 1980 through 1995. The models were able to explain ~50% of the variance of the observed data. Their analysis also indicated that a change from low rainfall to high rainfall shifts the 5 ppt isohaline ~15 km south,

and the 15 ppt isohaline ~8 km south, and a change from low riverflow to high riverflow shifts the 5 ppt isohaline 20 km south, and the 15 ppt isohaline ~10 km south.

Coastal Water Levels, and River Discharge

The Grand Isle station is being used as an indicator station for the Gulf of Mexico to characterize the large-scale water level patterns. The correlation of weekly average water level for the stations around the Gulf is presented in Table 2. These data indicate that the large scale water level patterns are quite consistent around the Gulf of Mexico. The Grand Isle station has correlation coefficients of ~ 0.8 to 0.9 with a majority of the other stations. Time series plots of weekly average water levels from January, 1999 through July, 2000 for the Gulf of Mexico stations shown in Figure 8 are presented in Figure 15 (the 25 hour filtered plots are shown in Appendix A). Note the large peak around September-October, 1999 which is followed by a period of low water levels in December-March, 2000. The observed and de-trended monthly mean water levels at Grand Isle, from 1955 through 2001 are shown in Figures 16 and 17 (the daily plots are in Appendix B). The long term trend (relative sea level rise) was removed from the water level data in order to more clearly show the seasonal pattern. It has been assumed that a marsh that is keeping pace with sea level would experience this de-trended water level signal. The mean monthly coastal water levels show a pattern in which there are two peaks. One is in May-June and the second (and larger) is in September-October (Figure 18). The water level at Grand Isle exhibits a statistically significant trend (which is also a major portion of the signal) of ~1.1 cm yr^{-1} over the time period from 1955 through 2001 (this is the trend that was removed from the data presented in Figure 17). The low coastal water levels that occurred during the Brown Marsh Event (1999 –2000) can be seen on the de-trended and filtered water level data (Figure 17). These low water levels occur on a fairly regular basis. However, the magnitude of the low water levels that occurred during the Brown Marsh Event were levels that occur infrequently. During this time, the levels decreased to ~25 centimeters below the mean, the lowest level over the period of record (1955-2001). Levels of ~20 centimeters below the mean have occurred only five times over the period of record. Figure 19 presents a comparison of the monthly average de-trended water levels for 1999 through 2002 in comparison to the long term (1955-2002) monthly averages. The water levels during first half of 1999 were close to the average where as the last half of 1999 was characterized by lower than average water levels. The time period from 2001 through 2002 was characterized by lower than normal water levels with the exception of September-October, 2002 which had higher than normal water levels. Table 3 ranks the monthly mean de-trended Grand Isle water levels for the period of record. The 1999-2000 time period was characterized by water levels in the lower 15-20% of the entire record

Figure 20 presents a summary of the river flow data from stations around the Gulf of Mexico (Figure7). This figure presents the month in which the maximum and minimum discharges occur. Time series plots of daily discharge for each station are presented in Appendix C and the monthly mean plots for each station are presented in Appendix D. The monthly mean Mississippi River discharge for the time period from 1935 through 2001 is shown in Figure 21. The Mississippi River discharge exhibits a typical seasonal pattern in which the maximum discharge of~22,000 m^3sec^{-1} occurs in April, and the minimum discharge of ~7,000 m^3sec^{-1} occurs in September (Figure 22). The central Gulf is characterized by this type of signal, with

peak river discharges in the spring-summer and minimum discharges in the fall. The exceptions are the south Texas and south Florida divisions which tend to exhibit fall peaks with summer minimums. The Mississippi River discharge during the Brown Marsh period (1999-2000) was one of the lowest on record. This low river discharge for 1999-2000 occurred at a majority of the rivers around the Gulf of Mexico (see time series plots in Appendix C). Figure 23 presents a comparison of the monthly average Mississippi River discharge for 1999 through 2002 in comparison to the long term (1955-2002) monthly averages. Discharge during first half of 1999 were average or higher than average, where as the last half of 1999 was characterized by lower than average discharge. The year 2000 stands out as a year characterized by lower than average water levels with the exception of July which was slightly higher than average. Discharge during 2001 was lower than average in January then was average (or above) for the remainder of the year. The spring flood during 2002 (April-June) was higher than average, with the rest of the year being close to average.

Climatic Characterization

Swenson and Turner (1998) used an overall "climatic characterization" to identify high freshwater inflow years and low freshwater inflow years for the Barataria System. The climatic regime was classified into "wet", "dry" and "normal" year classes for the upper and lower portions of the Barataria Estuary system using Mississippi River Discharge and the Palmer Drought Severity Index (PDSI) as classification variables. A value of +/- 1 standard deviation, was used for the cutoff point for Mississippi River flow for wet and dry years. The PDSI classifies the years into "drought" or "moist" conditions. The index has a numeric value, with zero indicating normal conditions, values equal to, or less than -4 indicate extreme drought conditions, values equal to, or greater than, +4 indicate extreme moist conditions. The "very moist" (>3) condition was used as an indicator of a high local runoff year, and the "moderate drought: (<-3) category was used as an indicator of a low local runoff year. The actual data were then used to classify the years from 1980 through 1995. A classification matrix was developed (Table 4) which classified the upper and lower portions of the estuary into "wet" and "dry" years (based upon river discharge and the PDSI). The actual data were then used to classify the years from 1980 through 1995. The data has been updated through 2002 as part of the present study. The overall characterization for the Barataria system is presented in Table 5. These data indicate that the time period from 1999 - 2000 was quite unique in the, being characterized by very dry conditions for an extended period of time (~18 months).

Time series plots of all of the NCDC Climate Division data are presented in Appendices E through I. The monthly pattern of surplus (precipitation minus evapotranspiration) for the Gulf of Mexico climate divisions (Figure 3) for the time period from 1950 through 2001 is presented in Figure 24. The monthly pattern of the PDSI from 1900 through 2001 is presented in Figure 25. In both case the blue colors represent wet conditions and the red colors represent dry (drought) conditions. The surplus pattern (Figure 24) shows an overall spatial difference around the gulf with the central gulf being wetter. Over the last 50 years there were several times when gulf wide dry conditions occurred, the most notable were in the 1950's, the early 1960's, and the recent Brown Marsh event. The temporal pattern is much more evident in the PDSI contour plot (Figure 25). The drought of the 1950's is the most severe in the record, lasting from 1950-1957,

with the most severe time period being 1955-1957. Texas was characterized by drought conditions over the entire time period. There was a short break in the drought for the most of the in late 1952 (south Texas remained under drought conditions). The next gulf wide droughts occurred in 1963-1964 and 1981. The 1963-1964 reached severe levels where as the 1981 drought did not. The most recent severe gulf wide drought covers the time period from mid-1998 to mid-2001. This drought was characterized by severe drought conditions (red color on plot) over a significant portion of the central gulf for 6-12 months.

The details of the 1999-2000 drought period are presented in Figures 26 through 29. Figure 26 presents a comparison of the monthly total precipitation for 1999 through 2001 in comparison to the long term (1950-2001) monthly averages. Precipitation for most of the climate divisions around the Gulf was below normal for 1999 through 2000. The drought ended in 2001, which was characterized by normal or higher than normal precipitation for all divisions around the gulf. Figure 27 presents a comparison of the monthly evapotranspiration for 1999 through 2001 in comparison to the long term (1950-2001) monthly averages. The evapotranspiration rates were slightly higher for 1999-2000 where as 2000 was closer to normal. In general the differences from normal were fairly small. Figure 28 presents a comparison of the monthly surplus for 1999 through 2001 in comparison to the long term (1950-2001) monthly averages. The time period from 1999-2000 stands out as having much lower than normal surplus for all climate divisions around the gulf. Figure 29 presents a comparison of the monthly average PDSI for 1999 through 2001 in comparison to the long term (1950-2001) monthly average. The long term behavior is "normal" conditions for most of the climate divisions around the gulf. The time period from 1999-2000 was characterized by drought conditions around the gulf with 2000 be more severe. In 2001 conditions became wetter than normal through most of the gulf.

There were some anecdotal observations stating that the winds during the drought period were different from the normal wind conditions. Plots of coastal wind data from Port Aransas, Sabine, Grand Isle, SW Pass, Dauphin Island, Keyton Beach, and Venice are presented in Appendix J. The Grand Isle station does show some slightly lower wind speeds during the time period. However this pattern is not observed at the other stations. In general, there we found no gulf wide wind anomaly as was the case for the drought indices.

Open Water Salinities

Time series plots of daily mean salinity (computed from hourly observations) from stations across the coast (from the Barataria system to Sabine), are presented in Figures 30 through 36). All plots have the same date axis to allow for visual comparison of the salinity data from various stations. Data from the Louisiana Department of Wildlife and Fisheries (LDWF) stations in the Barataria system (Station S315 - Grand Terre, Station S317 - St. Mary' Point, and Station S326 - Little Lake) are presented in Figure 30 through 32. Data from the LDWF station in Caillou Lake (Station 518) is shown in Figure 33, data from the LDWF station at Cypremort Point (Station 619) is shown in Figure 34, and data from the LDWF station at Cameron (Station 719) is presented in Figure 35. Examples of discrete salinity data from Lake Pontchartrain, Lake Cataouache, Lake Salvador, Bayou Chevreuil, Bayou Grand Caillou at Dulac, Vermillion Bay, and Sabine are presented in Figures 36 through 41. Although these data come from discrete data

sets, the data is presented in order to show the general patterns across the Louisiana coast. The most obvious feature of the salinity plots is the uniqueness of the 1999-2000 data. This time period is characterized by the highest salinities on record. The duration of the high salinities observed during the 1999 - 2000 time period for the Barataria system are summarized in Table 6. The normal high salinity patterns (for a two year time period) are ~ 4 months greater than 30 ppt for at Grand Terre, ~ 2 months greater than 20 ppt for at St. Mary's Point, and ~ 2 months greater than 7.5 ppt for at Little Lake. The 1999 - 2000 time period was characterized by high salinity patterns of 12 months greater than 30 ppt for at Grand Terre, 10 months greater than 20 ppt for at St. Mary's Point, and 8 months greater than 7.5 ppt for at Little Lake. This is a four fold increase in the high salinity levels observed in this system. Systems throughout the Louisiana coastal zone were characterized by much higher than normal salinities during this time period.

Climate Driver – Salinity Statistical Model Results

Regression models (SAS, 1990 a, b, c) were used to look at the importance of Mississippi River discharge, the Palmer Drought Severity Index, rainfall, and coastal water levels. Coastal water levels (as defined by the water levels at Grand Terre) were included to account for the possibility of extremely low or high water levels influencing the transport of water in and out of the system. Several models were run, using various lags for river flow, rainfall, and coastal water levels, in an approach that was similar to that of Gagliano et. al., (1973). Stepwise linear regression and Autoregressive models (SAS, 1988) were also used to produce a series of models using various combinations of variables (up to 9 variables). The results indicated that very little improvement in the model (5-7% improvement) was obtained by using more than three or four variables. In addition, any model used should be physically reasonable. A model using 1 month lag of the variables would be a physically reasonable model, whereas a model that used the 1 month lag and the 3 month lag, skipping the 2 month lag, would not be physically reasonable, although it might be statistically valid. Similar results were obtained by Wiseman, et. al., (1990) in their analysis of Mississippi River flow and salinity. Because the overall goal is to obtain a model that is both parsimonious and physically reasonable, it was decided to limit the models to three or four variables. The results presented here are for the Barataria system.

In all cases the most successful models were those that contained an autoregressive term. The models were run for the entire continuous data record for each station (1961-2000 for Station 315, 1973-2000 for Station 317, and 1988-2000 for Station 326). The details of the final statistical models are presented in Table 7, and results of the model predictions for the time period from 1995-2000 are presented in Figure 42. The measured values are shown by the solid line and the predicted results from the statistical model are shown as a dashed line (with solid dots). The model for station 315 (coastal station at Grand Terre) explained a total of 72 percent of the observed signal, with the linear portion of the model explaining 48 percent, using Mississippi River discharge, precipitation from Louisiana climate division 9, Grand Isle water levels, and the previous month's salinity. The model for station 317 (mid-estuary station at St. Mary's' Point) explained a total of 74 percent of the observed signal, with the linear portion of the model explaining 41 percent, using Mississippi River discharge, precipitation from Louisiana

climate division 9, Grand Isle water levels, and the previous month's salinity. The model for station 326 (upper-estuary station in Little Lake) explained a total of 63 percent of the observed signal, with the linear portion of the model explaining 16 percent, using Mississippi River discharge, precipitation from Louisiana climate division 9, and the previous 3 month's salinity. The results show a decrease in the magnitude of the effect of the Mississippi River discharge and coastal water levels from the coast inland. The effect of precipitation is maximum mid-estuary (St. Mary's' Point) and minimum at the upper station (Little Lake). This is not what would be expected but may be a result of the shorter data record at the Little Lake station. The autoregressive parameter seems to indicate a faster flushing in the lower portion of the system (one month lag at the coast and mid-estuary compared to three month lag at Little Lake). Previous studies by Wisemann, et al (1990) indicated that the effect of the Mississippi River plume is a factor in controlling coastal open water salinity throughout the entire Barataria-Terrebonne system.

The Role of ENSO for South Louisiana

Linkages between changes in large-scale atmospheric and oceanic circulation features and shifts in regional climate patterns in other parts of the world have been recognized for decades. These linkages between larger-scale circulation and regional scal climate are termed teleconnections. One of the most studied ocean-atmosphere circulation features is the ENSO (El Niño-Southern Oscillation). Principal ENSO features include sea-surface temperature (SST) variations in the eastern and central equatorial Pacific Ocean (the oceanic signal) and changes in pressure and wind patterns that occur over the greater Pacific basin (the atmospheric signal). La Niña is the term commonly applied to the negative (or "cold") SST phase of the ENSO cycle; El Niños, which have been more prevalent over the last thirty years, refer to periods of anomalously-warm SSTs over the equatorial Pacific. In addition, there exists a transition, or "neutral", phase in the cycle, sometimes referred to as La Nada (La Nada accounts for roughly 40% of all three-month periods from 1951-2000 based on the subjective ENSO classification provided by NWS Climate Prediction Center.).

Of key interest for the Gulf Coast region are the teleconnections that link ENSO phase with shifts in seasonal climatic patterns. Analyses have shown that the ENSO phase is linked to changes in atmospheric circulation patterns that impact the Gulf Coast. Shifts in the larger-scale upper-level atmospheric circulation can result in changes in longer-term (months to years) regional climatic patterns, which in turn affect the shorter-term (days to weeks) weather patterns as expressed at the surface. In effect, changes in atmospheric circulation over the Pacific basin may result in "downstream" modifications in the positions of upper-air ridges and troughs that drive regional and local weather. For the Gulf Coast region, one of the most notable atmospheric circulation features associated with the phase of ENSO is the presence/absence of a sub-tropical jet during the winter and spring months. An "active" sub-tropical jet (STJ) is associated with increased winter storminess in the Gulf Coast region; establishment and persistence of the STJ typically leads to greater rainfall totals during the low-sun months, especially along the Gulf Coast rim and the Florida Peninsula. Warm-phase periods (El Niño) are marked by runs of days and/or weeks with the STJ active over the Gulf Coast region, and these periods often correspond to enhanced cyclogenesis (formation of surface low-pressure centers and winter storms) in the northern Gulf. During a well-developed La Niña, the STJ during winters and springs tends to be

less permanent and more transitory in nature, although not entirely absent. While ENSO appears to play an important -- and predictable -- role in the winter-spring circulation patterns for the Gulf Coast region, associations between ENSO and high-sun (summer) season weather have not been successfully identified. The STJ is only occasionally observed in the summer months, and the focus of most upper-level circulation dynamics during the warm months shifts well to the north of the Gulf Coast region. Gulf Coast regional summer-fall weather -- and the amounts of rainfall -- tend to driven by the size, position and intensities of sub-tropical high-pressure centers (STHs). Most of the summertime precipitation along the central Gulf Coast is the result of convective showers and thunderstorms rather than frontal/low-pressure systems that are the primary drivers from late fall through spring. Summer convective activity may be suppressed or enhanced across the Gulf Coast during periods of expanded STHs; indeed the same high-pressure feature may serve to enhance summer rains for the western half of the Gulf while depressing shower formation over the eastern half. Of course, the importance of occasional rains generated by tropical waves and cyclones must also be recognized: in a given year, individual tropical systems have the potential of producing more than a month's worth of precipitation in just a few days.

To date, there is no compelling evidence of reliable linkages between STHs and ENSO phases. Evidence does suggest that the phase of ENSO may play some role in tropical storm frequencies: seasonal storm counts over the Atlantic basin tend to be lower during El Niño phases, while counts tend to be higher during La Niñas. However, the unpredictable nature of tropical weather serves as a "wild card" in any effort to provide extended-range forecasts of summer and fall seasonal rainfall. Regardless of the overall tropical activity -- and summer-fall ENSO phase -- an otherwise dry summer-fall period can end with above-normal seasonal rainfall due to a single tropical system. Given the inability to forecast tropical landfall threats and coastal impacts regardless of ENSO phase, and a lack of predictive skill for STHs based on ENSO phases, it is not surprising that little association between ENSO and summer-fall weather has been defined for the Gulf Coast region. Given the importance of upper-level circulation and the association between ENSO phase and the presence and intensity of the STJ over the Gulf during the winter and spring, it is not surprisingly to find that both ENSO phases are associated with departures from "normal" seasonal weather during the winter and spring across southern Louisiana and the Gulf Coast rim. Although linkages are weak for both phases with regard to winter and spring seasonal temperature across south Louisiana (and much of the Gulf Coast region), both ENSO phases show strong associations with Gulf Coast winter and spring precipitation trends. Indeed, the correlations between ENSO phase and Gulf Coast winter-spring rainfall are sufficiently strong to serve as an extended-range forecast tool for seasonal precipitation projections during that time of year. Established El Niños usually lead to wetter-than-normal winters and springs along the entire Gulf Coast. Over the last half-century for south Louisiana, November-thru-May (Nov-May) total rainfall was above the mean for virtually every winter-spring period occurring concurrent with moderate-to-strong El Niños. Conversely, Gulf Coast winter and spring rainfall is commonly below-normal during La Niñas, with Nov-May rainfall across south Louisiana being below Nov-May norms for all but one (1973-1974) of the recent La Niñas. (Analyses are based on a comparison of the Nov-May rainfall for south Louisiana with the NWS Climate Prediction Center's three-month subjective ENSO index for the period of October-December and January-March).

From a climatological and hydrological perspective, the winter and spring play important roles in terms of moisture recharge (upper-soils and deeper layers) for the Gulf Coast region. In a "normal" year, Louisiana winter-spring rainfall exceeds the environmental demand (potential evapotranspiration, PE) for moisture. Even following a dry fall season, normal winter rains will quickly restore upper-soil layers to near-saturation. In addition, excess precipitation serves as a recharging source for rivers and bayous, lakes and reservoirs. Under these conditions, overland runoff and rising water tables produce a "freshening" of the marshes, with seasonal salinity levels tending to reach the lowest levels of the year. However, during an unusually dry winter and spring, the environment may experience moisture deficits (stresses) not normally expected as the summer approaches. Should drier-than-normal weather persist into the summer, the impacts of these winter-spring deficits may be compounded, as environmental moisture demand (PE) often exceeds the local freshwater supply during the high-sun months.

ENSO-related indices clearly show that 1998 through 2000 was dominated by a La Niña event. The exact timing of the cold-phase event may be debated -- both in terms of the La Niña onset and the its termination -- but various measures of ENSO activity indicate that the La Niña cycle continued essentially uninterrupted for at least 18 months. Below-average SSTs persisted in the equatorial Pacific from mid-1998 through mid-2000; more conservative indices of ENSO activity suggest that the La Niña ran from late-1998 through early 2000. In addition, based on the NW Climate Prediction Center's 3-month subjective index, "cold" phase conditions dominated the period from mid-1998 into the first quarter of 2001. This period of time includes the winter-springs of 1999 and 2000 -- for south Louisiana, rainfall was far-below normal for both periods. Based on long-term data, areawide Nov-May rainfall across the southern parishes averages approximately 876 mm (34.5 in.). South Louisiana regional rainfall for that same six-month period averaged only two-thirds of normal (585 mm, 23.0 in.) in 1999; Nov-May rainfall for 2000 was less than half the norm (405 mm, 15.8 in.), and proved to be the driest Nov-May of the past fifty years.

CLIMATOLOGICAL OVERVIEW: 1998 - 2000

The period of 1998 through 2000 was marked by a well-developed La Niña, but the 1990s as a whole were dominated by the presence of El Nino. El Niño persisted throughout most of the period from late 1990 through early 1995, reaching its peak intensity during that cycle between late 1991 into mid-1992. In addition, a brief by strong El Niño developed in early-1997 and continued through the first half of 1998. Although SSTs briefly displayed anomalously-cool readings from late-1995 through early 1996, the 1998-2000 event as the only bona fide La Niña of the decade. The 1990s also displayed a continuation of a "wet" weather regime for the Bayou State that had become established over the last twenty years. Indeed, the 1980s and 1990s proved to be the "wettest" years, on average, in more than a century for the Bayou State. (Given the recent prolonged run of enhanced seasonal and annual rainfall over the last two decades, an obvious question arises: has this tendency towards wetter environmental conditions significantly affected and/or modified the freshwater hydrology and environmental response in the coastal zone?). The following is provided as a characterization of key monthly and seasonal climate/weather events during the period of 1998-2000. A general theme throughout the period quickly becomes evident: south Louisiana monthly rain totals throughout the period were

routinely below the norm, producing a slow, but steady intensification of moisture deficits and drought.

- In keeping with the twenty-year trend of enhanced precipitation during the waning months of the 1997-1998 El Niño, 1998 opened with record and near-record rainfall for the month of January over the Bayou State. Rainfall across the Louisiana coast averaged more than 250 mm (~10.0 in.) For the month, with some localized monthly totals exceeding 500 mm (~20.0 in.). Rainfall was also above the norm for February, with the 1997-1998 winter (DJF) proving to be among the "wettest" winters for Louisiana since the super El Niño of 1982-83.

- Louisiana's first run of dry weather during 1998 began during late March and continued across southern Louisiana through the first half of April. Indeed, the dry spell was deemed beneficial in some respects by eliminating moisture excesses that had accumulated during the winter, allowing saturated agricultural fields to drain, and permitting elevated water levels along many rivers and bayous to fall.

- Two frontal events during the latter half of April brought that brief dry spell to an end, but south Louisiana weather turned exceptionally dry and warm over the next four months. A persistent upper-level ridge over the southern U.S. blocked additional spring frontal passages, with the resulting fair weather allowing sunshine to add to the heat load. Rainfall during May 1998 averaged under 25 mm (0.5 in.) for most southern parishes, ranking among the driest Mays ever, and monthly rain totals for most south Louisiana sites remained below-normal through August. At the same time, monthly temperatures for the four-month period averaged nearly 2C (3-4F) above the norm, with the 1998 summer ranking among the warmest summers ever for Louisiana. (Note that elevated temperatures suggest above-average seasonal moisture demand -- elevated PE rates; this occurring at a time when precipitation inputs are well-below the seasonal norms.) Moisture deficits are evident in the monthly PDSI values for May, with all three Louisiana coastal climate divisions posted as under "mild drought".

- Although a weak tropical wave in late June provided temporary relief from excessive moisture shortages to a few areas of south Louisiana, the drought steadily intensified through the summer of 1998. By the end of August, Louisiana's three coastal climate divisions were rated as under "moderate to severe drought" according to the monthly PDSIs.

- September's active tropical weather provided a break for south Louisiana's on-going drought. Four tropical systems -- Earl, Frances, Hermine and Georges -- combined to produce one of the wettest September's ever for the state's southern parishes. Monthly rain totals typically ranged from 25 mm (~10.0 in.) to well over 50 mm (~20.0 in.), with isolated larger accumulations. The vast majority of that rain fell within a period of five to ten days, resulting in huge amounts of overland runoff and only a small portion of the total being available for upper-

level and deeper-layer soil-moisture recharge. Interestingly, September PDSI values indicate an end to drought conditions for the SW and SE climate divisions, but the SC division remained categorized as under "mild drought" for the month.

- The final three months of 1998 displayed a return to warmer-than-normal and drier-than-normal seasonal conditions for the southern parishes, although monthly rainfall departures were generally less extreme than those observed during the high-sun months. Warm-and-dry weather for the closing quarter of 1998 spelled a decline in moisture availability and a general decline in monthly PDSI values. December 1998 PDSI ratings across the three coastal parishes ranged from "near normal" for the SW division to "moderate drought" for the SC, with the SE division posted under "mild drought".

- Unlike the previous January, rainfall across most of Louisiana's southern parishes during January 1999 was below-normal. The dry pattern extended into and intensified during February, with winter (DJF) rainfall across the southern parishes averaging only about half the norm for the season. In addition, January and February temperatures averaged from 2 to 3C above normal (~4-6F), with the mild winter temperatures likely enhancing environmental ET rates.

- March marked the end of a ten-month run of above-normal monthly temperatures as well as an end to the string of drier-than-normal months for the southern three climate divisions. However, with near-normal March rainfall for the southern parishes, there was insufficient surplus moisture to significantly ease moisture deficits. As a result, spring 1999 began with "mild to moderate drought" (PDSI ranks) in effect for the coastal zone.

- For the second consecutive year, unusually warm-and-dry weather developed over southern Louisiana during April, as upper-level ridging became established once again over the central and eastern states. April monthly rainfall totaled less than 15 mm (~0.5 in.) for many southern parishes, with some south Louisiana sites reporting record-low April accumulations. Essentially rain-free weather continued into the first ten days of May before any relief arrived. May ended with near-normal rainfall totals for most southern parishes -- sufficient moisture to temporarily slow the intensification of drought conditions across the coastal zone, but not enough to dramatically ease the degree of drought over the southern parishes.

- June 1999 rainfall was well-above the norm across the southern parishes, with regional totals ranging from approximately 180 mm (~7.0 in.) to 300 mm (~12.0 in.), with localized totals exceeding 450 mm (~18.0 in.). Daily data indicate that much of the month's rain fell in a series of locally-heavy downpours, with several incidents producing extensive urban/suburban flooding. The unusually wet weather was certain to have delivered a large volume of freshwater to the coastal zone -- both as direct rain and overland runoff. Yet PDSI values as of the end of June indicate that only the SW division slipped out of "mild drought", with the SE

division remaining in "mild drought" and the SC division ranked as still under "moderate drought".

- June's respite from drier-than-normal weather was short-lived, with July rain totals returning to below-normal. Excessive heat during August 1999 resulted in one of the warmest Augusts in history for the Bayou State, with south Louisiana rainfall running from 66% of normal for the SE division down to less than 25% of the norm for the SW (the lowest August total ever for the SW division). Elevated temperatures (elevated PE) coupled with the dry weather prompted a decline in PDSI values, with the SC division dropping into the "severe drought" category as of summer's end.

- September rainfall was below normal across the coastal zone, with October rains running below-normal for the SW division but above the norm for the SC and SE divisions. November was also a month of below-normal rainfall across the southern parishes, with several parishes recording under 25 mm (~1.0 in.) for the month. December followed the pattern of drier-than-normal weather for he coastal region, with 1999 ending a second consecutive year of below-normal rainfall across the southern half of the state. PDSIs for the close of 1999 rated the SE division as under "moderate drought", with "severe drought" posted for both the SC and SW divisions.

- The La Niña effect on winter-spring rain was evident across all of the southern parishes for 2000, with monthly rainfall for all three climate divisions being below the mean for each of the first four months of the new year. In addition, temperatures were above-normal from January through March, suggesting above-average seasonal ET rates. January rainfall averaged less than 50% of normal for the coastal zone as a whole, with regionwide February rainfall running less than 25% of normal. After yet another "dry" month in March, 2000's first quarter total for the SE division was among the ten lowest January-to-March (Jan-Mar) totals in a century, among the five lowest ever for the SC division, and established an all-time record low Jan-Mar cumulative total for the SW division! Not surprisingly, the SW division PDSI for March 2000 indicates "extreme drought", with "severe drought" posted for the SC division and "moderate drought" in effect for the SE.

- Although April proved to be cooler-than-normal, ending the temperature trend that began the year, rainfall remained below the norm for most southern parishes, especially those in the eastern half of the coastal region. Assessments of the January-to-April (Jan-Apr) 2000 four-month totals indicate that not only does this period rank among the all-time record low Jan-Apr totals in the 100-year precipitation record for southern Louisiana, but that these four-month totals rank among the twenty "driest" four-month totals regardless of season (out of a possible ~1300 cases!)

- May rainfall across the coastal zone displayed a steep west-to-east gradient; rainfall for the SW division averaged more than 165 mm (6.5 in) for the month, yet totals for the SC and SE divisions failed to reach 15 mm (0.6 in.). June rains offered a respite to the intensifying drought, with monthly totals running near normal to slightly above normal for the southern parishes, but once again the relief was brief as July rainfall averaged between 66% (SW division) and just 44% (SE division).

- Unusually warm weather during August, with rainfall running from 45% to 65% of normal, pushed drought conditions across south Louisiana parishes to their most intense levels during the late summer of 2000. Although summer rainfall totals were not records, eight-month (January-through-August) totals for 2000 rank among the lowest January-August totals of the century, and establish all-time record lows for the SC and SE divisions.

- September rain totals were quite variable over the coastal parishes, partly due to a poorly-defined tropical depression (T.D. #9) that made landfall along Cameron Parish. September monthly totals across the region ranged from less than 50 mm (2.0 in.) to more than 250 mm (~10.0 in.). October rainfall was below-normal regionwide, with a number of parishes reporting under 15 mm (0.6 in.) for the month.

- The on-going La Niña weakened substantially during the latter half of 2000, with various ENSO indices indicating either weak La Niña or neutral conditions in effect during the last quarter of the year. November upper-level circulation patterns, and the resulting south Louisiana rainfall, appear to have responded to this modification in the ENSO phase (or at least the weakened intensity of the La Niña). A series of fronts -- and a number of developing lows over the northwestern Gulf -- delivered heavy rains during November 2000 to the southern parishes. November rains were two to three times the monthly norm, with totals over the southern parishes ranging from 250 mm (~10.0 in.) to as much as 380 mm (~15.0 in.) or more. November PDSIs indicate an end to the drought for the SW and SC divisions, with a two-category reduction in drought classification for the SE division (from "extreme" to "moderate drought"). 2000 closed with a "dry" December for the coastal zone, with the SE division still in drought (based on the PDSI).

- Weak La Niña to neutral conditions were in effect for 2001, with neutral conditions in early 2002 giving way to a moderate El Niño by the latter half of that year. For the SE division, which ended 2000 still in PDSI drought, the 1998-2000 drought extended well into 2001 before ending in the spring. The SC and SW division also demonstrated brief spells of PDSI drought during the spring of 2001. Another short run of drought is evident for all three climate divisions from late 2001 into early-to-mid 2002, with "moist to very moist conditions" indicated by PDSI values for the three divisions for the latter half of 2002.

- In summary, the south Louisiana drought of 1998-2000 -- as referenced by monthly PDSI values -- displayed some regional variability in terms of onset, duration and intensity. Tropical weather during September 1998 briefly eased the intensifying drought for many parishes, and effectively terminated the drought for a short period in other sections of coastal Louisiana.

- Drought returned to all of south Louisiana during 1999, with all three coastal climate divisions in "mild to moderate drought" by mid-year and "moderate to severe drought" in effect by the end of 1999. Yet the most intense period of drought was to come in 2000, with periods of "extreme drought" occurring across the entire coastal zone for several months that year.

SUMMARY

The salinities in the open waters of the estuaries is controlled by several forcing functions. These forcing functions range from local precipitation derived runoff to larger scale forcing from near shore coastal waters which are influenced by the Mississippi River Plume. The forcing function patterns over the time period from 1950 through 2002 are summarized in Table 8 and presented in graphic form in Figure 43. The gulf wide drought observed during the "Brown Marsh Event" of 1999 – 2000 was one of the most extensive on record. In addition to the gulf wide drought conditions, the Mississippi River discharge during 2000 was the second lowest on record (over the time period from 1935 – 2002). The lowest discharge year over this time period was 1954.

The previous gulf wide drought (1963-1964) was of a much shorter duration and was not as severe in magnitude. The 1963-1964 drought was also coupled with Mississippi River discharges that were average to slightly below average. The time period from 1951 to 1957 were also characterized by a gulf wide drought that reached severe levels. However during this drought the Mississippi River discharge was close to average for most years, with the exception of 1954 which was below average.

The major findings of this Task are summarized below:

- Estuaries in the northern Gulf of Mexico are influenced by (1) exchange between the estuarine waters and the waters in the coastal zone; and (2) local forcing (river discharge, precipitation) occurring within the estuary proper. Mississippi river discharge is the dominant forcing function influencing salinity in the coastal waters.

- The large scale water level patterns are quite consistent around the Gulf of Mexico. The Grand Isle station has correlation coefficients of ~ 0.8 to 0.9 with a majority of the other stations.

- The Mississippi-Atchafalaya discharge dominates the input in the central portion of the Gulf, while the western (Texas) and eastern (Mississippi to Florida) portions of the Gulf are more heavily influence by local river flow.

- The northern gulf of Mexico precipitation-evaporation exhibits a general characterized by a decrease in precipitation from east (Florida) to west (Texas), while surface evaporation rates generally increase from east to west across the Gulf. This results in an overall pattern in which there is a precipitation deficit in the western part of the Gulf (and southern Florida) and a precipitation surplus in the central portion of the Gulf.

- Isohaline data from the Barataria estuary in Louisiana indicated that a change from low rainfall to high rainfall shifts the 5 ppt isohaline ~15 km south, and the 15 ppt isohaline ~8 km south, and a change from low Mississippi River discharge to high Mississippi River discharge shifts the 5 ppt isohaline 20 km south, and the 15 ppt isohaline ~10 km south. Literature data for Gulf of Mexico estuaries (Orlando et. al., 1993) show salinity decreases of 2 to 5 ppt for high freshwater input years and increases of 5 to 7 ppt for low freshwater input years. These are the magnitude of the salinity changes that might be expected with global climate changes.

- Literature data for Gulf of Mexico estuaries (Orlando et. al., 1993) show salinity decreases of 2 to 5 ppt for high freshwater input years and increases of 5 to 7 ppt for low freshwater input years. These are the magnitude of the salinity changes that might be expected with global climate changes.

- The Mississippi River discharge exhibits a seasonal pattern in which the maximum discharge of ~22,000 m^3sec^{-1} occurs in April, and the minimum discharge of ~6,000 m^3sec^{-1} occurs in September.

- The central Gulf is characterized by this type of signal, with peak river discharges in the spring-summer and minimum discharges in the fall. The exceptions are the south Texas and south Florida divisions which tend to exhibit fall peaks with summer minimums.
- The mean monthly coastal water levels (at Grand Isle, Louisiana) show a pattern in which there are two peaks. One is in May-June and the second (and larger) is in September-October. The water level at Grand Isle also exhibits a statistically significant trend (which is also a major portion of the signal) of ~1.17 cm yr^{-1} over the time period from 1955 through 2000.

- Regression models (SAS, 1988) were used to look at the importance of Mississippi River discharge, the Palmer Drought Severity Index, rainfall, and coastal water levels on salinity in the Barataria estuary, Louisiana. The most successful models were those that contained an autoregressive term. The model for station 315 (coastal station at Grand Terre) explained a total of 72 percent of

the observed signal, with the linear portion of the model explaining 48 percent, using Mississippi River discharge, precipitation, Grand Isle water levels, and the previous months salinity. The model for station 317 (mid-estuary station at St. Mary's' Point) explained a total of 74 percent of the observed signal, with the linear portion of the model explaining 41 percent, using Mississippi River discharge, precipitation, Grand Isle water levels, and the previous months salinity. The model for station 326 (upper-estuary station in Little Lake) explained a total of 63 percent of the observed signal, with the linear portion of the model explaining 16 percent, using Mississippi River discharge, precipitation, and the previous 3 month's salinity.

- In comparing PDSI scores for the 1998-2000 drought with past drought periods, it is apparent that the recent drought ranks among the most intense droughts of the past 100 years for the three Louisiana coastal climate divisions. Although a number of past events demonstrate longer durations and greater temporal persistence than the 1998-2000 event, the 1998-2000 event (based on PDSI scores) shows similar peak intensities. Most notable is the intensity of the drought for the South Centrall division, where the absolute values of the extreme PDSI values during the 1998-2000 event are the most severe PDSI drought scores (i.e., most negative PDSI values) to be found in the entire time series.

- The drought of the 1950's was the most severe in the record, lasting from 1950-1957, with the most severe time period being 1955-1957. Texas was characterized by drought conditions over the entire time period. There was a short break in the drought for the most of the in late 1952 (south Texas remained under drought conditions). The next gulf wide droughts occurred in 1963-1964 and 1981. The 1963-1964 reached severe levels where as the 1981 drought did not. The most recent severe gulf wide drought covers the time period from mid-1998 to mid-2001. This drought was characterized by severe drought conditions over a significant portion of the central gulf for 6-12 months. Estuarine systems throughout the Louisiana coastal zone were characterized by much higher than normal salinities during this time period.

- Both ENSO phases show strong associations with Gulf Coast winter and spring precipitation trends. Indeed, the correlations between ENSO phase and Gulf Coast winter-spring rainfall are sufficiently strong to serve as an extended-range forecast tool for seasonal precipitation projections during that time of year. Established El Niños usually lead to wetter-than-normal winters and springs along the entire Gulf Coast. Conversely, Gulf Coast winter and spring rainfall is commonly below-normal during La Niñas, with Nov-May rainfall across south Louisiana being below Nov-May norms for all but one (1973-1974) of the recent La Niñas.

- ENSO-related indices clearly show that 1998 through 2000 was dominated by a La Niña event. The exact timing of the cold-phase event may be debated -- both in terms of the La Niña onset and the its termination -- but various measures of

ENSO activity indicate that the La Niña cycle continued essentially uninterrupted for at least 18 months. This period of time includes the winter-springs of 1999 and 2000 -- for south Louisiana, rainfall was far-below normal for both periods. Based on long-term data, areawide Nov-May rainfall across the southern parishes averages approximately 876 mm (34.5 in.). South Louisiana regional rainfall for that same six-month period averaged only two-thirds of normal (585 mm, 23.0 in.) in 1999; Nov-May rainfall for 2000 was less than half the norm (405 mm, 15.8 in.), and proved to be the driest Nov-May of the past fifty years.

LITERATURE CITED

Barrett, B. B. 1971. Cooperative Gulf of Mexico Estuarine Inventory and Study, Louisiana, Phase II, Hydrology and Phase III, Sedimentology. Louisiana Wildlife and Fisheries Commission, New Orleans. 190 pp.

Baumann, R. H. 1987. Chapter 2, Physical Variables. in W. H. Conner and J. W. Day, Jr. , editors. The Ecology of Barataria Basin, Louisiana: An estuarine profile. U. S. Fish and Wildlife Service Biological Report 85(7.13). 165 pp.

Gagliano, S. M., P. Light, R. Muller, M. Al-Awady. 1973. Water balance in Louisiana estuaries. Hydrologic and Geologic Studies of Coastal Louisiana, Report No. 3. Coastal Resources Unit, Center for Wetland Resources, Louisiana State University, Baton Rouge, LA, 70803. 177 pp.

Geyer, R. A. 1950. The occurrence of pronounced salinity variations in Louisiana coastal waters. Journal of Marine Research IX-2: 100-110.

Hart, W. E. and S. P. Murray. 1978. Energy balance and wind effects in a shallow sound. Journal of Geophysical Research 83(C8): 4097-4106.

Kjerfve, B. 1975. Tide and fair-weather effects in a bar-built Louisiana estuary. Estuarine Research, Vol II. Geology and Engineering. Academic Press, Inc. New York.

Mitsch, W J. and J. G. Gosselink. 1993. Wetlands, Second Edition. Van Nostrand Reinhold, New York. 722 pp.

Morris, J. T. 1995. The Mass Balance of Salt and Water in Intertidal Sediments: Results From North Inlet, South Carolina. Estuaries 18(4): 556-567.

Orlando, S. P. Jr., L. P. Rozas, G. H. Ward, and C. J. Klein. 1993. Salinity characteristics of Gulf of Mexico estuaries. Silver Spring, MD: National Oceanic and Atmospheric Administration, Office of Ocean Resources Conservation and Assessment. 209 pp.

SAS, 1990a. SAS procedures guide, version 6, third edition. SAS Institute, Inc., Cary, North Carolina. 705 pp.

SAS, 1990b. SAS language reference, version 6, first edition. SAS Institute, Inc., Cary, North Carolina. 1042 pp.

SAS, 1990c. SAS /STAT user's guide, release 6.03 edition. SAS Institute, Inc., Cary, North Carolina. 1028 pp.

Swenson, E. M. and R. E. Turner. 1998. Past, Present and Probable Future Salinity Variations in the Barataria Estuarine System. Final report to the Coastal Restoration Division of

the Louisiana Department of Natural Resources. Coastal Ecology Institute, Baton Rouge, LA 70803. 112 pp. with appendices.

Ward, G. H. Jr. 1980. Hydrography and Circulation Processes of Gulf Estuaries. In P. Hamilton and K. B. MacDonald. Editors. Estuaries and Wetland Processes with Emphasis on Modeling. Plenum Press, New York, NY.

Wiseman, Wm. J. Jr. 1986. Estuarine-shelf interactions. in C. N. K. Mooers, Editor. Baroclinic processes on continental shelves. Coastal and Estuarine Sciences 3, American Geophysical Union, Washington, D.C. 130 pp.

Wiseman Wm. J. Jr., E. M. Swenson, F. J. Kelley. 1990. Control of estuarine salinities by coastal ocean salinity. in R. T. Cheng, Editor. Residual Currents and Long-term Transport. Coastal and Estuarine Studies, Volume 38. Sprnger-Verlag, New York. 544 pp.

Table 1. Summary of the major and secondary freshwater sources influencing salinities in the 26 northern Gulf of Mexico estuaries presented in Figure 2. Data was taken from Orlando et. al., (1995).

State	Estuarine system	Major freshwater source	Other freshwater source
Texas	Laguna Madre	Rainfall (65%)	Local riverflow (17%)
Texas	Corpus Christie Bay	Local riverflow (92%)	Rainfall (8%)
Texas	Aransas Bay	Local riverflow (54%)	Rainfall (46%)
Texas	San Antonio Bay	Local riverflow	Rainfall
Texas	Matagorda Bay	Local riverflow (25-80%)	Rainfall
Texas	Brazos River	Local riverflow	
Texas	Galveston Bay	Local riverflow	
Texas	Sabine Lake	Local riverflow	
Louisiana	Calcasieu Lake	Local riverflow	
Louisiana	Mermentau River	Local riverflow	Atchafalaya River flow
Louisiana	Atchafalaya/Vermillion	Atchafalaya River flow	
Louisiana	Terrebonne.Timbalier	Mississippi River flow	Rainfall
Louisiana	Barataria Bay	Mississippi River flow	Rainfall
Louisiana	Breton Sound	Mississippi River flow	Pearl River flow
Louisiana	Pontchartrain/Borgne	Local riverflow (90%)	Rainfall (5%)
Mississippi	Mississippi Sound	Local riverflow	Mississippi River flow
Alabama	Mobile Bay	Local riverflow	
Florida	Perdido Bay	Local riverflow	
Florida	Pensacola Bay	Local riverflow	
Florida	Choctawhatchee Bay	Local riverflow	
Florida	St. Andrew Bay	Rainfall	
Florida	Apalachicola Bay	Local riverflow	
Florida	Apalachee Bay	Local riverflow	
Florida	Suwannee River	Local riverflow	Groundwater flow
Florida	Tampa Bay	Local riverflow	Rainfall
Florida	Sarasota Bay	Rainfall	Local riverflow

Table 2. Correlation matrix for weekly average water levels for ten stations around the Gulf of Mexico (Figure 8).

	Corpus Christie	Galveston	Sabine	Cocodrie	**Grand Isle**	Waveland	Pensacola	Panama City	St. Pete.	Naples
Port Isabel	0.948	0.921	0.756	0.752	**0.772**	0.753	0.638	0.604	0.427	0.547
Corpus Christie		0.926	0.860	0.831	**0.823**	0.797	0.663	0.609	0.412	0.510
Galveston			0.930	0.930	**0.892**	0.877	0.740	0.697	0.479	0.543
Sabine				0.941	**0.903**	0.866	0.767	0.715	0.500	0.509
Cocodrie					**0.963**	0.939	0.852	0.785	0.587	0.513
Grand Isle						**0.936**	**0.942**	**0.908**	**0.752**	**0.748**
Waveland							0.882	0.843	0.660	0.621
Pensacola								0.990	0.905	0.845
Panama City									0.934	0.880
St. Petersburg										0.947

Table 3. Ranking of observed water levels for the NOS Grand Isle station for June, 1999 through July 2000. The percentile ranking for each month is presented. The percentile ranking was computed using the observed hourly water level data from January 1955 through July, 2000. The long-term trend was removed from the data before analysis.

Month	Ranking
June, 1999	Upper 40%
July 1999	Upper 40%
August, 1999	Upper 10%
September, 1999	Lower 20%
October, 1999	Lower 30%
November, 1999	Lower 15%
December, 1999	Lower 20%
January, 2000	Lower 10%
February, 2000	Lower 10%
March, 2000	Lower 40%
April, 2000	Lower 20%
May, 2000	Lower 30%
June, 2000	Lower 20%
July, 2000	Lower 10%

Table 4. Classification matrix for the Barataria estuarine system based upon the Palmer Drought Severity Index (PDSI) and Mississippi River discharge. The matrix classifies the upper (north of Little Lake) and lower portions of the system as either a "high salinity year" a "low salinity year" or a "normal year". Values of river discharge greater than 1 standard deviation (S. D.) above the mean were considered high river discharge years, and values of river discharge less than 1 standard deviation (S. D.) below the mean were considered low river discharge years. The Palmer Drought Severity Index classifies the years into "drought" conditions. The index has a numeric value with 0 indicating normal conditions. Values equal to, or less than, -4 indicate extreme drought conditions. Values equal to, or greater than, +4 indicate extreme moist conditions. Very moist (>3) was used as an indicator of a high local runoff year, and moderate drought (<-3) as an indicator of a low local runoff year.

Palmer Drought Severity Index

	Moderate Drought Index		**Normal Drought Index**		**Very Moist Drought Index**	
	Lower Estuary	Upper Estuary	Lower Estuary	Upper Estuary	Lower Estuary	Upper Estuary
Mississippi River Discharge >1 S. D. Above Mean	Low Salinity or "Wet Year"	Low Salinity or "Wet Year"	Low Salinity or "Wet Year"	"Normal Year"	Low Salinity or "Wet Year"	High Salinity or "Dry Year"
Mississippi River Normal River Discharge	"Normal Year"	Low Salinity or "Wet Year"	"Normal Year"	"Normal Year"	"Normal Year"	High Salinity or "Dry Year"
Mississippi River Discharge <1 S. D. Below Mean	High Salinity or "Dry Year"	Low Salinity or "Wet Year"	High Salinity or "Dry Year"	"Normal Year"	High Salinity or "Dry Year"	High Salinity or "Dry Year"

Table 5. Climatic classification for the Barataria Estuarine System based upon the Palmer Drought Severity Index (PDSI) and Mississippi River discharge.

				Year Classification	
Year	Season	Drought Severity	River Flow	Upper Estuary	Lower Estuary
1980	Jan. - Jun.	moist	normal	normal	normal
1980	Jul. - Dec.	mild drought	-1 SD	normal	dry
1981	Jan. - Jun.	mild drought	-1 SD	normal	dry
1981	Jul. - Dec.	moderate drought	normal	dry	normal
1982	Jan. - Jun.	incipient drought	normal	normal	normal
1982	Jul. - Dec.	normal	+1 SD	normal	wet
1983	Jan. - Jun.	very moist	+1 SD	wet	wet
1983	Jul. - Dec.	unusual moist	normal	wet	normal
1984	Jan. - Jun.	moist	+1 SD	normal	wet
1984	Jul. - Dec.	normal	+1 SD	normal	wet
1985	Jan. - Jun.	mild drought	normal	normal	normal
1985	Jul. - Dec.	incipient drought	+1 SD	normal	wet
1986	Jan. - Jun.	mild drought	-1 SD	normal	dry
1986	Jul. - Dec.	mild drought	+1 SD	normal	wet
1987	Jan. - Jun.	moist	normal	normal	normal
1987	Jul. - Dec.	normal	-1 SD	normal	dry
1988	Jan. - Jun.	moist	normal	normal	normal
1988	Jul. - Dec.	moist	-1 SD	normal	dry
1989	Jan. - Jun.	mild drought	+1 SD	normal	wet
1989	Jul. - Dec.	normal	normal	normal	normal
1990	Jan. - Jun.	incipient moist	+1 SD	normal	wet
1990	Jul. - Dec.	moderate drought	normal	dry	normal
1991	Jan. - Jun.	extreme moist	+1 SD	wet	wet
1991	Jul. - Dec.	extreme moist	normal	wet	normal
1992	Jan. - Jun.	extreme moist	-1 SD	wet	dry
1992	Jul. - Dec.	very moist	+1 SD	wet	wet
1993	Jan. - Jun.	extreme moist	+1 SD	wet	wet
1993	Jul. - Dec.	normal	+1 SD	normal	wet
1994	Jan. - Jun.	incipient drought	+1 SD	normal	wet
1994	Jul. - Dec.	incipient moist	normal	normal	normal
1995	Jan. - Jun.	normal	normal	normal	normal
1995	Jul. - Dec.	incipient drought	normal	normal	normal
1996	Jan. - Jun.	mild drought	normal	normal	normal
1996	Jul. - Dec.	normal	+ 1 SD	normal	wet
1997	Jan. - Jun.	incipient moist	+ 1 SD	normal	wet
1997	Jul. - Dec.	normal	normal	normal	normal
1998	Jan. - Jun.	moist	+1 SD	normal	wet
1998	Jul. - Dec.	incipient drought	+1 SD	normal	wet
1999	Jan. - Jun.	moderate drought	normal	normal	normal
1999	Jul. - Dec.	mild drought	-1 SD	normal	dry
2000	Jan. - Jun.	severe drought	-1 SD	dry	dry
2000	Jul. - Dec.	extreme drought	-1 SD	dry	dry
2001	Jan. – Jun	mild drought	normal	normal	normal
2001	Jul. - Dec.	very moist	normal	wet	normal
2002	Jan. – Jun	mild drought	+1 SD	normal	wet
2002	Jul. - Dec.	moist	normal	normal	normal

Table 6. Consecutive number of months that the monthly mean salinity equals (or exceeds) the listed salinity level for LDWF salinity stations in the Barataria system. The monthly means were calculated using hourly observations. The year classes are 24 month classes (1965-1966 - January, 1965 through December, 1966). The symbol indicates no data.

Year Class	Grand Terre >= 30 ppt	St. Mary's' Point >= 20 ppt	Little Lake >= 7.5 ppt
1965-1966	1	nd	nd
1967-1968	5	nd	nd
1969-1970	4	nd	nd
1971-1972	4	nd	nd
1973-1974	3	0	nd
1975-1976	5	3	nd
1977-1978	4	2	nd
1979-1980	0	2	nd
1981-1982	5	2	nd
1983-1984	2	1	nd
1985-1986	3	2	nd
1987-1988	4	3	0
1989-1990	4	1	1
1991-1992	2	1	2
1993-1994	2	0	0
1995-1996	4	1	2
1997-1998	4	2	2
1999-2000	12	10	8
Mean	3.9	2.3	2.1
Standard Deviation	2.8	2.5	2.7

Table 7. Summary of regression results to predict salinity in the Barataria system using Mississippi River discharge, Precipitation at Louisiana climate region 9, and de-trended coastal water levels.

LDWF S315: Grand Terre

Overall Model R-square = 0.72
Linear portion R-square = 0.48

Variable	Estimate	F-value	Probability > F
Intercept	19.99		
Mississippi Discharge	-0.00029	544.38	0.0001
Region 9 Precipitation	-0.2761	99.56	0.0001
Grand Isle Water Level	-0.0329	83.50	0.0001
1 month previous salinity	+0.5466	354.00	0.0001

LDWF S317: St. Mary's' Point

Overall Model R-square = 0.74
Linear portion R-square = 0.41

Variable	Estimate	F-value	Probability > F
Intercept	9.66		
Mississippi Discharge	-0.00024	277.17	0.0001
Region 9 Precipitation	-0.3806	88.96	0.0001
Grand Isle Water Level	-0.0065	22.74	0.0001
1 month previous salinity	+0.6297	330.94	0.0001

LDWF S326: Little Lake

Overall Model R-square = 0.63
Linear portion R-square = 0.16

Variable	Estimate	F-value	Probability > F
Intercept	2.916		
Mississippi Discharge	-0.00007	47.25	0.0001
Region 9 Precipitation	-0.1522	11.55	0.0009
Previous month salinity	+0.8728	145.63	0.0001
2 months previous salinity	-0.4220	7.37	0.0075
3 months previous salinity	+0.2511	6.96	0.0094

Table 8. Summary of Gulf of Mexico salinity forcing functions over the time period from 1950 though 2002. The years and magnitudes of the major drought or wet periods are listed along with the Mississippi River discharge classification (low, average, high) and the coastal water levels (low, average, high). The years in bold red represent the most severe gulfwide drought years over the time period from 1950 – 2002.

Years	Drought Index	Mississippi River Discharge	Coastal Water Levels
1951 – 1953	TX-LA: moderate drought MS-FL: normal to moderate drought	average	
1954 – 1957	TX: moderate to severe drought LA-MS: normal to moderate drought FL: moderate to severe drought	54 low 55-57 average	
1958 – 1962	TX-FL: normal to wet	58-60 average 61-62 high	
1963 – 1964	TX-AL: moderate to severe drought Florida: normal	average – low	
1965 – 1980	Normal throughout the gulf some short duration wet and dry	73, 79 high 67, 76, 77 low remainder average	
1981 – 1982	TX: wet LA-FL: moderate drought	83 high	
1983 – 1984	TX: normal LA – FL: wet	high	
1984 – 1989	Normal throughout the gulf some short duration wet and dry	normal	
1990	TX and FL: moderate drought LA - AL: wet	high	
1991 – 1993	FL: normal to wet TX – AL: wet	91 low 92-93 average	
1994 – 1998	Normal to wet throughout the gulf	average	
1998 – 2000	Moderate to severe drought entire gulf	low	
2001 - 2002	Mild to wet entire gulf	average-high	

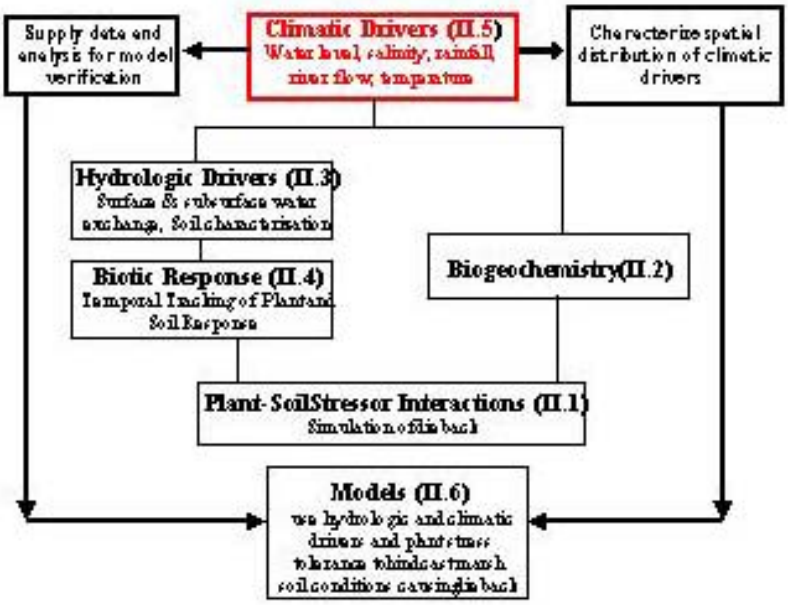

Figure 1. Diagram illustrating the connections among the various Sub-tasks on the overall causes Task for the Brown Marsh studies. The contributions of this specific Task (Task II.5) are shown in bold.

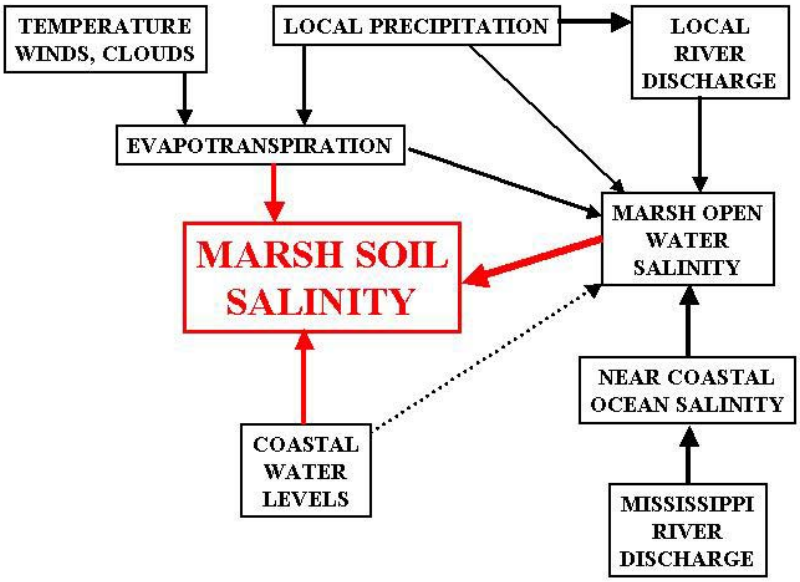

Figure 2. Conceptual model detailing the role of the major environmental forcing functions in controlling open water salinity and marsh soil salinity.

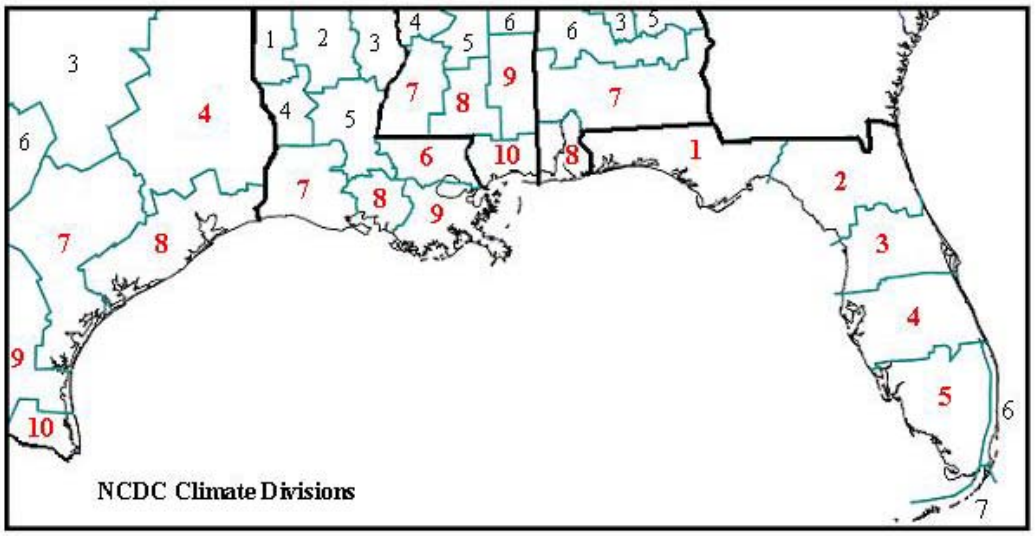

Figure 3. NCDC Climate Divisions for the states around the Gulf of Mexico. Monthly summary data from the sites numbered in red was used for this study.

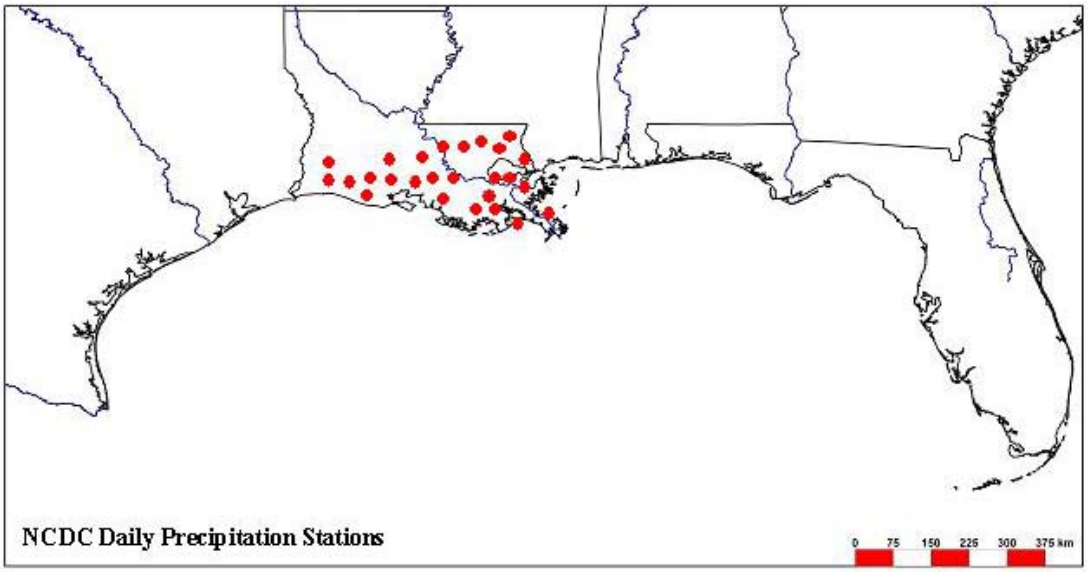

Figure 4. Map showing the climate stations from which daily data was obtained.

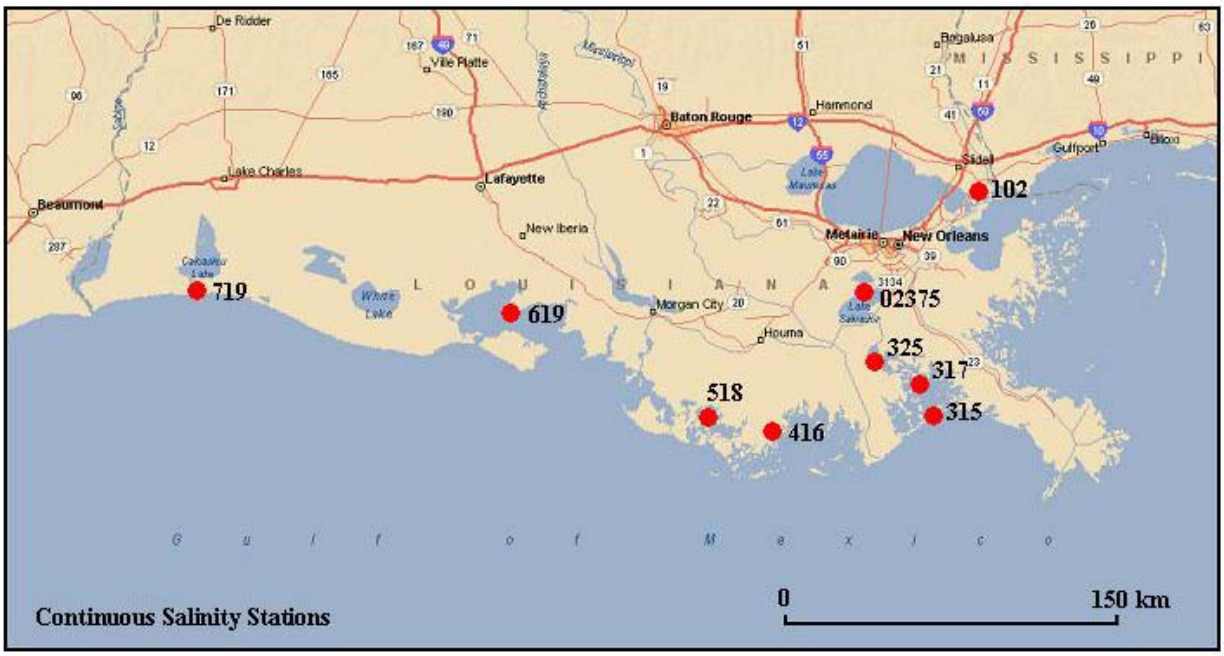

Figure 5. Map showing the LDWF-USGS continuous salinity stations.

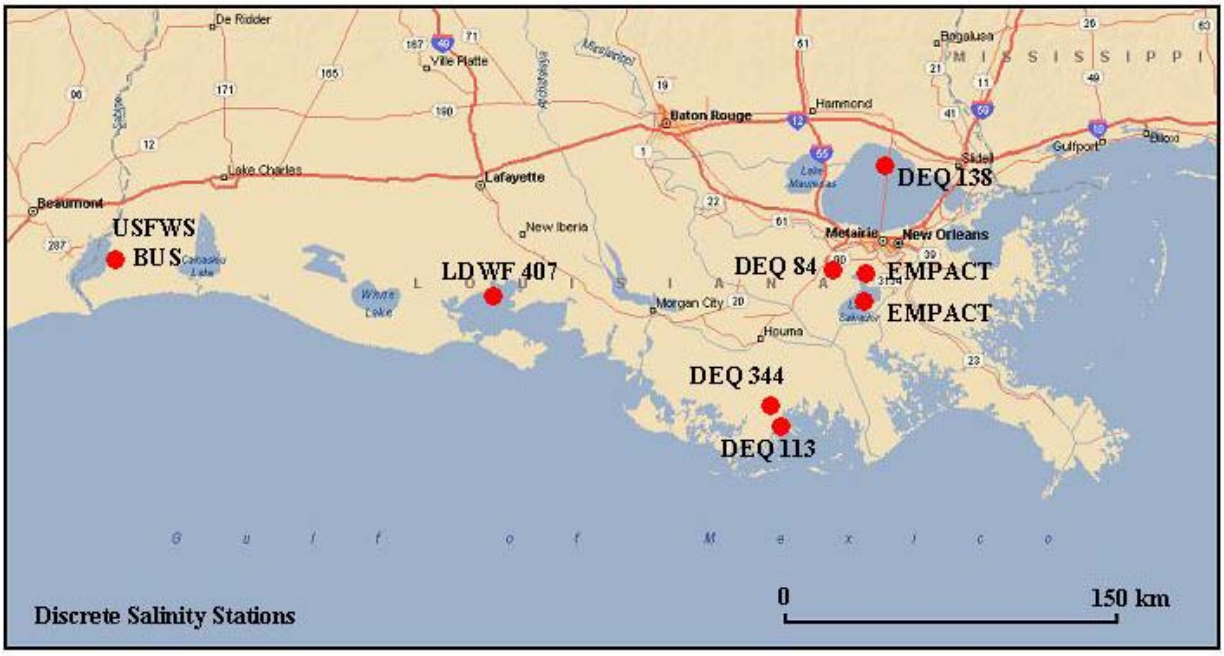

Figure 6. Map showing discrete salinity stations.

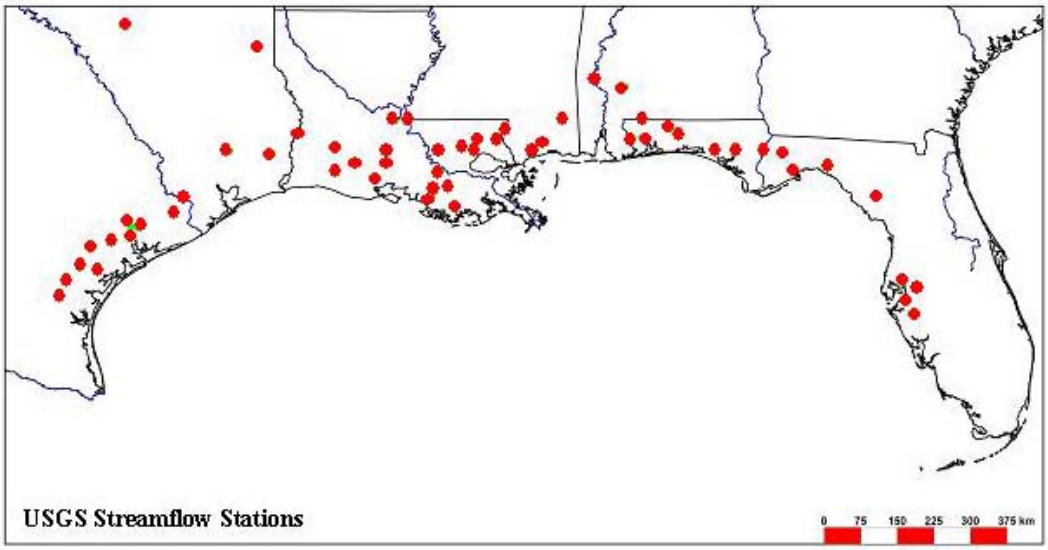

Figure 7. Map showing the USCE and USGS stream discharge stations.

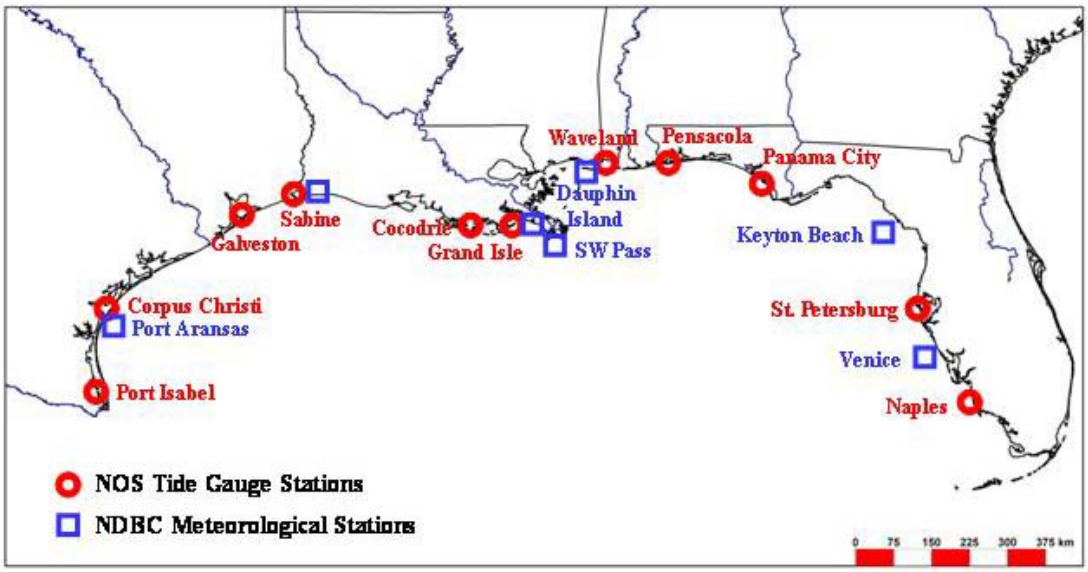

Figure 8. Map of the Gulf of Mexico showing the National Ocean Survey (NOS) stations and the National Data Buoy Center (NDBC) stations from which hourly water level and meteorological observations were obtained

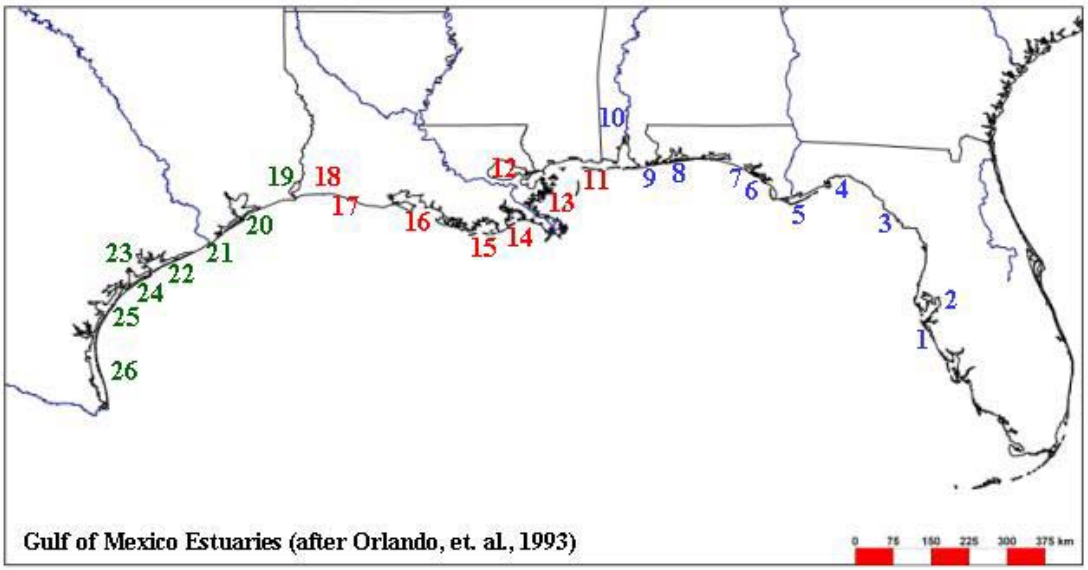

Western Gulf

19. Sabine Lake
20. Galveston Bay
21. Brazos River
22. Matagorda Bay
23. San Antonio Bay
24. Aransas Bay
25. Corpus Christi Bay
26. Laguna Madre

Central Gulf

11. Mississippi Sound
12. Pontchartrain/Borgne and Chandeleur Sound
13. Breton Sound
14. Barataria Bay
15. Terrebonne-Timbalier Bays
16. Atchafalaya/Vermillion Bays
17. Mermentau River
18. Calcasieu Lake

Eastern Gulf

1. Sarasota Bay
2. Tampa Bay
3. Suwanee River
4. Apalachee Bay
5. Apalachicola Bay
6. St. Andrew Bay
7. Choctawhatchee Bay
8. Pensacola Bay
9. Perdido Bay
10. Mobile Bay

Figure 9. Map of the Gulf of Mexico showing the estuaries characterized by Orlando, et. al., (1993).

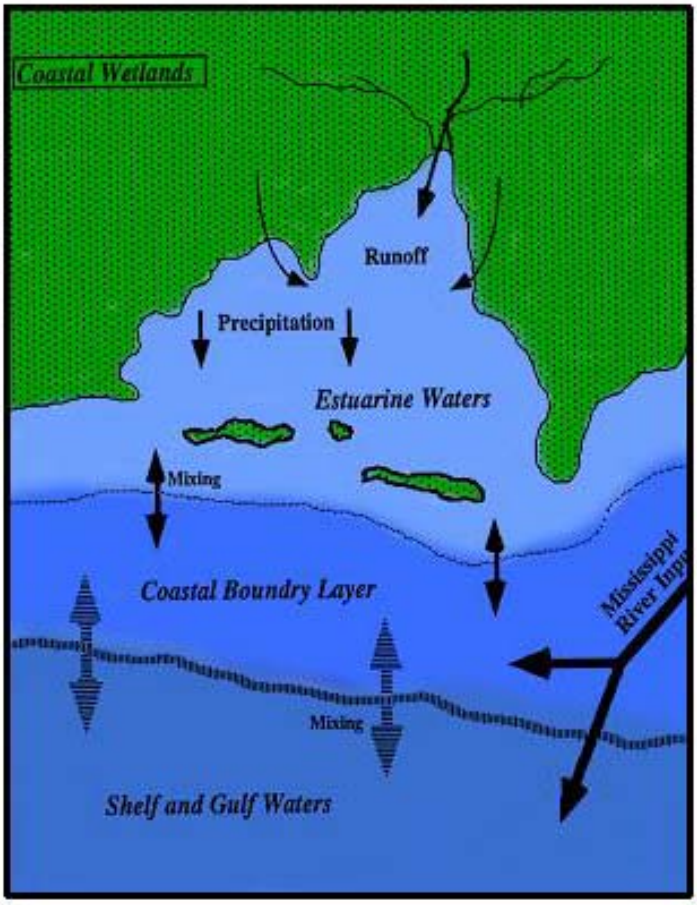

Figure 10. Schematic of an estuarine system illustrating the major pathways of fresh water and coastal ocean water inputs to the system.

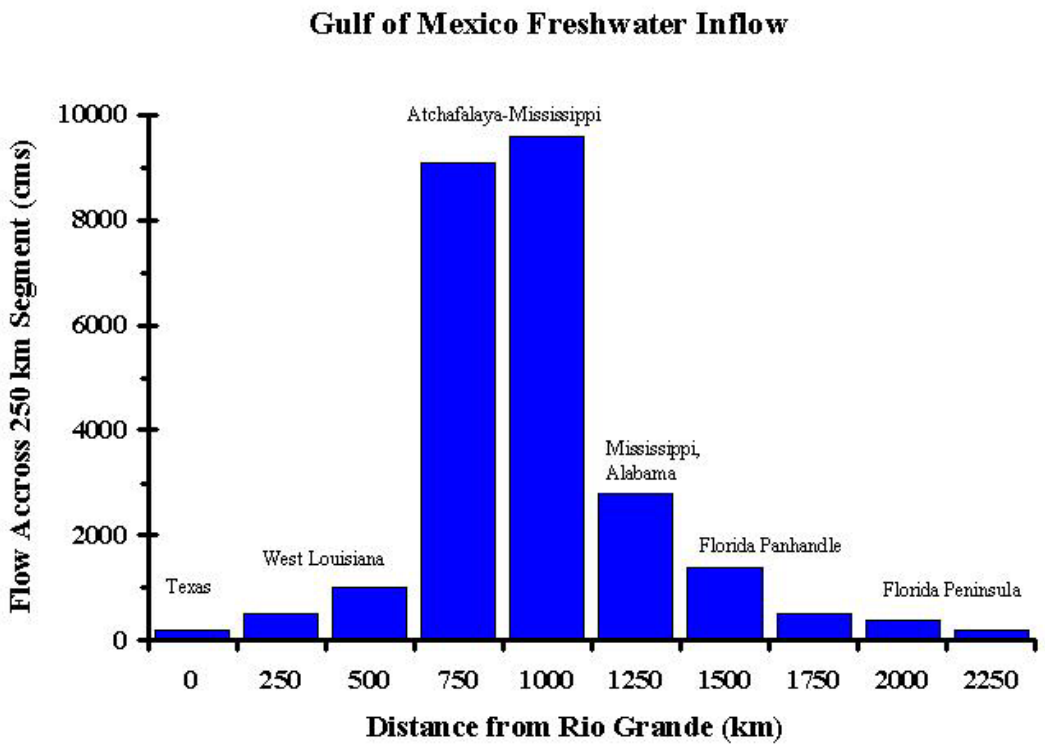

Figure 11. Distribution of river input into the Northern Gulf of Mexico. Modified from Orlando et. al., (1993).

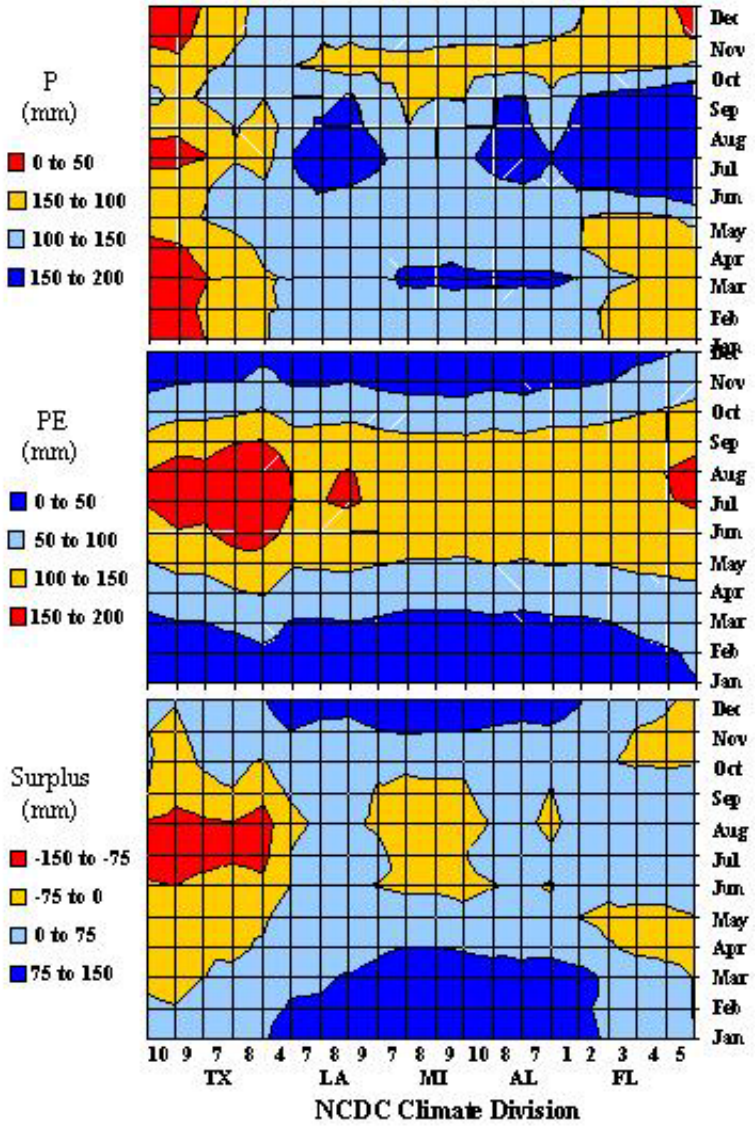

Figure 12. Monthly average patterns of (top to bottom) precipitation, potential evapotranspiration, and surplus for the NCDC Climatic Divisions (Figure 3) around the Gulf of Mexico. The values are the monthly means from 1950 through 2002. The data is from the National Climatic Data Center (NCDC).

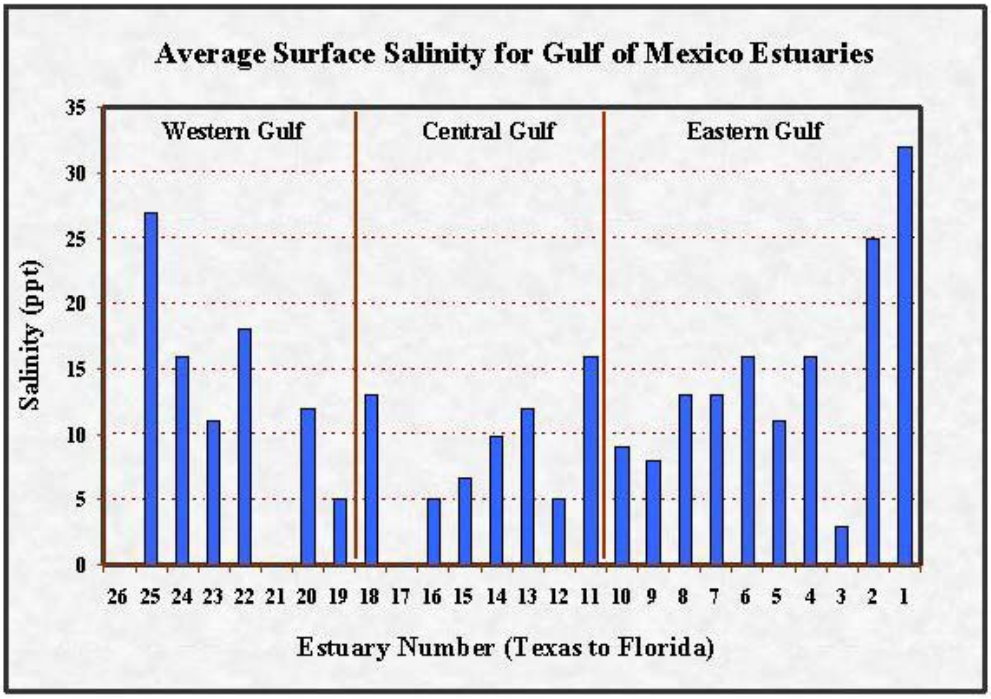

Figure 13. Distribution of surface salinity for 26 estuaries around the Gulf of Mexico. Data is from Orlando et. al., (1993), and updated as part of this study.

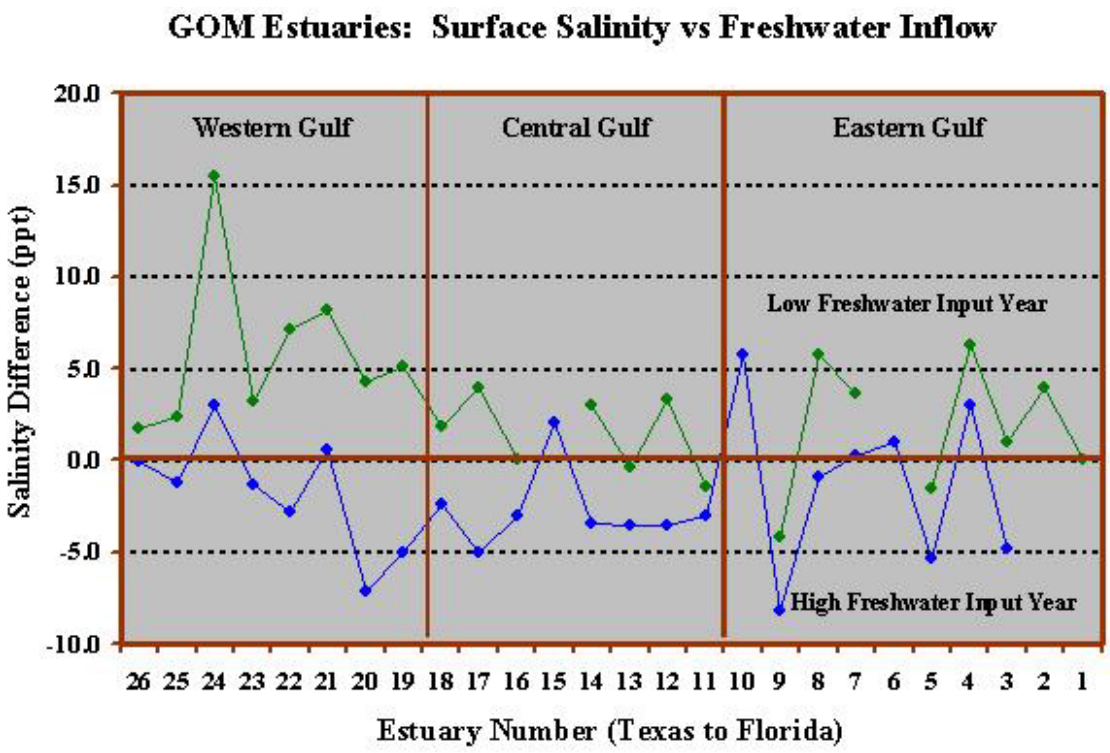

Figure 14. Changes in surface salinity (in ppt) for 26 estuaries around the Gulf of Mexico resulting from either a high freshwater input year (filled circles) or a low freshwater input year (open circles). Data are from Orlando et. al., (1993), and updated as part of this study.

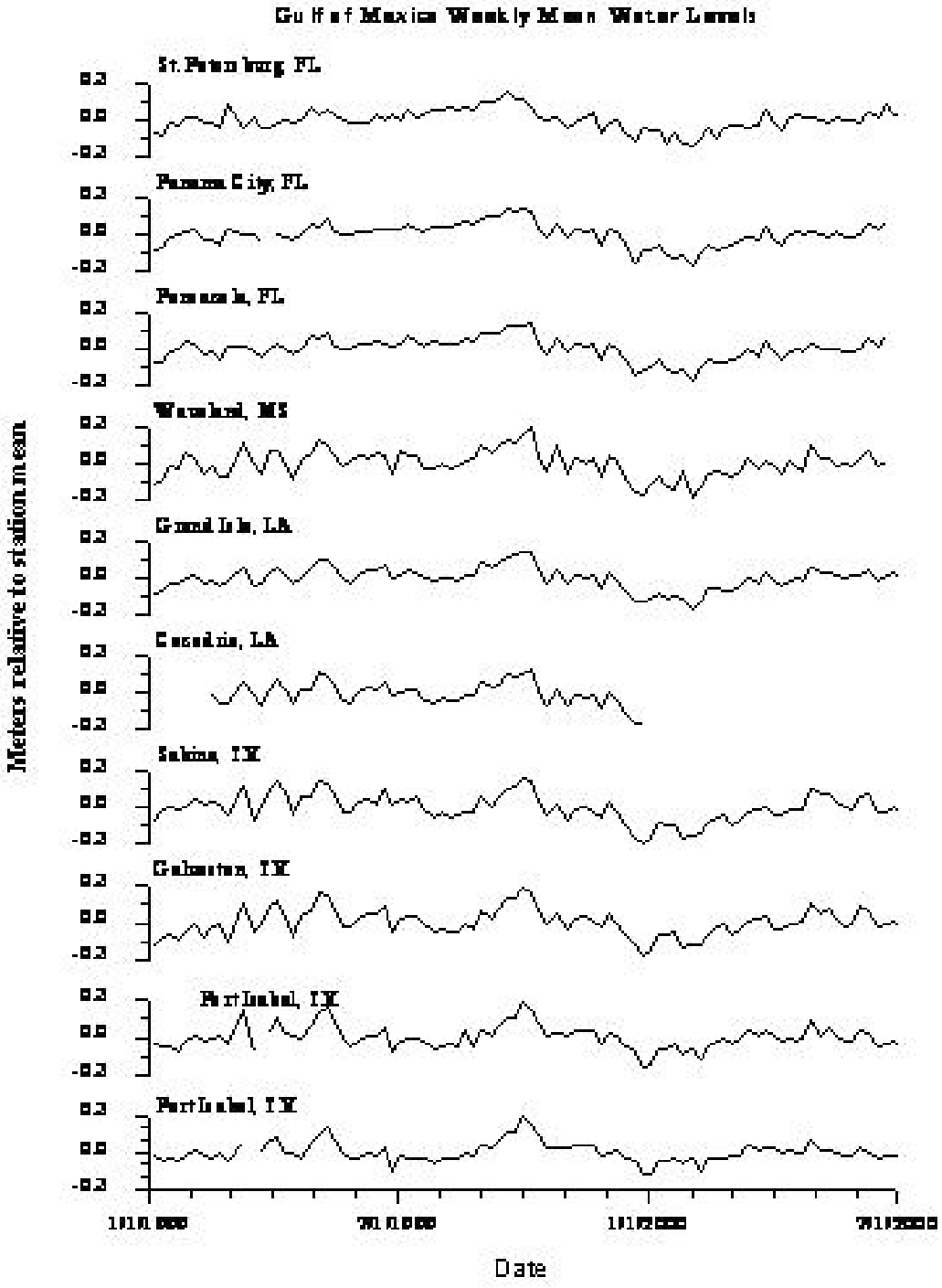

Figure 15. Plot of weekly average water levels for stations around the Gulf of Mexico (Figure 8). The values are in meters above or below the series mean. Hourly data from the National Oceanic Survey (NOS) was used in this analysis..

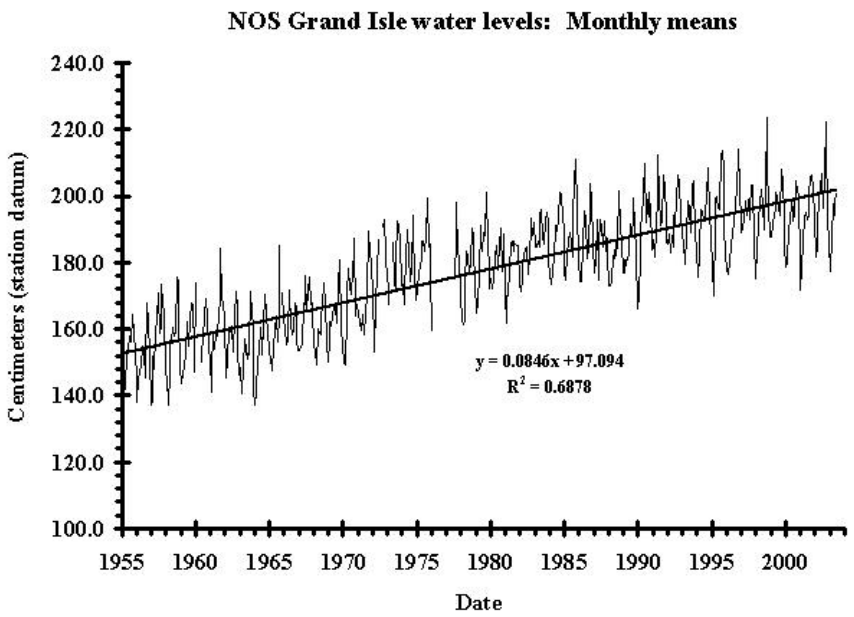

Figure 16. Plot of monthly mean water levels for Grand Isle, Louisiana, in centimeters relative to the station datum. The results of a linear regression using water level as the dependent variable and time as the independent variable are indicated. Hourly data from the National Oceanic Survey (NOS) was used in this analysis..

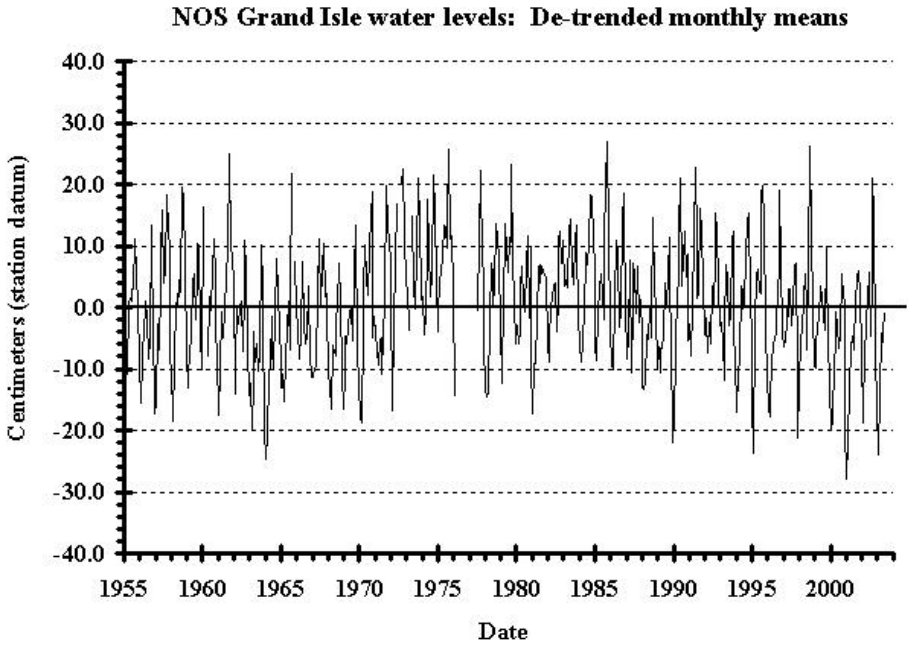

Figure 17. Plot of de-trended monthly mean water levels for Grand Isle, Louisiana, in centimeters relative to the station datum. The data were de-trended by removing the long term trend determined from linear regression analysis. Hourly data from the National Oceanic Survey (NOS) was used in this analysis.

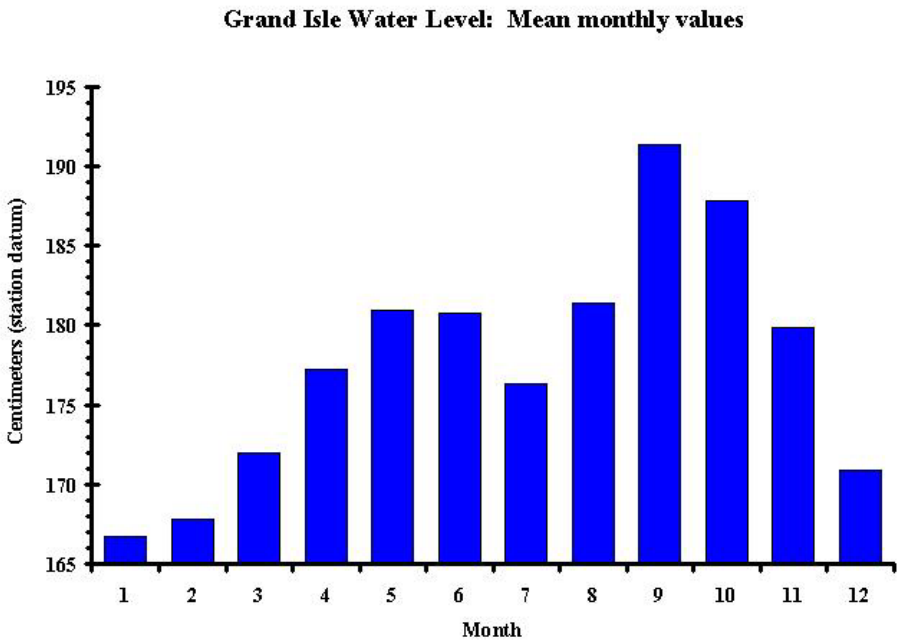

Figure 18. Plot of mean monthly water level at Grand Isle. Hourly data from the National Oceanic Survey (NOS) was used in this analysis.

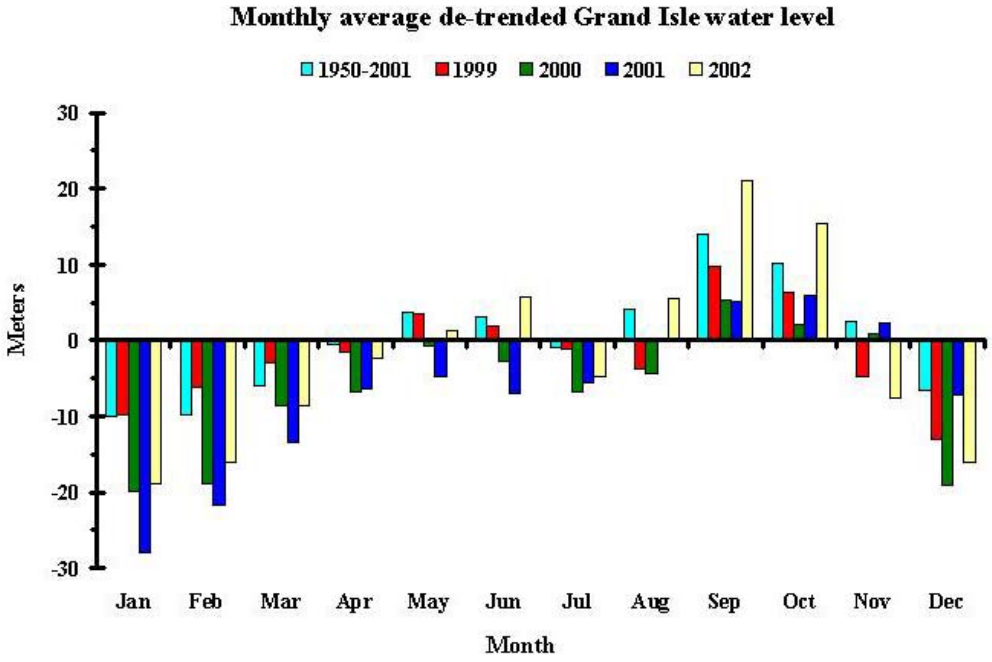

Figure 19. Plot of long-term (1955-2002) average monthly water level at Grand Terre (light blue) versus average monthly water levels for 1999 (red), 2000 (green), 2001 (dark blue), and 2002 (beige). Hourly data from the National Oceanic Survey (NOS) was used in this analysis.

Minimum Maximum

State	Estuary	Station	Station Name	Dates	J	F	M	A	M	J	J	A	S	O	N	D
TX	Laguna Madre	8211900	San Fernando Canal	1943-2000												
TX	Corpus Christi Bay	8211000	Nueces River	1939-2000												
TX	Aransas Bay	8189500	Mission River	1939-2000												
TX	Aransas Bay	8189700	Aransas River	1944-2000												
TX	San Antonio Bay	8188500	San Antonio River	1924-2000												
TX	San Antonio Bay	8174500	Guadalupe River	1934-2000												
TX	Matagorda Bay	8164500	Navidad River	1939-2000												
TX	Matagorda Bay	8164000	Lavaca River	1938-2000												
TX	Galveston Bay	8117500	San Bernard River	1934-2000												
TX	Galveston Bay	8114000	Brazos River	1903-2000												
TX	Galveston Bay	8066500	Trinity River 1	1924-2000												
TX	Galveston Bay	8057000	Trinity River 2	1902-2000												
TX	Sabine	8041000	Neches River	1904-2000												
TX	Sabine	8028500	Sabine River 1	1923-2000												
TX	Sabine	8022040	Sabine River 2	1938-2000												
LA	Calcasieu	8015500	Calcasieu River	1922-2000												
LA	Mermentau	8012470	Bayou Lacassine	1968-2000												
LA	Vermillion	7384980	Vermillion River 1	1978-2000												
LA	Vermillion	7384880	Vermillion River 2	1967-2000												
LA	Vermillion	7385500	Bayou Tache	1949-2000												
LA	Atchafalaya	3045	Atchafalaya River	1953-2000												
LA	Barataria	1100	Mississippi River	1953-2000												
LA	Barataria	7381000	Amite River	1938-2000												
LA	Pontchartrain Bayou	7376500	Natalbany River	1943-2000												
LA	Pontchartrain Bayou	7375500	Tangipahoa River	1938-2000												
LA	Pontchartrain Bayou	7375000	Tchefuncta River	1943-2000												
LA	Pontchartrain Bayou	2489500	Pearl River	1938-2000												
LA	Pontchartrain Bayou	2492000	Bogue Chitto Canal	1957-2000												
MS	Mississippi Sound	2479000	Pascagoula River	1930-2000												
MS	Mississippi Sound	2481510	Wolf River	1971-2000												
MS	Mississippi Sound	2481000	Biloxi River	1932-2000												
AL	Mobile Bay	2428400	Alabama River	1973-2000												
AL	Mobile Bay	2469761	Tombigbee River	1940-2000												
FL	Perdido Bay	2376000	Perdido River	1941-2000												
FL	Pensacola Bay	2375500	Escambia River 1	1934-2000												
FL	Pensacola Bay	2374033	Escambia River 2	1988-2000												
FL	Pensacola Bay	2370000	Blackwater River	1930-2000												
FL	Pensacola Bay	2368000	Yellow River	1938-1998												
FL	Choctawhatchee Bay	2366500	Choctawhatchee River	1930-2000												
FL	St. Andrews Bay	2359500	Econfina Canal	1953-2000												
FL	Apalachicola Bay	2358700	Apalachicola River	1957-2000												
FL	Apalachee Bay	2330000	Ochlockonee River	1926-2000												
FL	Apalachee Bay	2327100	Sopchoppy River	1944-2000												
FL	Apalachee Bay	2326000	Econfina River	1930-2000												
FL	Suwanee River	2323500	Suwanee River	1930-2000												
FL	Tampa Bay	2304500	Hillsborough River	1938-2000												
FL	Tampa Bay	2300500	Little Manatee River	1939-2000												
FL	Tampa Bay	2301500	Alafia River	1932-2000												
FL	Tampa Bay	2299950	Manatee River	1966-2000												

Figure 20. Monthly changes in freshwater input for rivers around the Gulf of Mexico (Figure 7.) Indicated, for each river, are the months during which high (blue) and low (red) freshwater input occur.

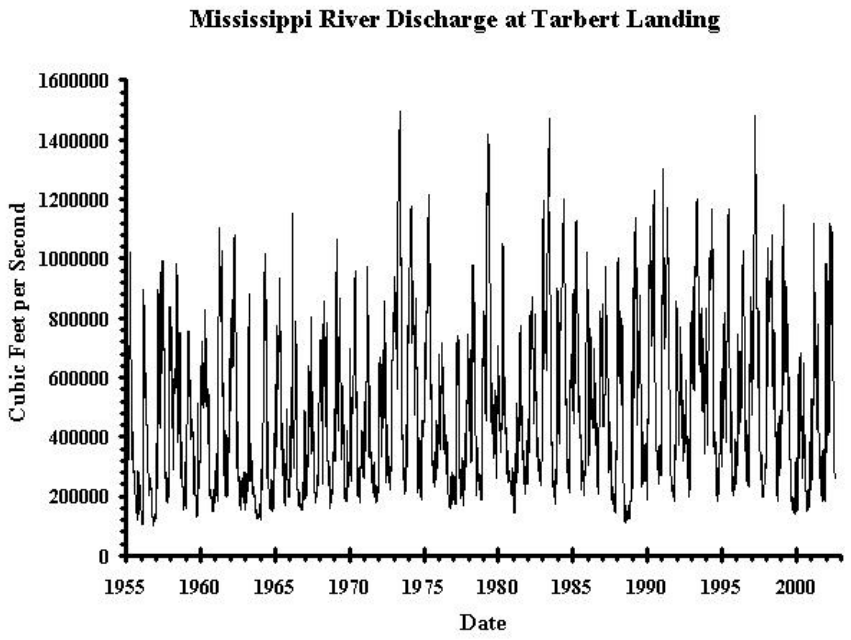

Figure 21. Time series plot of monthly mean Mississippi River discharge at Tarberts Landing. The monthly totals were computed from daily discharge from the United States Army Corps. of Engineers.

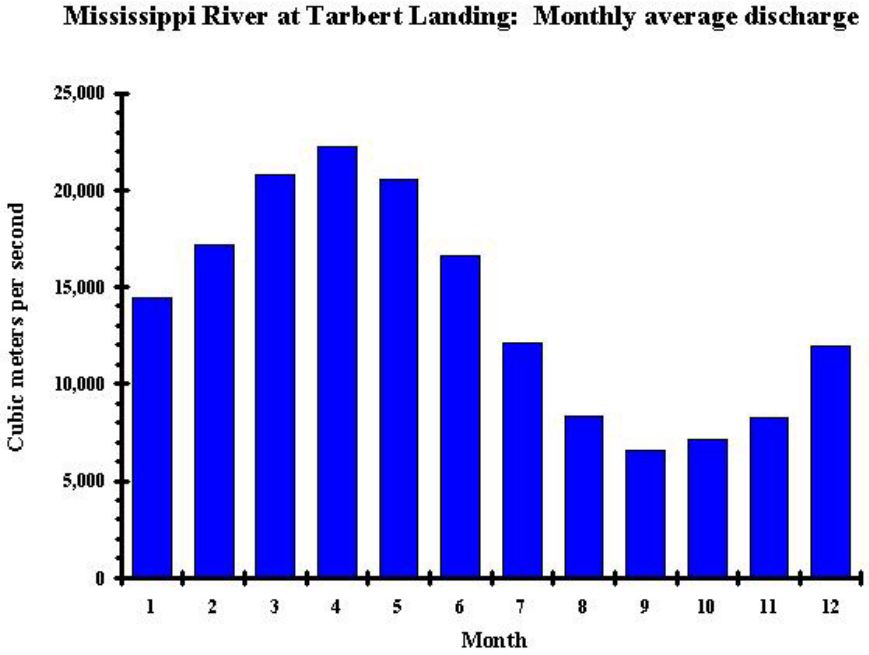

Figure 22. Plot of mean monthly Mississippi River discharge at Tarberts Landing. The mean monthly values were computed from daily discharge from the United States Army Corps. of Engineers.

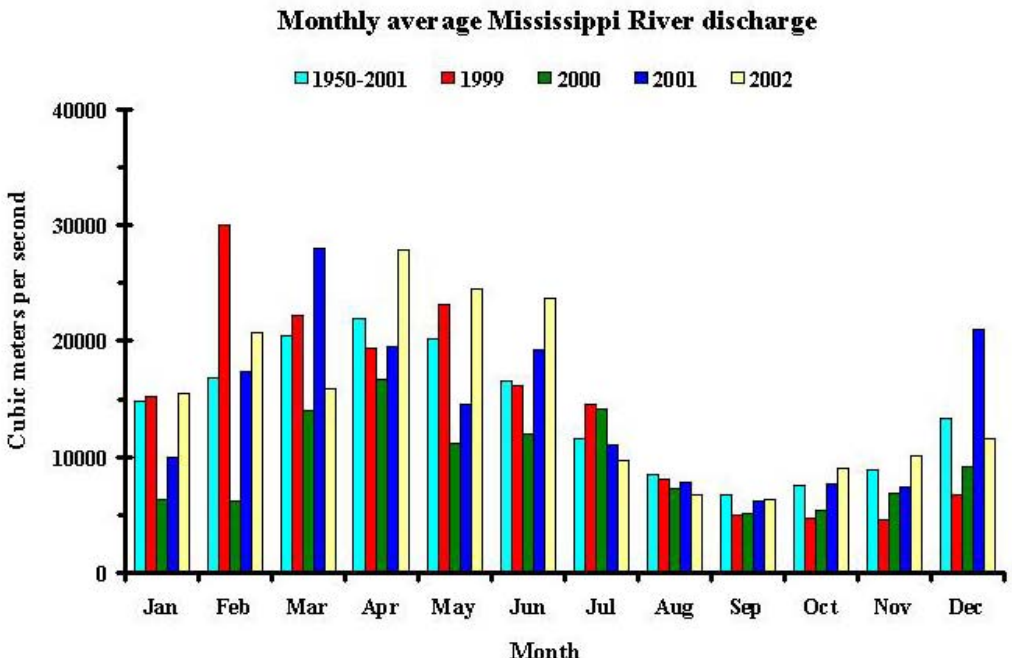

Figure 23. Plot of long-term (1955-2002) average monthly Mississippi River discharge (light blue) versus average monthly discharge for 1999 (red), 2000 (green), 2001 (dark blue), and 2002 (beige). Daily data from the U. S. Army Corps of Engineers (USCE) was used in this analysis.

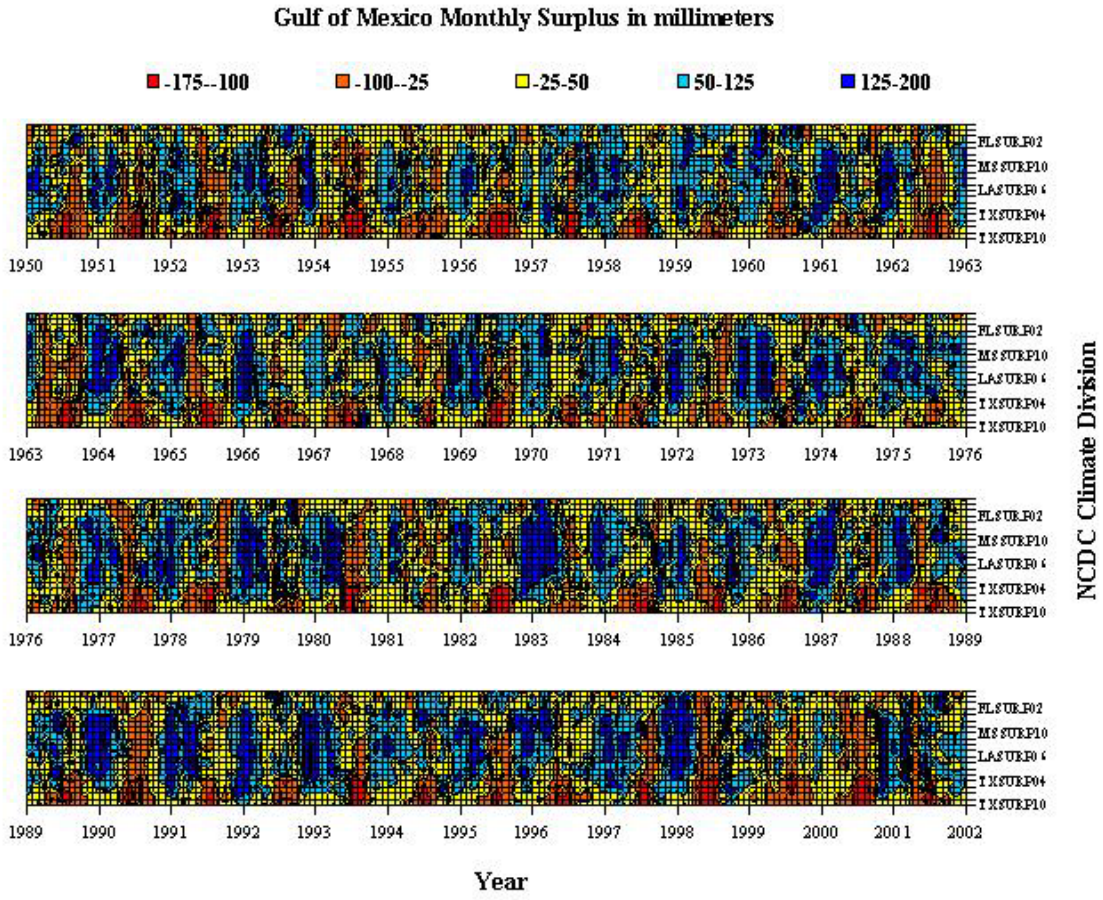

Figure 24. Contour plot of monthly surplus (rainfall-evapotranspiration), in millimeters, for the NCDC Climate divisions around the Gulf of Mexico. The horizontal axis is time and the vertical axis is the climate division arranged from Texas (bottom of each panel) to Florida (top of each panel). Blue values indicate wet conditions and red values indicate dry conditions.

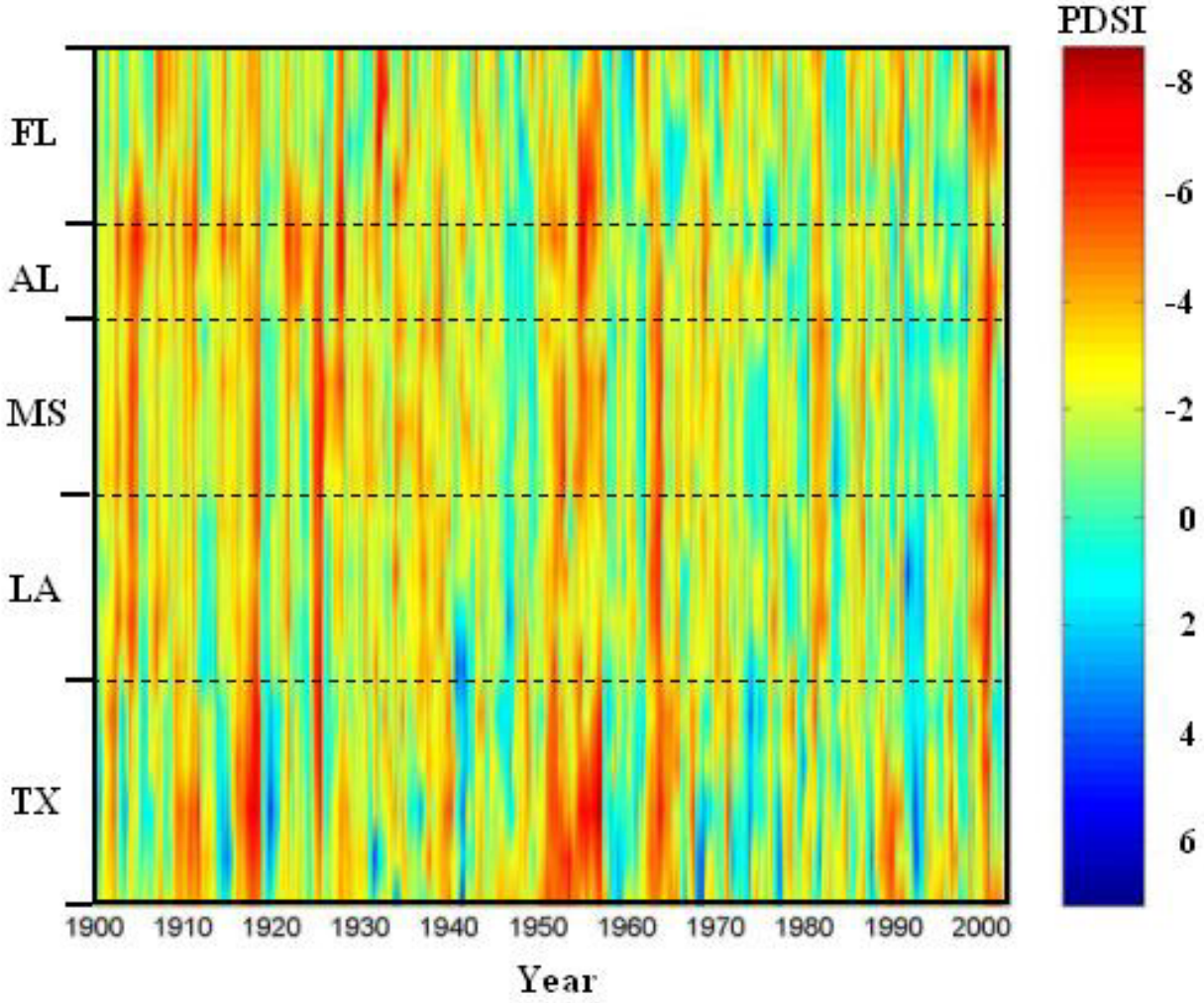

Figure 25. Contour plot of monthly Palmer Drought Severity Index for the NCDC Climate divisions around the Gulf of Mexico. The horizontal axis is time and the vertical axis is the climate division arranged from Texas (bottom) to Florida (top). Blue values indicate wet conditions and red values indicate dry conditions.

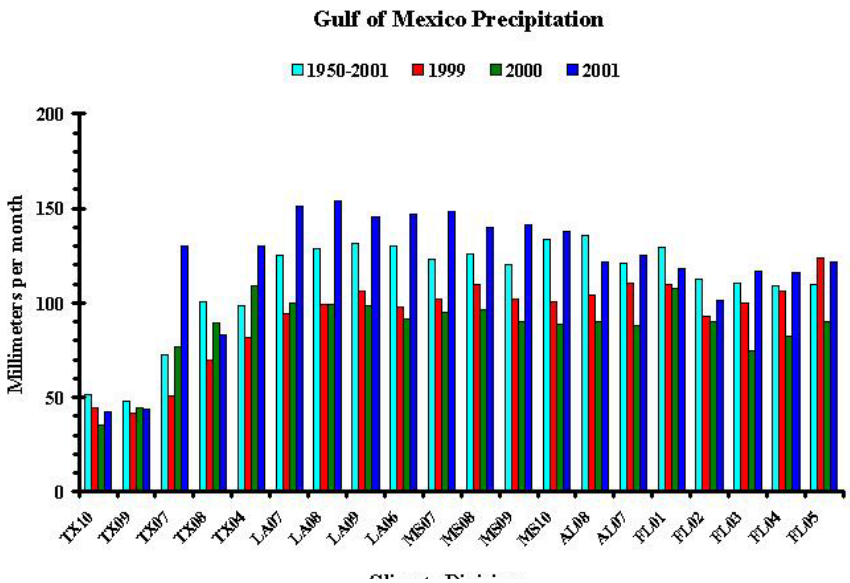

Figure 26. Plot of long-term (1955-2002) monthly total precipitation (light blue) versus monthly total precipitation for 1999 (red), 2000 (green), 2001 (dark blue), and 2002 (beige). Monthly climate division data from the National Climatic Data Center was used for this analysis.

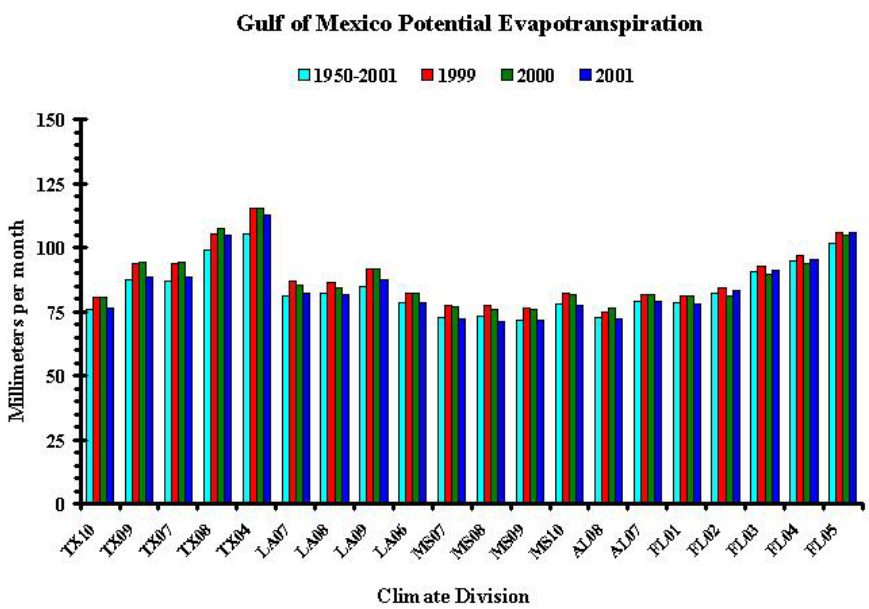

Figure 27. Plot of long-term (1955-2002) monthly total evapotranspiration (light blue) versus monthly total evapotranspiration for 1999 (red), 2000 (green), 2001 (dark blue), and 2002 (beige). Monthly climate division data from the National Climatic Data Center was used for this analysis.

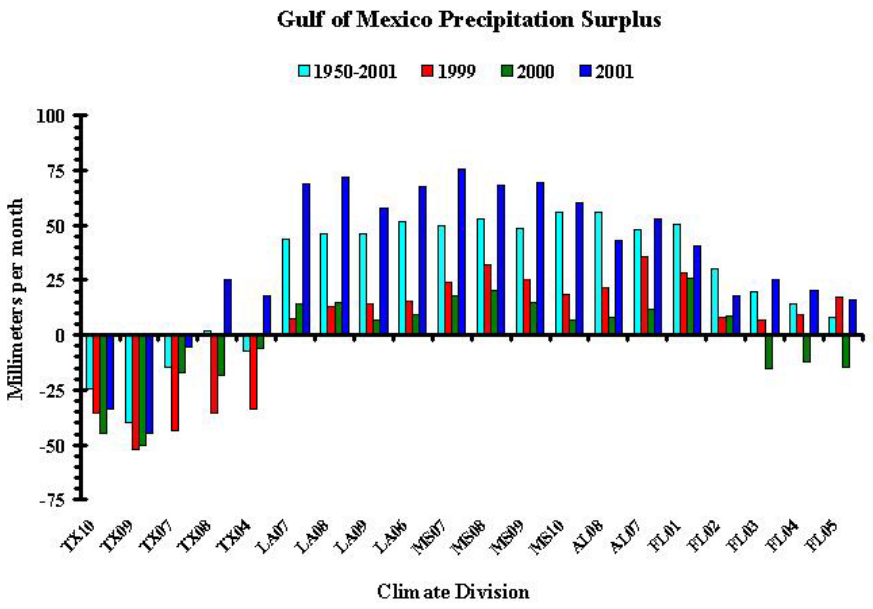

Figure 28. Plot of long-term (1955-2002) monthly total surplus (light blue) versus monthly total surplus for 1999 (red), 2000 (green), 2001 (dark blue), and 2002 (beige). Monthly climate division data from the National Climatic Data Center was used for this analysis.

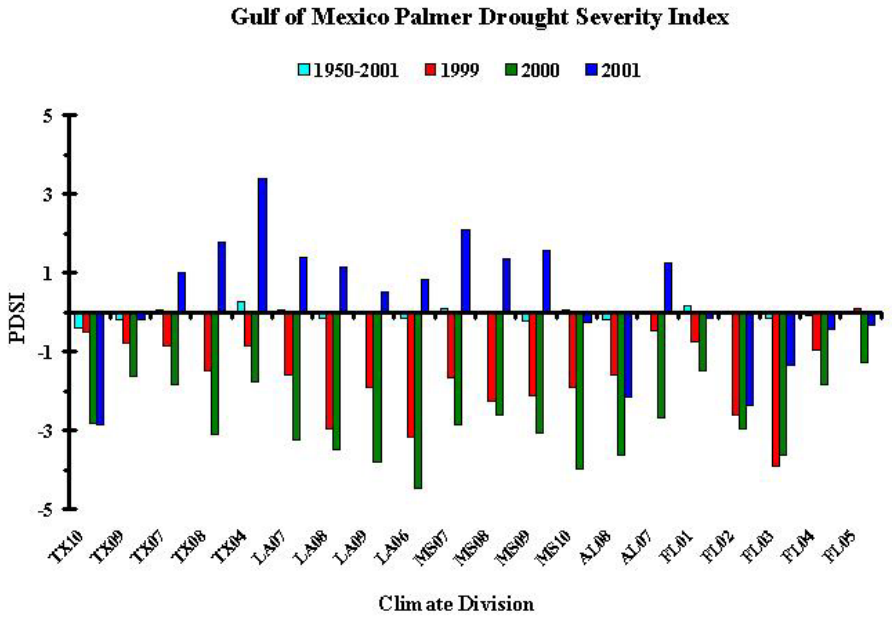

Figure 29. Plot of long-term (1955-2002) monthly Palmer Drought Severity Index (light blue) versus monthly Palmer Drought Severity Index for 1999 (red), 2000 (green), 2001 (dark blue), and 2002 (beige). Monthly climate division data from the National Climatic Data Center was used for this analysis.

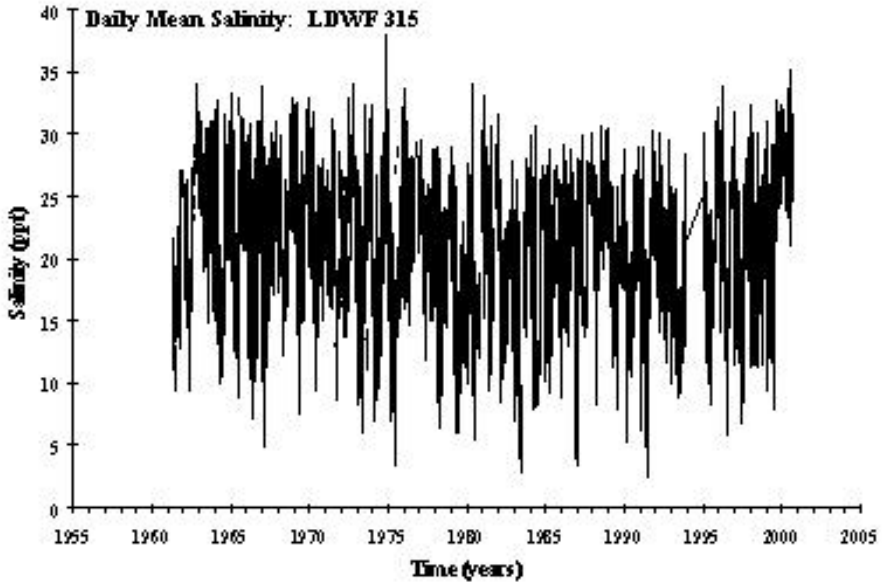

Figure 30. Time series plot of daily mean salinity from the Louisiana Department of Wildlife and Fisheries continuous monitoring station at Grand Terre, Louisiana (Station 315). Hourly data was used for this analysis.

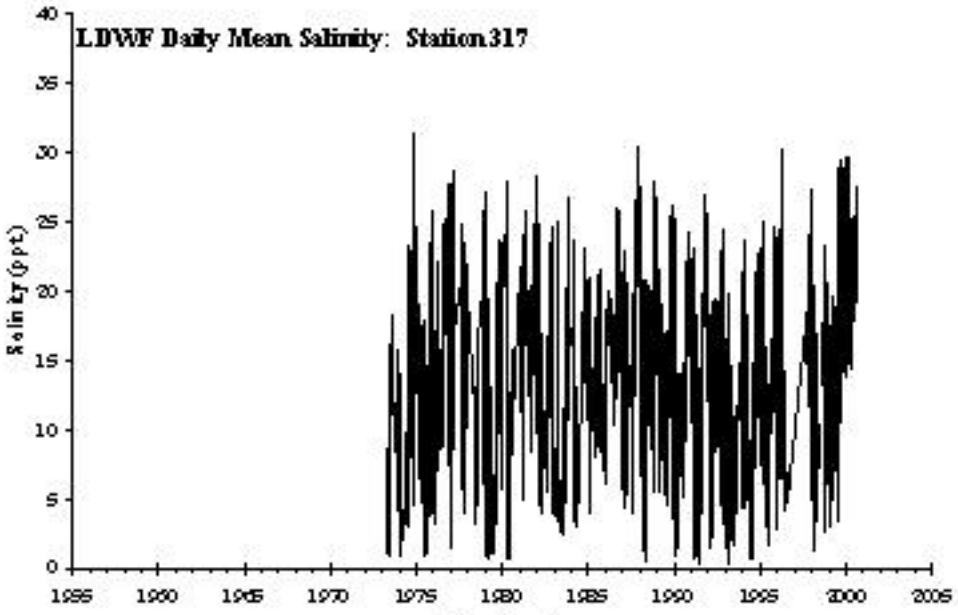

Figure 31. Time series plot of daily mean salinity from the Louisiana Department of Wildlife and Fisheries continuous monitoring station at St. Mary's Point, Louisiana (Station 317). Hourly data was used for this analysis.

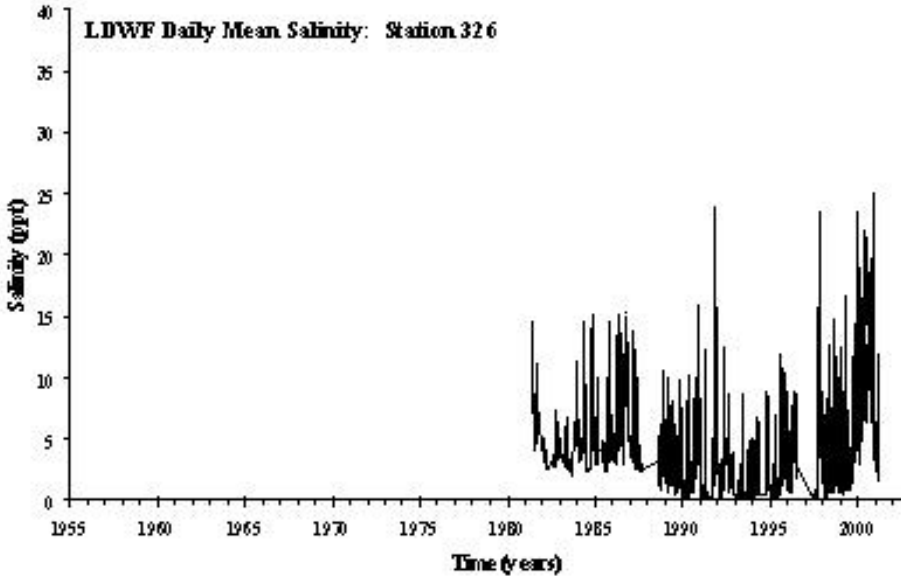

Figure 32. Time series plot of daily mean salinity from the Louisiana Department of Wildlife and Fisheries continuous monitoring station in Little Lake, Louisiana (Station 326). Hourly data was used for this analysis.

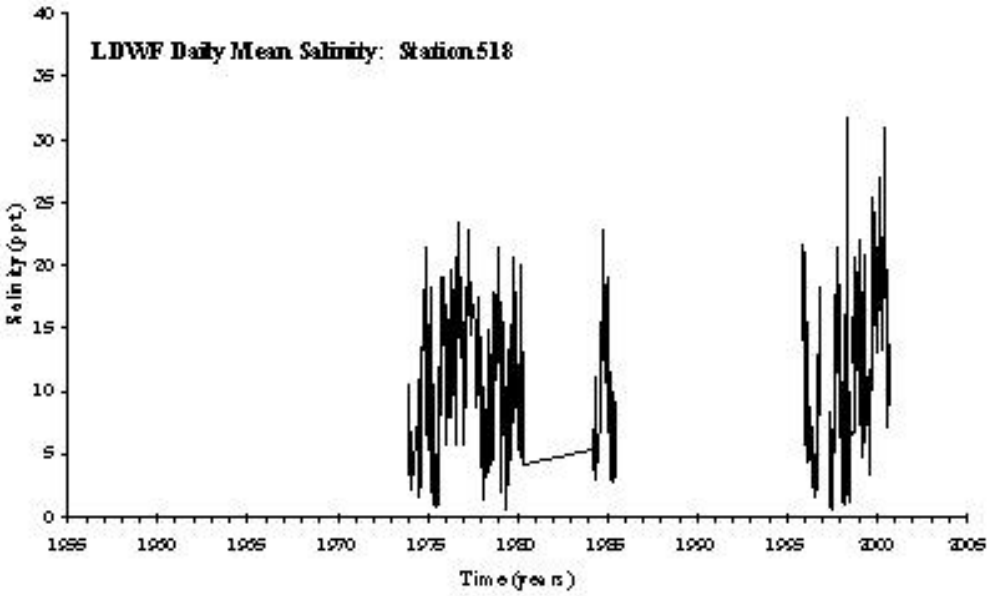

Figure 33. Time series plot of daily mean salinity from the Louisiana Department of Wildlife and Fisheries continuous monitoring station in Caillou lake, Louisiana (Station 518). Hourly data was used for this analysis.

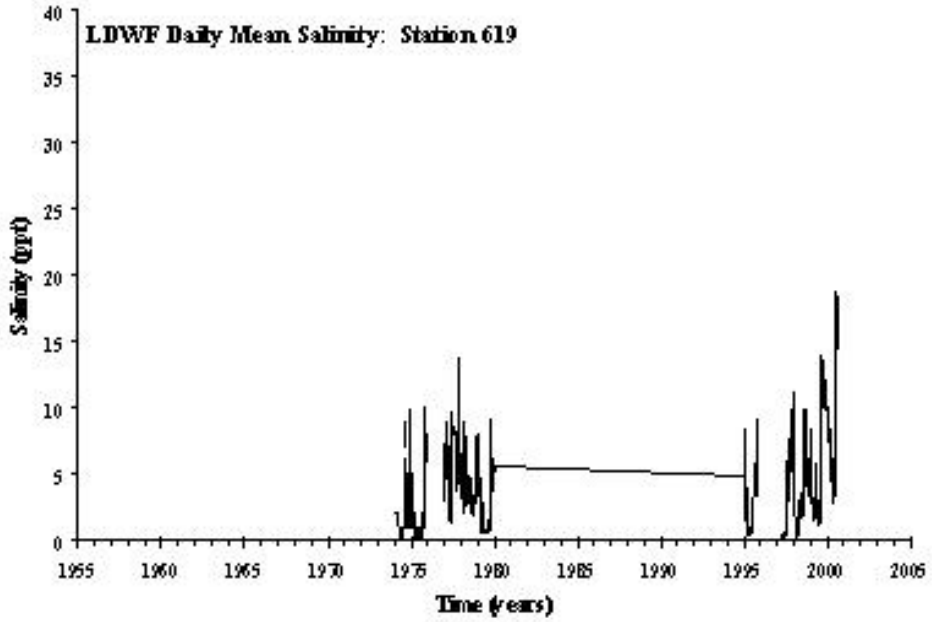

Figure 34. Time series plot of mean daily salinity from the Louisiana Department of Wildlife and Fisheries continuous monitoring station at Cypremort Point, Louisiana (Station 619). Hourly data was used for this analysis.

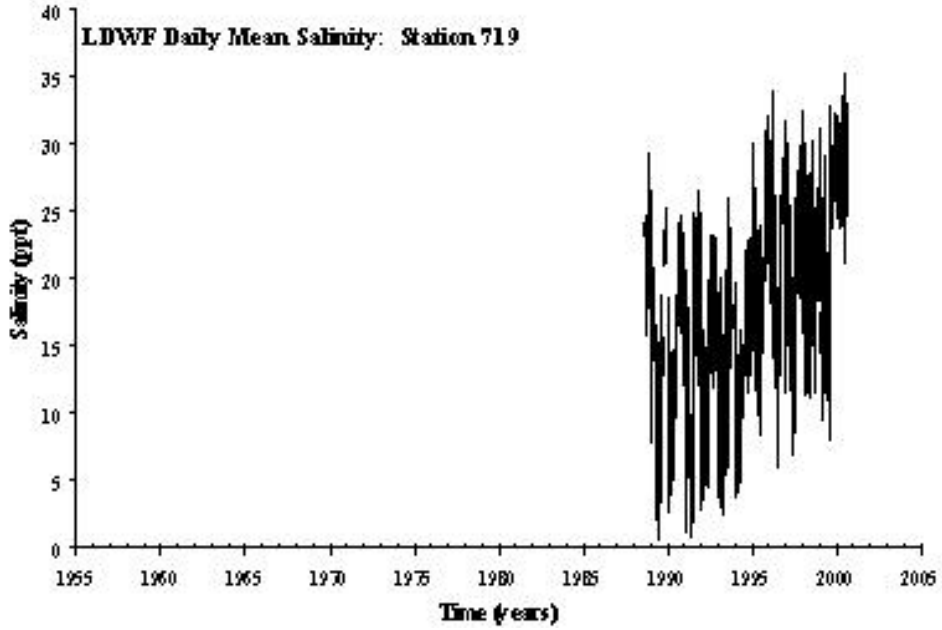

Figure 35. Time series plot of mean daily salinity from the Louisiana Department of Wildlife and Fisheries continuous monitoring station at Cameron Louisiana (Station 719). Hourly data was used for this analysis.

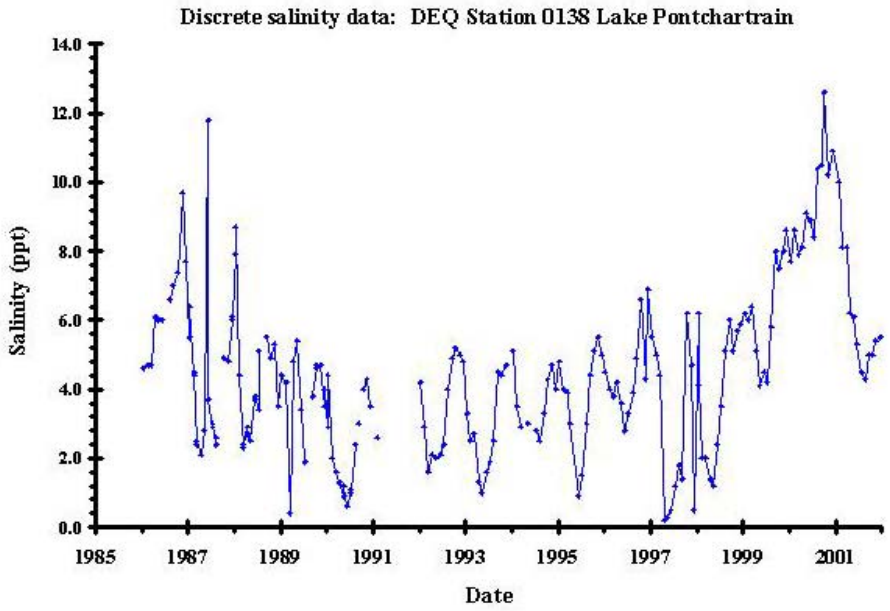

Figure 36. Time series plot of discrete salinity data from DEQ station 0138, Lake Pontchartrain Causeway at crossover number 4. The data were sampled on an approximately one month schedule.

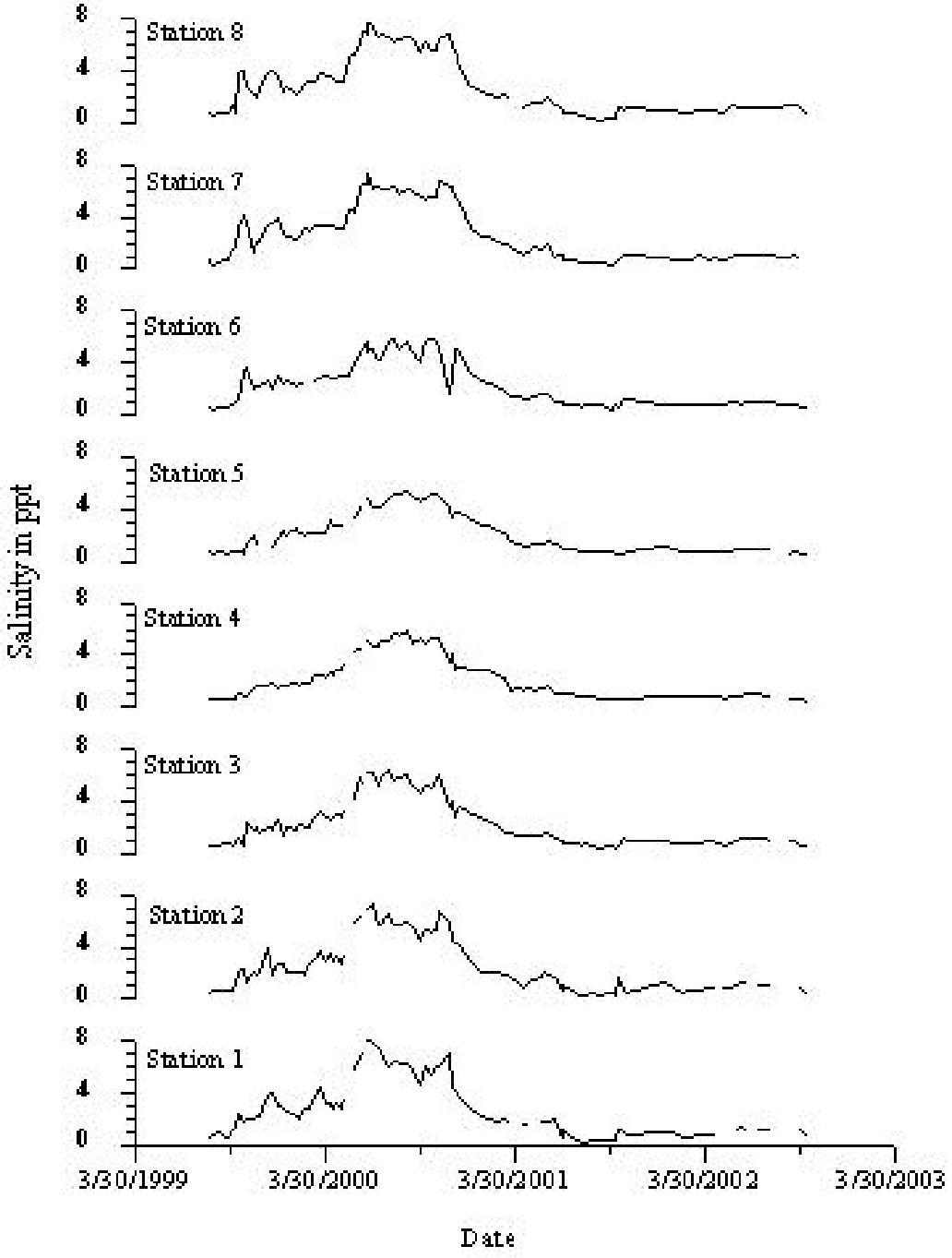

Figure 37. Time series plot of discrete salinity data from the Jefferson Parish EMPACT project (EPA funded) jointly conducted by the Coastal Ecology Institute at LSU and the USGS Baton Rouge office. The data are weekly observations.

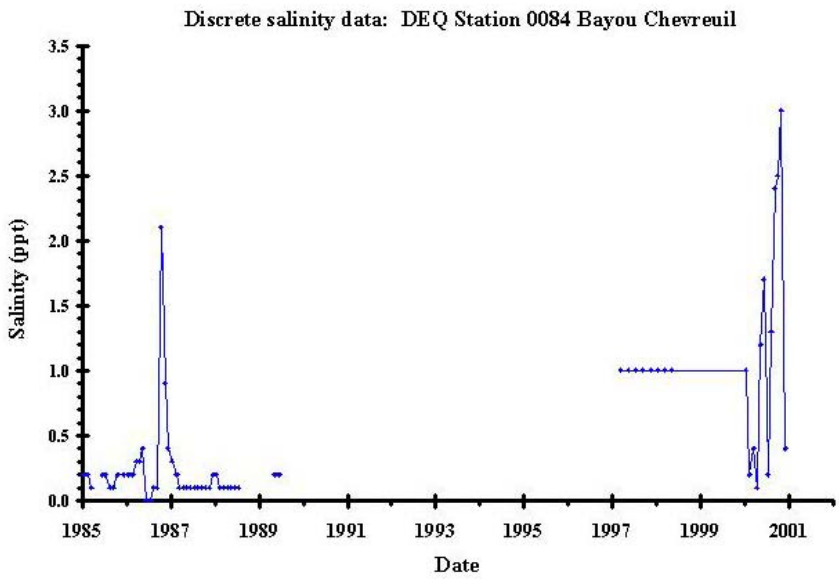

Figure 38. Time series plot of discrete salinity data from DEQ station 0084, Bayou Chevreuil at Chegby. The data were sampled on an approximately one month schedule.

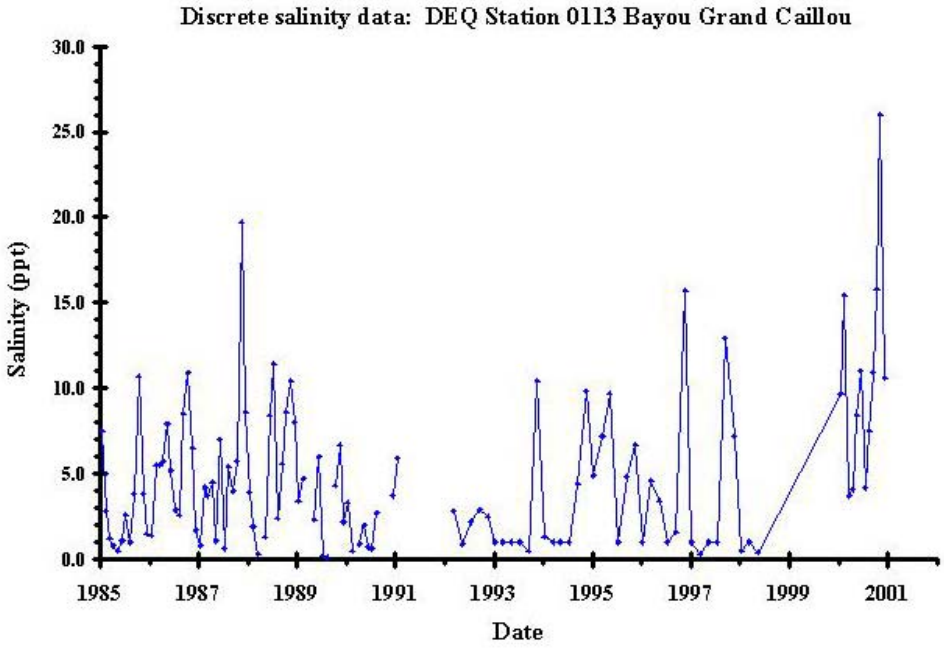

Figure 39. Time series plot of discrete salinity data from DEQ station 0113, Bayou Grand Caillou at Dulac. The data were sampled on an approximately one month schedule.

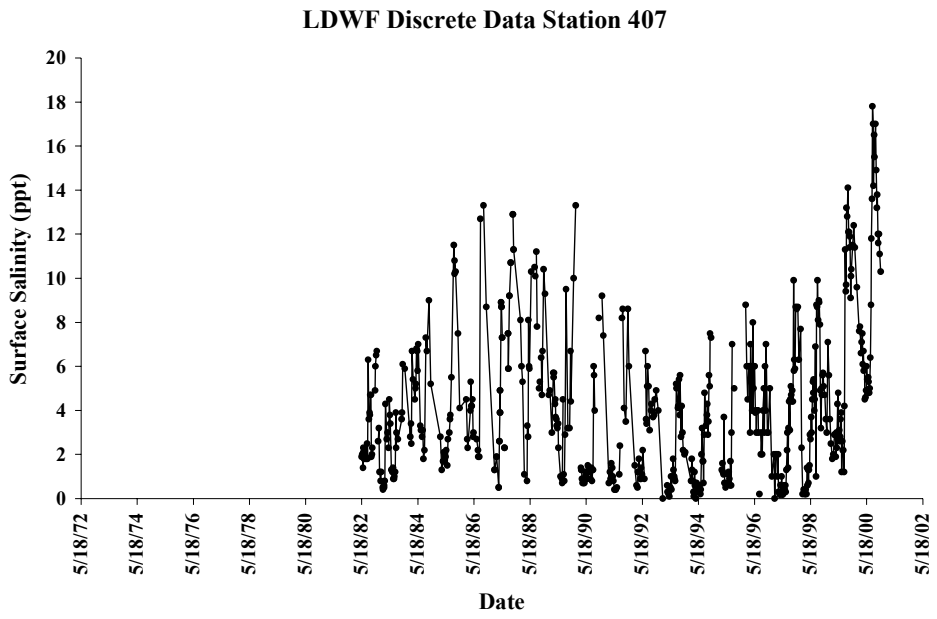

Figure 40. Time series plot of discrete salinity data from Louisiana Department of Wildlife and Fishereis Station 407 in Vermillion Bay. The data are monthly observations.

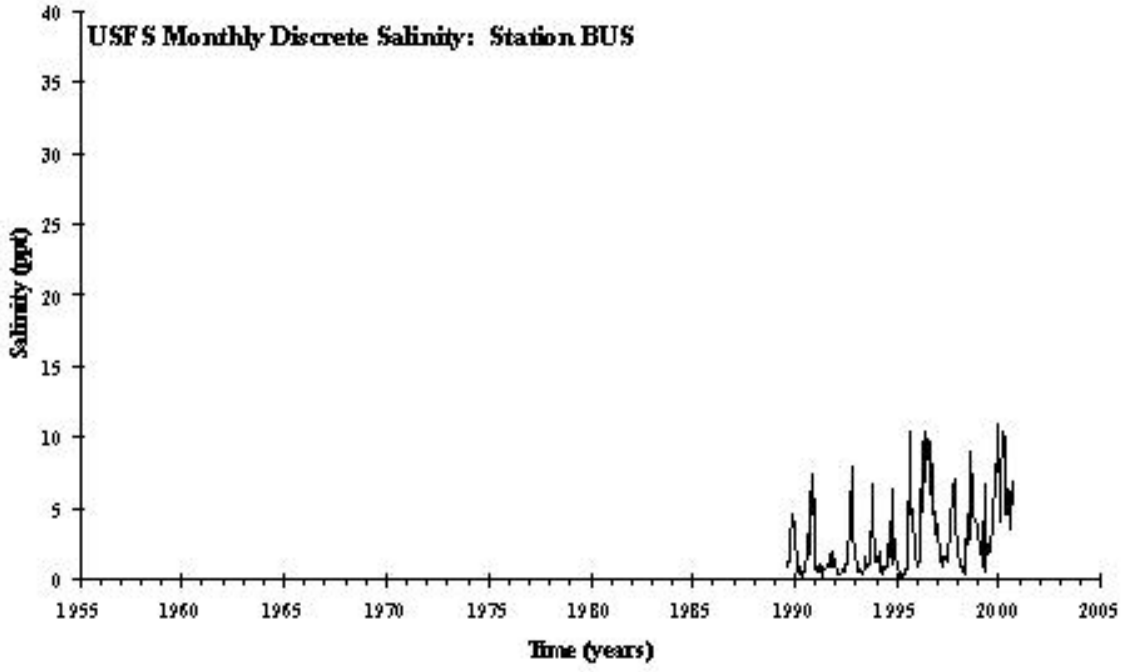

Figure 41. Time series plot of discrete salinity data from the United States Fish and Wildlife Service in the Sabine National Wildlife Refuge(Station BUS). The data are monthly observations.

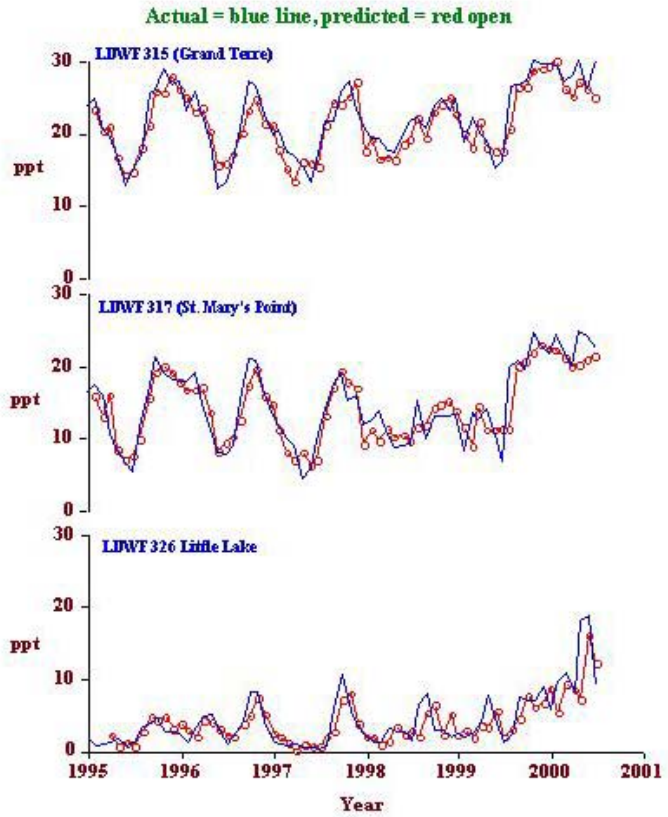

Figure 42. Plots of measured monthly mean salinity (solid line) and predicted monthly salinity (dashed line) for LDWF Station 315 (Top), LDWF Station 317 (middle) and LDWF Station 326 (bottom) in the Barataria system. The following models were used: Station 315 - Salinity = 19.99 - 0.00029 Q - 2761 P - 0.0329 WL _ 0.5466 S_{-1}; Station 317 - Salinity = 9.66 - 0.00024 Q - 0.3806 P - 0.00655 WL +0.6297 S_{-1}, and Station 317 - Salinity = 2.92- 0.00007 Q - 0.1522 P + 0.8728 S_{-1}, - 0.4220 S_{-2}, + 0.2511 S_{-3} where Q = total monthly Mississippi River Discharge (m^3s^{-1}), P = total monthly precipitation (cm), WL = de-trended water level at Grand Isle (cm), S_{-1} = salinity (ppt) of previous month, S_{-2} = salinity (ppt) two months previous, S_{-3} = salinity (ppt) three months previous.

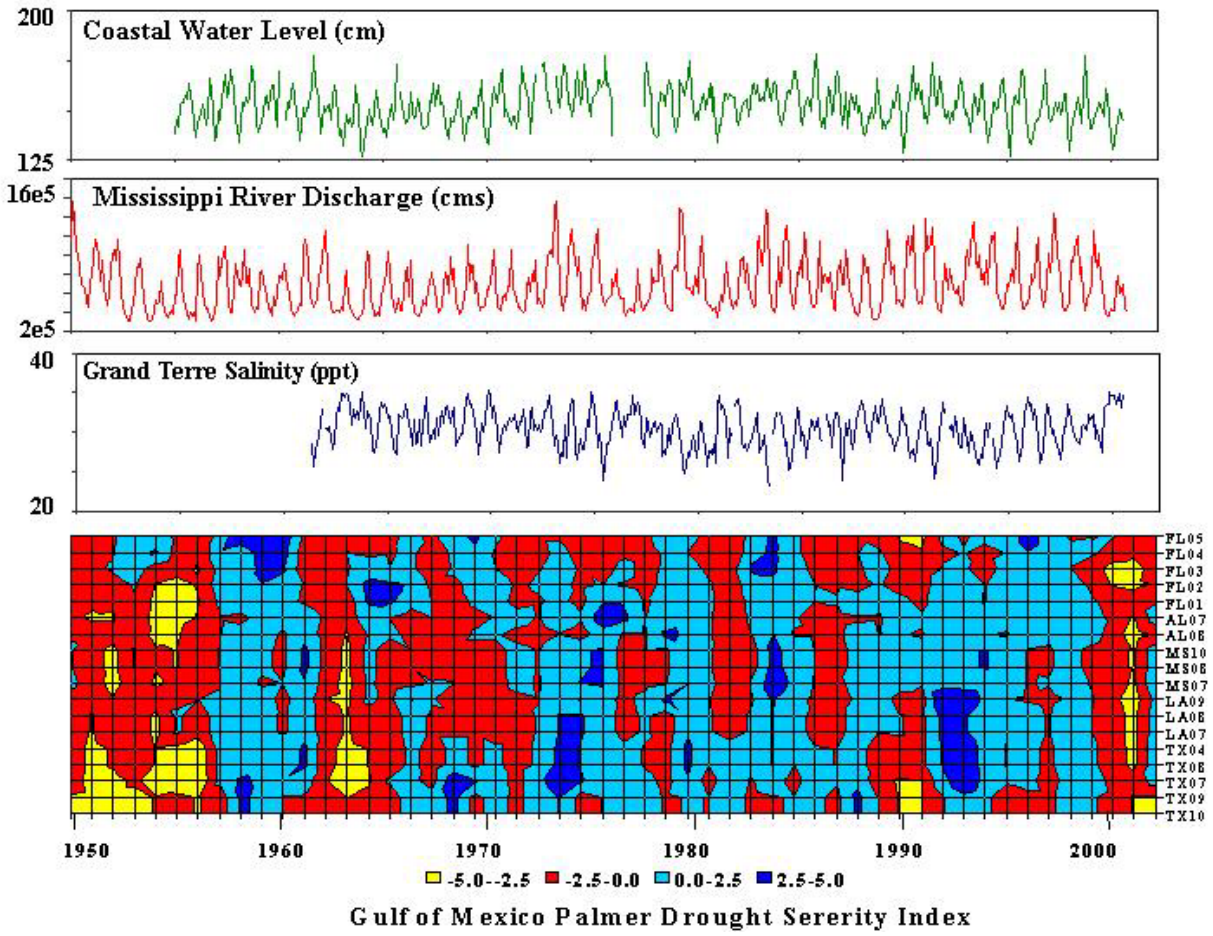

Figure 43. Summary of forcing function patters over the time period from 1950 through 2001. Indicated are the coastal water level pattern (de-trended Grand Isle record), the Mississippi River discharge, and the Palmer Drought Severity Index (PDSI) for the NCDC Climate Divisions around the Gulf of Mexico, red and yellow colors indicate dry or drought conditions and blue colors indicate wet conditions.

DATA APPENDICES

The following appendices presents plots of the data used for this project. These data files are also available in digital form on CD. The following appendices are included:

Appendix A: Tidally filtered Gulf of Mexico water level from January, 1999 through July, 2000.

Appendix B: Daily water level plots from Grand Isle, Louisiana from 1955 through 2002.

Appendix C: Gulf of Mexico daily stream discharge from 1935 through 2001.

Appendix D: Gulf of Mexico mean monthly stream discharge.

Appendix E: Plots of monthly Palmer Drought Severity Index for NCDC climate divisions around the Gulf of Mexico from 1950 through 2002.

Appendix F: Plots of monthly total precipitation for NCDC climate divisions around the Gulf of Mexico from 1950 through 2002.

Appendix G: Plots of monthly temperature for NCDC climate divisions around the Gulf of Mexico from 1950 through 2002.

Appendix H: Plots of monthly total potential evapotranspiration for NCDC climate divisions around the Gulf of Mexico from 1950 through 2002.

Appendix I: Plots of monthly total surplus (precipitation – evapotranspiration) for NCDC climate divisions around the Gulf of Mexico from 1950 through 2002.

Appendix A: Gulf of Mexico Water Level Plots.

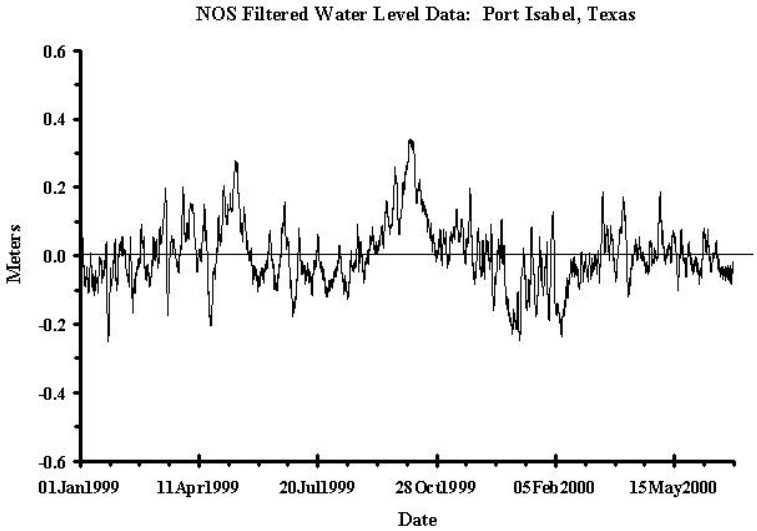

Figure A-1. Plot of filtered (25 hour running mean) hourly water levels from Port Isabel, Texas. Data is from the National Oceanic Survey (NOS).

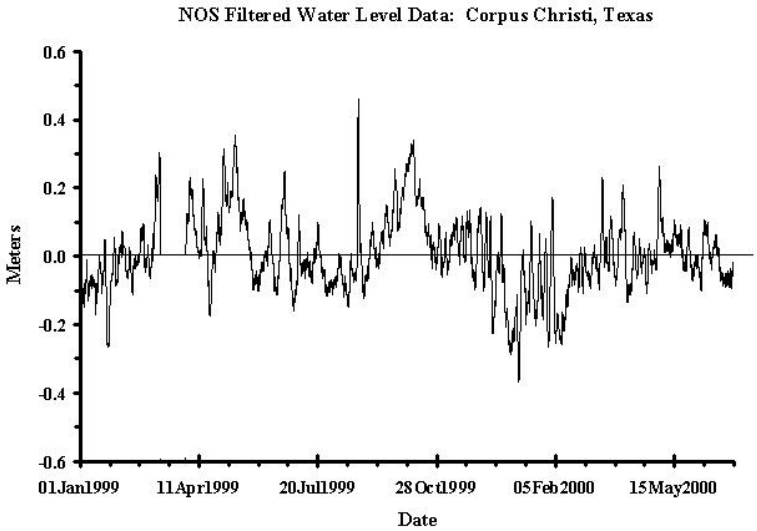

Figure A-2. Plot of filtered (25 hour running mean) hourly water levels from Corpus Christi, Texas. Data is from the National Oceanic Survey (NOS).

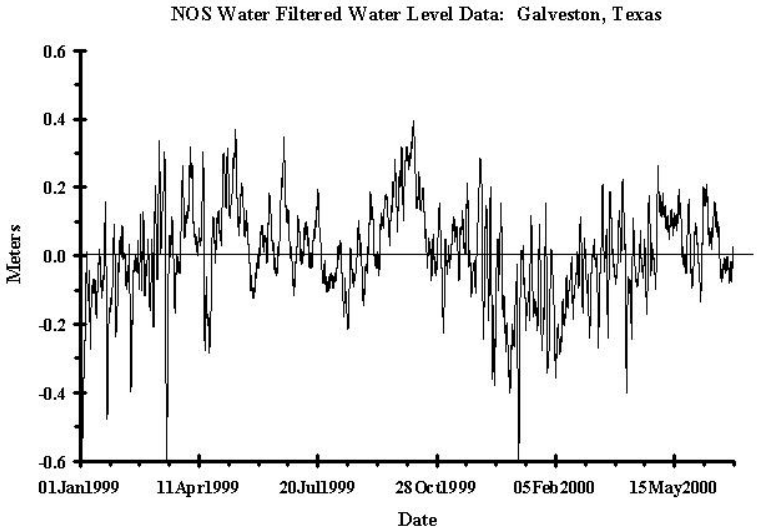

Figure A-3. Plot of filtered (25 hour running mean) hourly water levels from Galveston, Texas. Data is from the National Oceanic Survey (NOS).

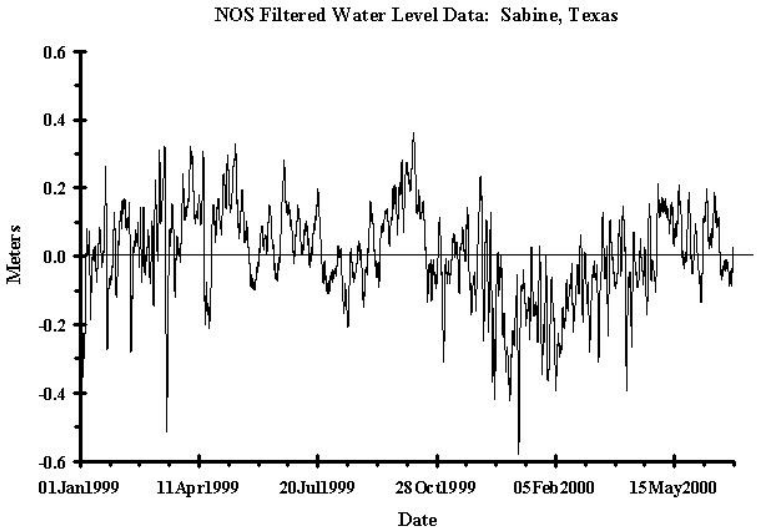

Figure A-4. Plot of filtered (25 hour running mean) hourly water levels from Sabine, Texas. Data is from the National Oceanic Survey (NOS).

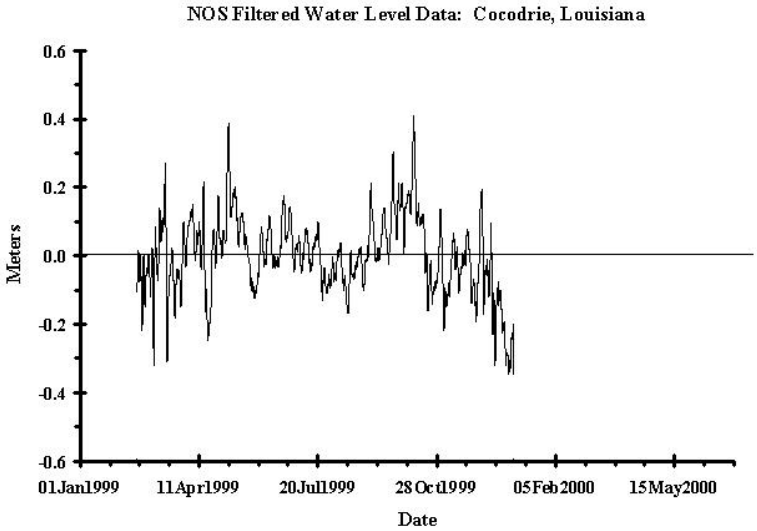

Figure A-5. Plot of filtered (25 hour running mean) hourly water levels from Cocodrie, Louisiana. Data is from the National Oceanic Survey (NOS).

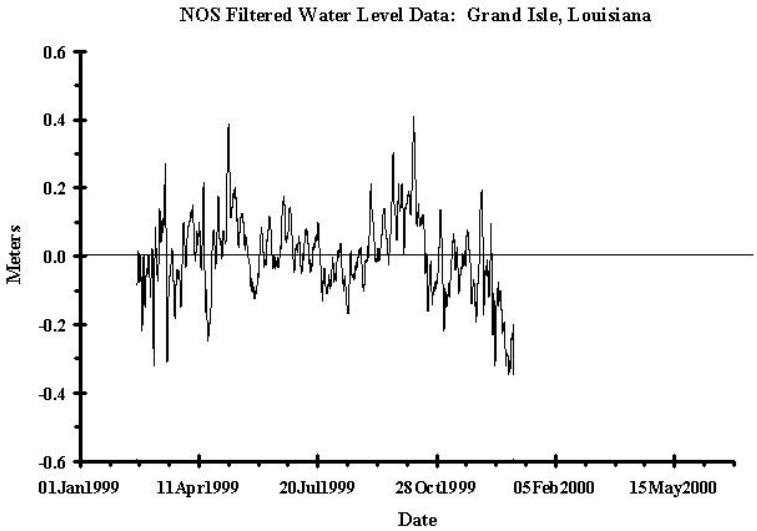

Figure A-6. Plot of filtered (25 hour running mean) hourly water levels from Grand Isle, Louisiana. Data is from the National Oceanic Survey (NOS).

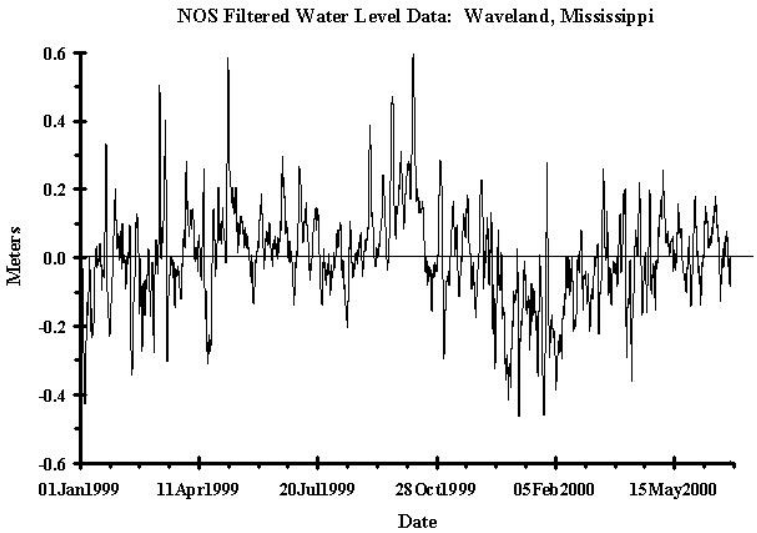

Figure A-7. Plot of filtered (25 hour running mean) hourly water levels from Waveland, Mississippi. Data is from the National Oceanic Survey (NOS).

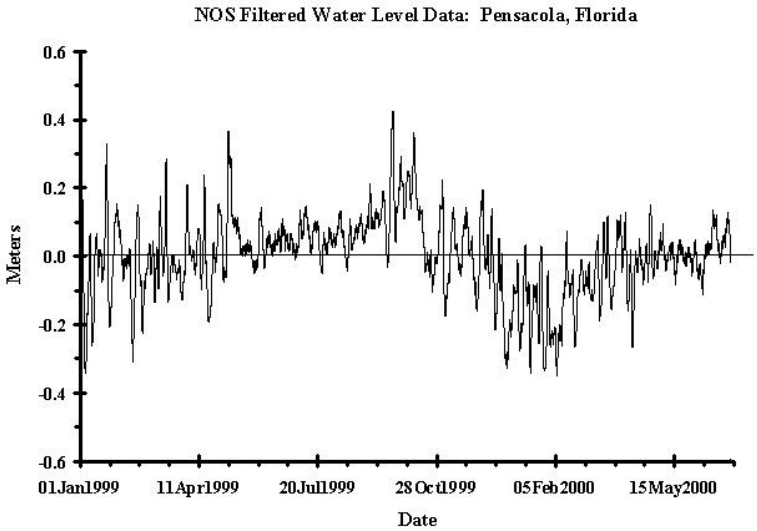

Figure A-8. Plot of filtered (25 hour running mean) hourly water levels from Pensacola, Florida. Data is from the National Oceanic Survey (NOS).

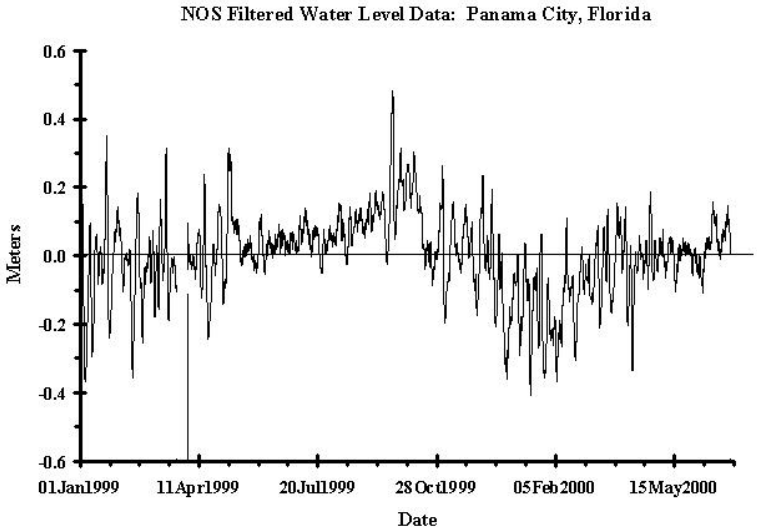

Figure A-9. Plot of filtered (25 hour running mean) hourly water levels from Panama City, Florida. Data is from the National Oceanic Survey (NOS).

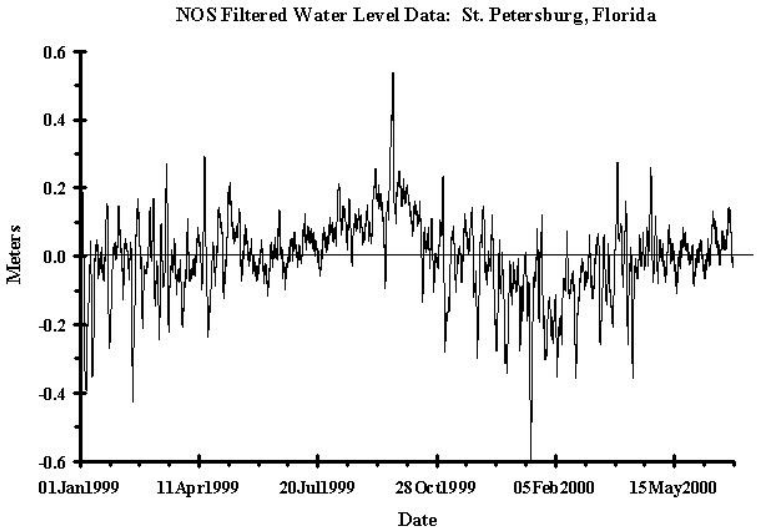

Figure A-10. Plot of filtered (25 hour running mean) hourly water levels from St. Petersburg, Florida. Data is from the National Oceanic Survey (NOS).

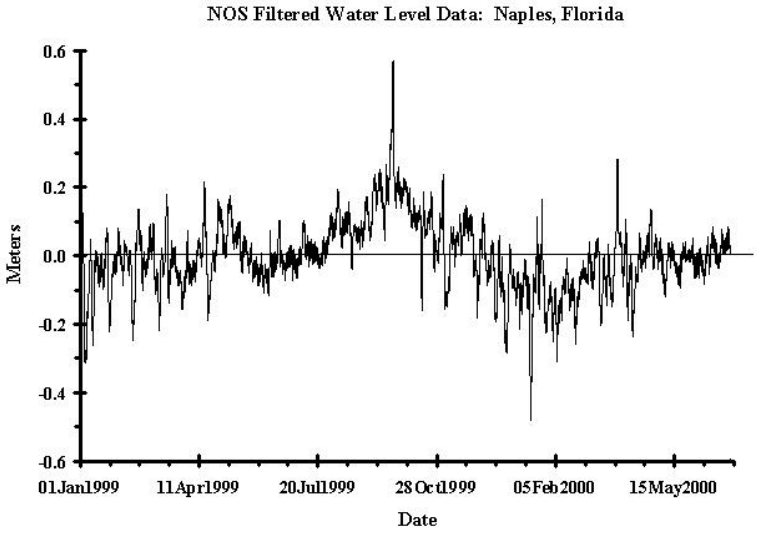

Figure A-11. Plot of filtered (25 hour running mean) hourly water levels from Naples, Florida. Data is from the National Oceanic Survey (NOS).

Appendix B: Grand Isle Water Level Plots.

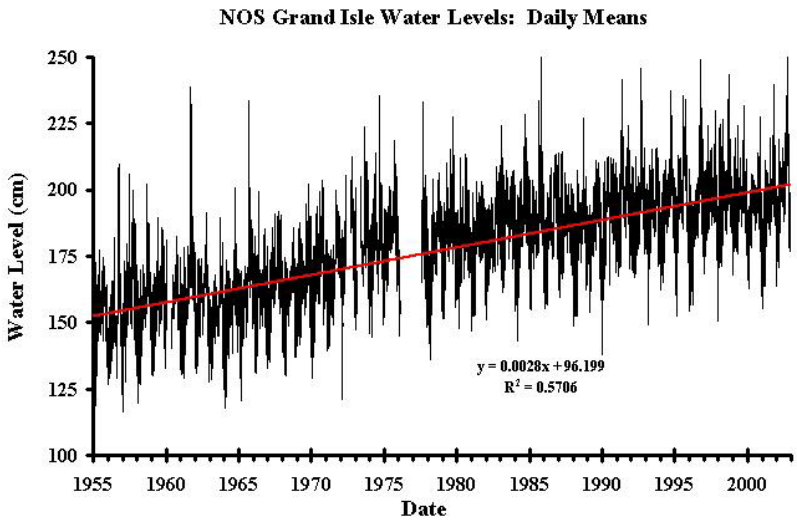

Figure B-1. Plot of daily mean water levels for Grand Isle, Louisiana, in centimeters relative to the station datum. The results of a linear regression using water level as the dependent variable and time as the independent variable are indicated. Hourly data from the National Oceanic Survey (NOS) was used in this analysis.

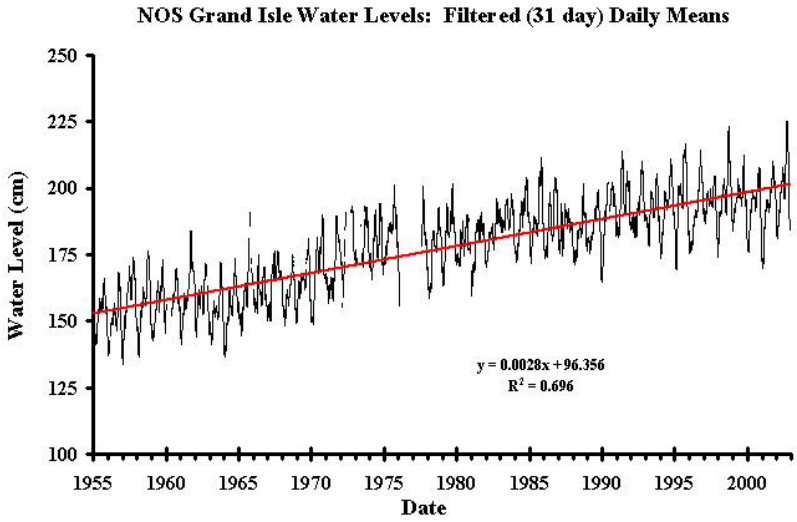

Figure B-2. Plot of filtered daily mean water level for Grand Isle, Louisiana, in centimeters relative to the station datum. The data were filtered using a 31-day running mean. The results of a linear regression using water level as the dependent variable and time as the independent variable are indicated. Hourly data from the National Oceanic Survey (NOS) was used in this analysis.

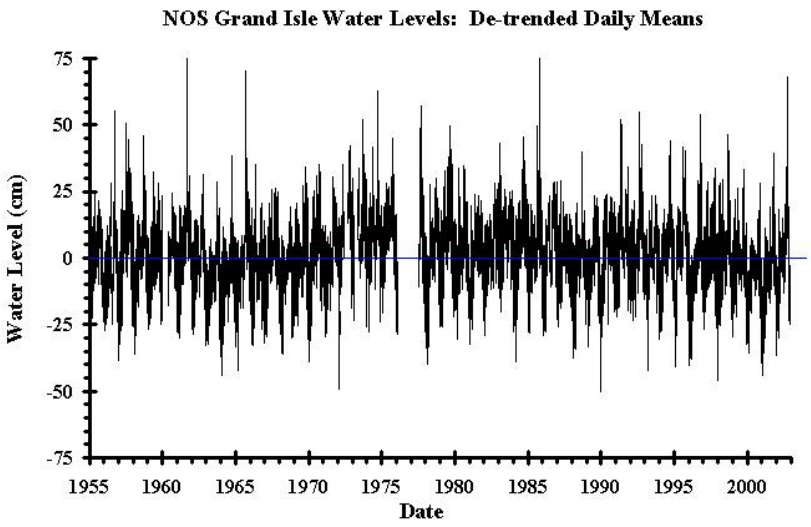

Figure B-3. Plot of de-trended daily mean water level for Grand Isle, Louisiana, in centimeters relative to the station datum. The data were de-trended by removing the long term trend determined from linear regression analysis. Hourly data from the National Oceanic Survey (NOS) was used in this analysis.

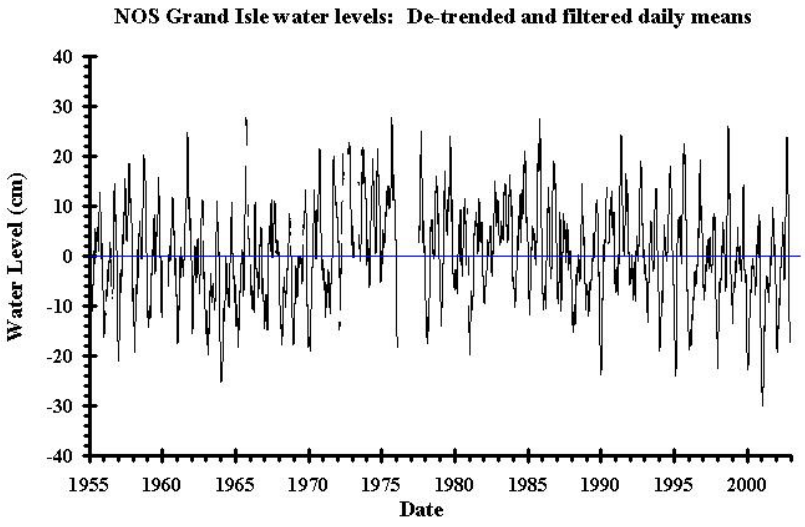

Figure B-4. Plot of de-trended and filtered daily mean water level for Grand Isle, Louisiana, in centimeters relative to the station datum. The data were de-trended by removing the long term trend determined from linear regression analysis, and filtered using a 31 day running mean. Hourly data from the National Oceanic Survey (NOS) was used in this analysis.

Appendix C: Daily river discharge plots.

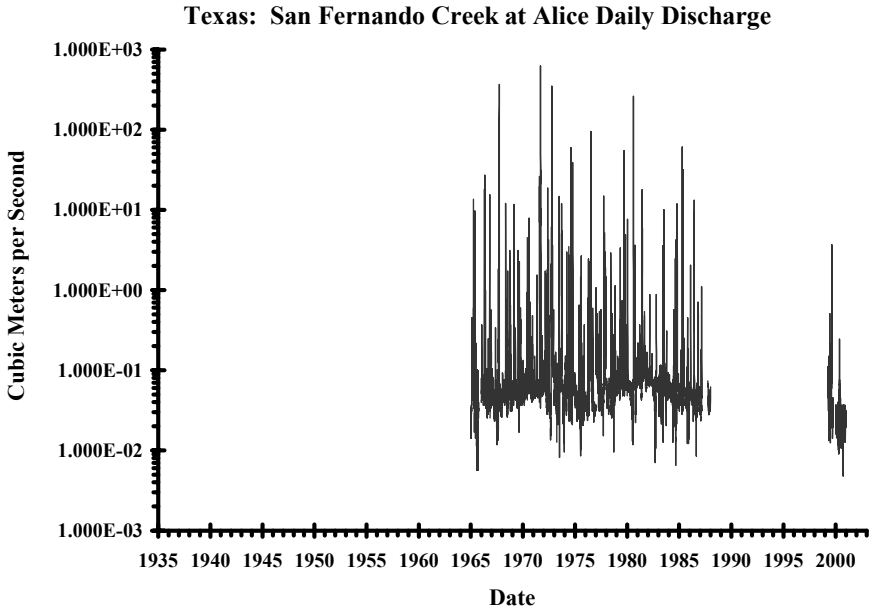

Figure C-1. Daily data from the USGS streamflow station 8211900, San Fernando Creek at Alice, Texas.

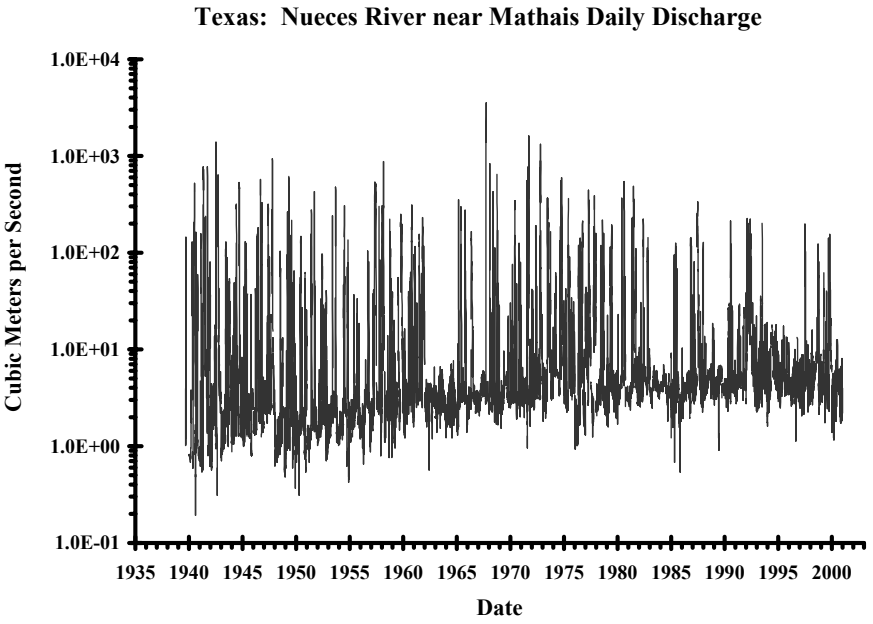

Figure C-2. Daily data from the USGS streamflow station 8211000, Nueses River near Mathais, Texas.

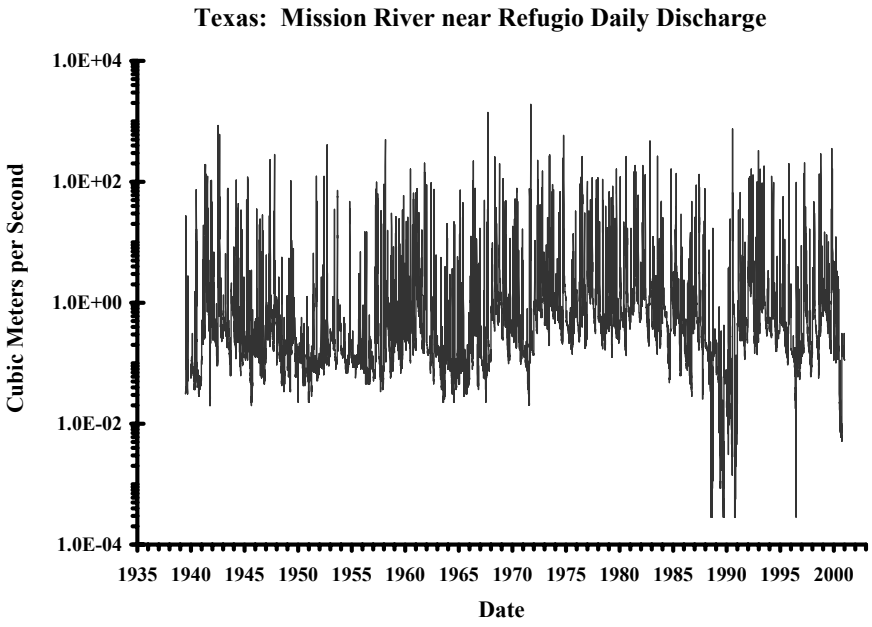

Figure C-3. Daily data from the USGS streamflow station 8189500, Mission River near Refugio, Texas.

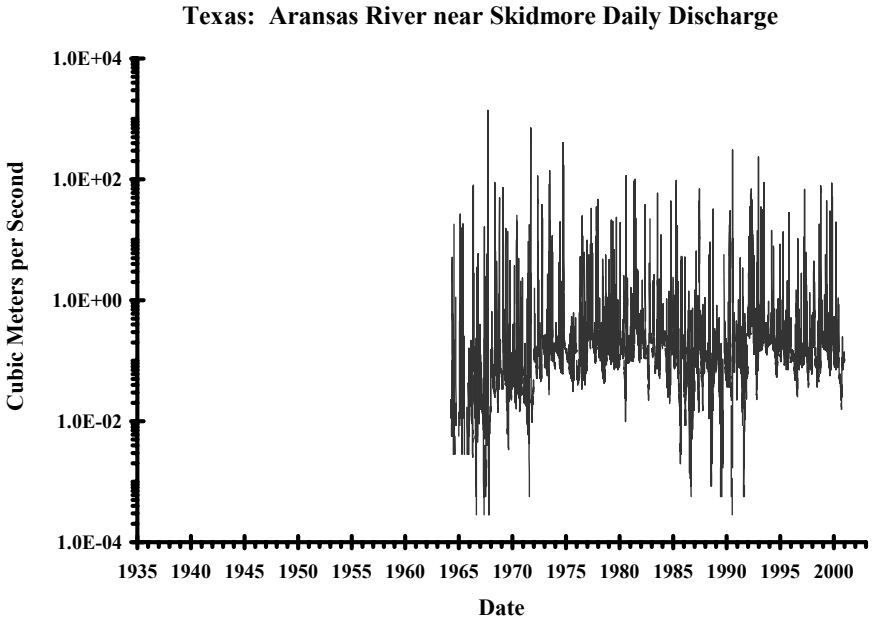

Figure C-4. Daily data from the USGS streamflow station 8189700, Aransas River near Skidmore, Texas.

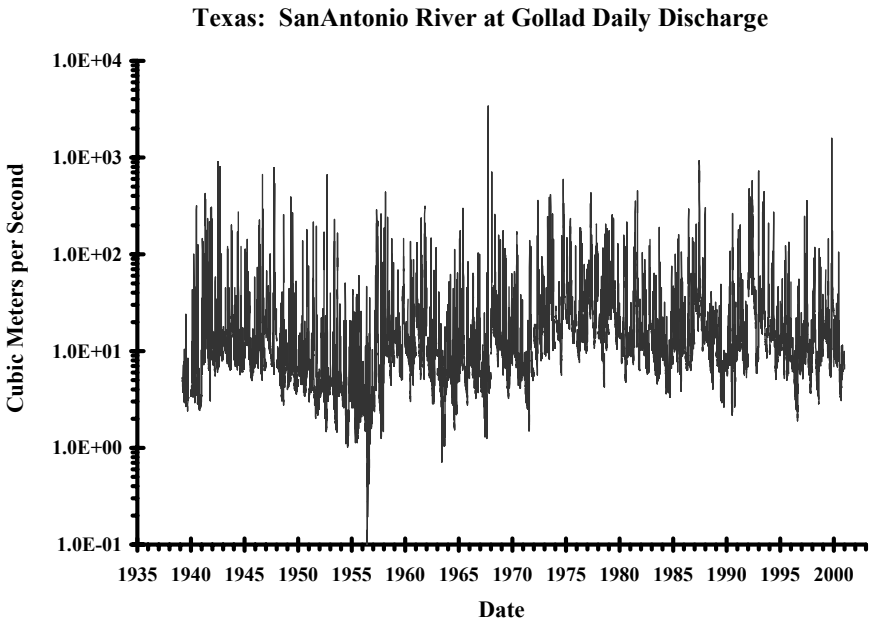

Figure C-5. Daily data from the USGS streamflow station 8188500, San Antonio Rivera at Golliad, Texas.

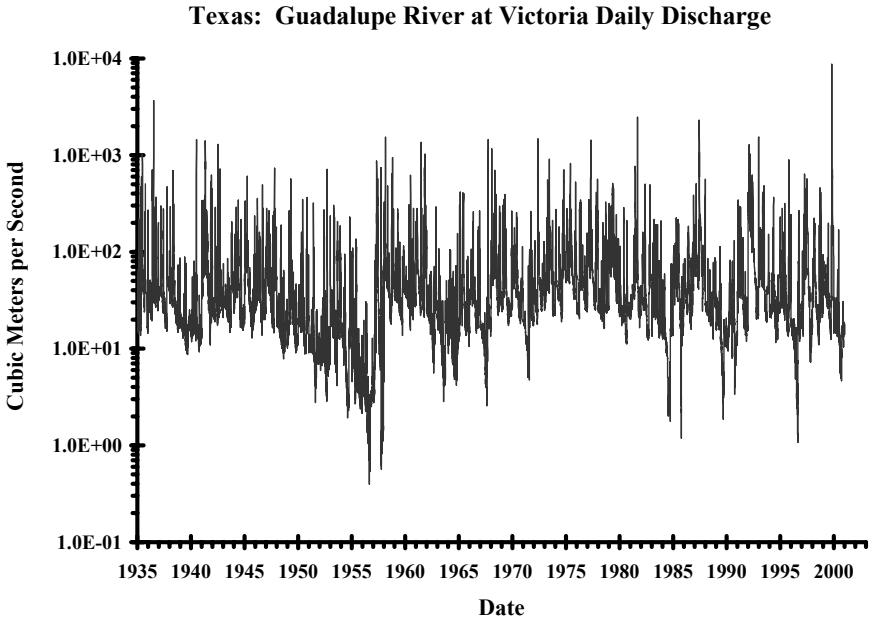

Figure C-6. Daily data from the USGS streamflow station 8176500, Guadalupe River at Victoria, Texas.

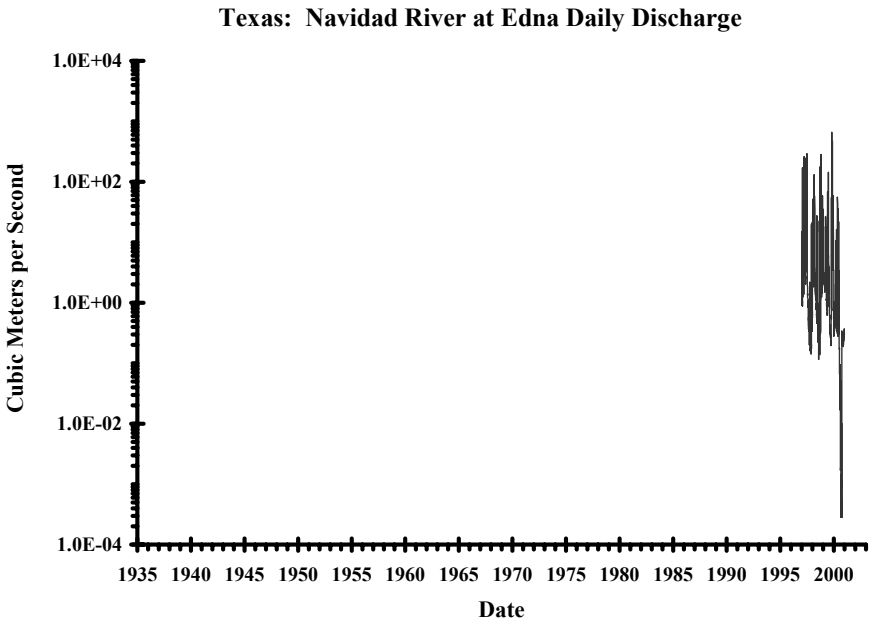

Figure C-7. Daily data from the USGS streamflow station 8164390, Navidad River at Edna, Texas.

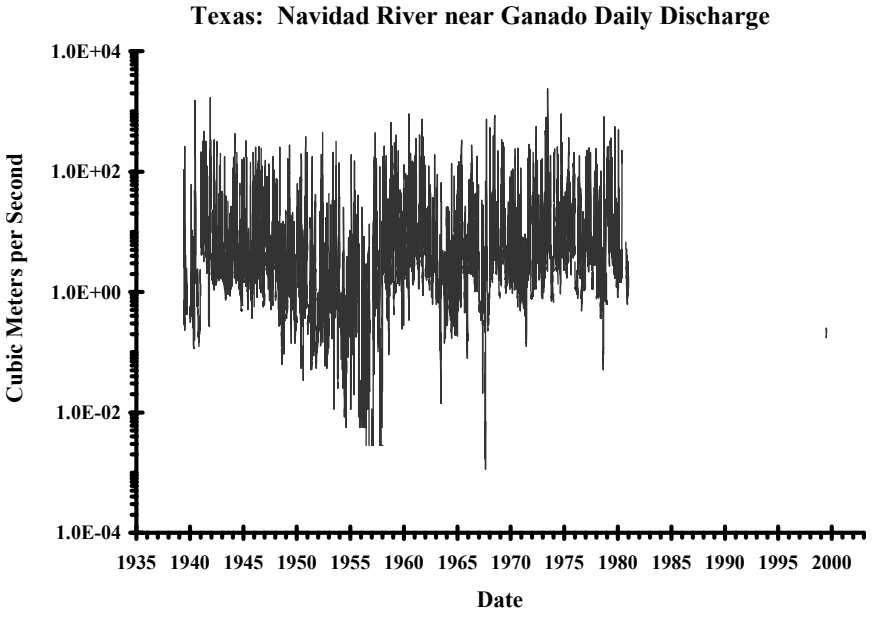

Figure C-8. Daily data from the USGS streamflow station 8164500, Navidad River near Ganado, Texas.

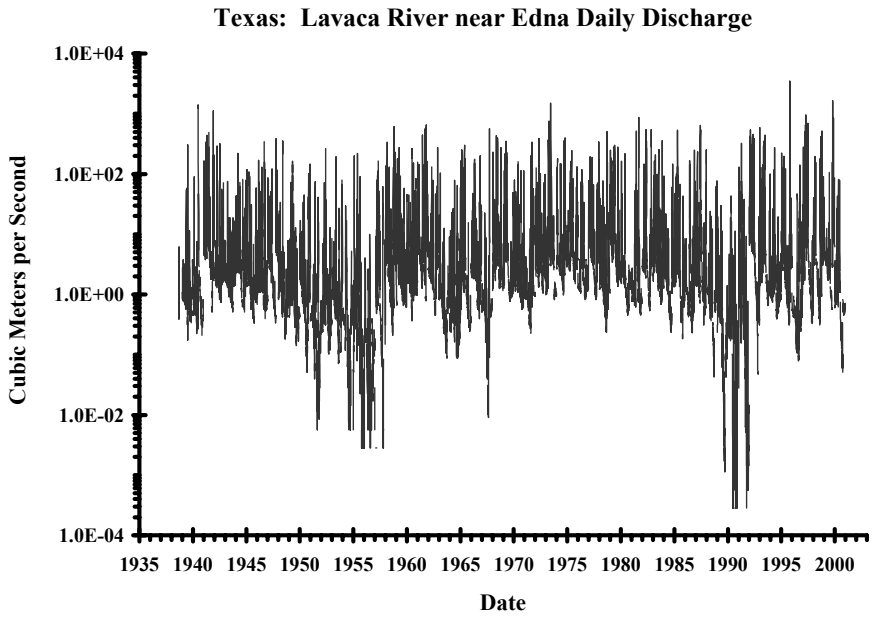

Figure C-9. Daily data from the USGS streamflow station 8164000, Lavaca River near Edna, Texas.

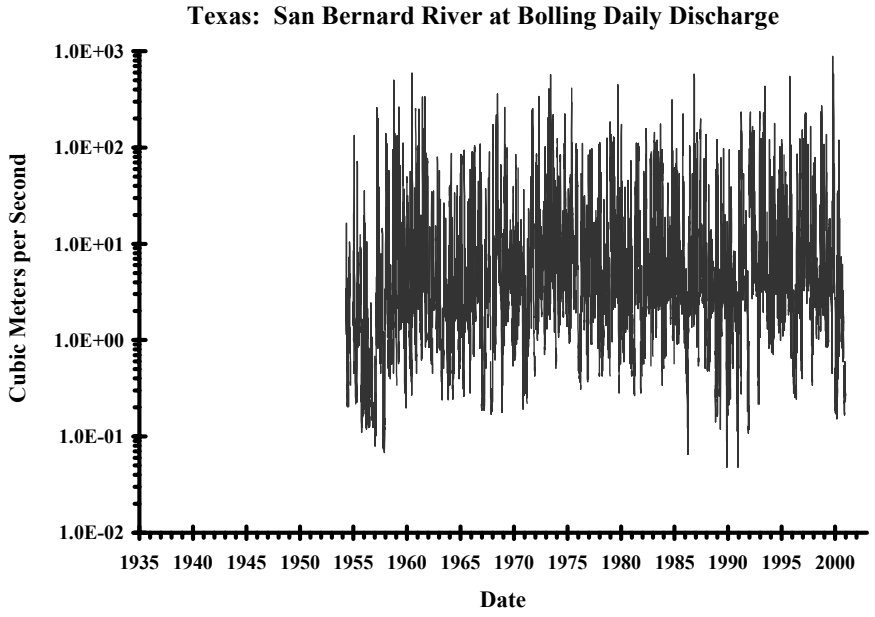

Figure C-10. Daily data from the USGS streamflow station 8117500, San Bernard River at Bolling, Texas.

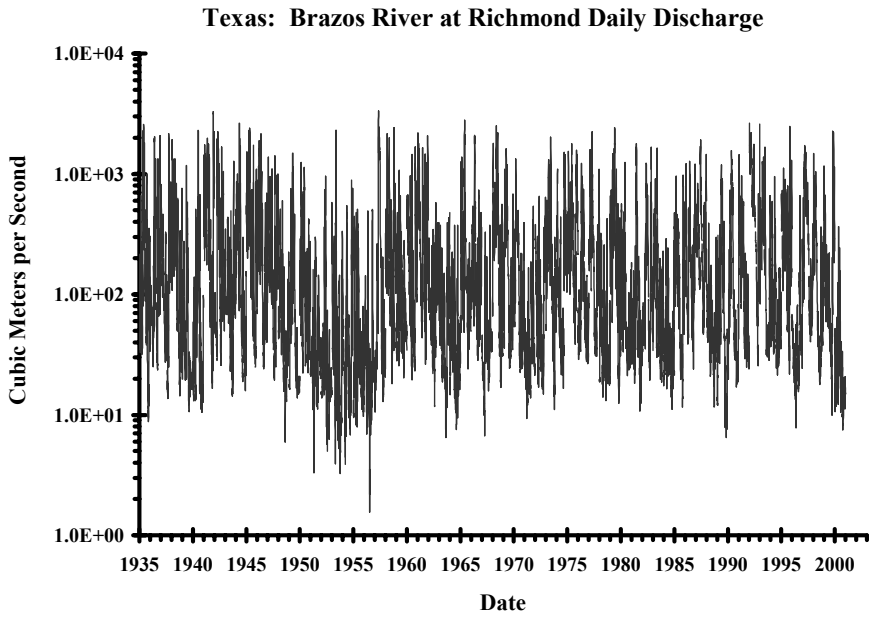

Figure C-11. Daily data from the USGS streamflow station 8114000, Brazos River at Richmond, Texas.

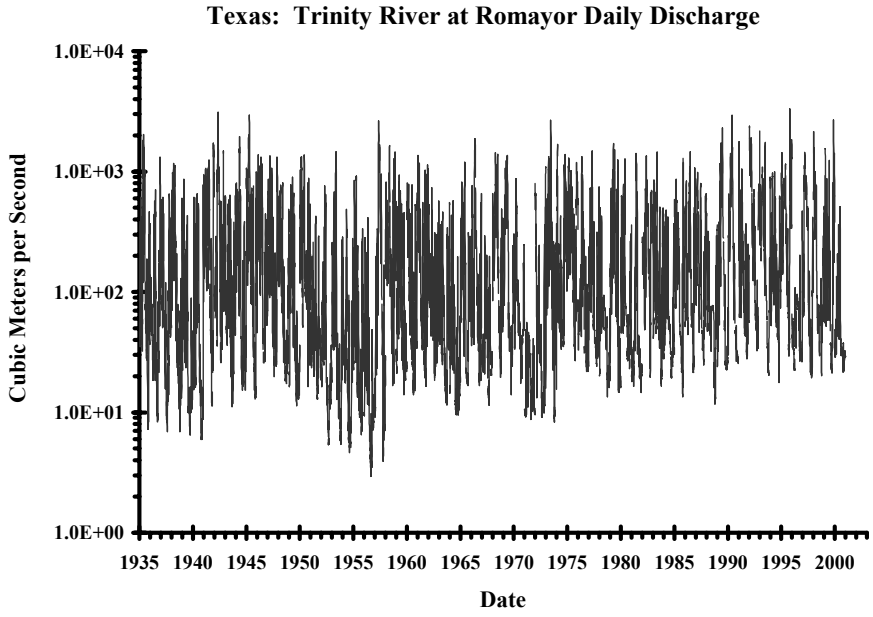

Figure C-12. Daily data from the USGS streamflow station 8066500, Trinity River at Romayor, Texas.

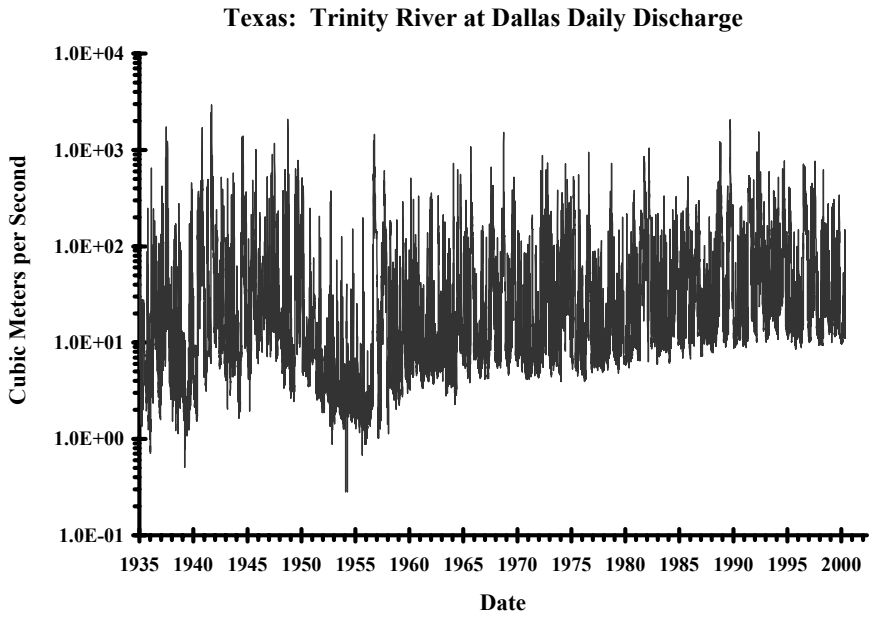

Figure C-13. Daily data from the USGS streamflow station 8057000, Trinity River at Dallas, Texas.

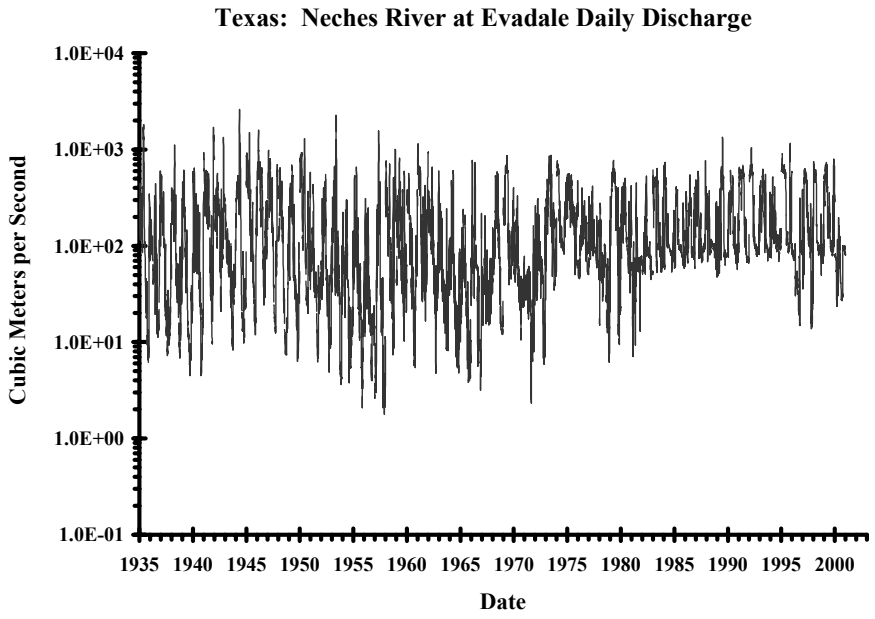

Figure C-14. Daily data from the USGS streamflow station 8041000, Neches River at Evadale, Texas.

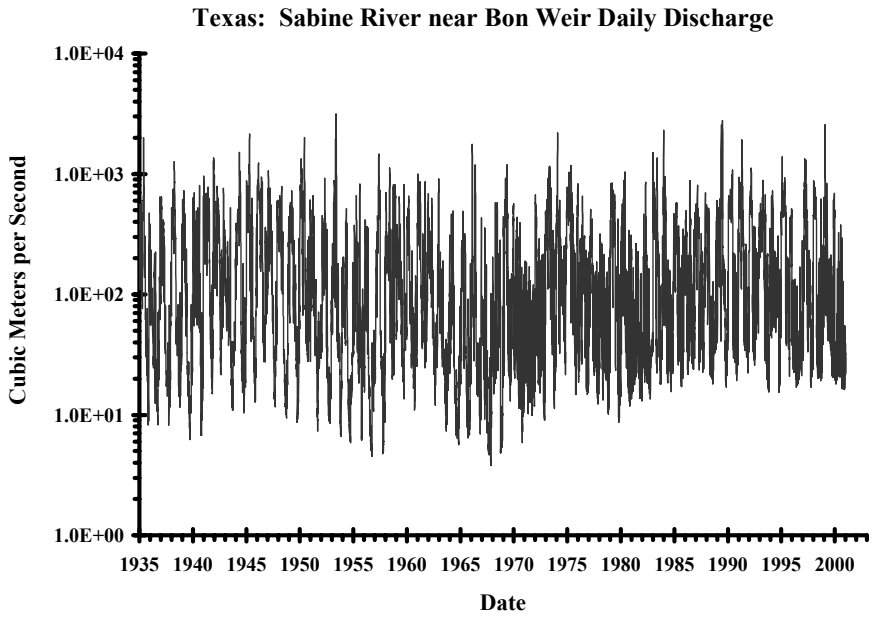

Figure C-15. Daily data from the USGS streamflow station 8028500, Sabine River near Bon Weir, Texas.

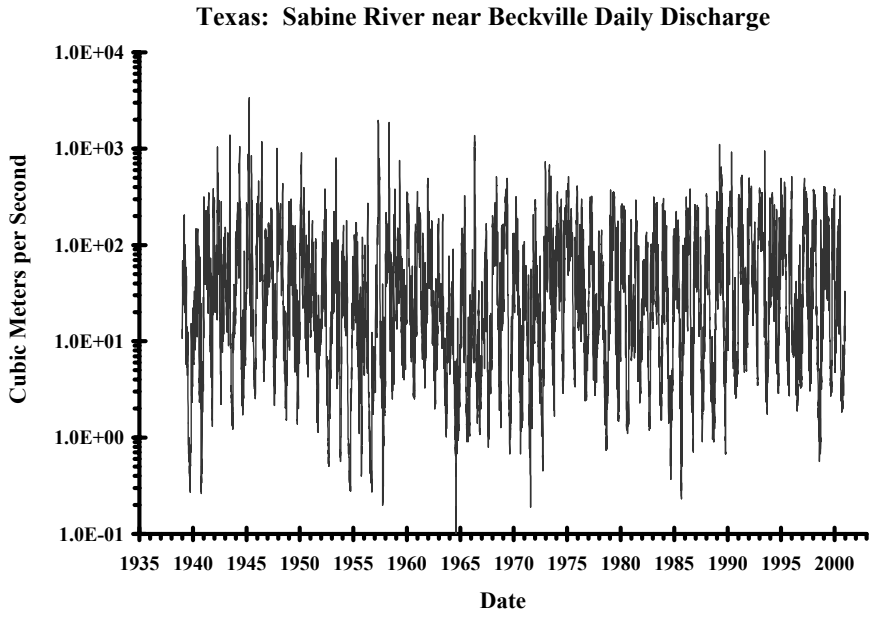

Figure C-16. Daily data from the USGS streamflow station 8022040, Sabine River near Beckville, Texas.

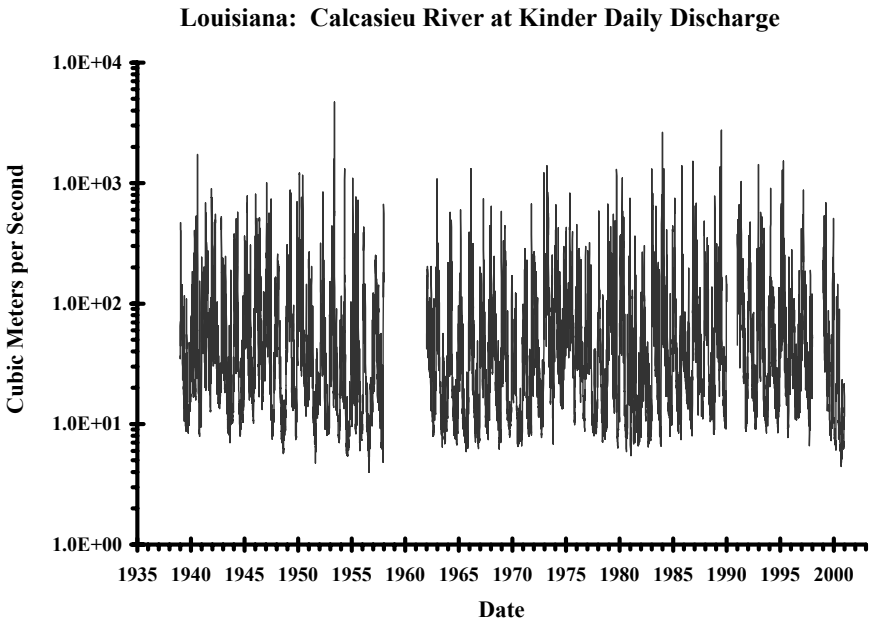

Figure C-17. Daily data from the USGS streamflow station 8015500, Calcasieu River at Kinder, Louisiana.

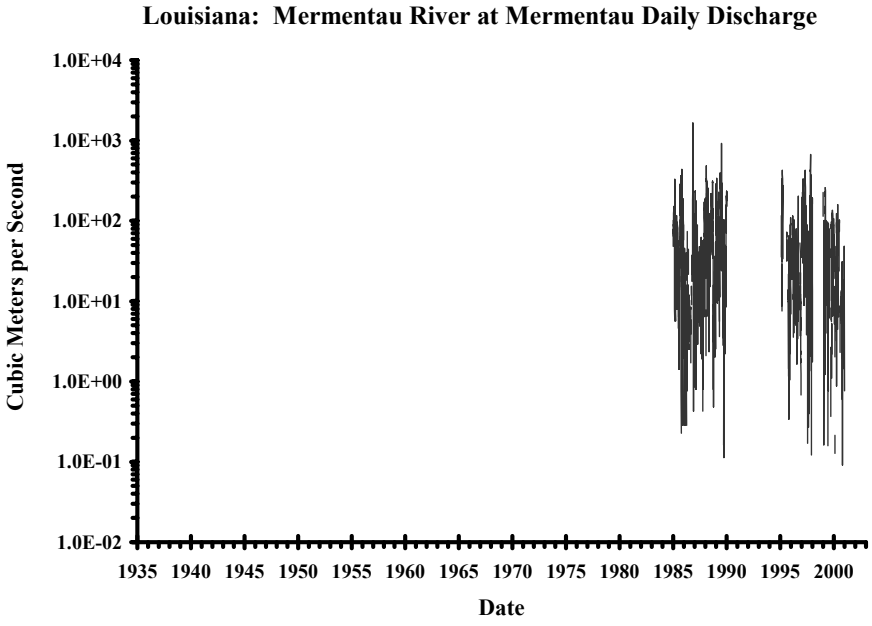

Figure C-18. Daily data from the USGS streamflow station 8012150, Mermentau River at Mermentau, Louisiana.

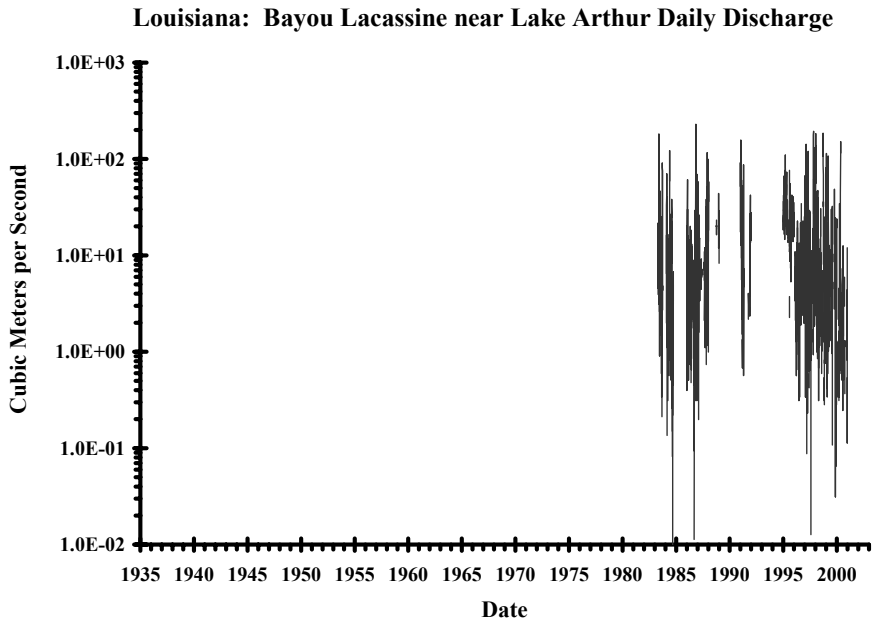

Figure C-19. Daily data from the USGS streamflow station 8012470, Bayou Lacassine near Lake Arthur, Louisiana.

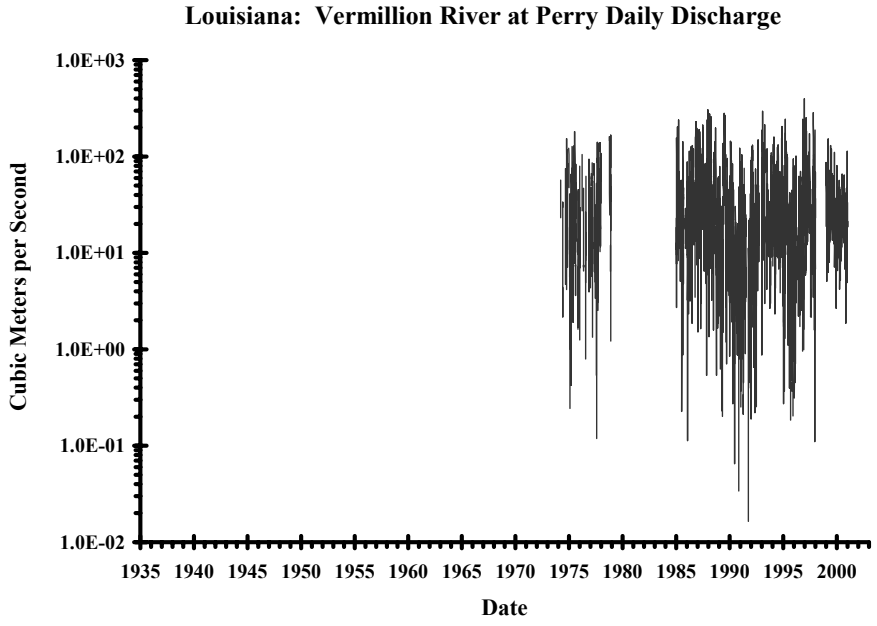

Figure C-20. Daily data from the USGS streamflow station 7386980, Vermillion River at Perry, Louisiana.

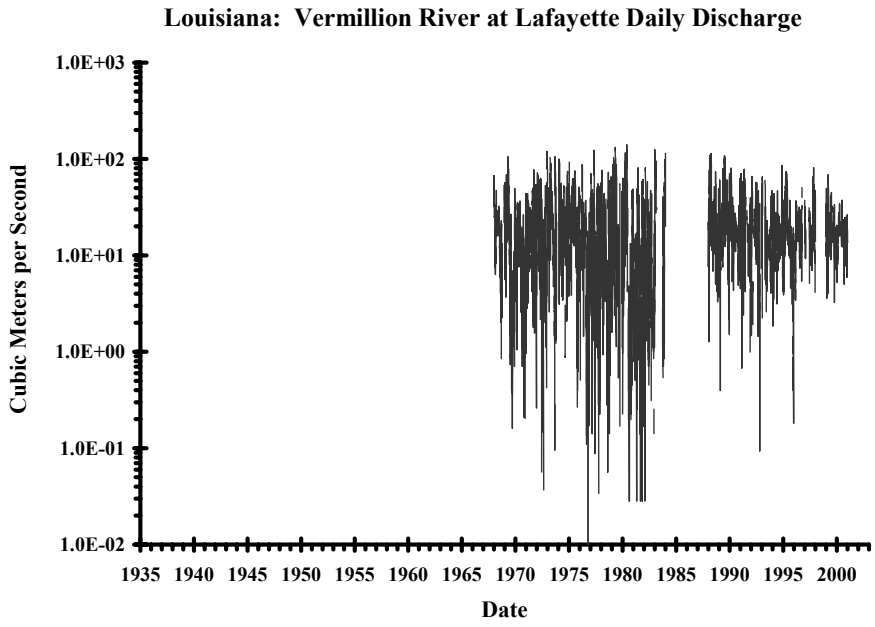

Figure C-21. Daily data from the USGS streamflow station 7386880, Vermillion River at Lafayette, Louisiana.

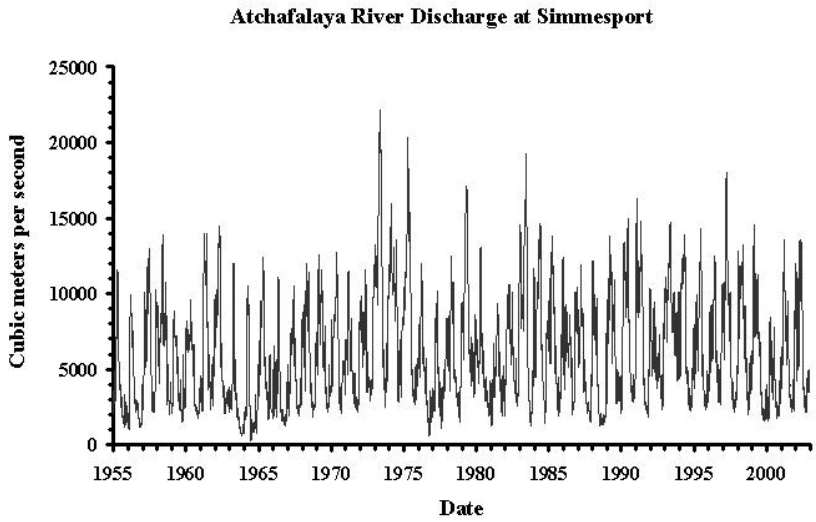

Figure C-22. Daily data from the USCE streamflow station 3045, Atchafalaya River at Simmesport. Louisiana.

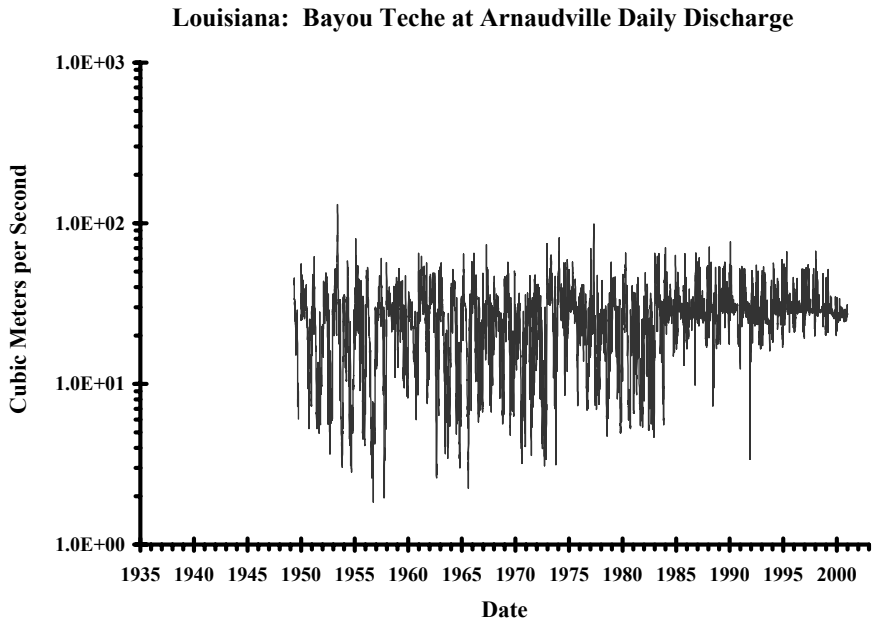

Figure C-23. Daily data from the USGS streamflow station7 385500,Bayou Teche at Arnaudville, Louisiana.

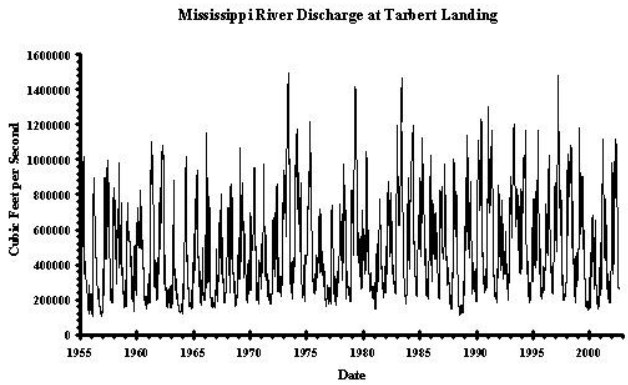

Figure C-24. Daily data from the USCE streamflow 1100, station Mississippi River at Tarbert Landing, Mississippi.

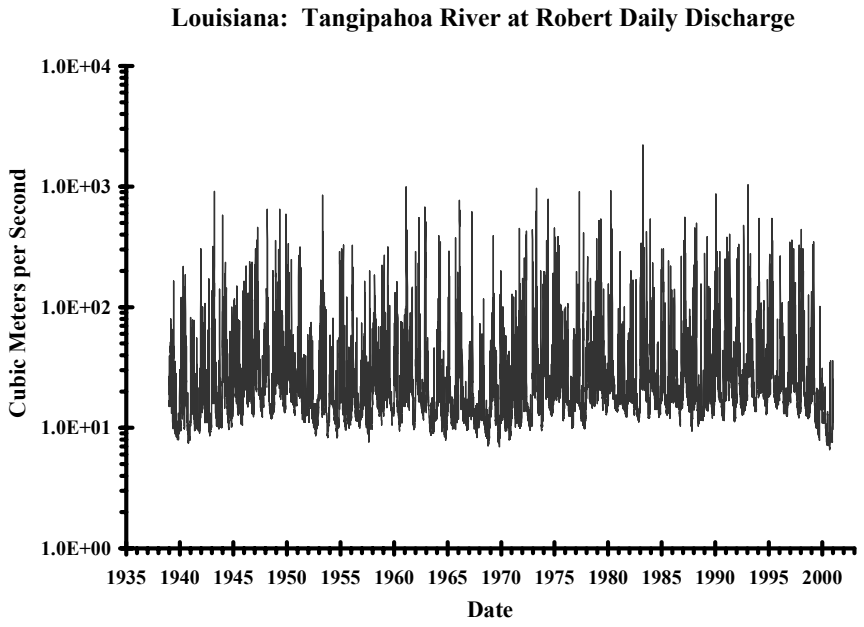

Figure C-25. Daily data from the USGS streamflow station 7375500, Tangipahoa River at Robert, Louisiana.

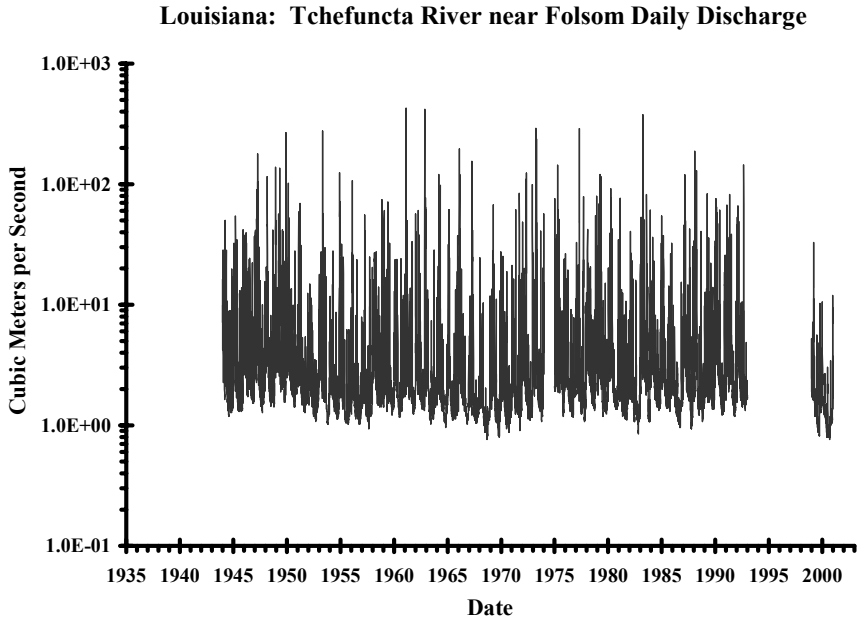

Figure C-26. Daily data from the USGS streamflow station 7375000, Tchefuncta River near Folsom, Louisiana.

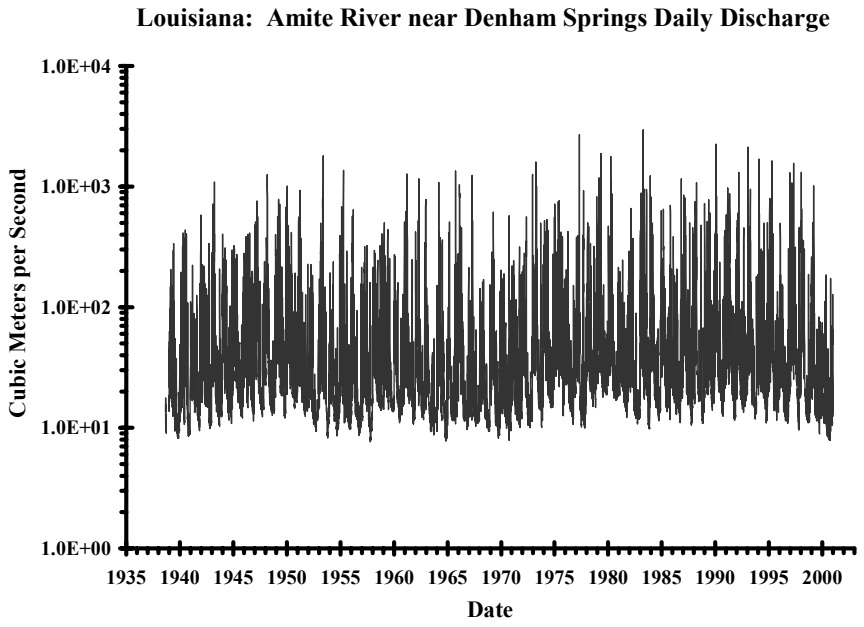

Figure C-27. Daily data from the USGS streamflow station 7378500, Amite River near Denham Springs, Louisiana.

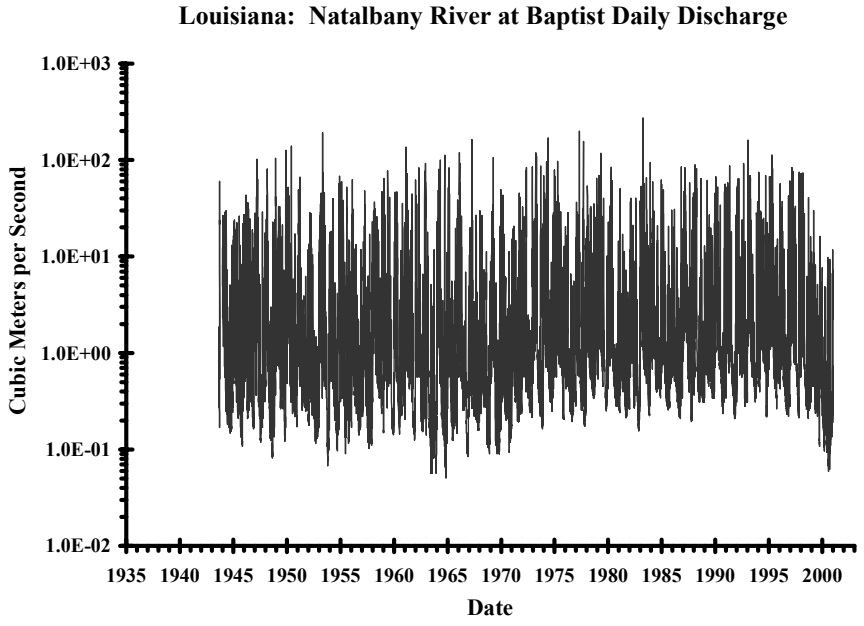

Figure C-28. Daily data from the USGS streamflow station 7376500, Natalbany River at Baptist, Louisiana.

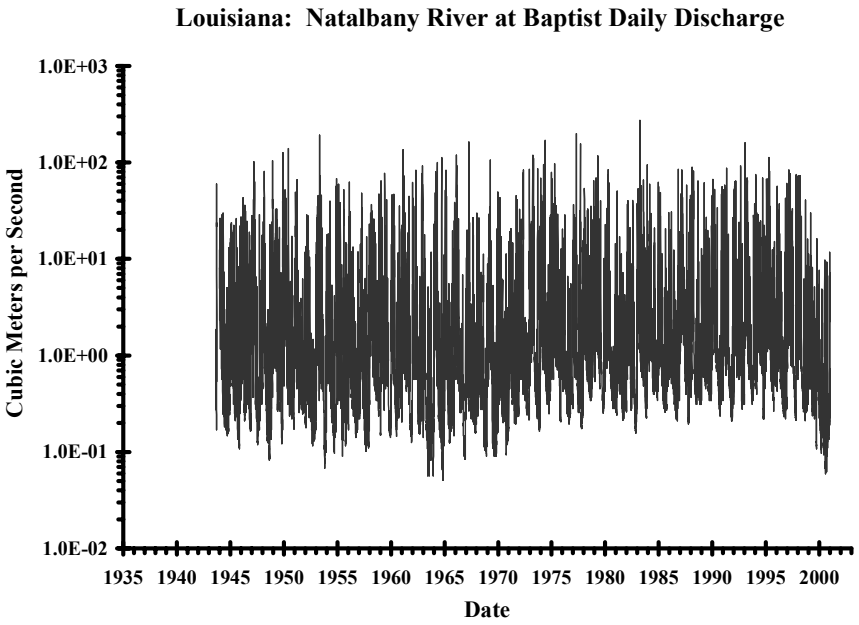

Figure C-29. Daily data from the USGS streamflow station 2489500, Pearl River near Bogalusa, Louisiana.

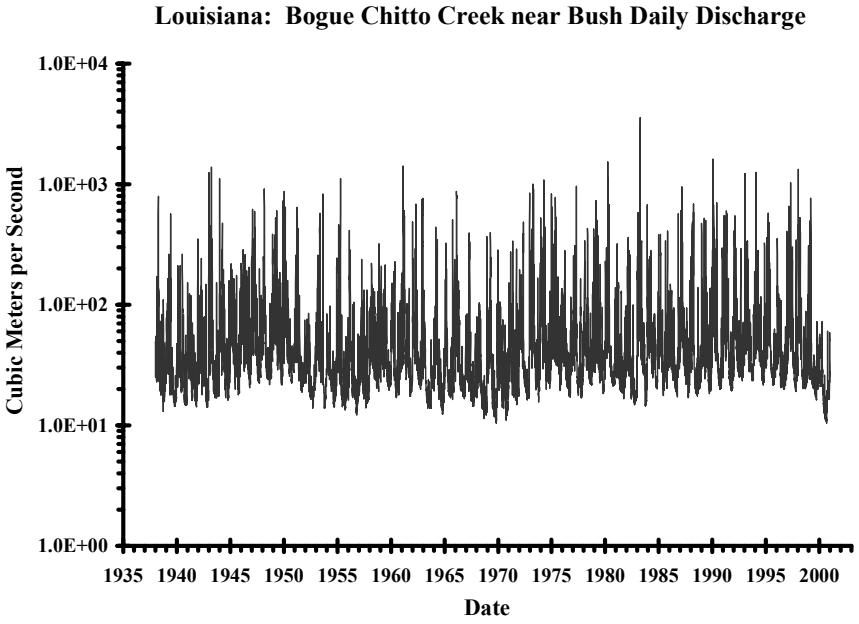

Figure C-30. Daily data from the USGS streamflow station 2492000, Bogue Chitto near Bush, Louisiana.

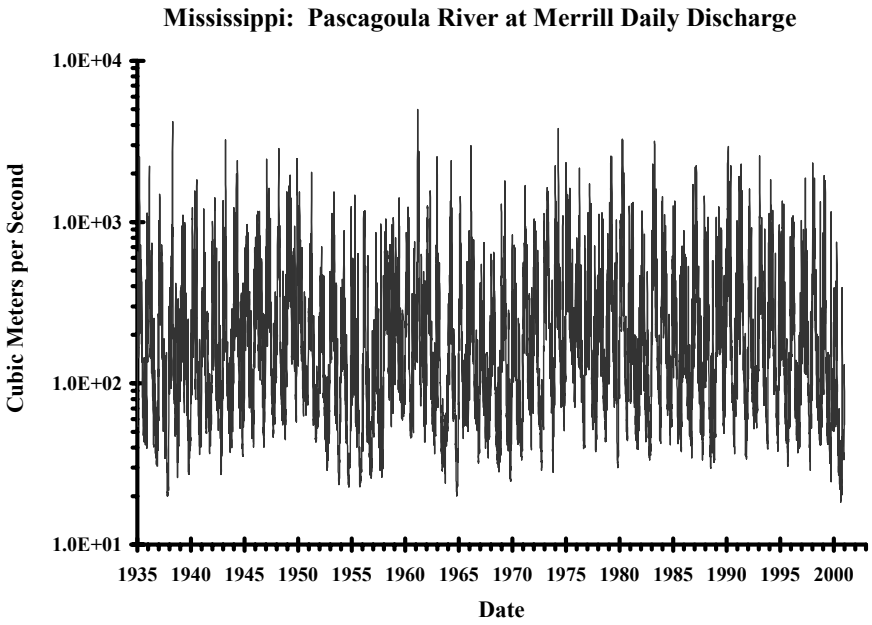

Figure C-31. Daily data from the USGS streamflow station 2479000, Pascagoula River at Merrill, Mississippi.

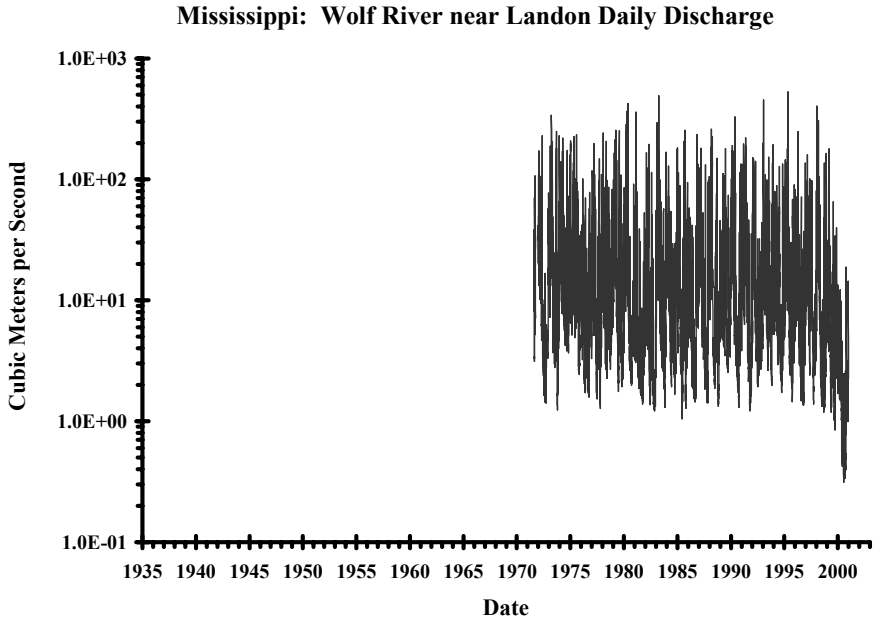

Figure C-32. Daily data from the USGS streamflow station 2481510, Wolf River near Landon, Mississippi.

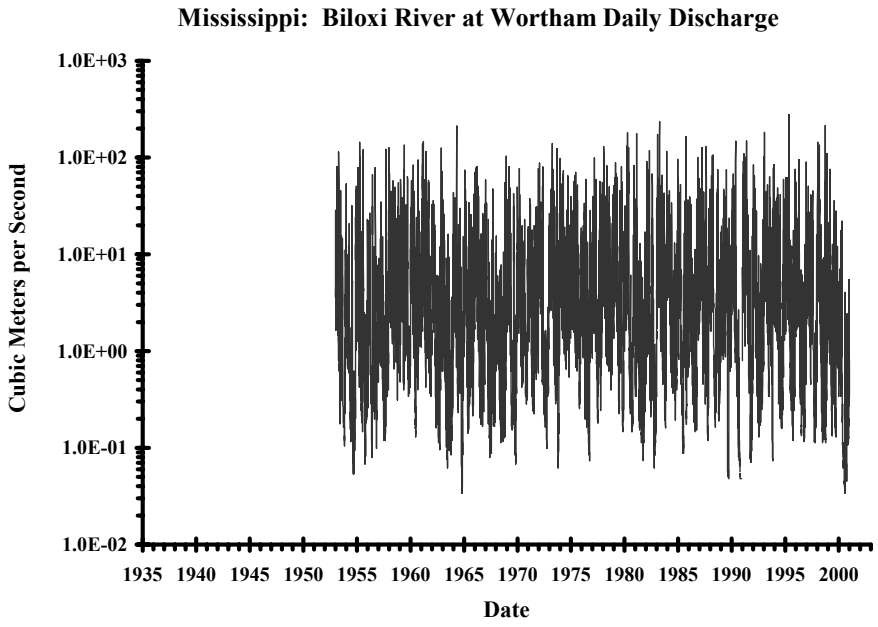

Figure C-33. Daily data from the USGS streamflow station 2481000, Biloxi River at Wortham, Mississippi.

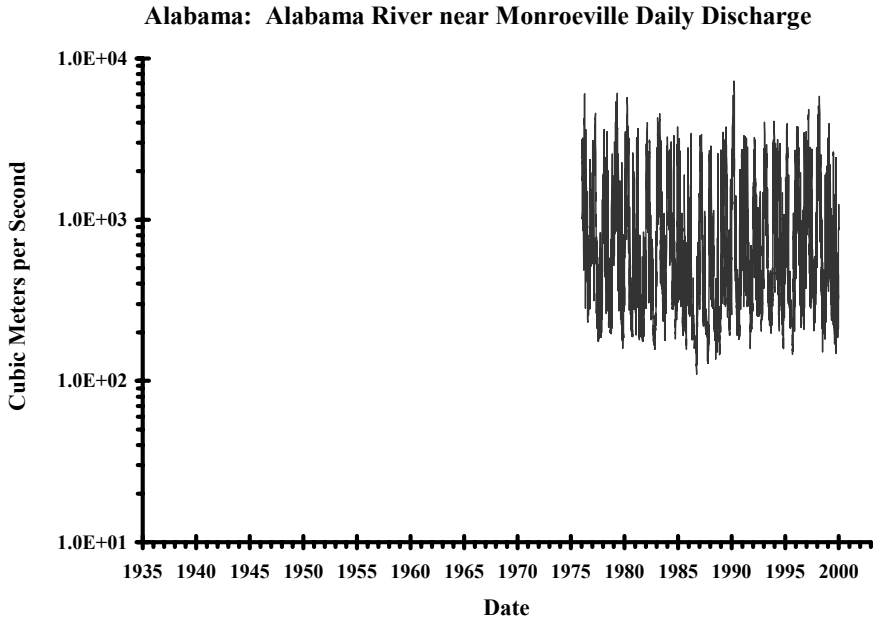

Figure C-34. Daily data from the USGS streamflow station 2428400, Alabama River near Monroeville, Alabama.

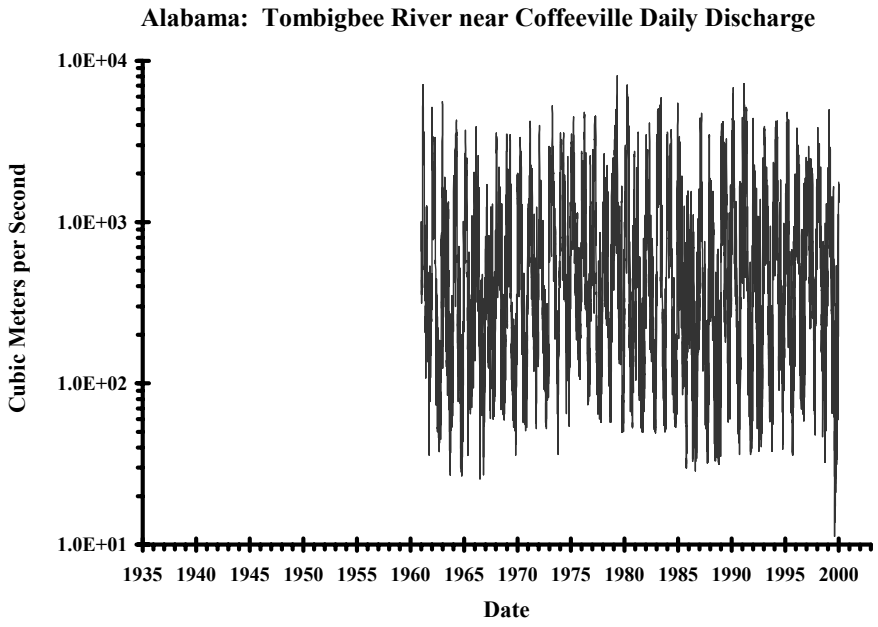

Figure C-35. Daily data from the USGS streamflow station 2469761, Tombigbee River near Coffeeville, Alabama.

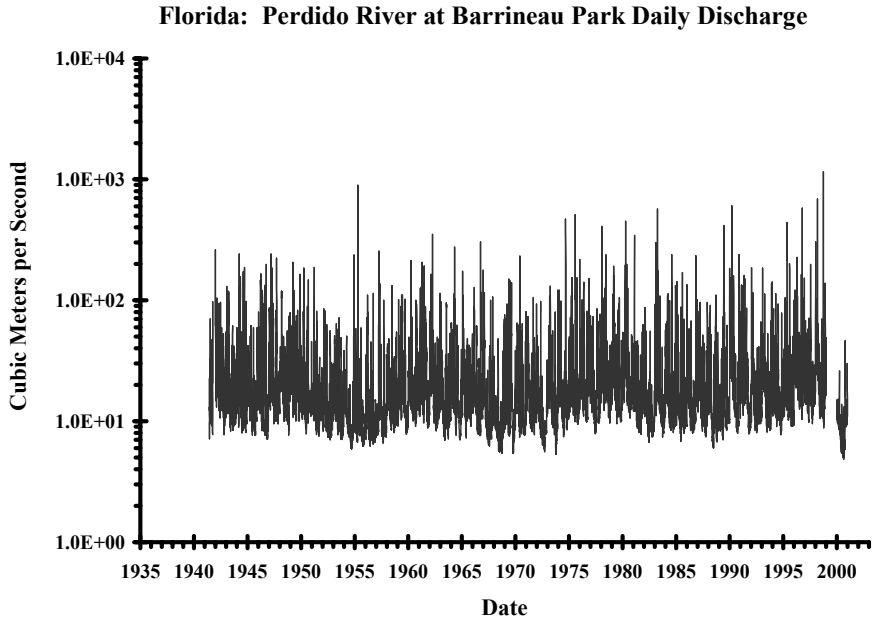

Figure C-36. Daily data from the USGS streamflow station 23765000, Perdido River at Barrineau Park, Florida.

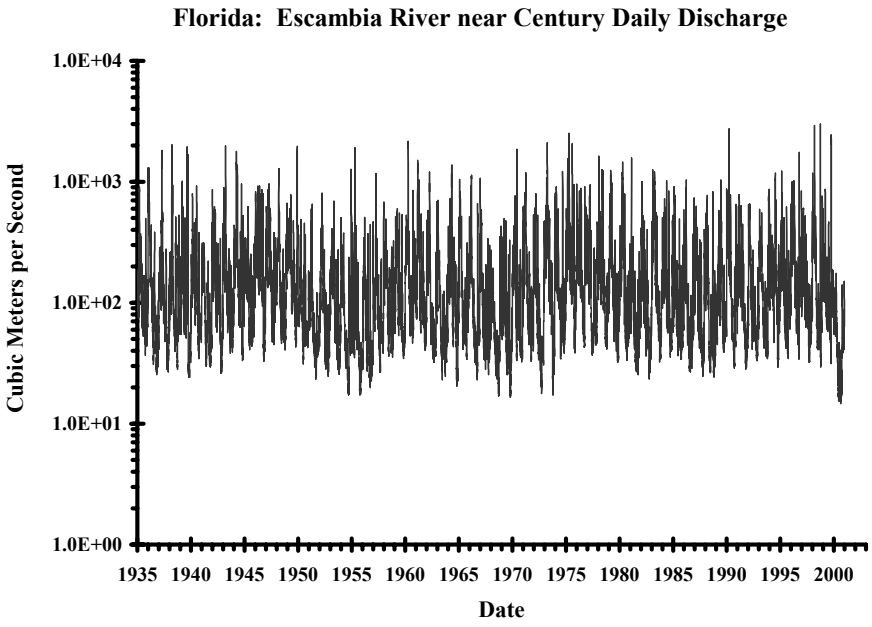

Figure C-37. Daily data from the USGS streamflow station 2375500, Escambia River near Century, Florida.

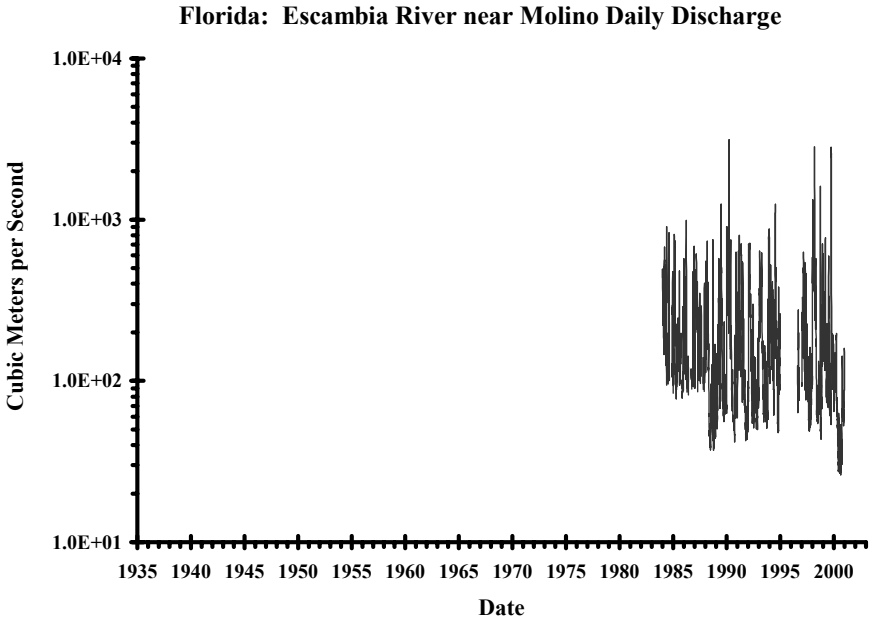

Figure C-38. Daily data from the USGS streamflow station 2376033, Escambia River near Molino, Florida.

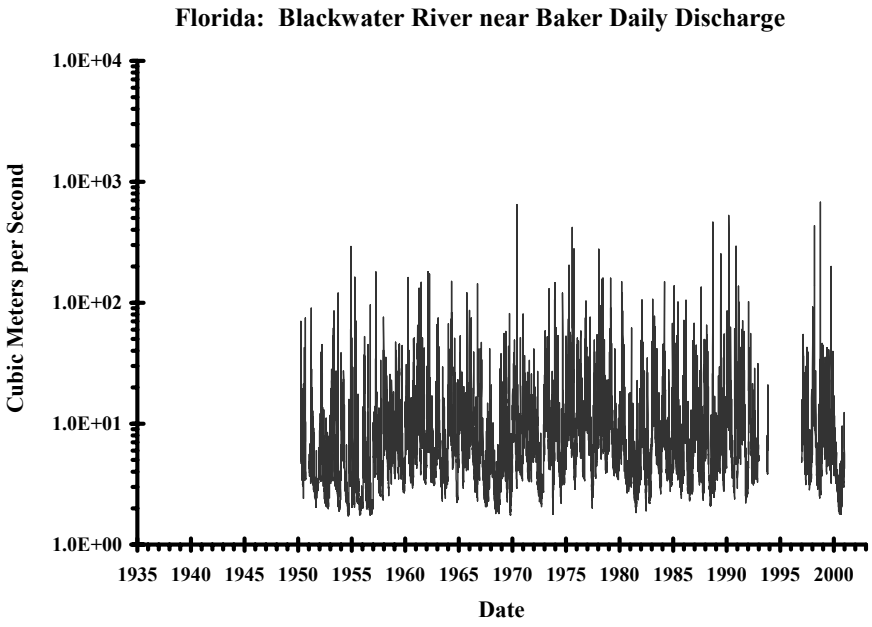

Figure C-39. Daily data from the USGS streamflow station 2370000, Blackwater River near Baker, Florida.

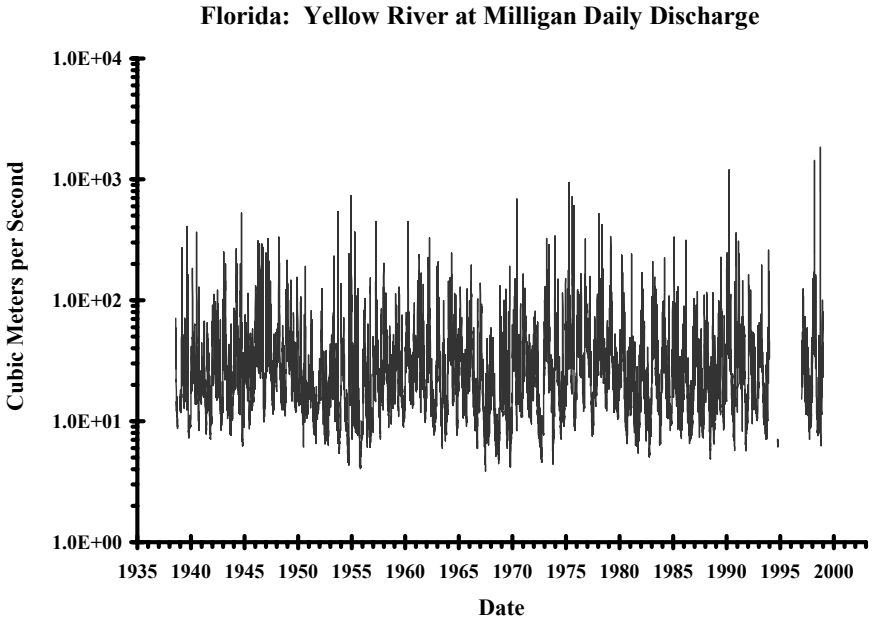

Figure C-40. Daily data from the USGS streamflow station 2368000, Yellow River at Milligan, Florida.

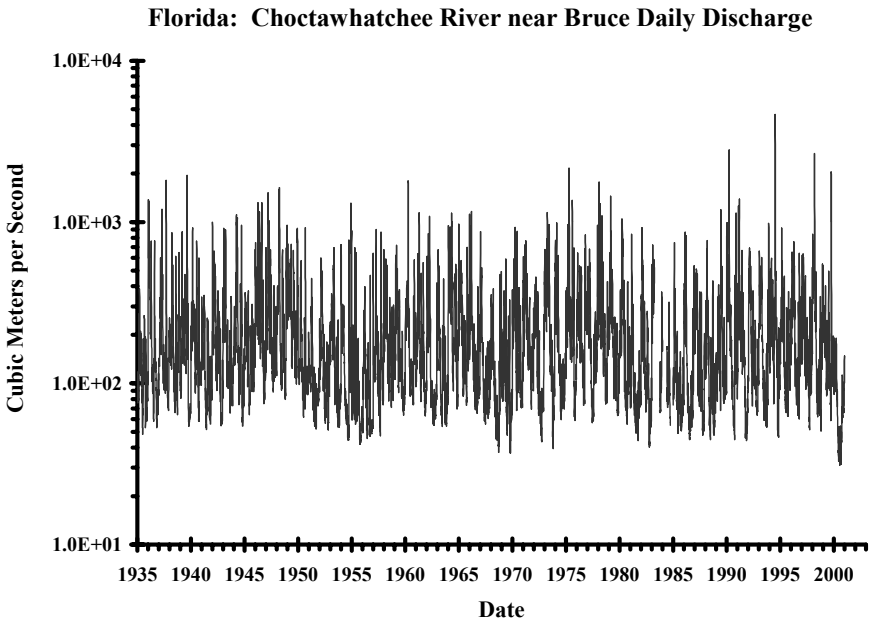

Figure C-41. Daily data from the USGS streamflow station 2366500, Choctawhatchee River near Bruce, Florida.

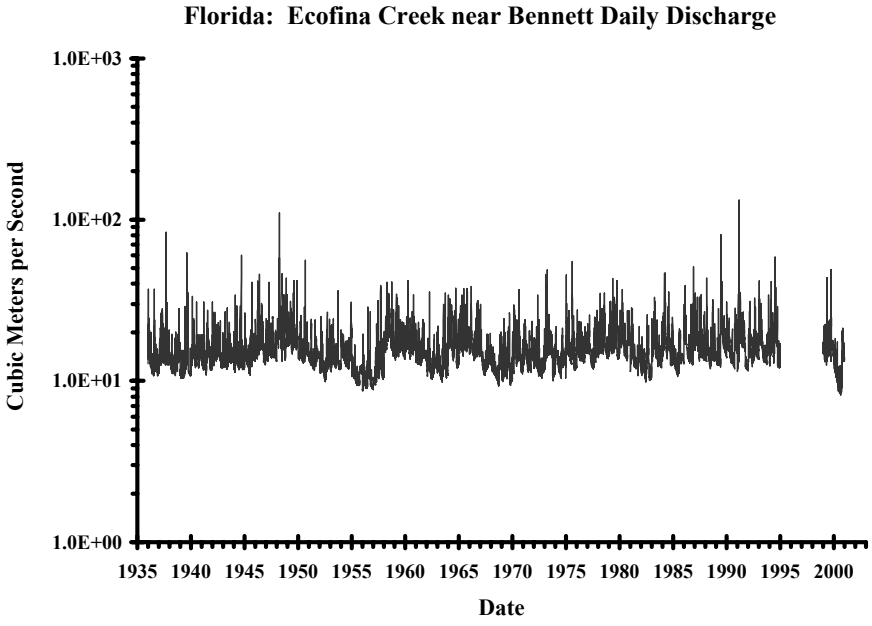

Figure C-42. Daily data from the USGS streamflow station 2359500, Ecofina Creek near Bennett, Florida.

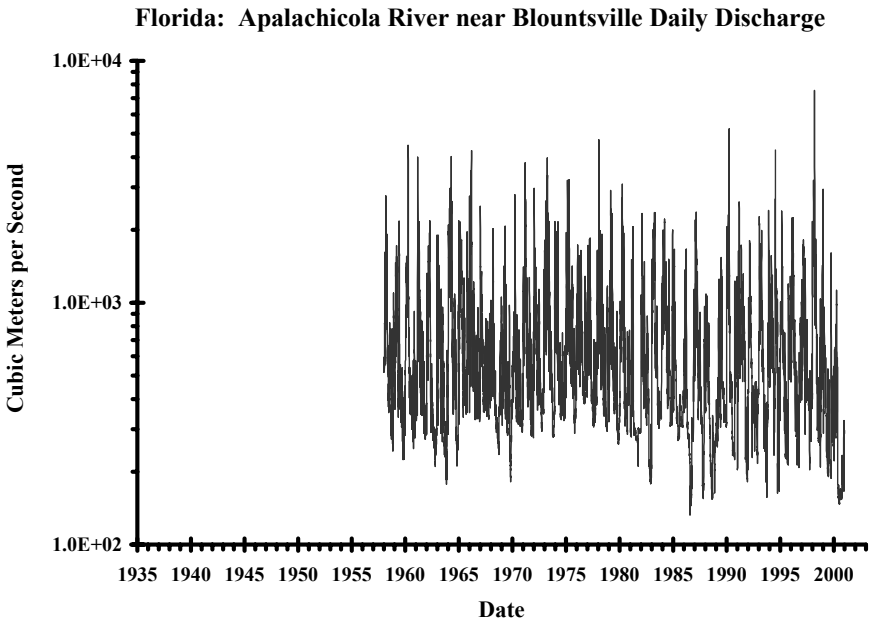

Figure C-43. Daily data from the USGS streamflow station 2358700, Apalachicola River near Blontsville, Florida.

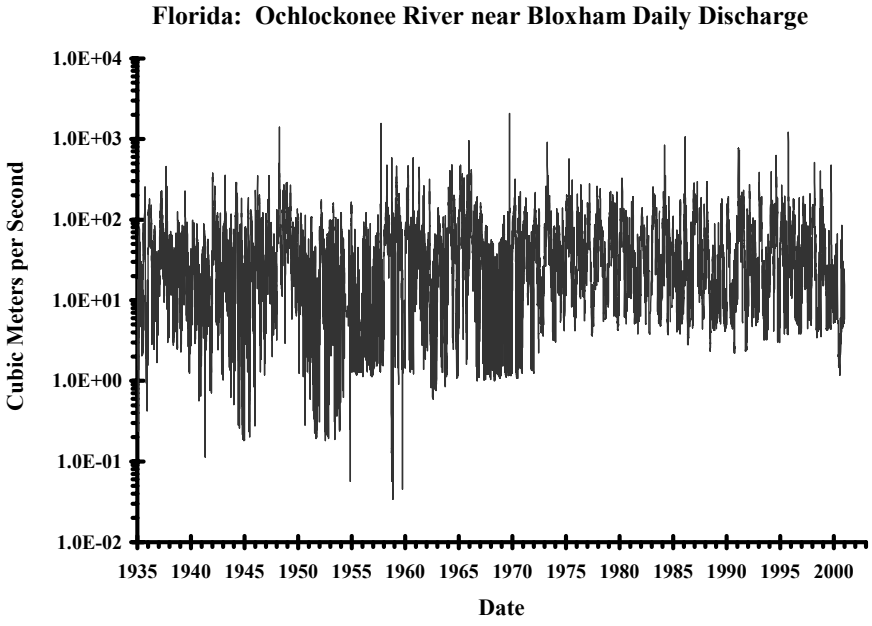

Figure C-44. Daily data from the USGS streamflow station 2330000, Ochlockonee River near Bloxham, Florida.

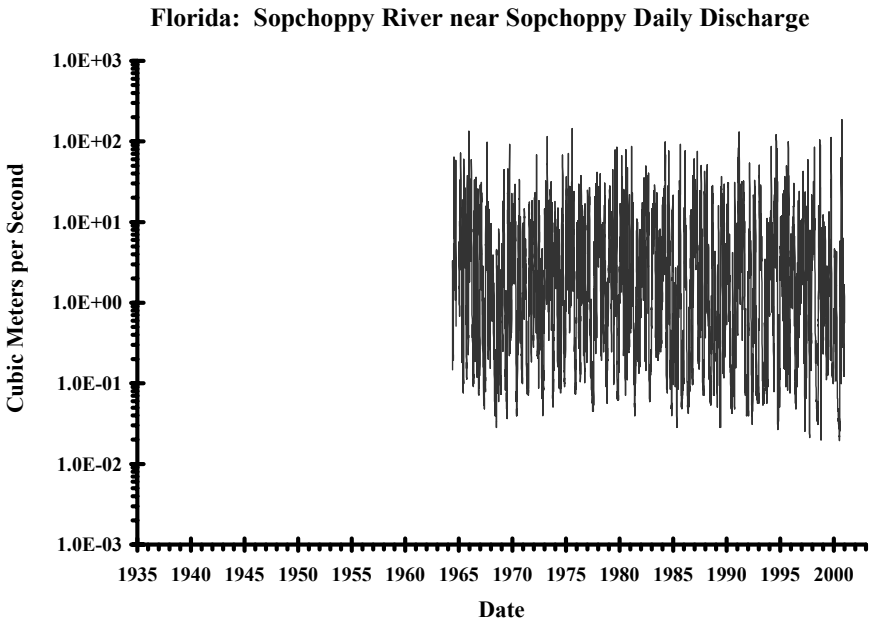

Figure C-45. Daily data from the USGS streamflow station 2327100, Sopchoppy River near Sopchoppy, Florida.

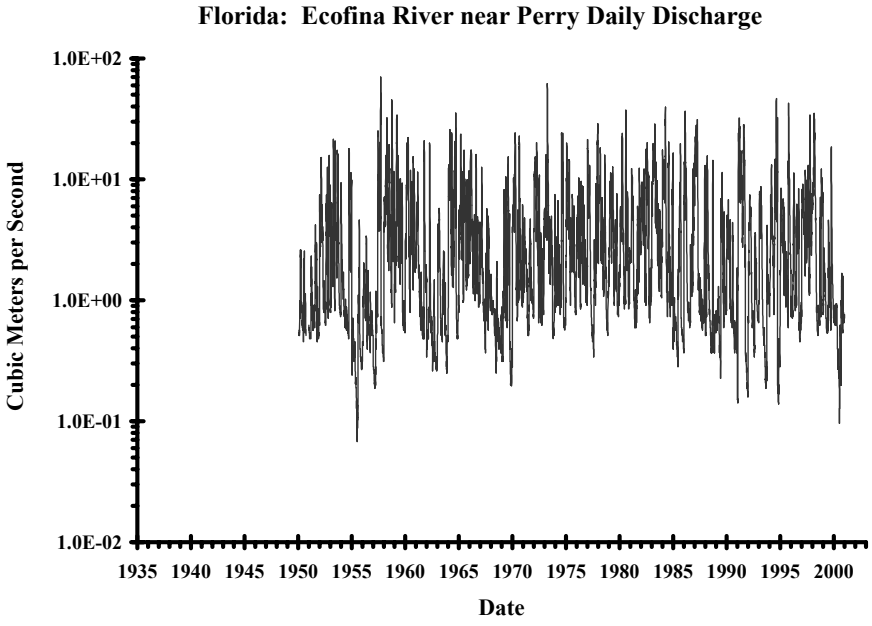

Figure C-46. Daily data from the USGS streamflow station 2326000, Ecofina River near Perry, Florida.

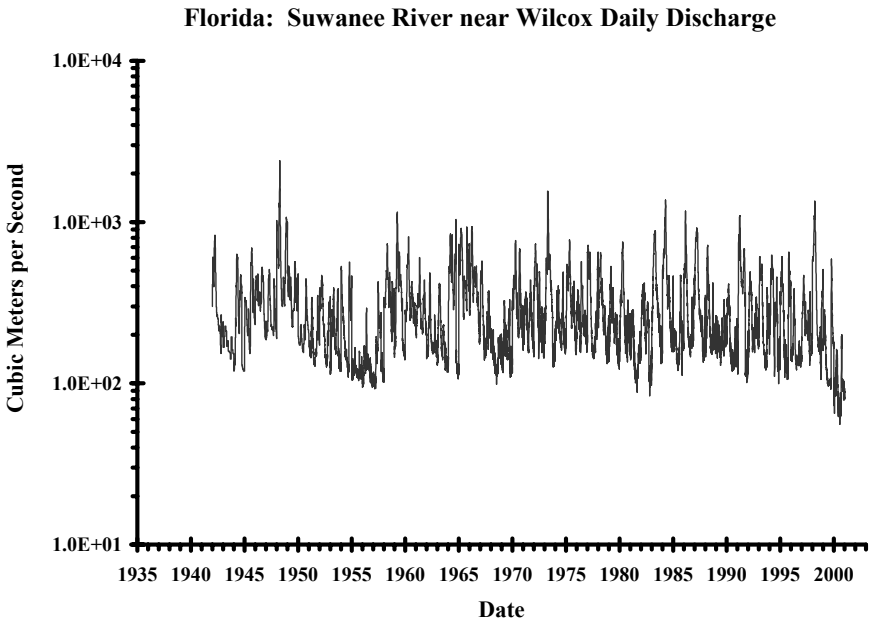

Figure C-47. Daily data from the USGS streamflow station 2323500, Suwanee River near Wilcox, Florida.

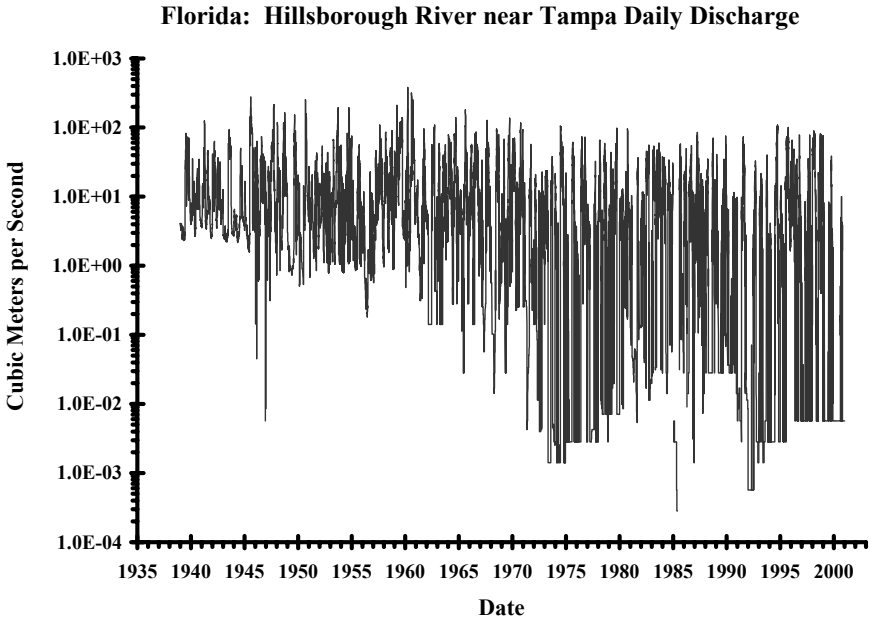

Figure C-48. Daily data from the USGS streamflow station 2304500, Hillsborough River near Tampa, Florida.

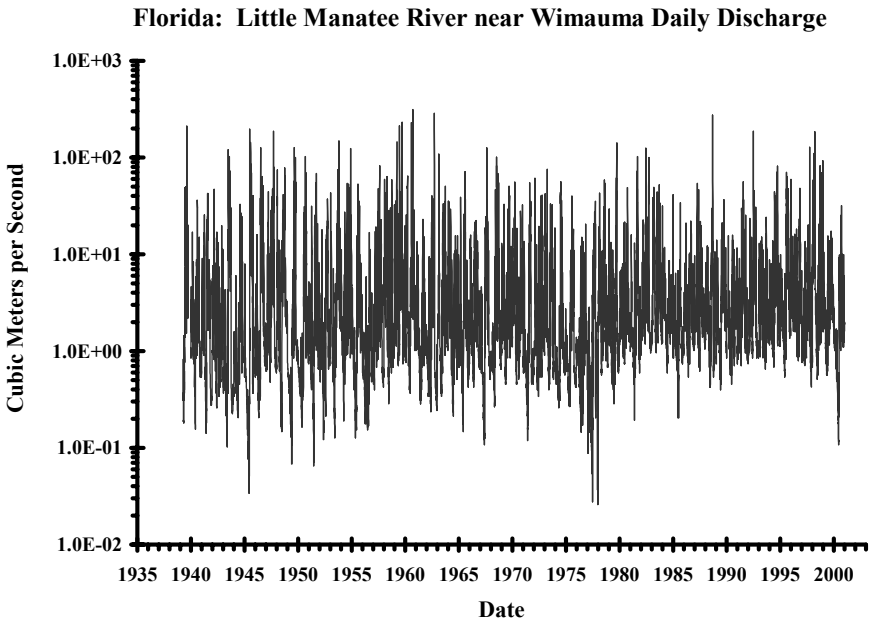

Figure C-49. Daily data from the USGS streamflow station 2300500, Little Manatee River near Wimauma, Florida.

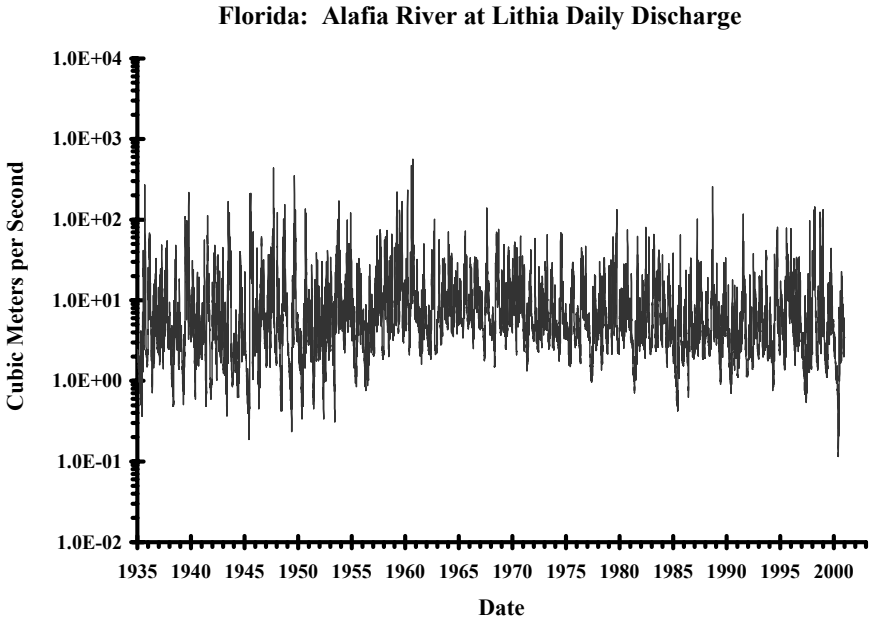

Figure C-50. Daily data from the USGS streamflow station 2301500, Alafia River at Lithia, Florida.

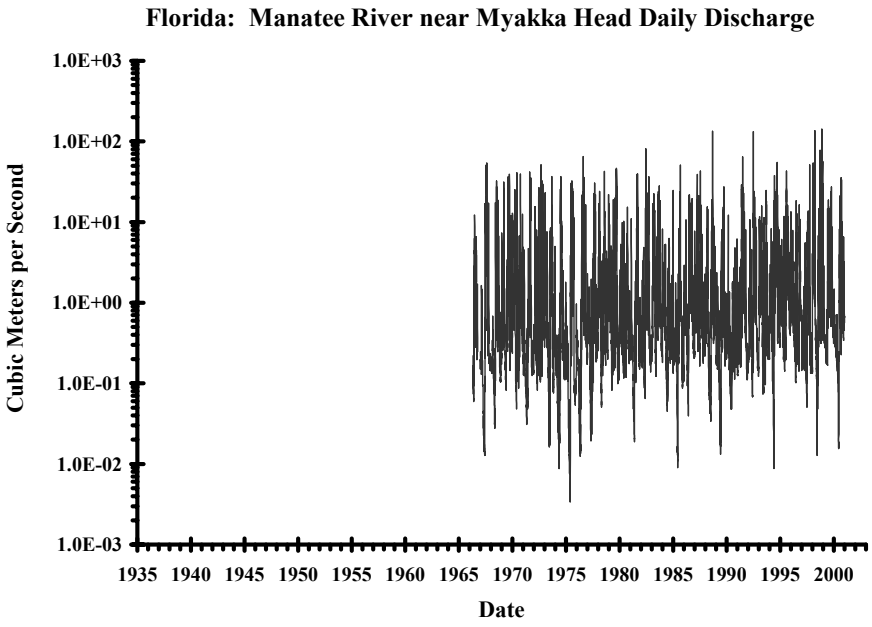

Figure C-51. Daily data from the USGS streamflow station 2299950, Manatee River near Myakka Head, Florida.

Appendix D: Mean Monthly Water Level Plots.

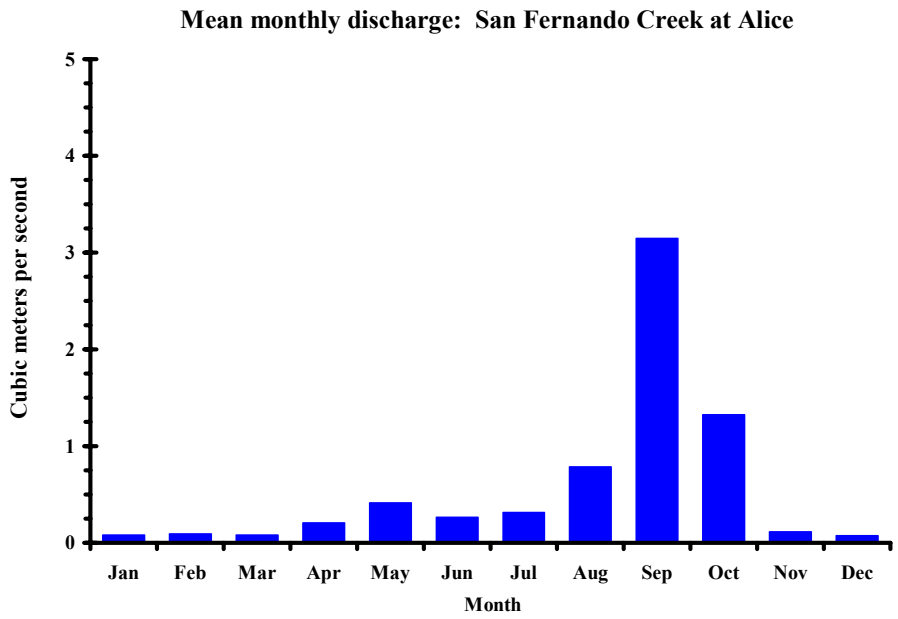

Figure D-1. Mean monthly data from the USGS streamflow station 8211900, San Fernando Creek at Alice, Texas.

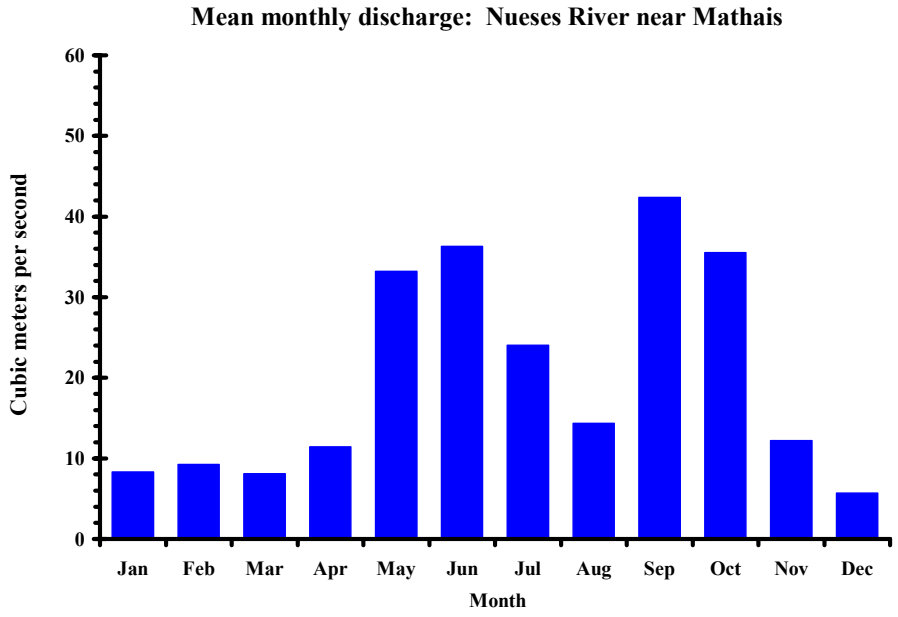

Figure D-2. Mean monthly data from the, Nueses River near Mathais, Texas.

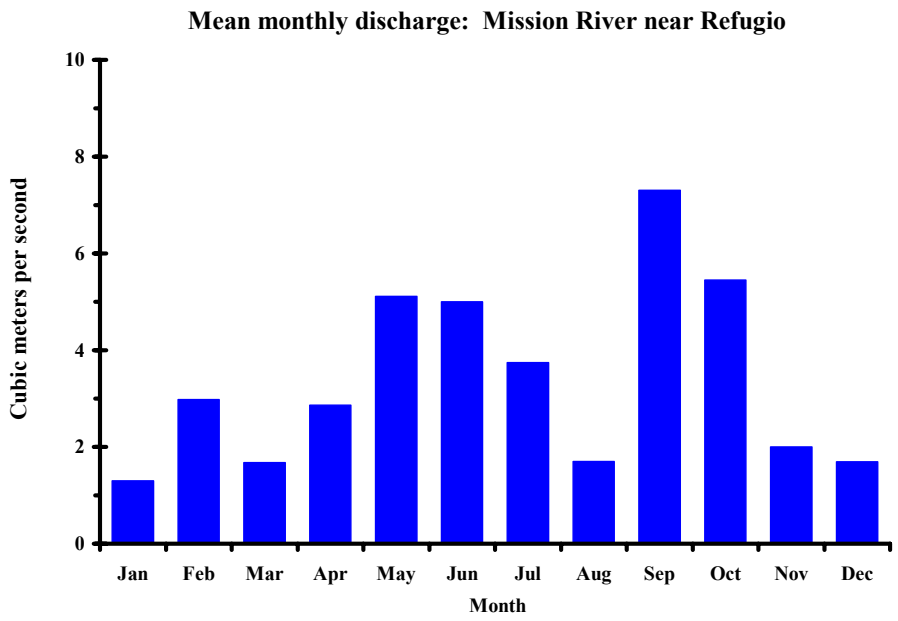

Figure D-3. Mean monthly data from the USGS streamflow station 8189500, Mission River near Refugio, Texas.

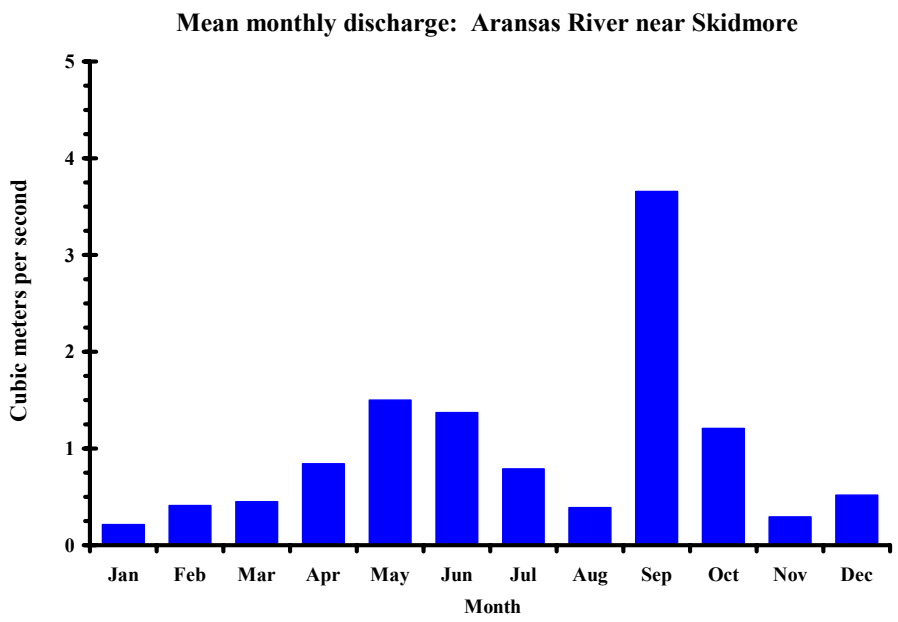

Figure D-4. Mean monthly data from the USGS streamflow station 8189700, Aransas River near Skidmore, Texas.

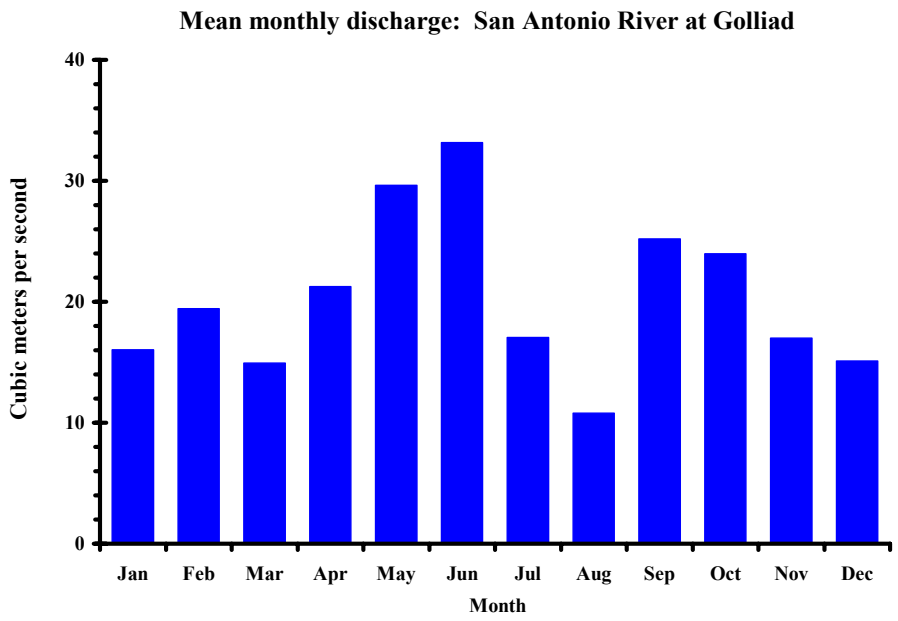

Figure D-5. Mean monthly data from the USGS streamflow station 8188500, San Antonio Rivera at Golliad, Texas.

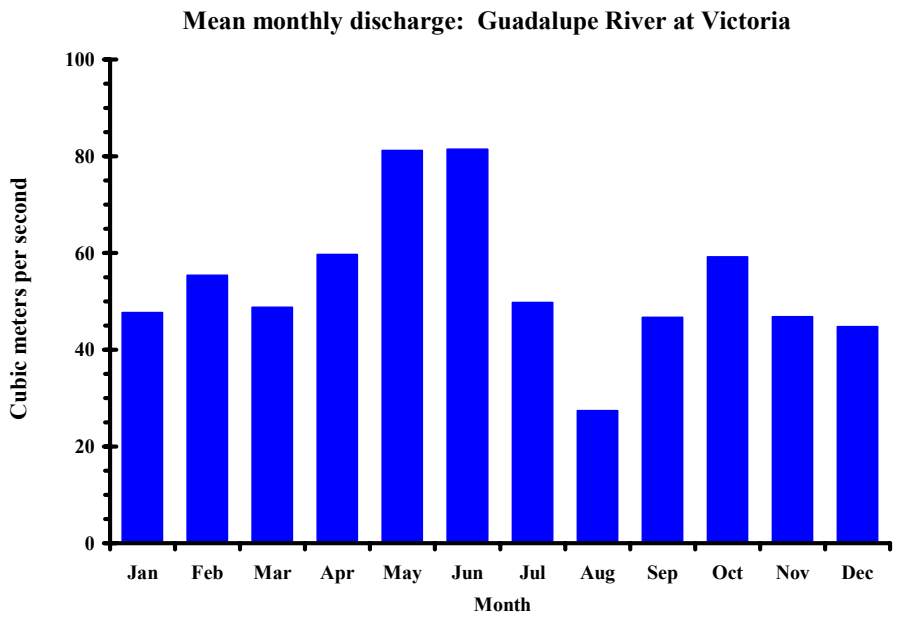

Figure D-6. Mean monthly data from the USGS streamflow station 8176500, Guadalupe River at Victoria, USGS streamflow station 8211000Texas.

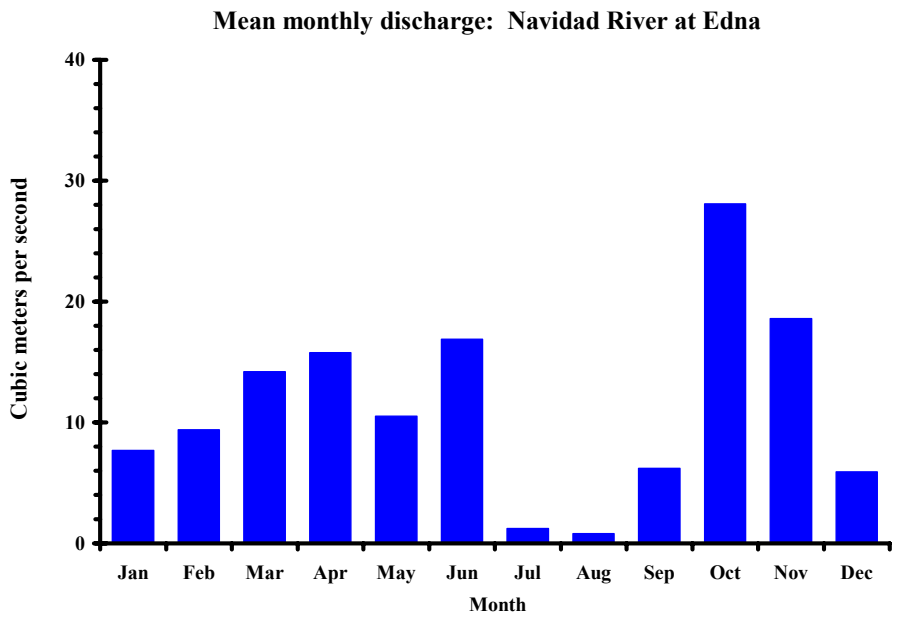

Figure D-7. Mean monthly data from the USGS streamflow station 8164390, Navidad River at Edna, Texas.

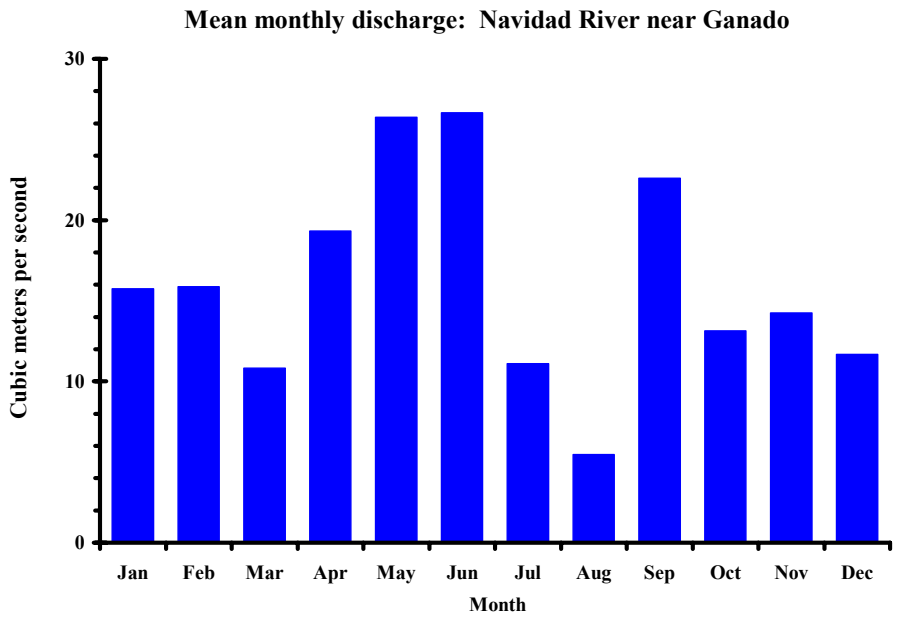

Figure D-8. Mean monthly data from the USGS streamflow station 8164500, Navidad River near Ganado, Texas.

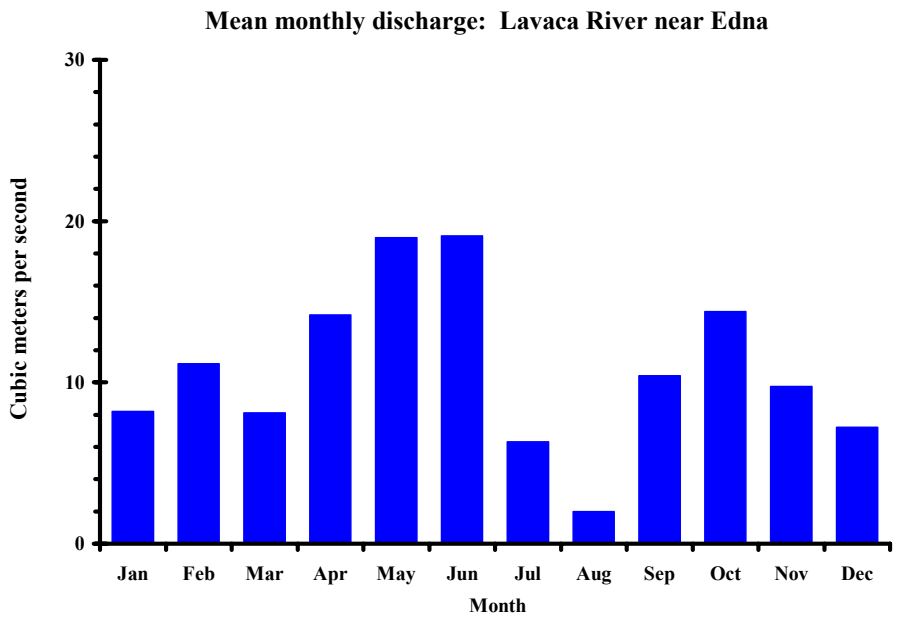

Figure D-9. Mean monthly data from the USGS streamflow station 8164000, Lavaca River near Edna, Texas.

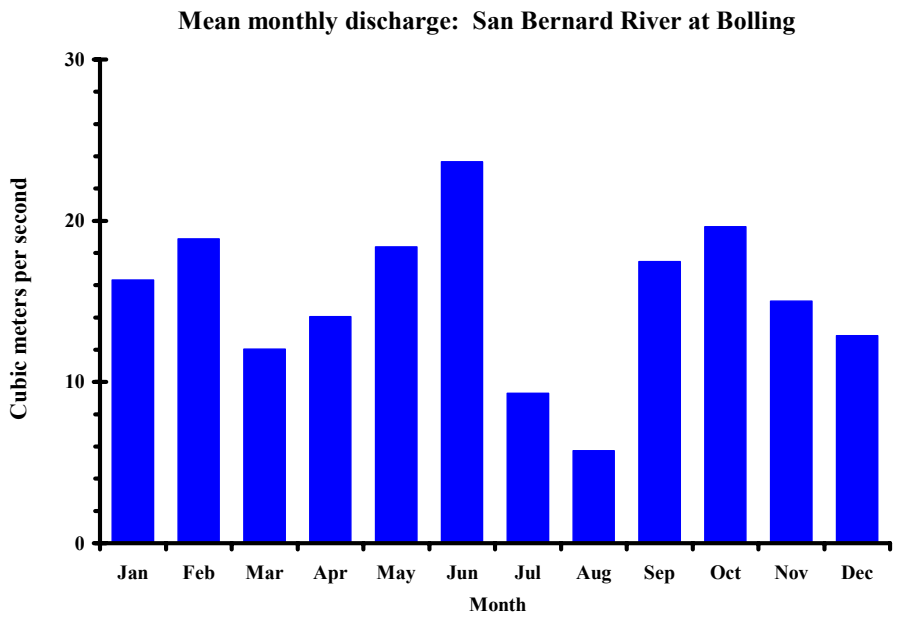

Figure D-10. Mean monthly data from the USGS streamflow station 8117500, San Bernard River at Bolling, Texas.

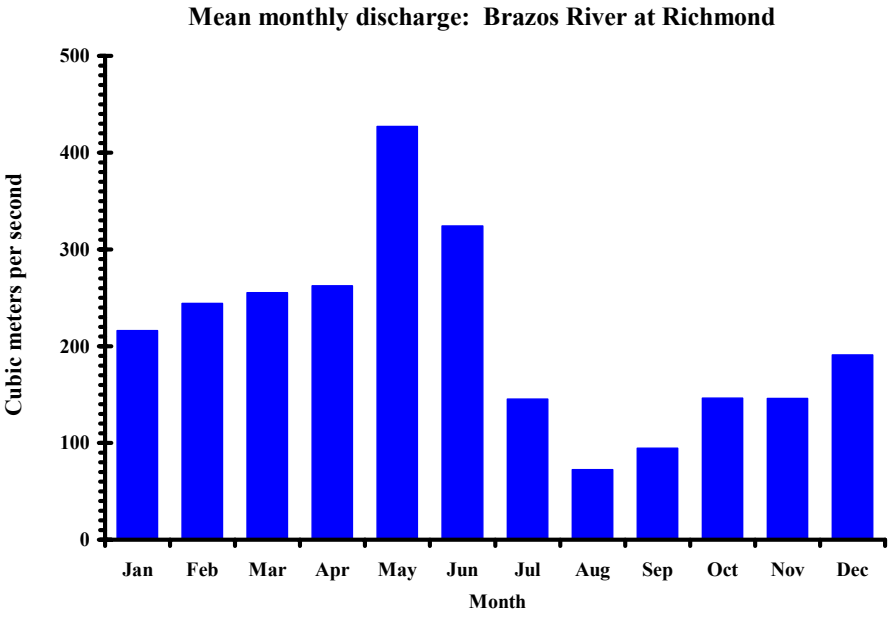

Figure D-11. Mean monthly data from the USGS streamflow station 8114000, Brazos River at Richmond, Texas.

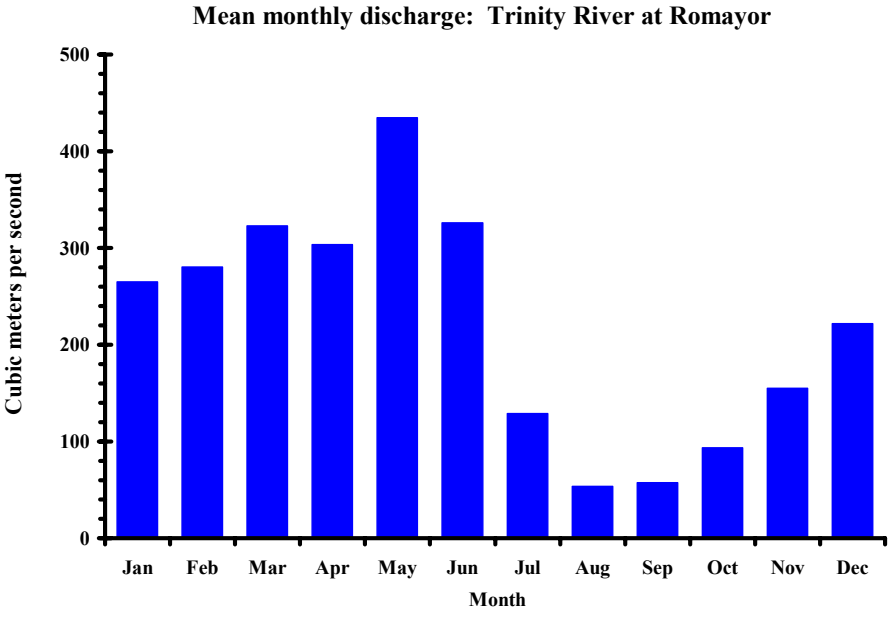

Figure D-12. Mean monthly data from the USGS streamflow station 8066500, Trinity River at Romayor, Texas.

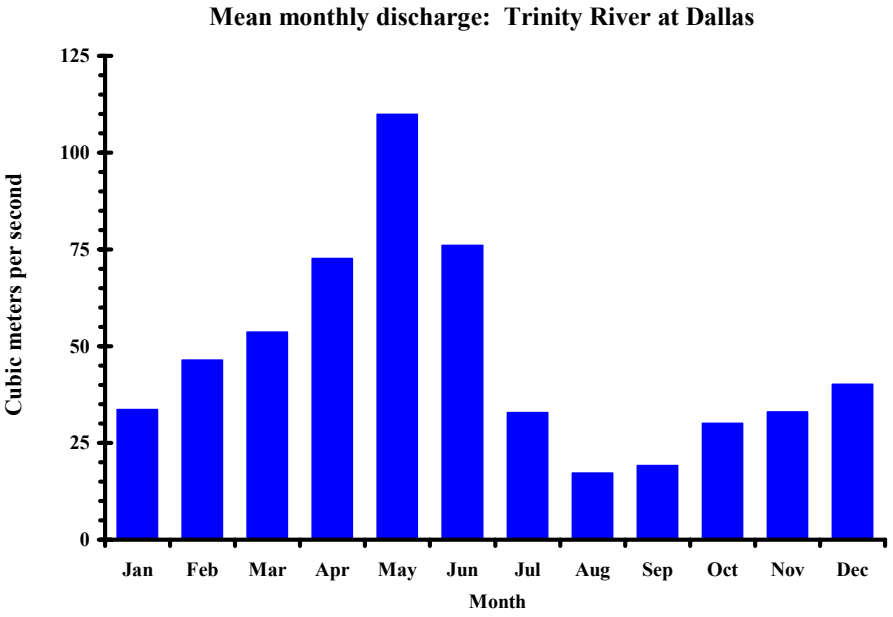

Figure D-13. Mean monthly data from the USGS streamflow station 8057000, Trinity River at Dallas, Texas.

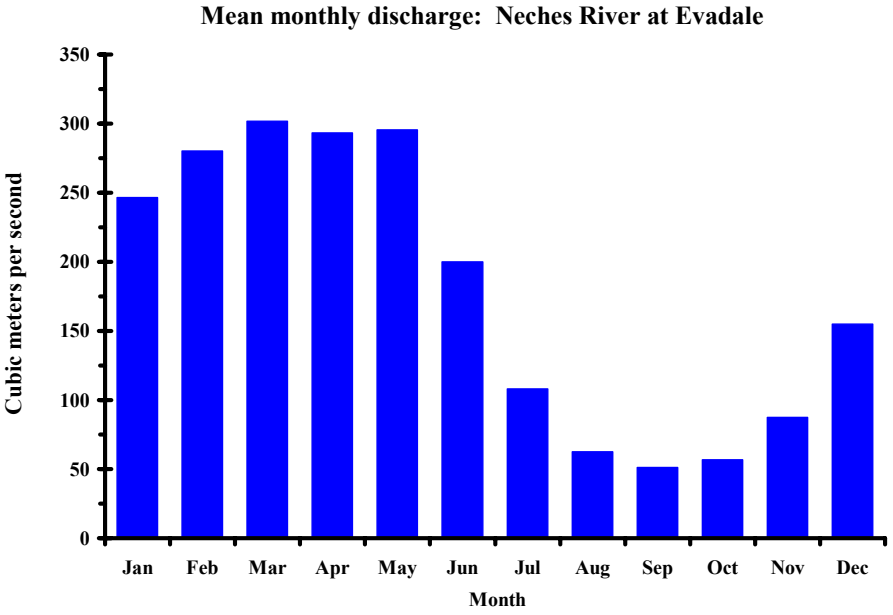

Figure D-14. Mean monthly data from the USGS streamflow station 8041000, Neches River at Evadale, Texas.

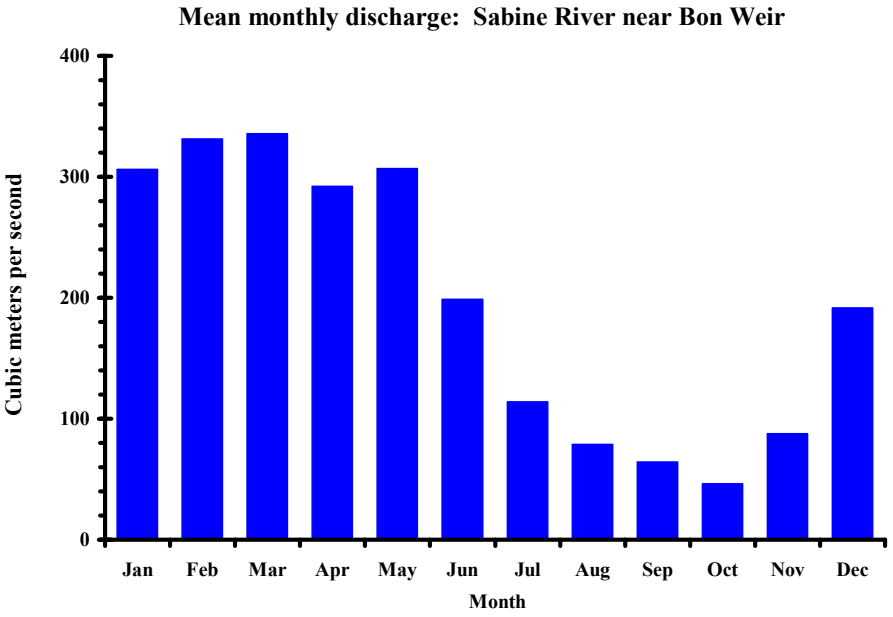

Figure D-15. Mean monthly data from the USGS streamflow station 8028500, Sabine River near Bon Weir, Texas.

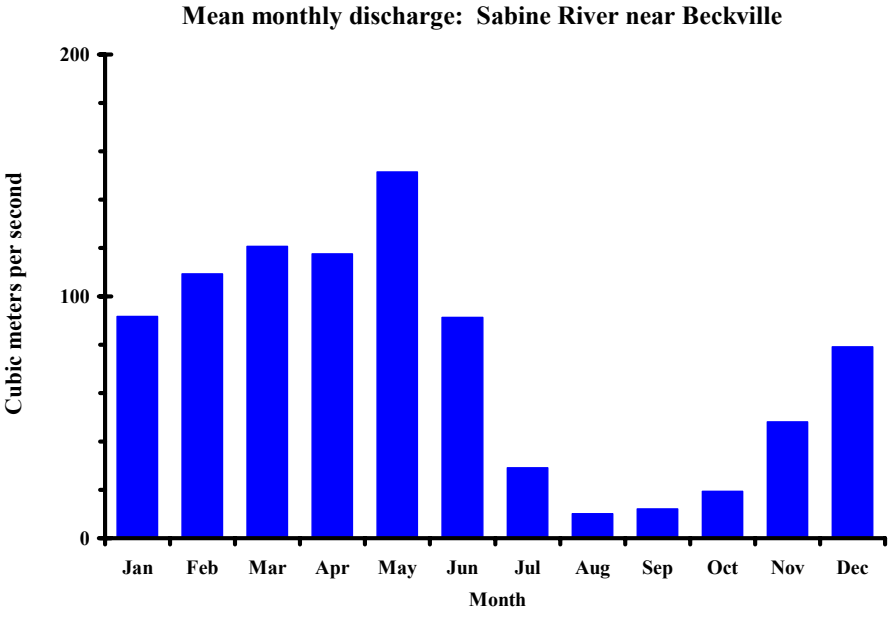

Figure D-16. Mean monthly data from the USGS streamflow station 8022040, Sabine River near Beckville, Texas.

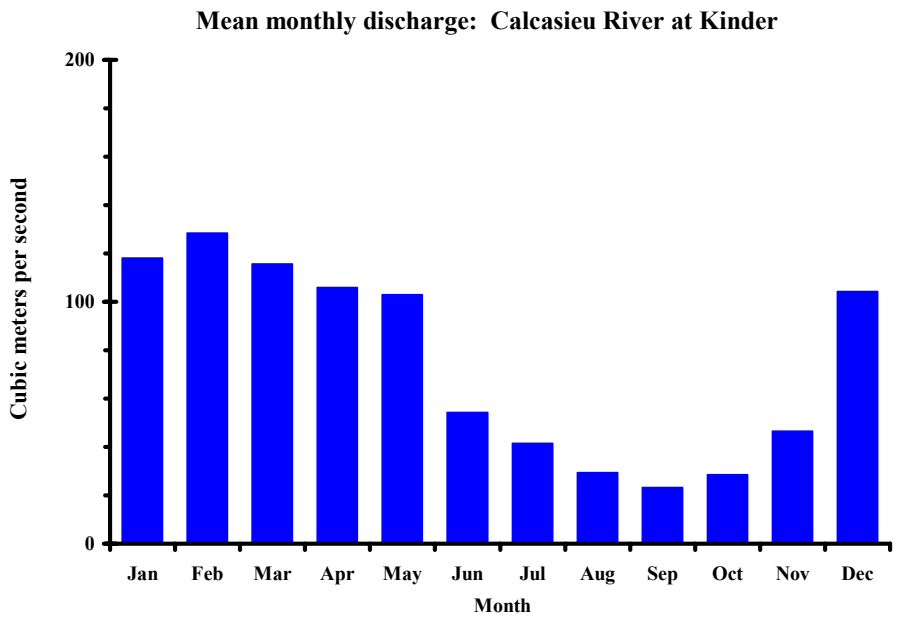

Figure D-17. Mean monthly data from the USGS streamflow station 8015500, Calcasieu River at Kinder, Louisiana.

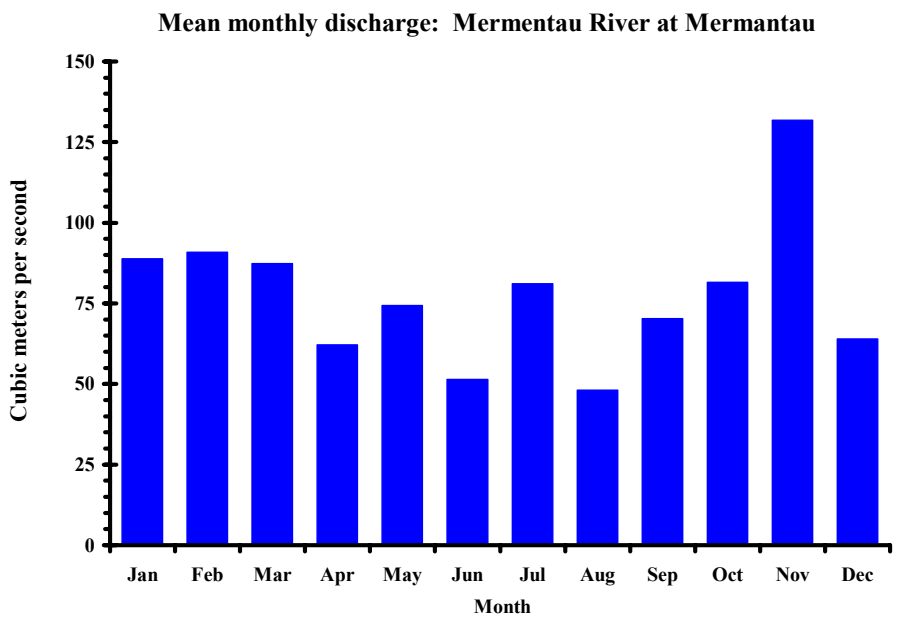

Figure D-18. Mean monthly data from the USGS streamflow station 8012150, Mermentau River at Mermentau, Louisiana.

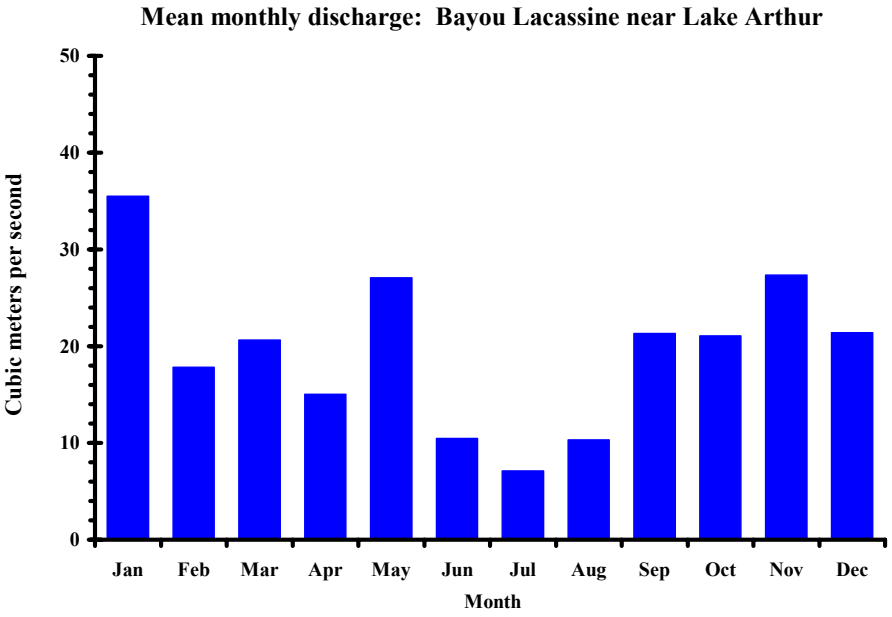

Figure D-19. Mean monthly data from the USGS streamflow station 8012470, Bayou Lacassine near Lake Arthur, Louisiana.

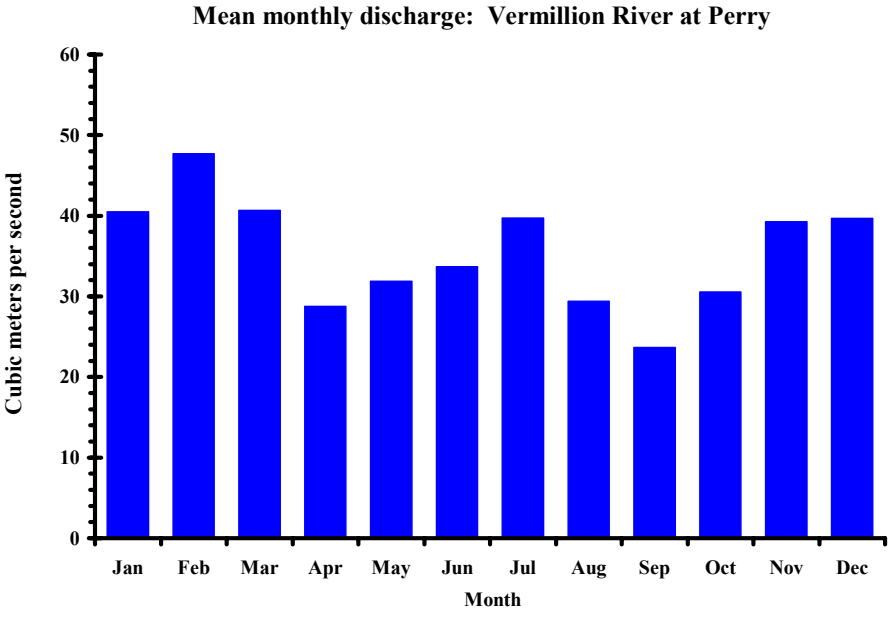

Figure D-20. Mean monthly data from the USGS streamflow station 7386980, Vermillion River at Perry, Louisiana.

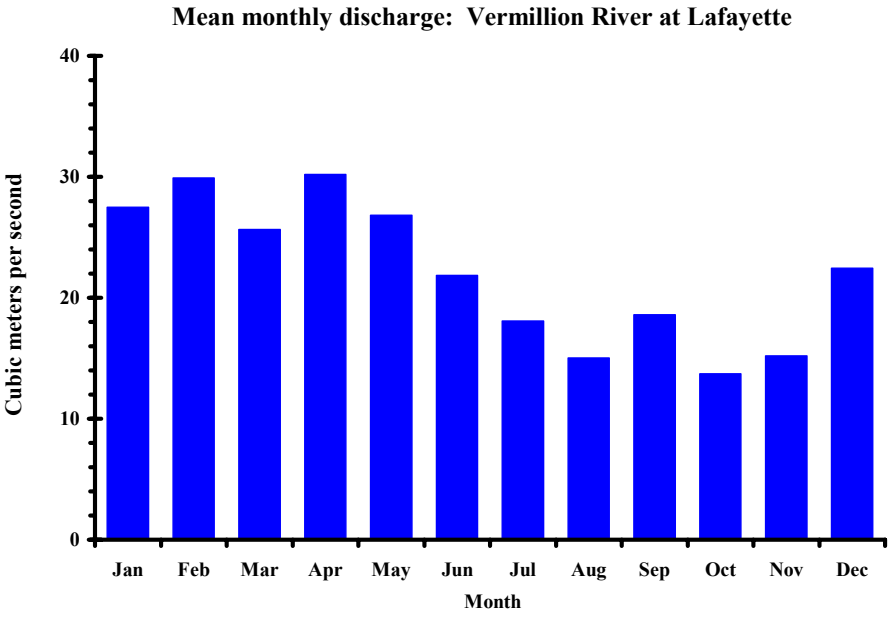

Figure D-21. Mean monthly data from the USGS streamflow station 7386880, Vermillion River at Lafayette, Louisiana.

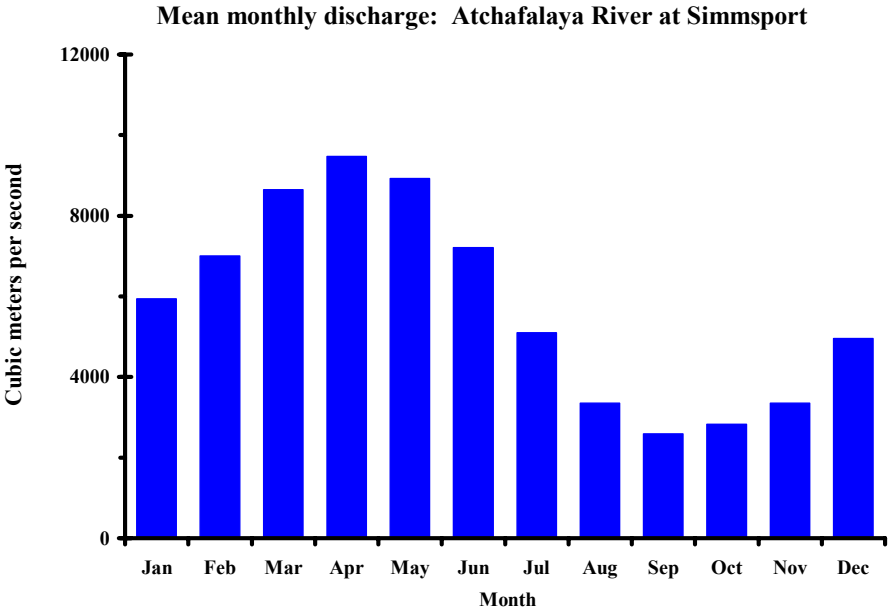

Figure D-22. Mean monthly data from the USCE streamflow station 3045, Atchafalaya River at Simmesport. Louisiana.

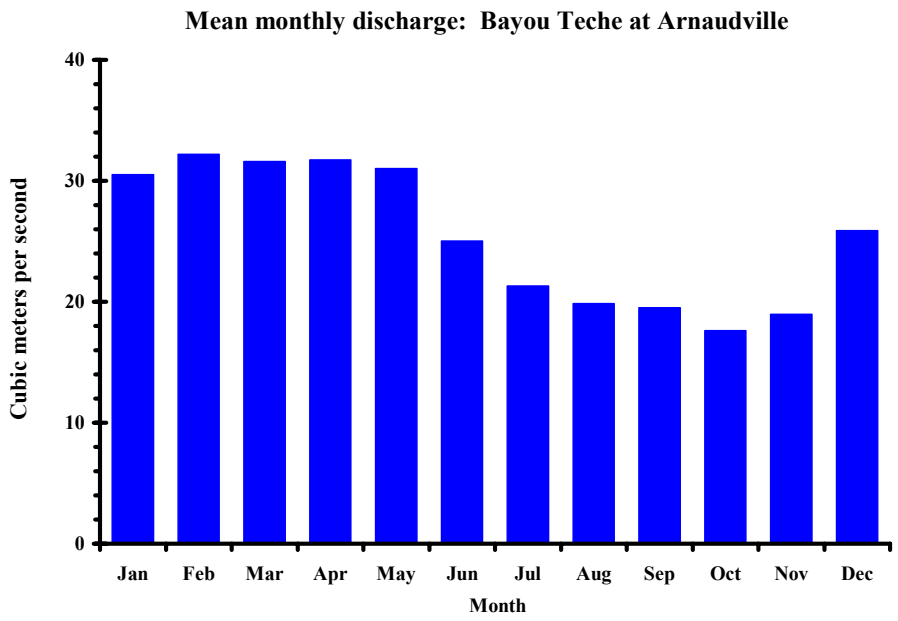

Figure D-23. Mean monthly data from the USGS streamflow station7 385500,Bayou Teche at Arnaudville, Louisiana.

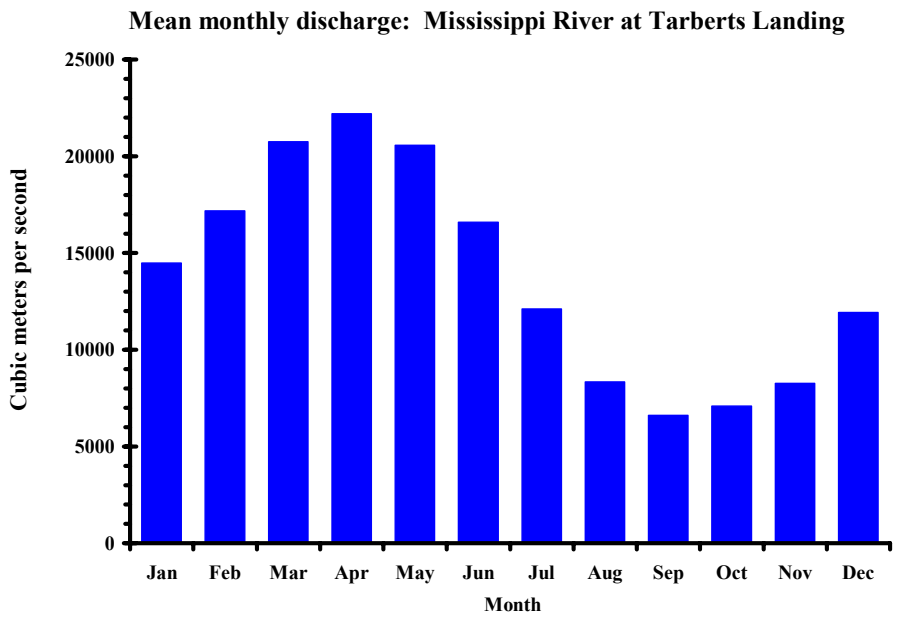

Figure D-24. Mean monthly data from the USCE streamflow 1100, station Mississippi River at Tarbert Landing, Mississippi.

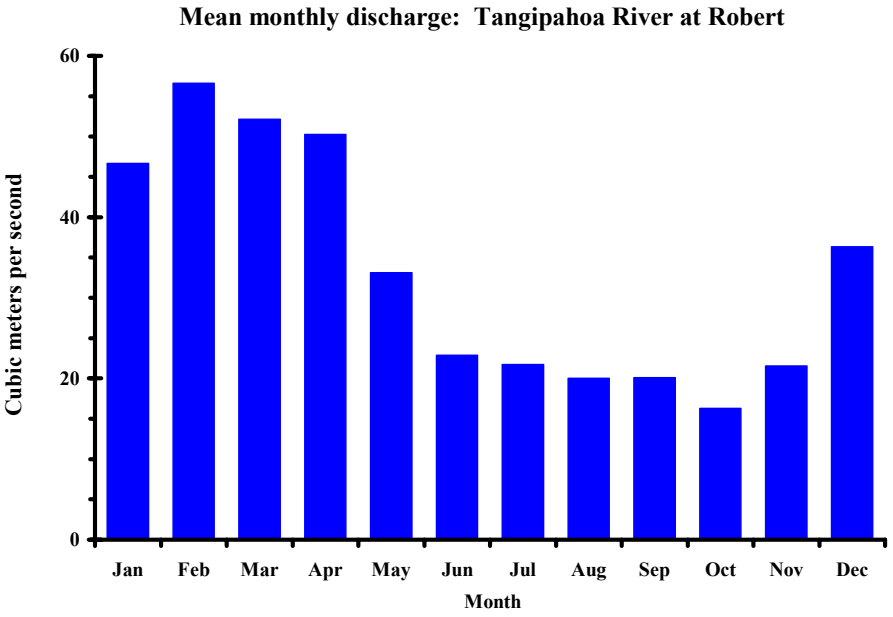

Figure D-25. Mean monthly data from the USGS streamflow station 7375500, Tangipahoa River at Robert, Louisiana.

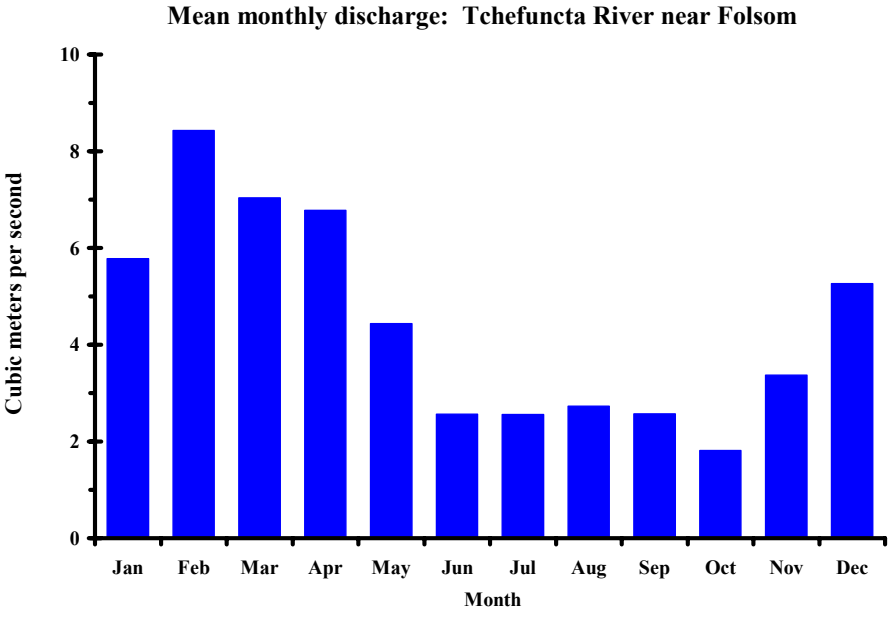

Figure D-26. Mean monthly data from the USGS streamflow station 7375000, Tchefuncta River near Folsom, Louisiana.

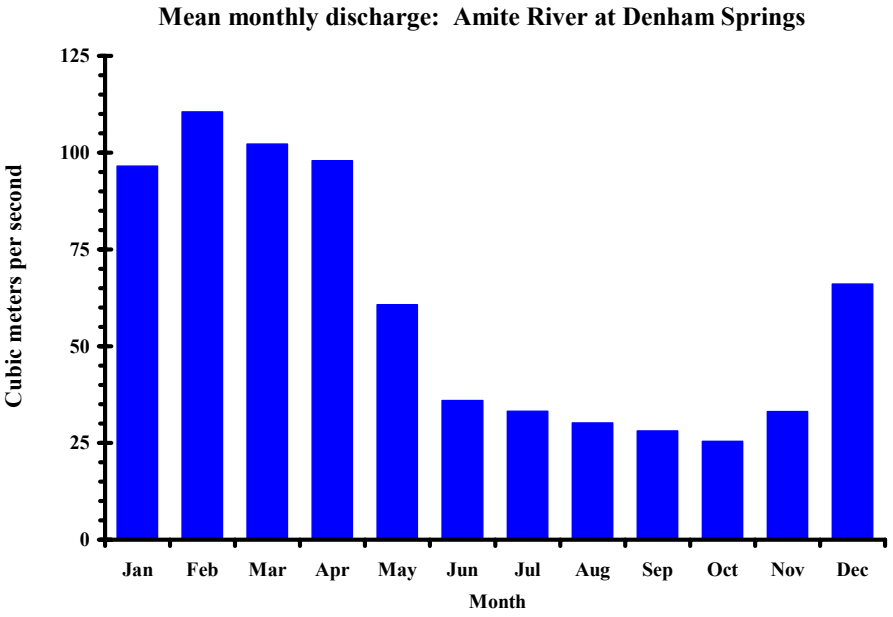

Figure D-27. Mean monthly data from the USGS streamflow station 7378500, Amite River near Denham Springs, Louisiana.

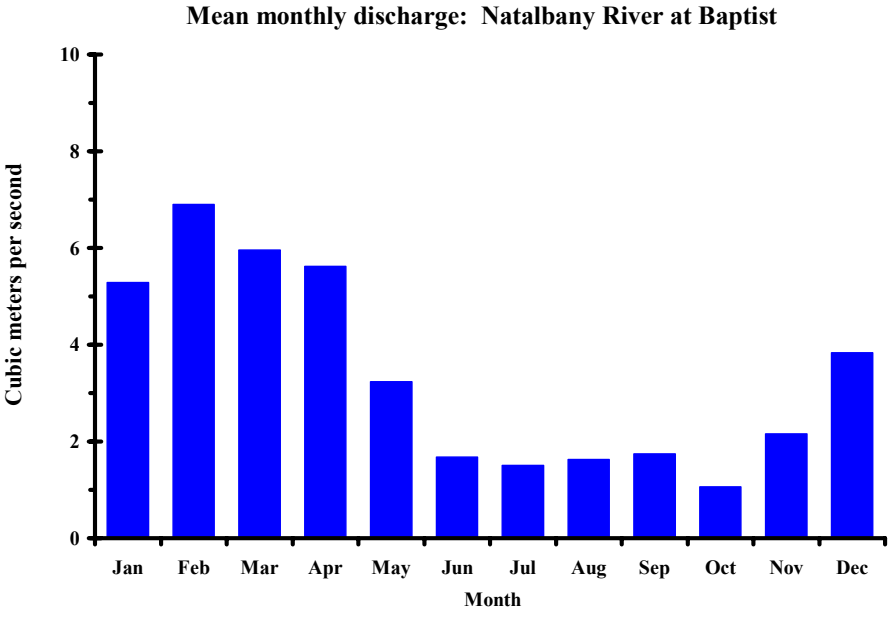

Figure D-28. Mean monthly data from the USGS streamflow station 7376500, Natalbany River at Baptist, Louisiana.

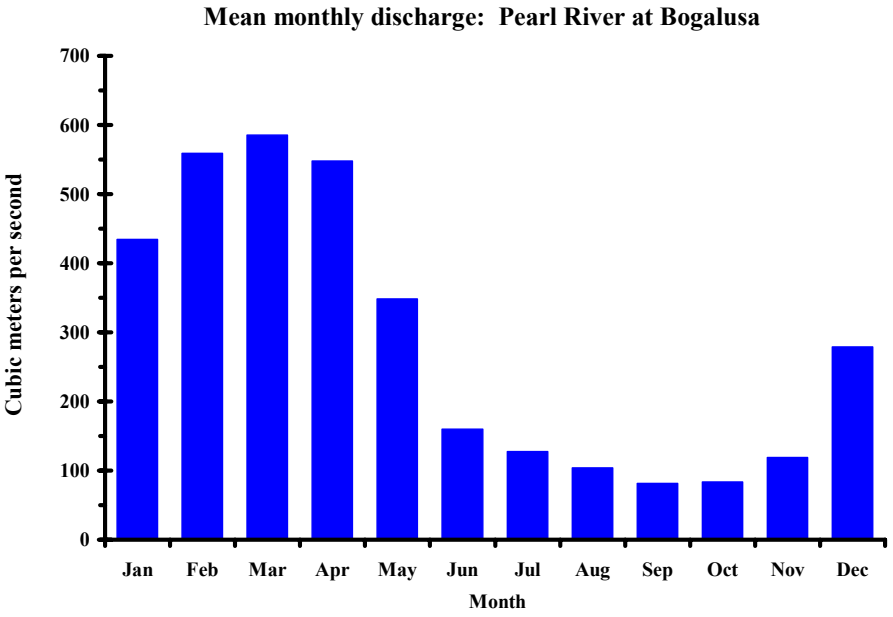

Figure D-29. Mean monthly data from the USGS streamflow station 2489500, Pearl River near Bogalusa, Louisiana.

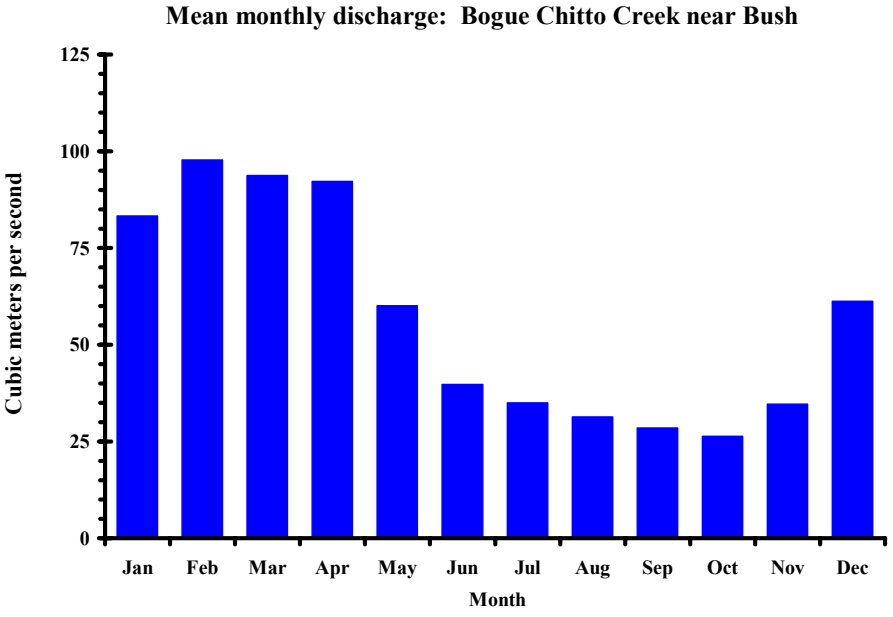

Figure D-30. Mean monthly data from the USGS streamflow station 2492000, Bogue Chitto near Bush, Louisiana.

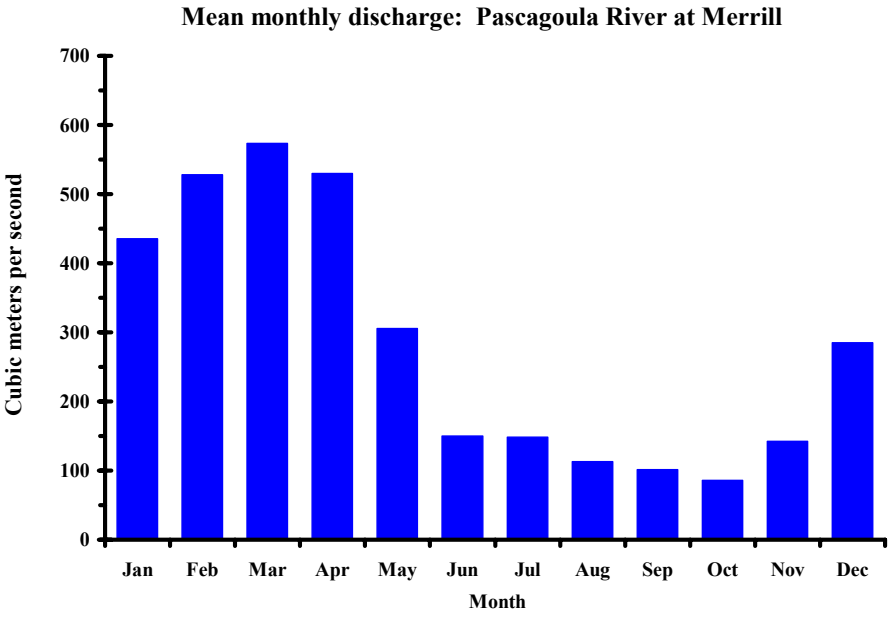

Figure D-31. Mean monthly data from the USGS streamflow station 2479000, Pascagoula River at Merrill, Mississippi.

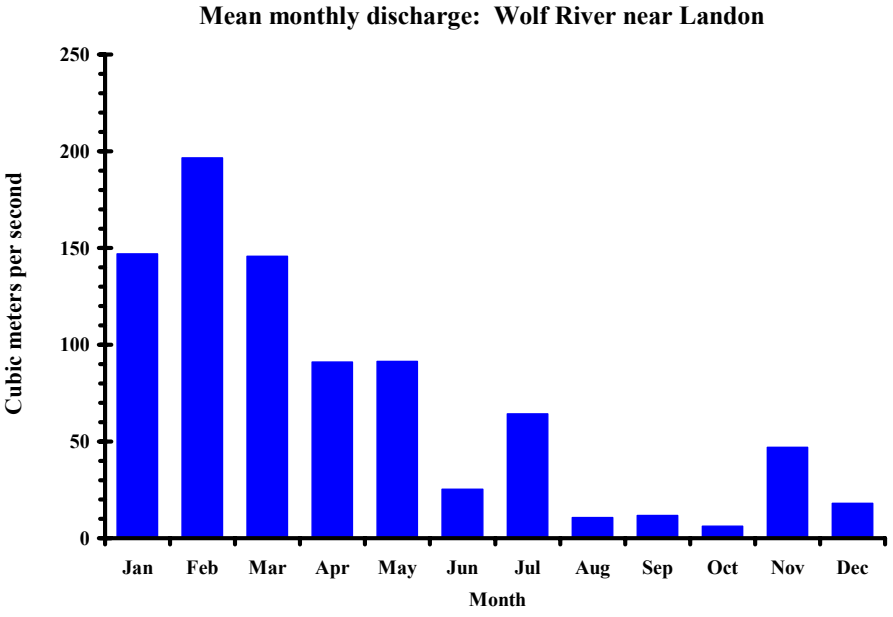

Figure D-32. Mean monthly data from the USGS streamflow station 2481510, Wolf River near Landon, Mississippi.

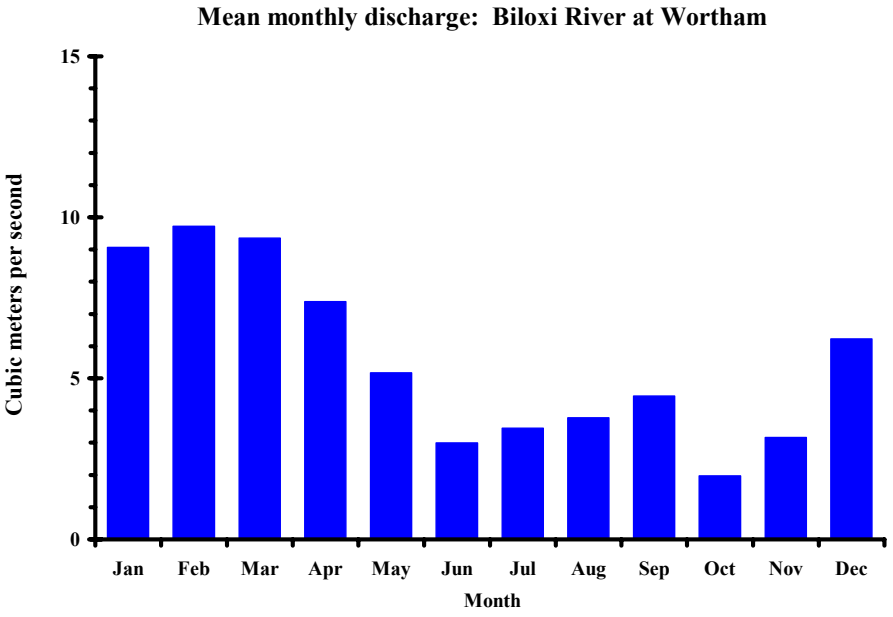

Figure D-33. Mean monthly data from the USGS streamflow station 2481000, Biloxi River at Wortham, Mississippi.

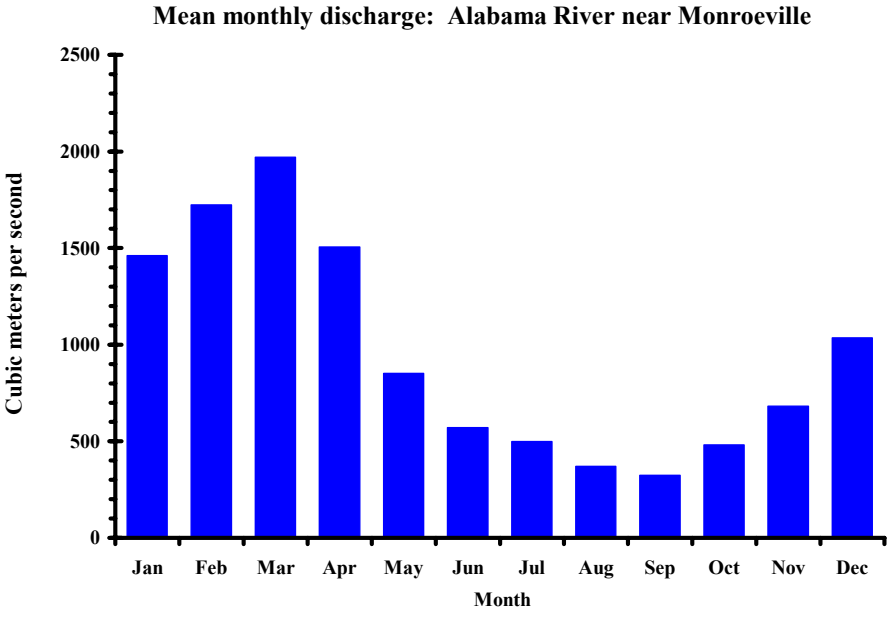

Figure D-34. Mean monthly data from the USGS streamflow station 2428400, Alabama River near Monroeville, Alabama.

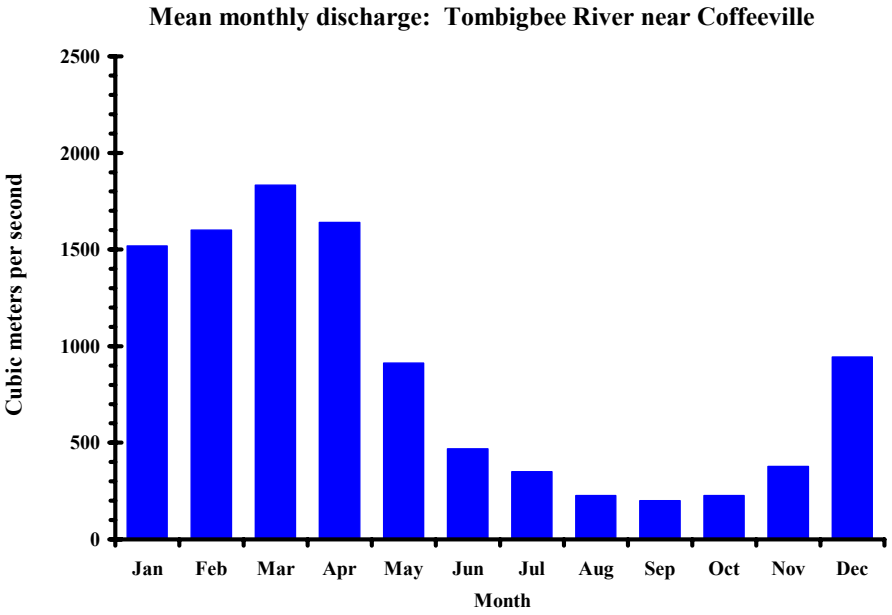

Figure D-35. Mean monthly data from the USGS streamflow station 2469761, Tombigbee River near Coffeeville, Alabama.

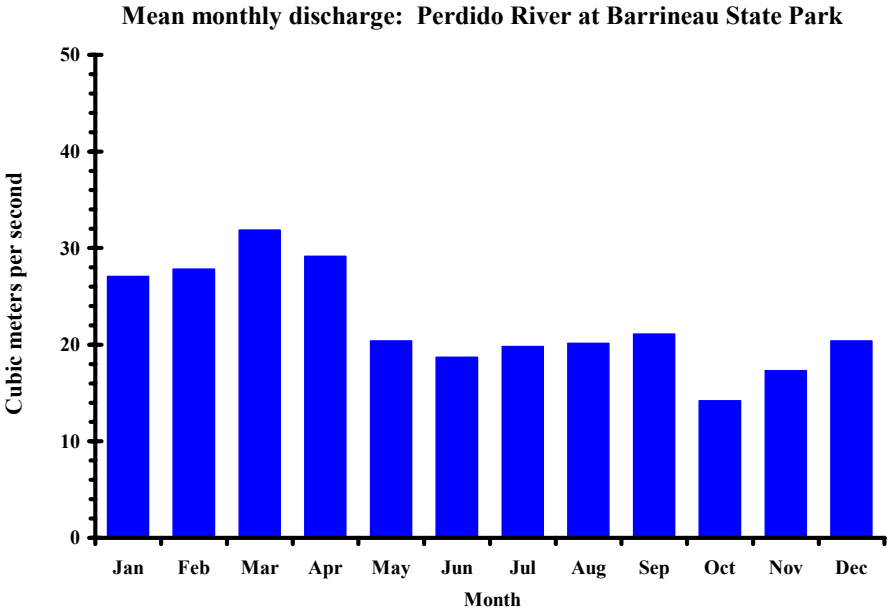

Figure D-36. Mean monthly data from the USGS streamflow station 23765000, Perdido River at Barrineau Park, Florida.

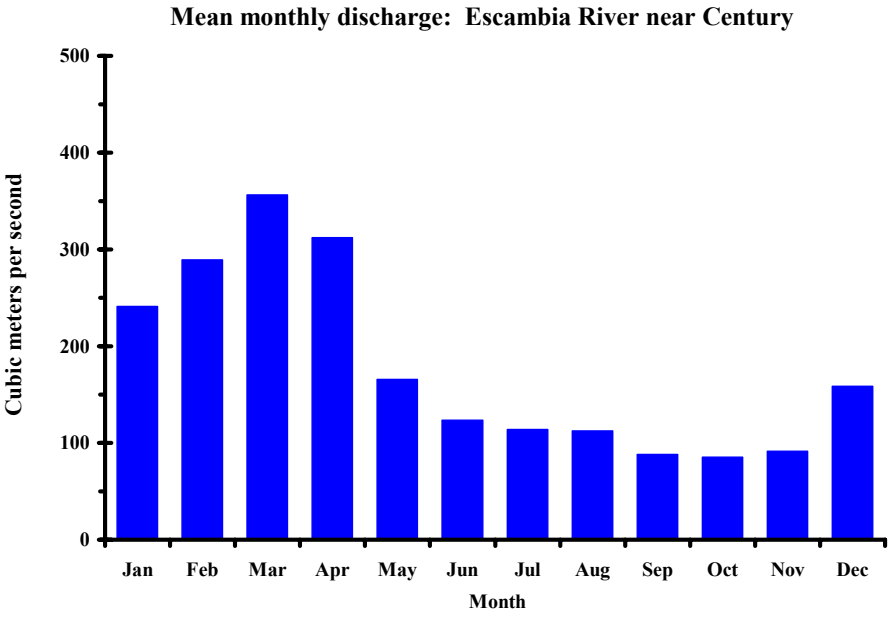

Figure D-37. Mean monthly data from the USGS streamflow station 2375500, Escambia River near Century, Florida.

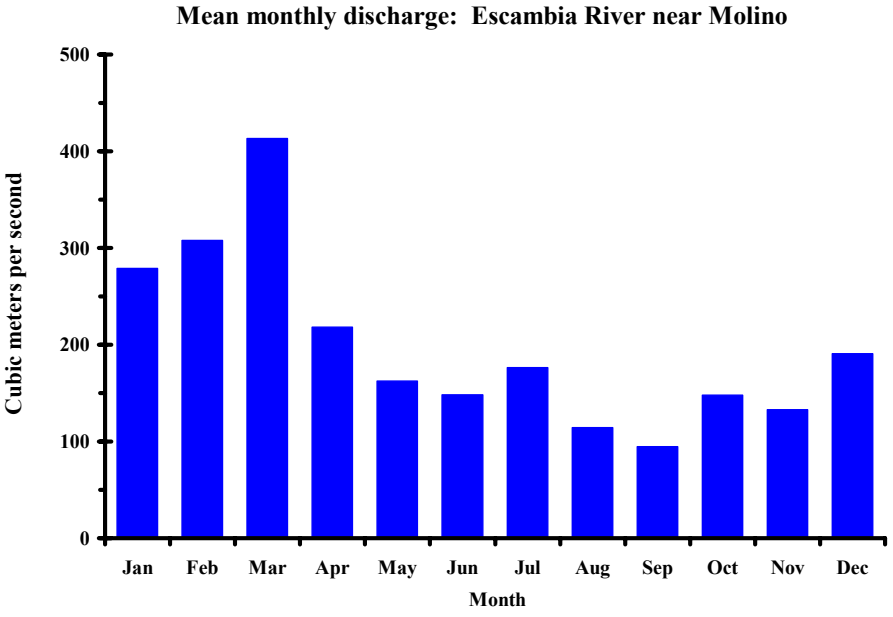

Figure D-38. Mean monthly data from the USGS streamflow station 2376033, Escambia River near Molino, Florida.

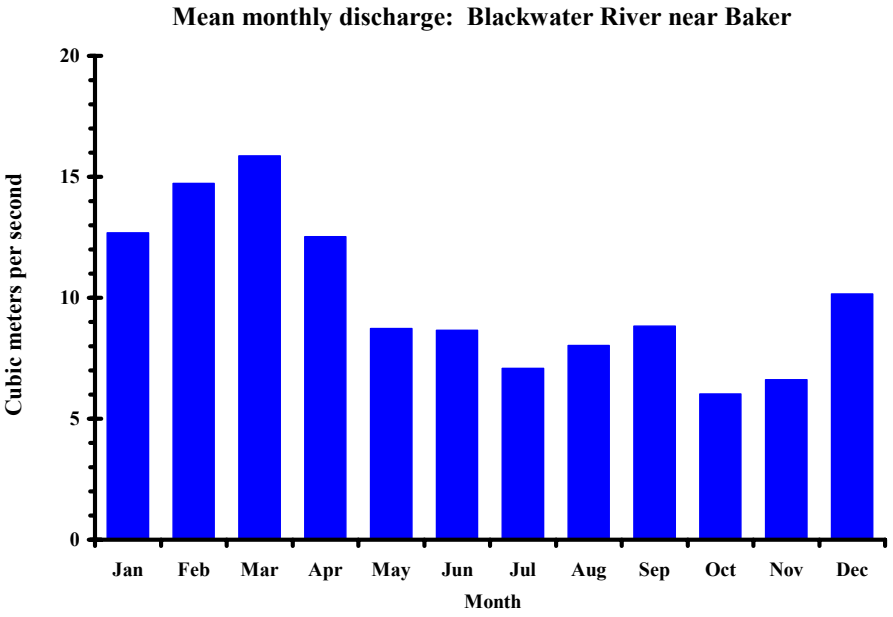

Figure D-39. Mean monthly data from the USGS streamflow station 2370000, Blackwater River near Baker, Florida.

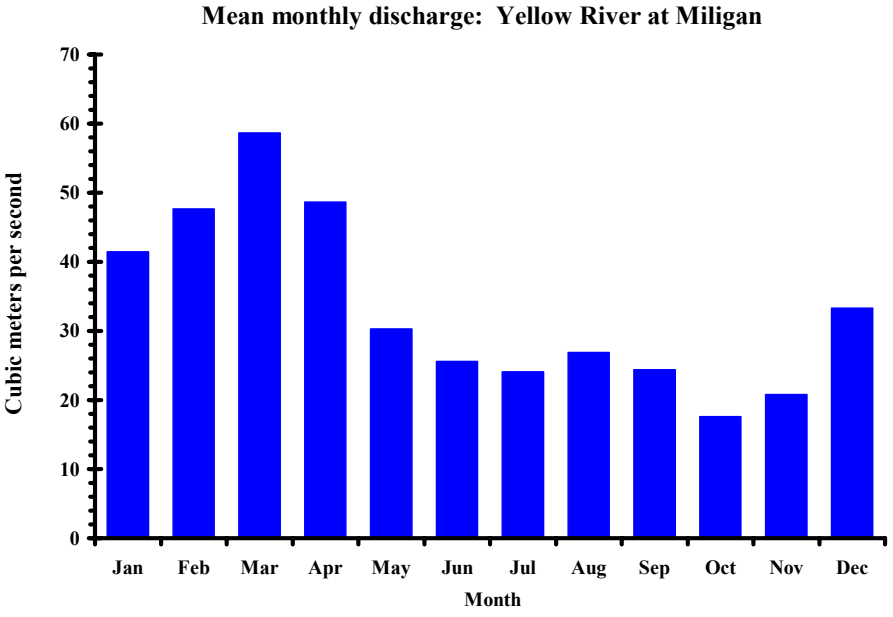

Figure D-40. Mean monthly data from the USGS streamflow station 2368000, Yellow River at Milligan, Florida.

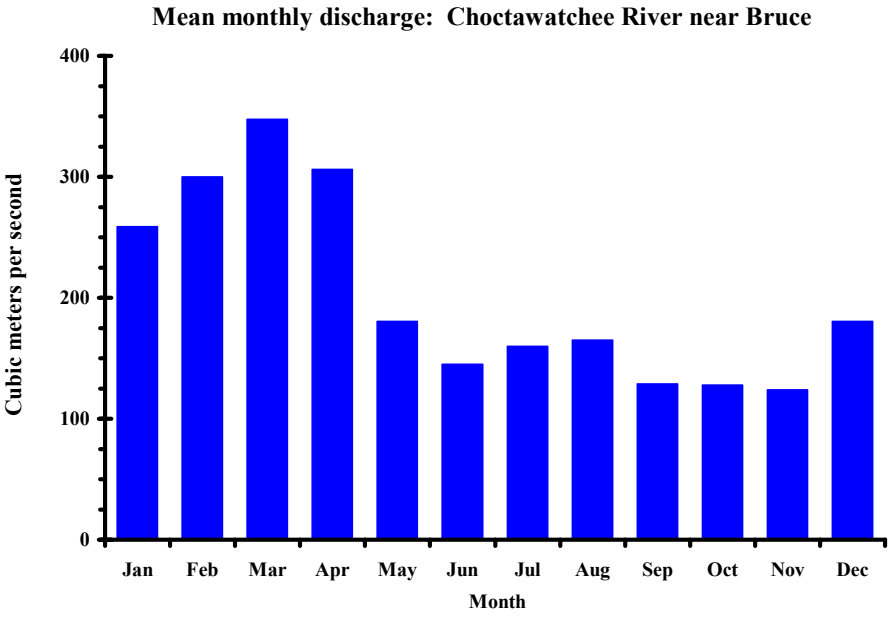

Figure D-41. Mean monthly data from the USGS streamflow station 2366500, Choctawhatchee River near Bruce, Florida.

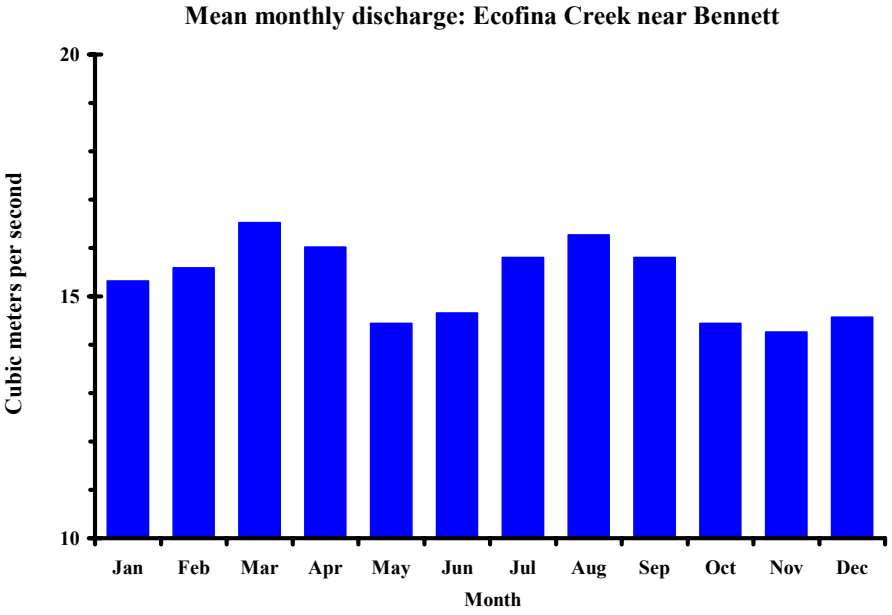

Figure D-42. Mean monthly data from the USGS streamflow station 2359500, Ecofina Creek near Bennett, Florida.

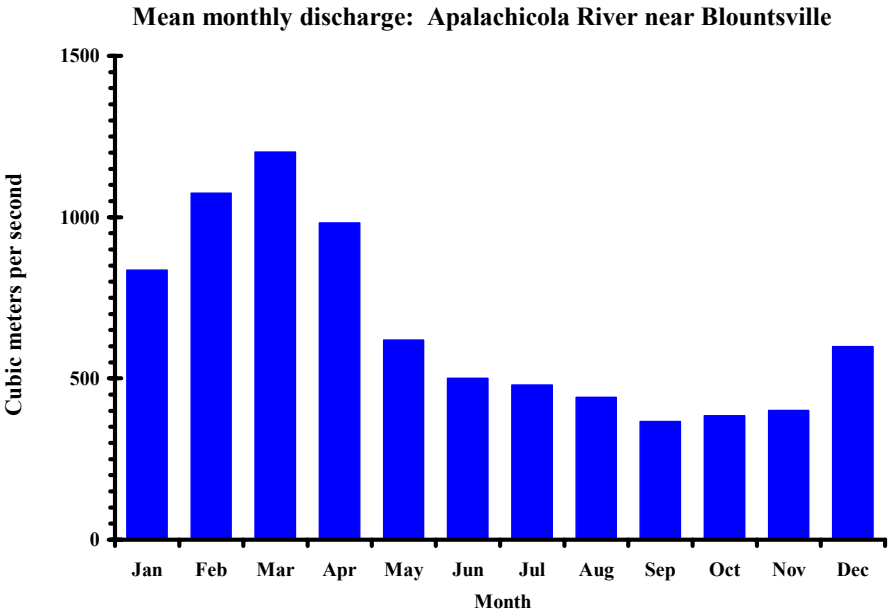

Figure D-43. Mean monthly data from the USGS streamflow station 2358700, Apalachicola River near Blontsville, Florida.

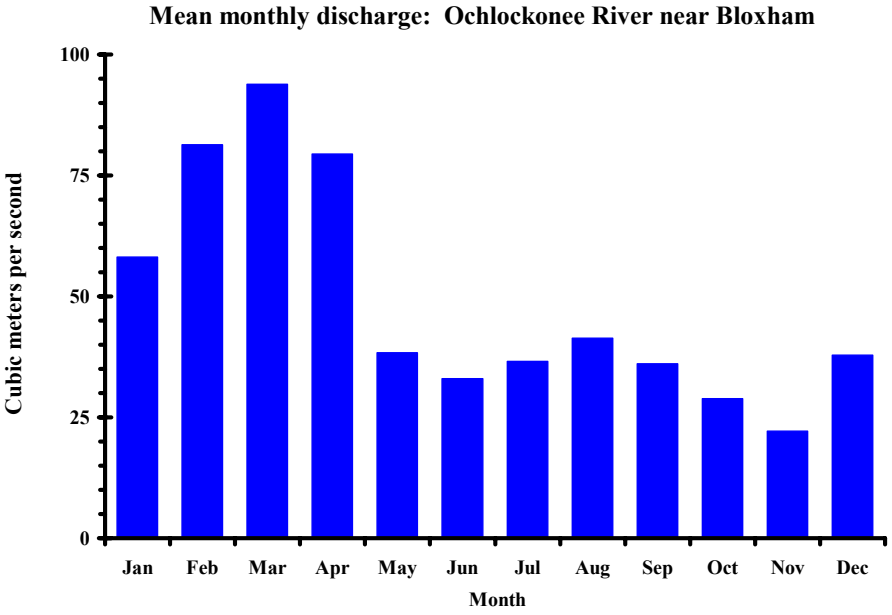

Figure D-44. Mean monthly data from the USGS streamflow station 2330000, Ochlockonee River near Bloxham, Florida.

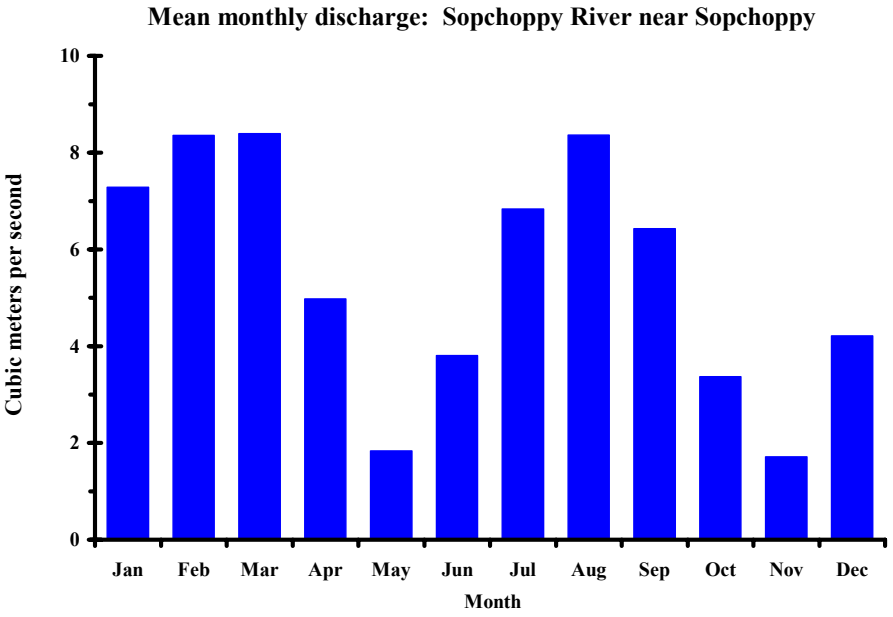

Figure D-45. Mean monthly data from the USGS streamflow station 2327100, Sopchoppy River near Sopchoppy, Florida.

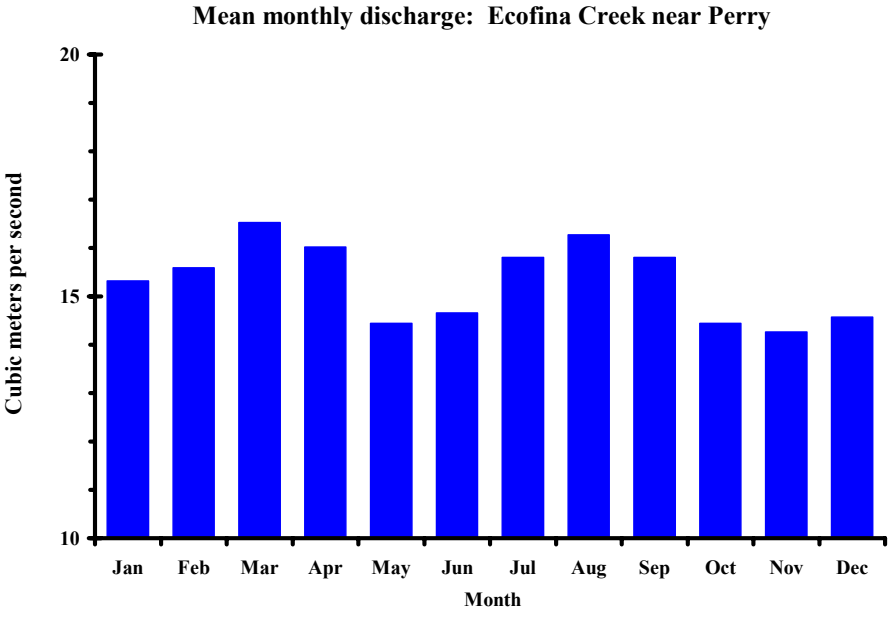

Figure D-46. Mean monthly data from the USGS streamflow station 2326000, Ecofina Creek near Perry, Florida.

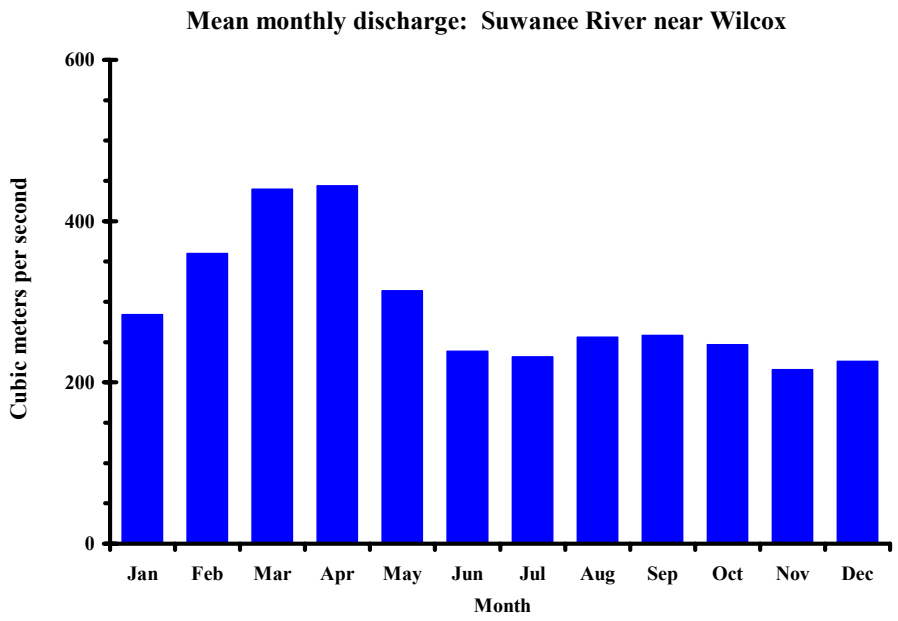

Figure D-47. Mean monthly data from the USGS streamflow station 2323500, Suwanee River near Wilcox, Florida.

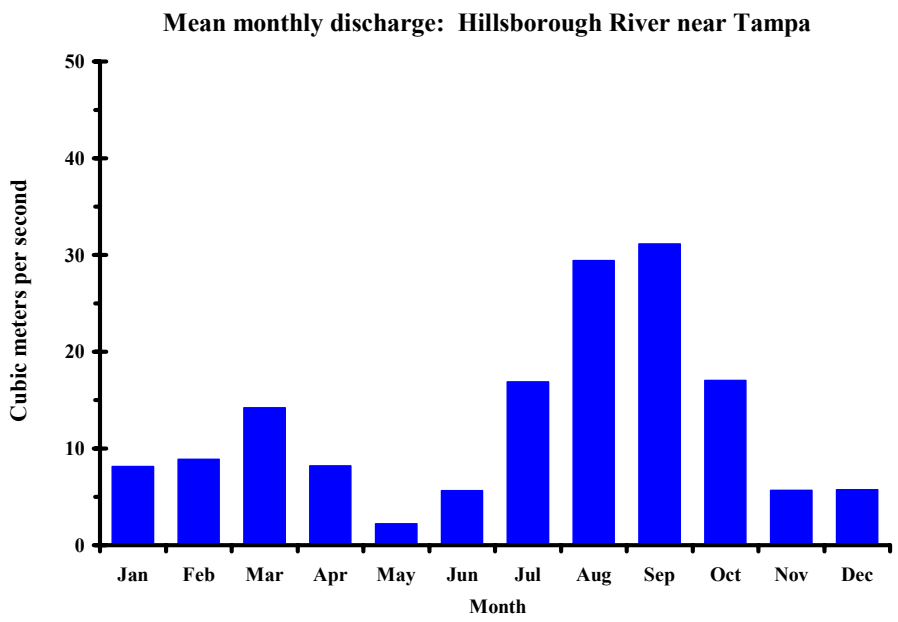

Figure D-48. Mean monthly data from the USGS streamflow station 2304500, Hillsborough River near Tampa, Florida.

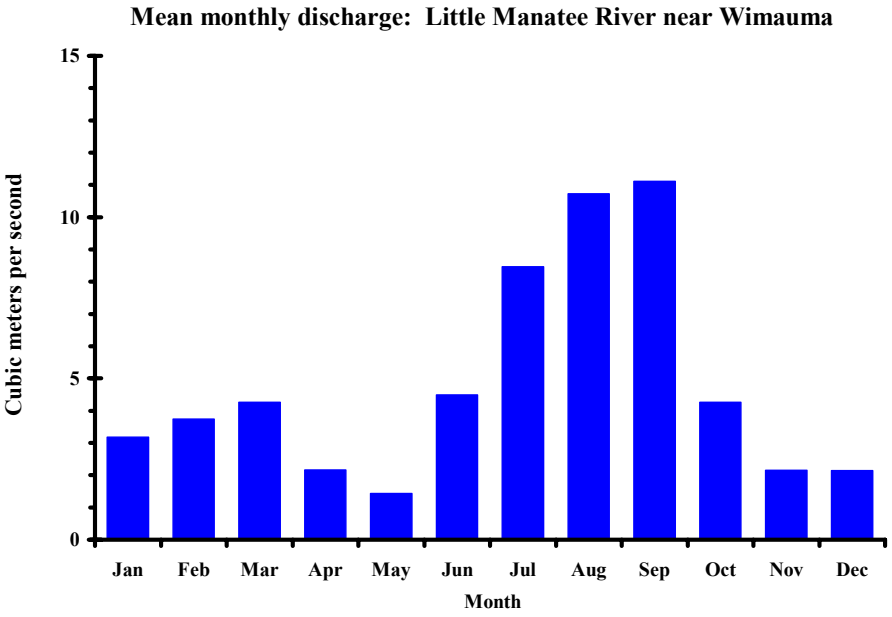

Figure D-49. Mean monthly data from the USGS streamflow station 2300500, Little Manatee River near Wimauma, Florida.

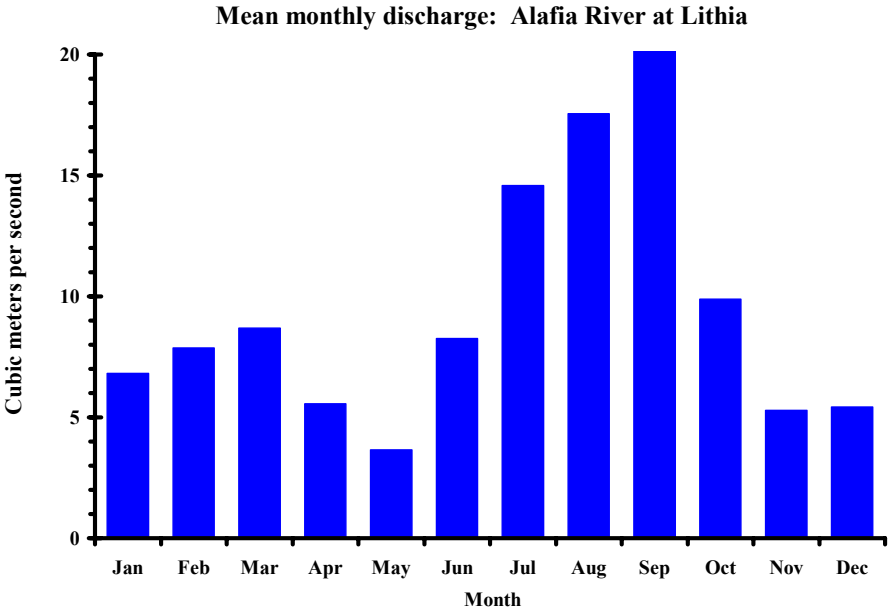

Figure D-50. Mean monthly data from the USGS streamflow station 2301500, Alafia River at Lithia, Florida.

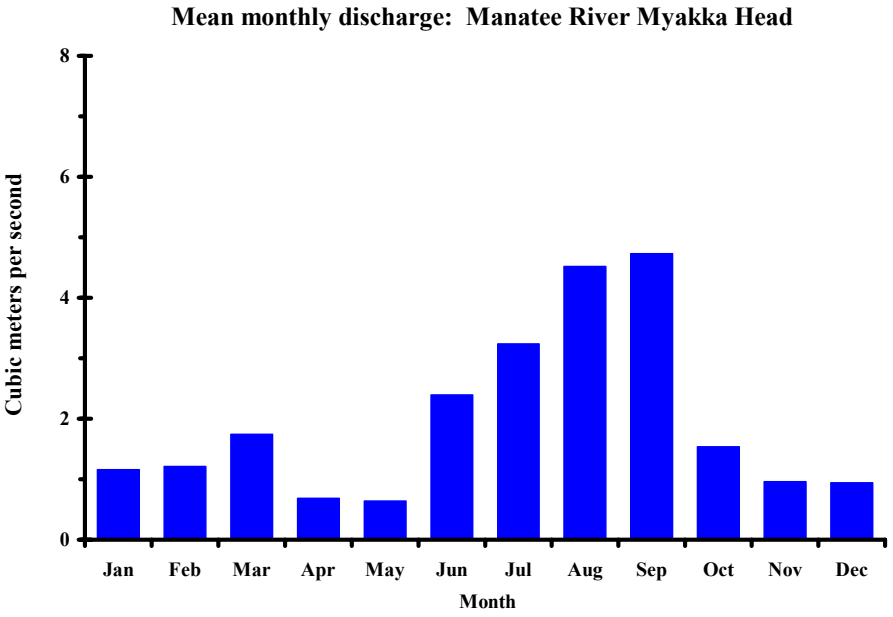

Figure D-51. Mean monthly data from the USGS streamflow station 2299950, Manatee River near Myakka Head, Florida.

Appendix E: Palmer Drought Severity Index (PDSI) data plots.

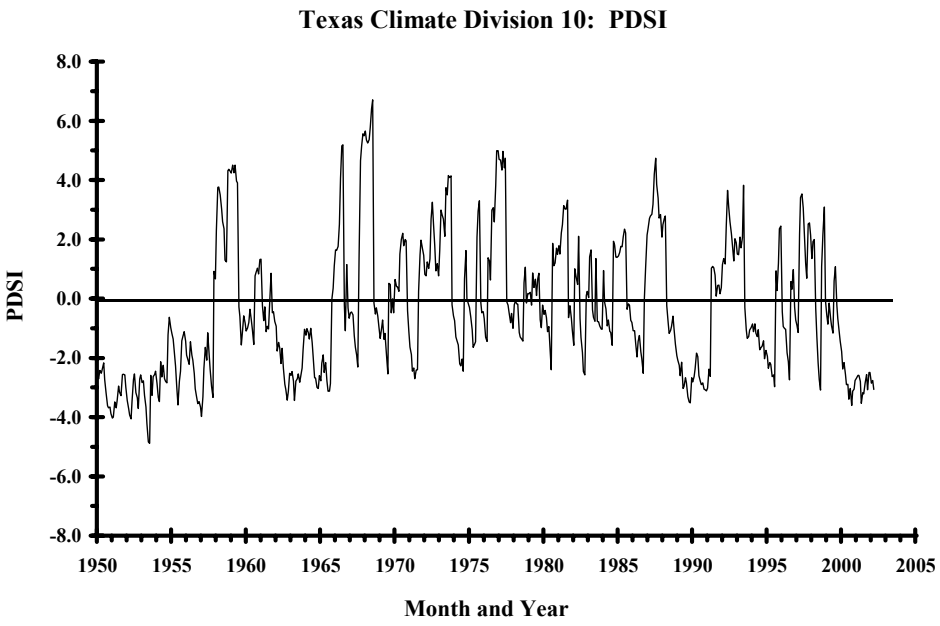

Figure E-1. Plot of monthly Palmer Drought Severity Index (PDSI) for Texas Climate Division 10. Data is from the National Climatic Data Center.

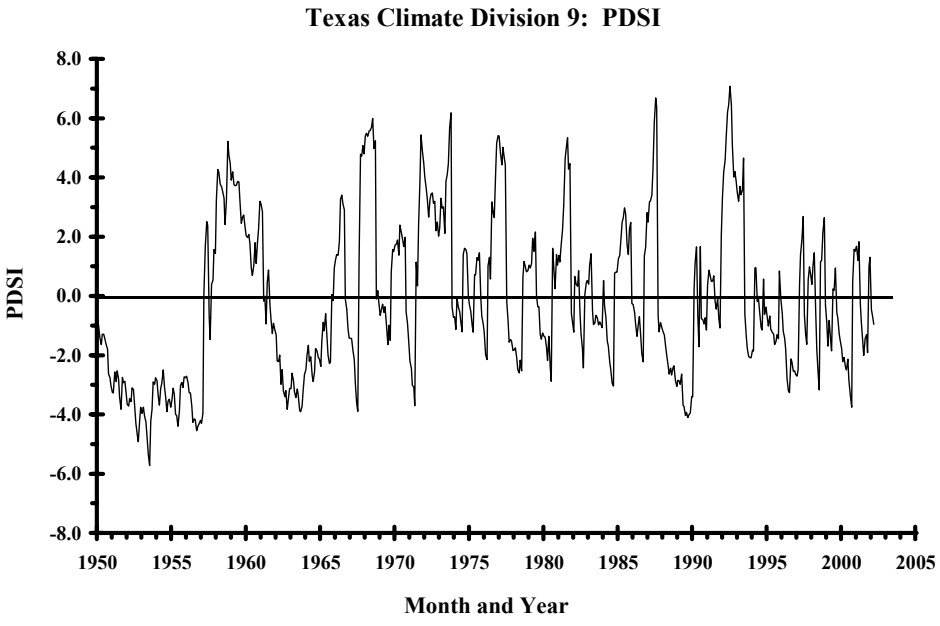

Figure E-2. Plot of monthly Palmer Drought Severity Index (PDSI) for Texas Climate Division 9. Data is from the National Climatic Data Center.

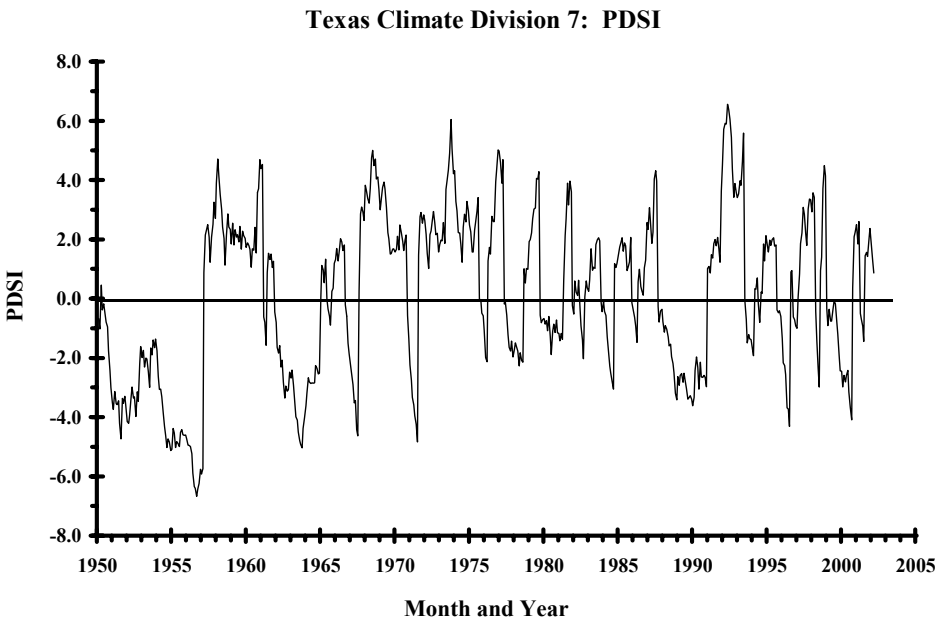

Figure E-3. Plot of monthly Palmer Drought Severity Index (PDSI) for Texas Climate Division 7. Data is from the National Climatic Data Center.

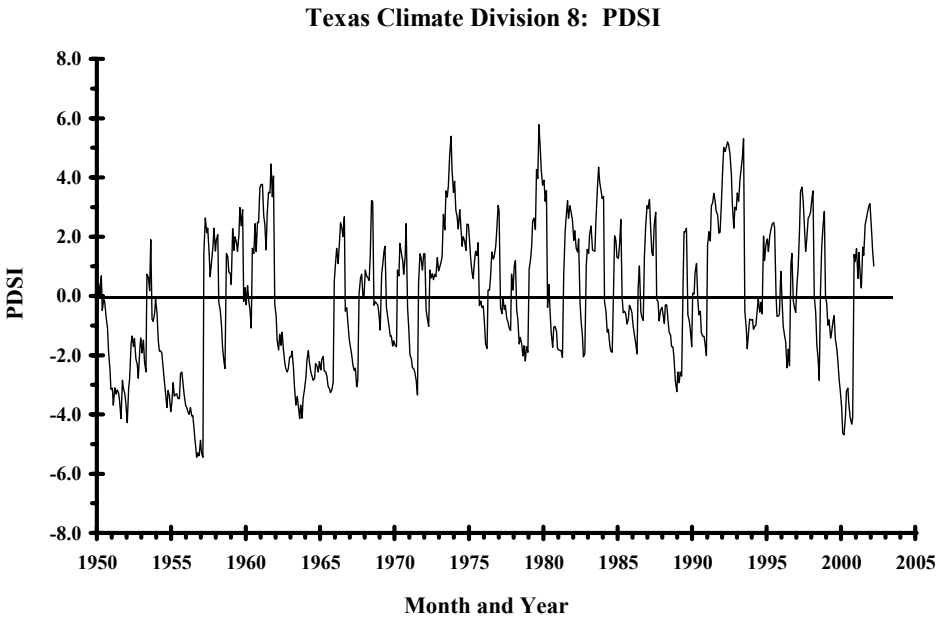

Figure E-4. Plot of monthly Palmer Drought Severity Index (PDSI) for Texas Climate Division 8. Data is from the National Climatic Data Center.

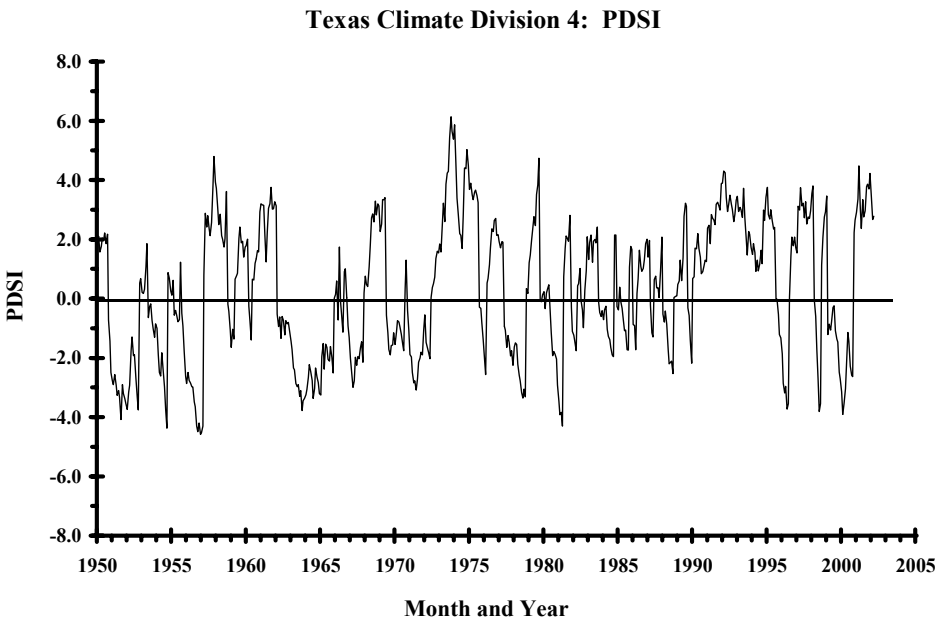

Figure E-5. Plot of monthly Palmer Drought Severity Index (PDSI) for Texas Climate Division 4. Data is from the National Climatic Data Center.

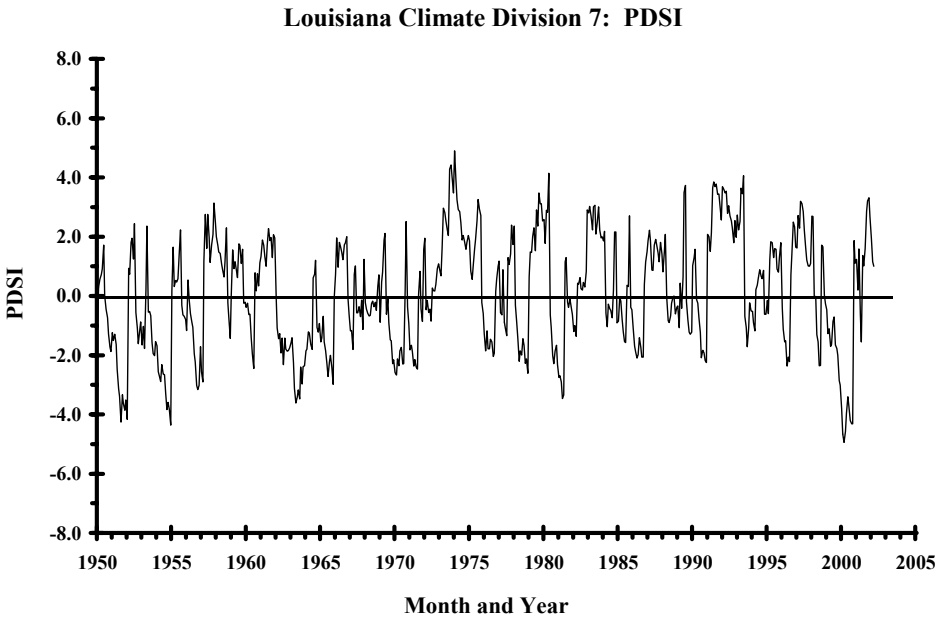

Figure E-6. Plot of monthly Palmer Drought Severity Index (PDSI) for Louisiana Climate Division 7. Data is from the National Climatic Data Center.

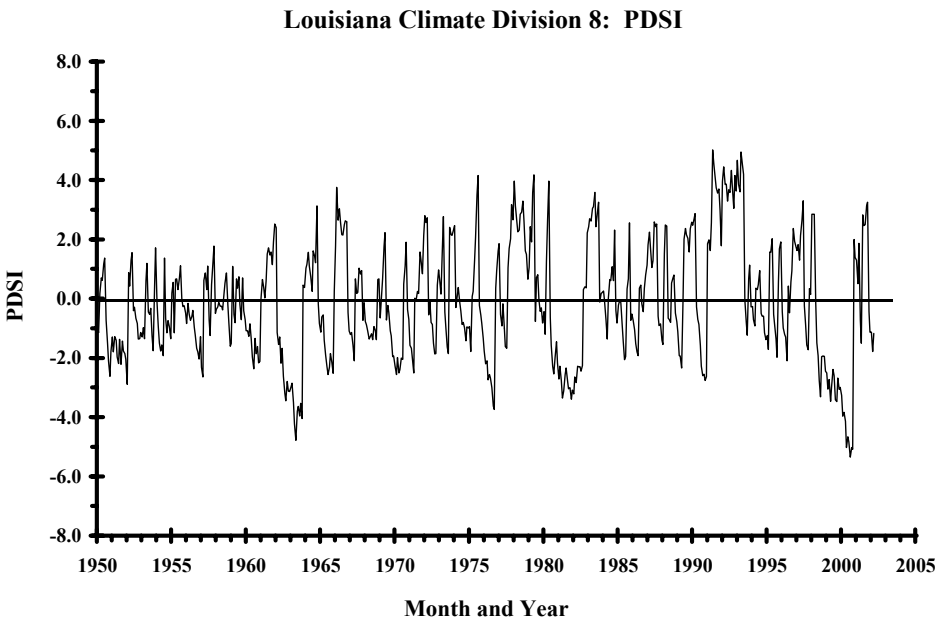

Figure E-7. Plot of monthly Palmer Drought Severity Index (PDSI) for Louisiana Climate Division 8. Data is from the National Climatic Data Center.

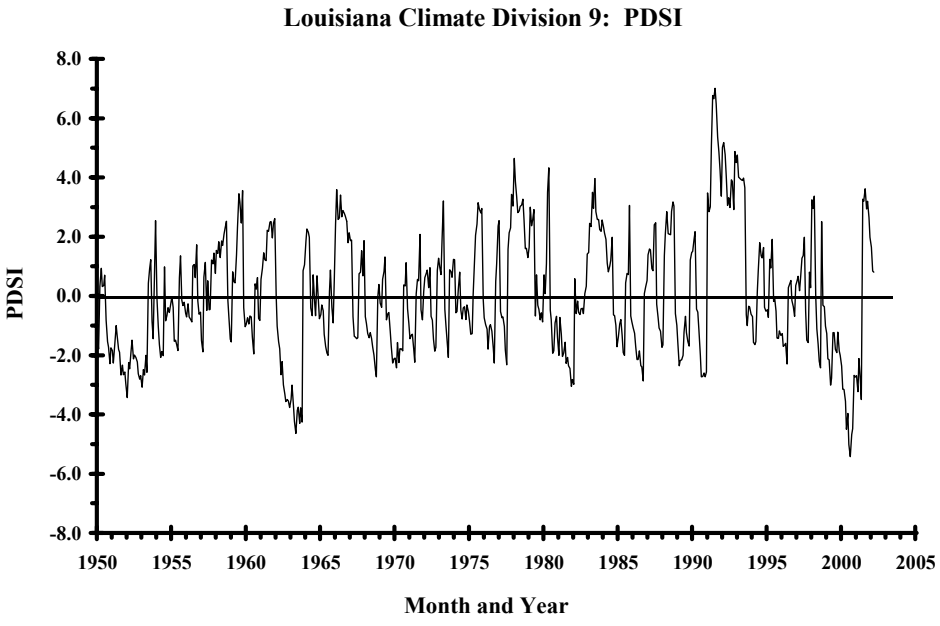

Figure E-8. Plot of monthly Palmer Drought Severity Index (PDSI) for Louisiana Climate Division 9. Data is from the National Climatic Data Center.

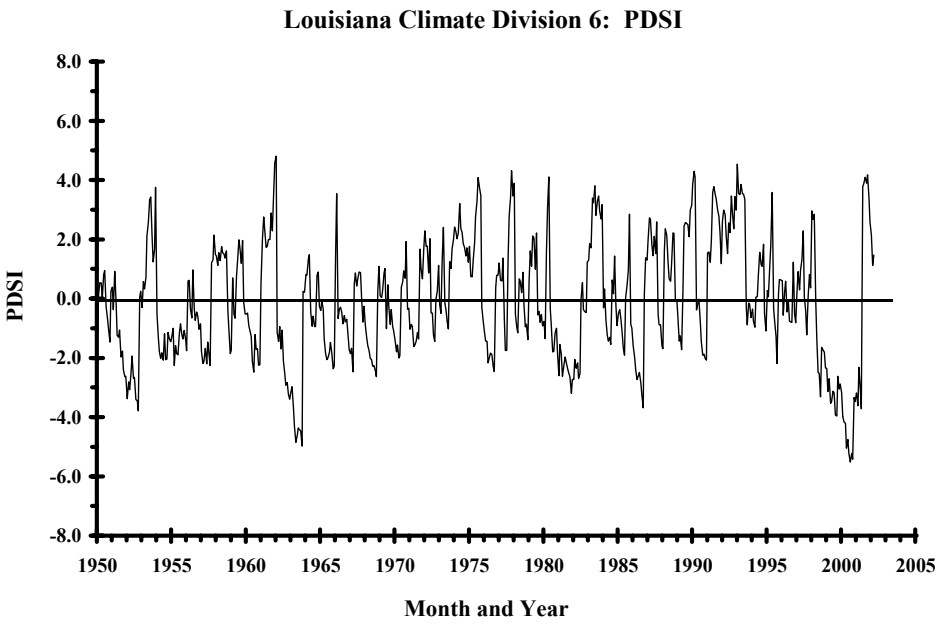

Figure E-9. Plot of monthly Palmer Drought Severity Index (PDSI) for Louisiana Climate Division 6. Data is from the National Climatic Data Center.

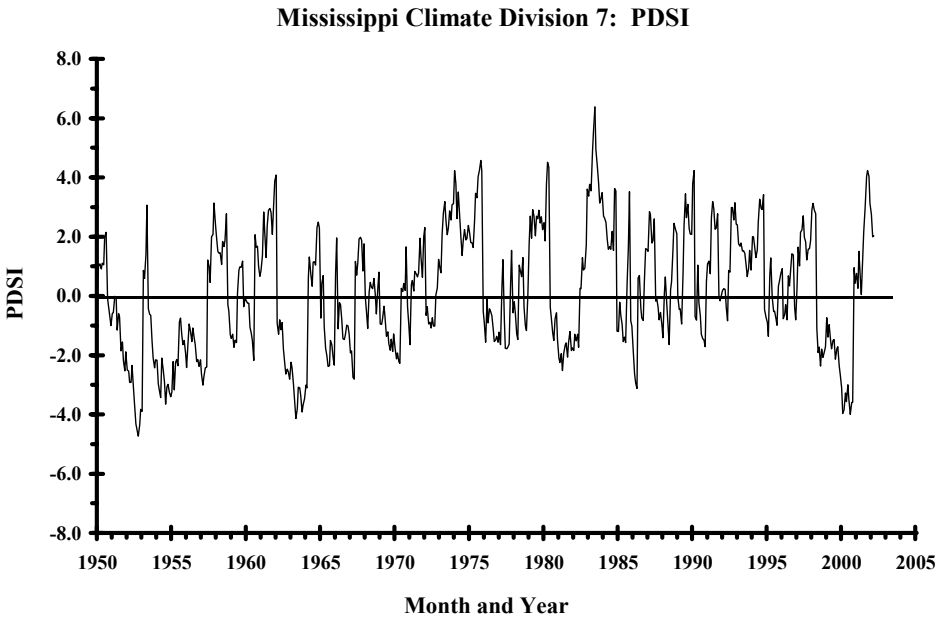

Figure E-10. Plot of monthly Palmer Drought Severity Index (PDSI) for Mississippi Climate Division 7. Data is from the National Climatic Data Center.

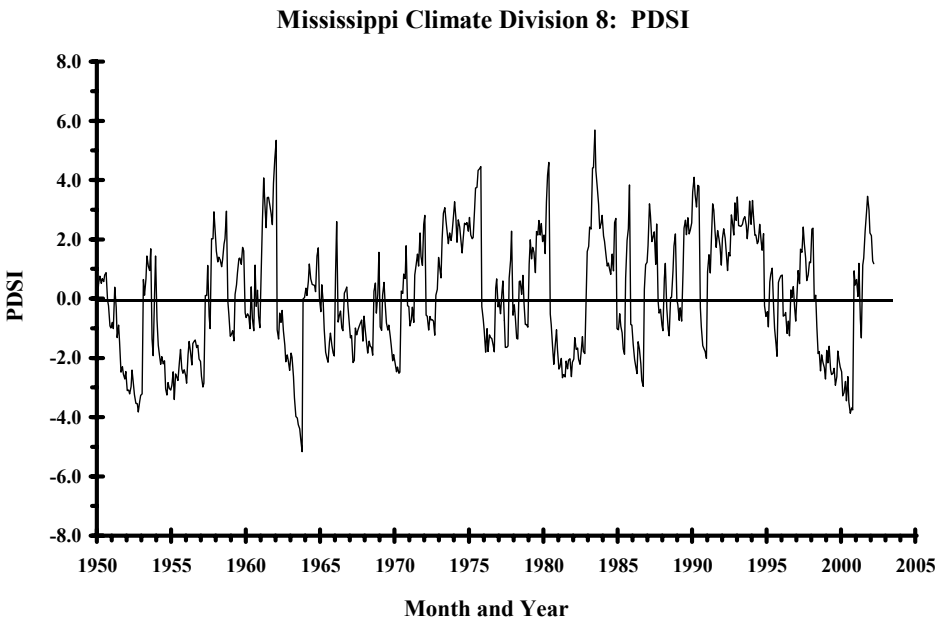

Figure E-11. Plot of monthly Palmer Drought Severity Index (PDSI) for Mississippi Climate Division 8. Data is from the National Climatic Data Center.

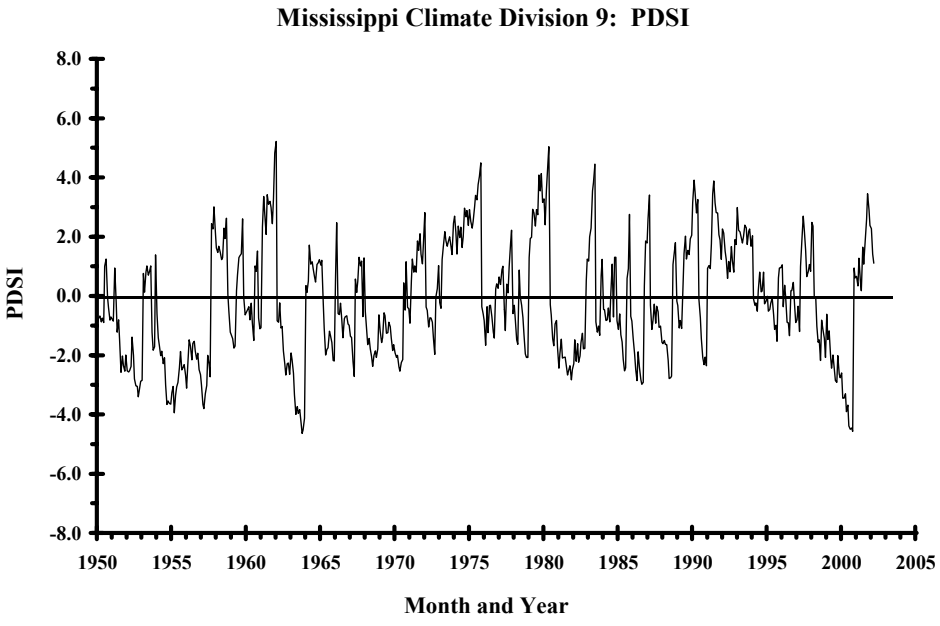

Figure E-12. Plot of monthly Palmer Drought Severity Index (PDSI) for Mississippi Climate Division 9. Data is from the National Climatic Data Center.

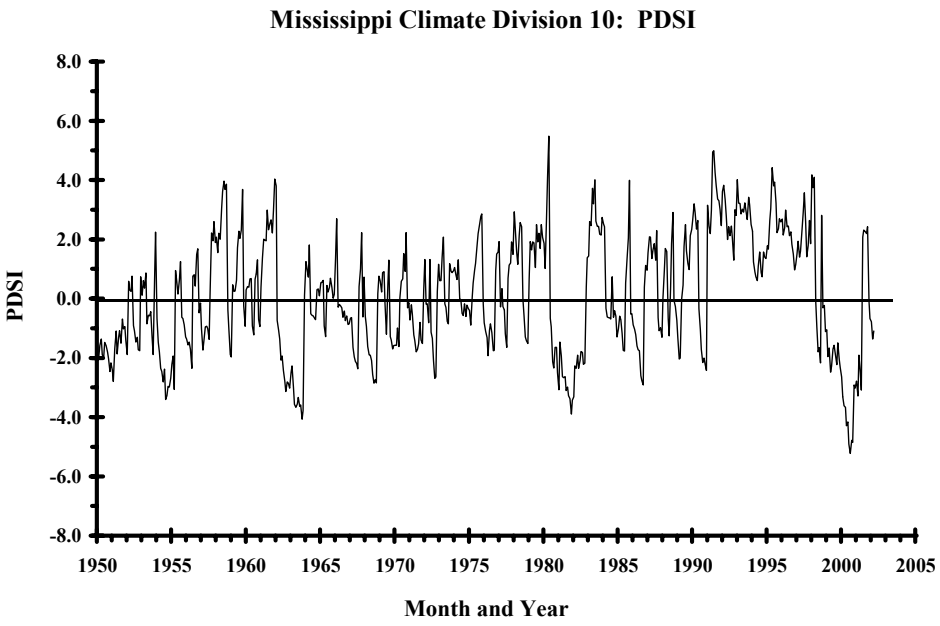

Figure E-13. Plot of monthly Palmer Drought Severity Index (PDSI) for Mississippi Climate Division 10. Data is from the National Climatic Data Center.

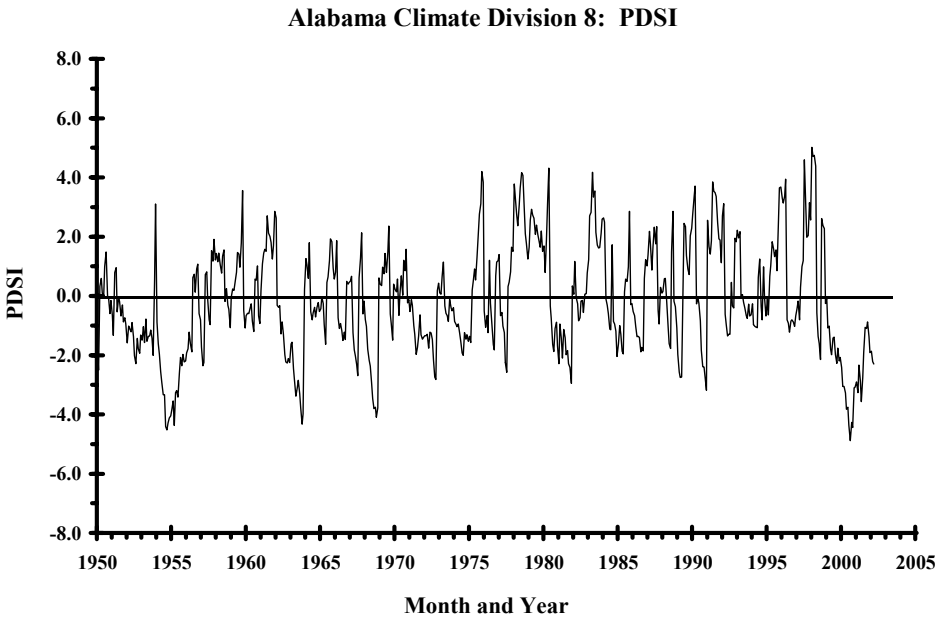

Figure E-14. Plot of monthly Palmer Drought Severity Index (PDSI) for Alabama Climate Division 8. Data is from the National Climatic Data Center.

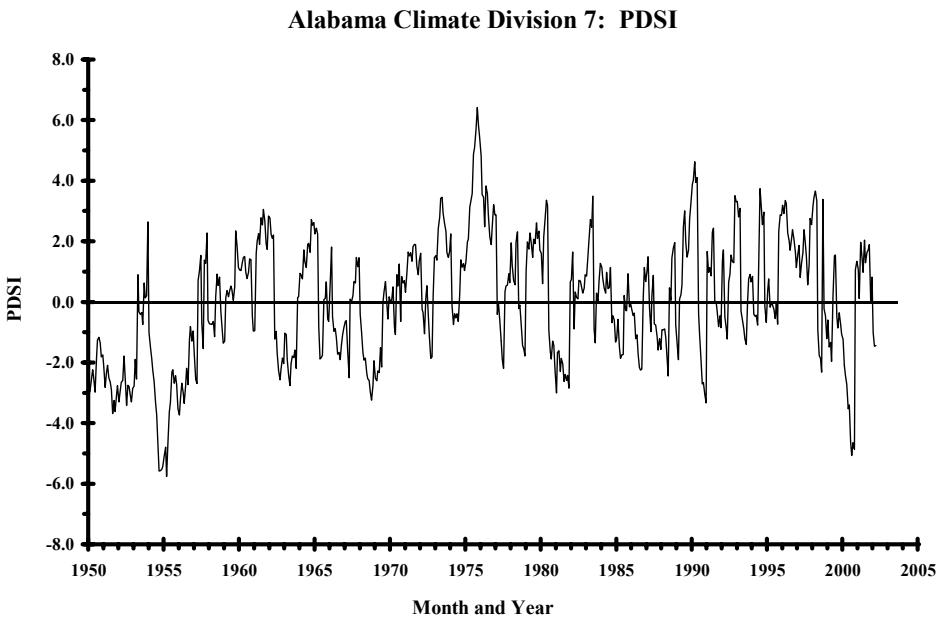

Figure E-15. Plot of monthly Palmer Drought Severity Index (PDSI) for Alabama Climate Division 7. Data is from the National Climatic Data Center.

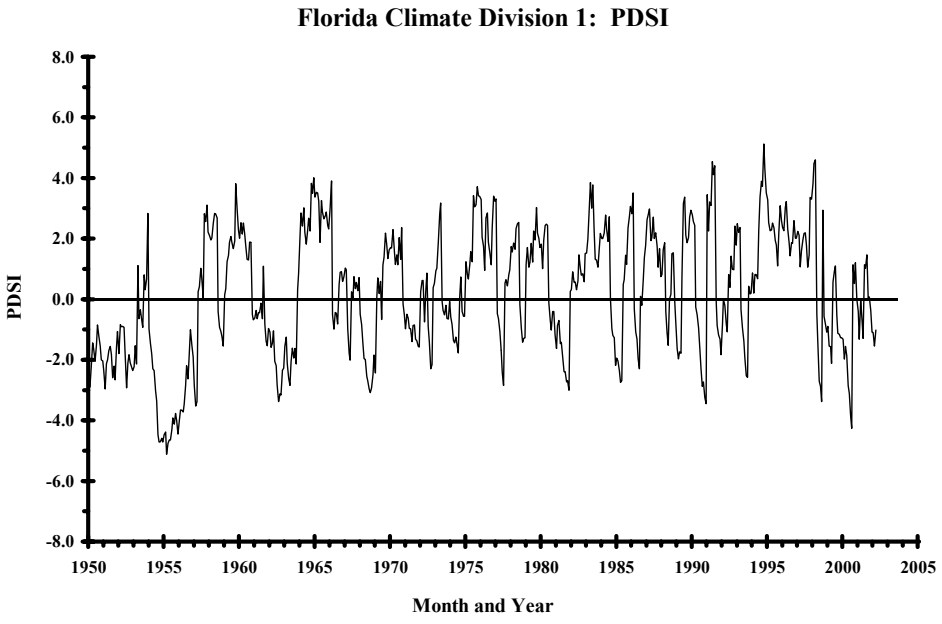

Figure E-16. Plot of monthly Palmer Drought Severity Index (PDSI) for Florida Climate Division 1. Data is from the National Climatic Data Center.

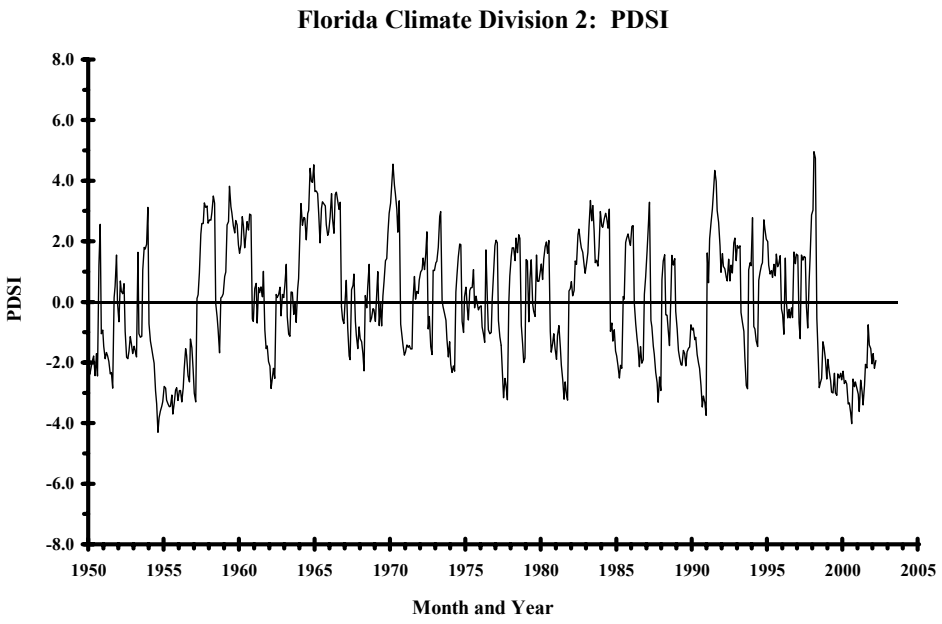

Figure E-17. Plot of monthly Palmer Drought Severity Index (PDSI) for Florida Climate Division 2. Data is from the National Climatic Data Center.

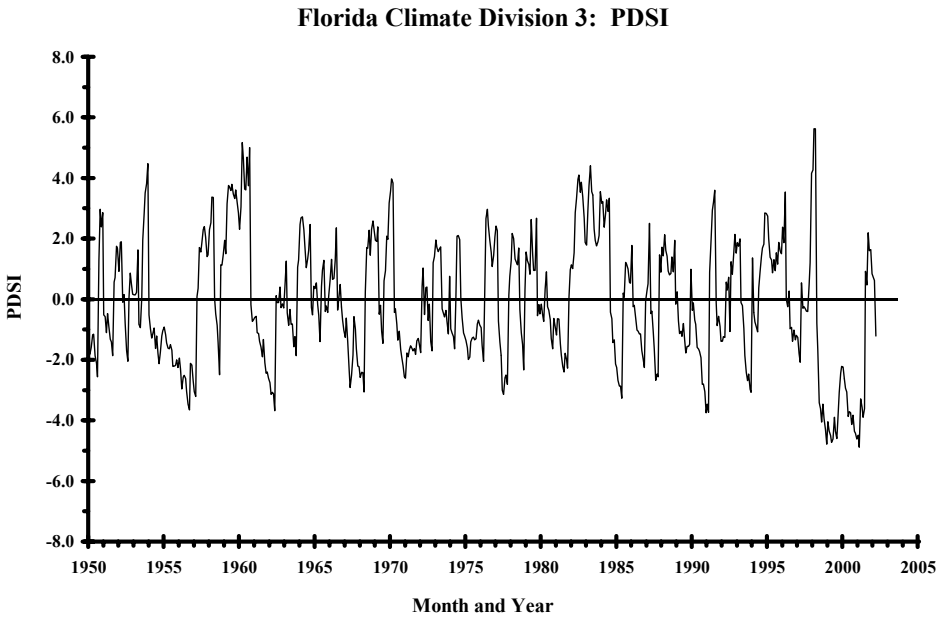

Figure E-18. Plot of monthly Palmer Drought Severity Index (PDSI) for Florida Climate Division 3. Data is from the National Climatic Data Center.

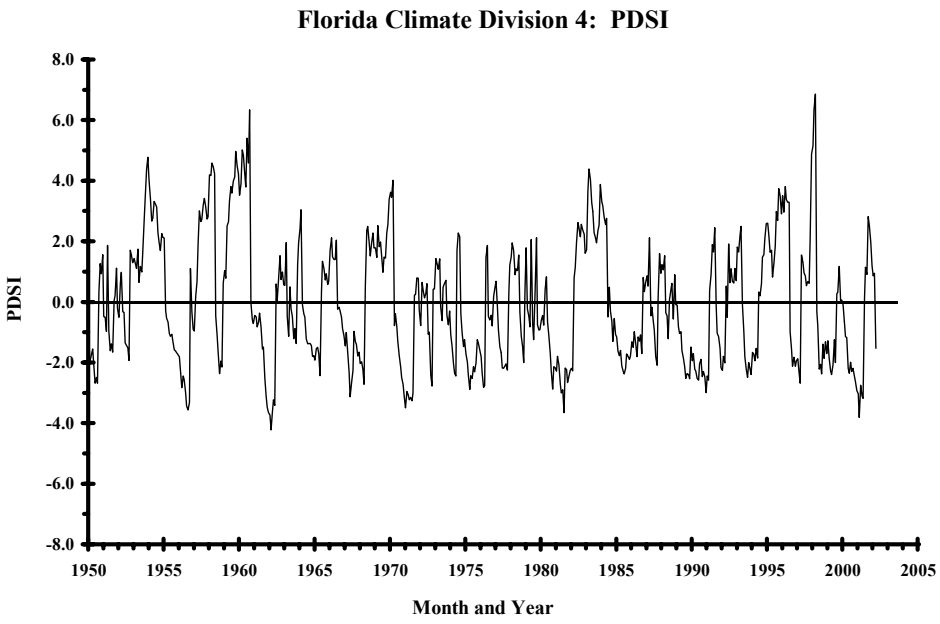

Figure E-19. Plot of monthly Palmer Drought Severity Index (PDSI) for Florida Climate Division 4. Data is from the National Climatic Data Center.

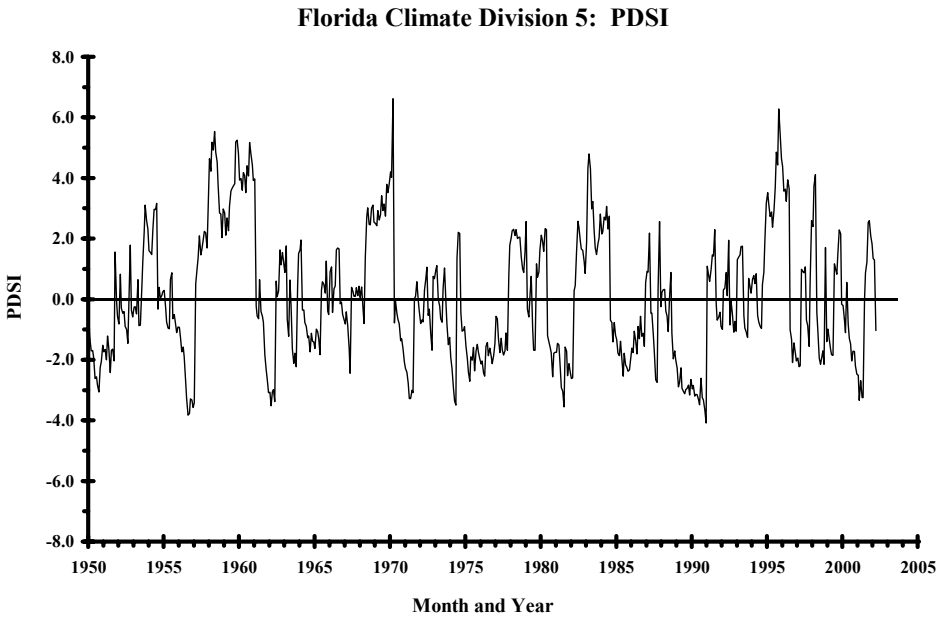

Figure E-20. Plot of monthly Palmer Drought Severity Index (PDSI) for Florida Climate Division 5. Data is from the National Climatic Data Center.

Appendix F: Precipitation data plots.

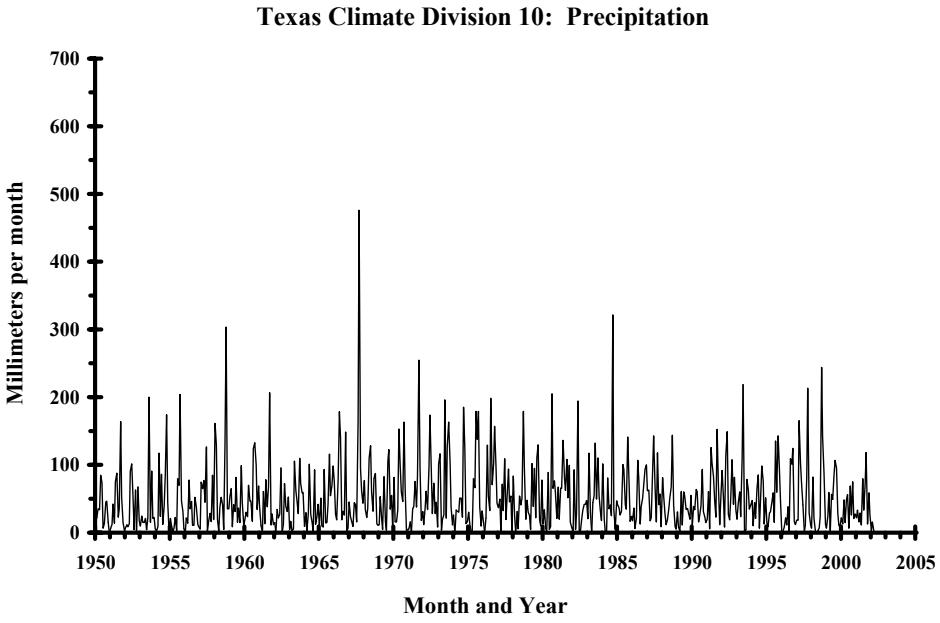

Figure F-1. Plot of monthly total precipitation (millimeters) for Texas Climate Division 10. Data is from the National Climatic Data Center.

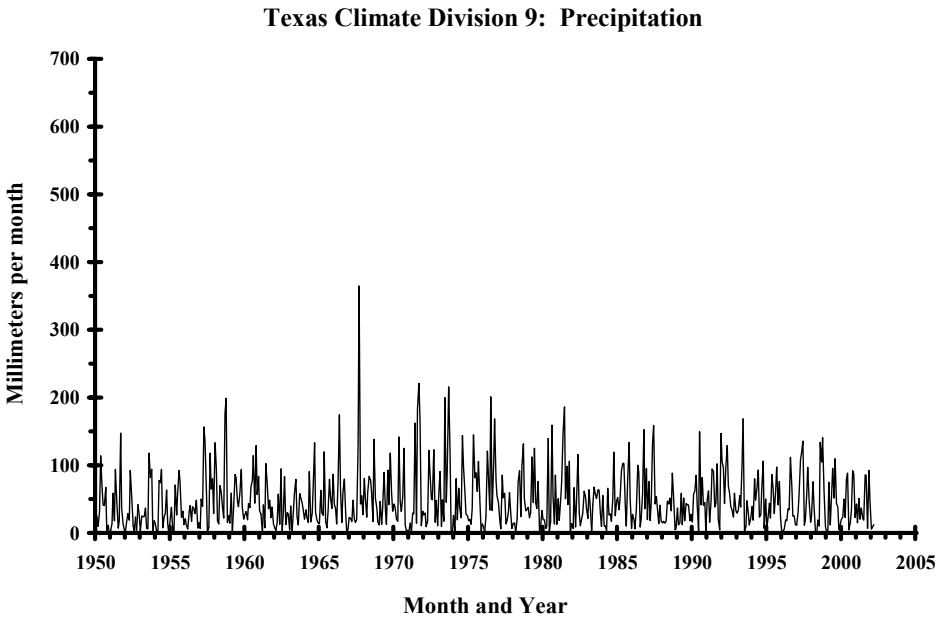

Figure F-2. Plot of monthly total precipitation (millimeters) for Texas Climate Division 9. Data is from the National Climatic Data Center.

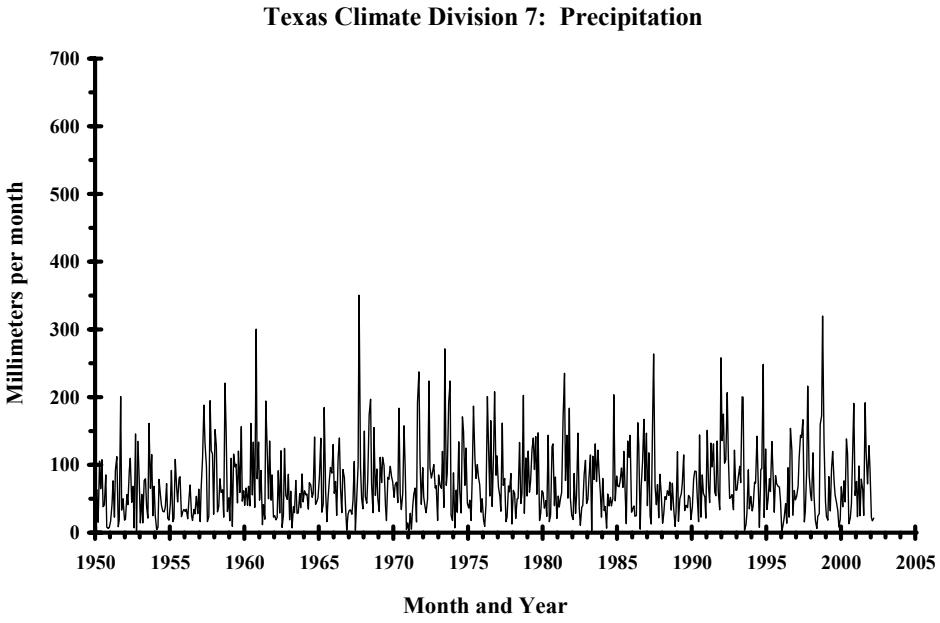

Figure F-3. Plot of monthly total precipitation (millimeters) for Texas Climate Division 7. Data is from the National Climatic Data Center.

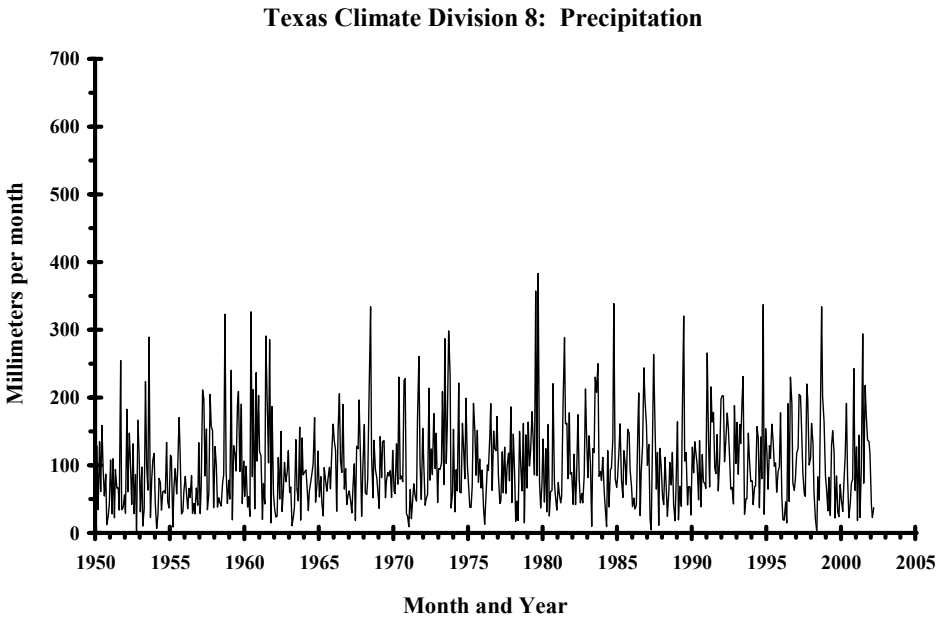

Figure F-4. Plot of monthly total precipitation (millimeters) for Texas Climate Division 8. Data is from the National Climatic Data Center.

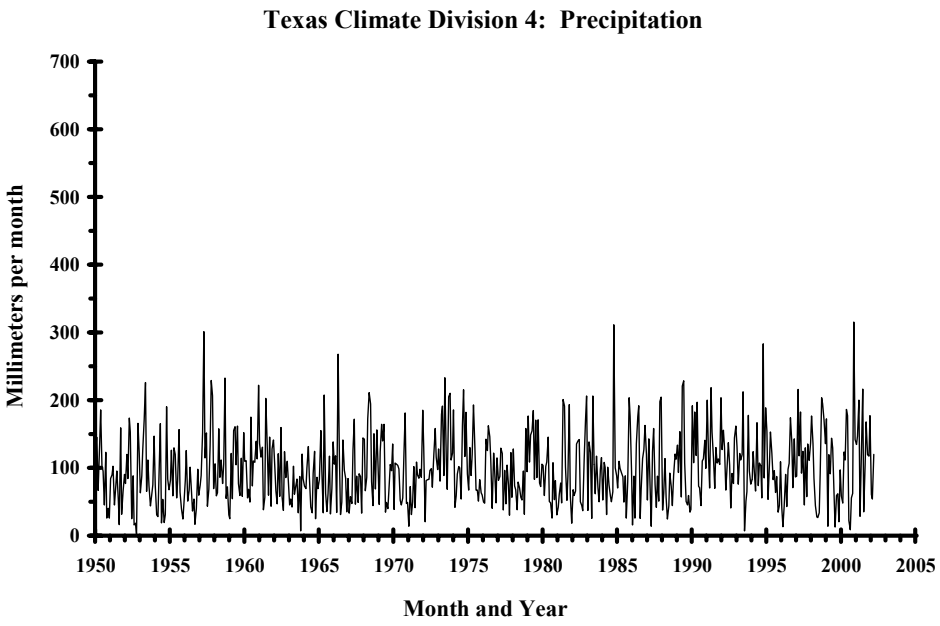

Figure F-5. Plot of monthly total precipitation (millimeters) for Texas Climate Division 4. Data is from the National Climatic Data Center.

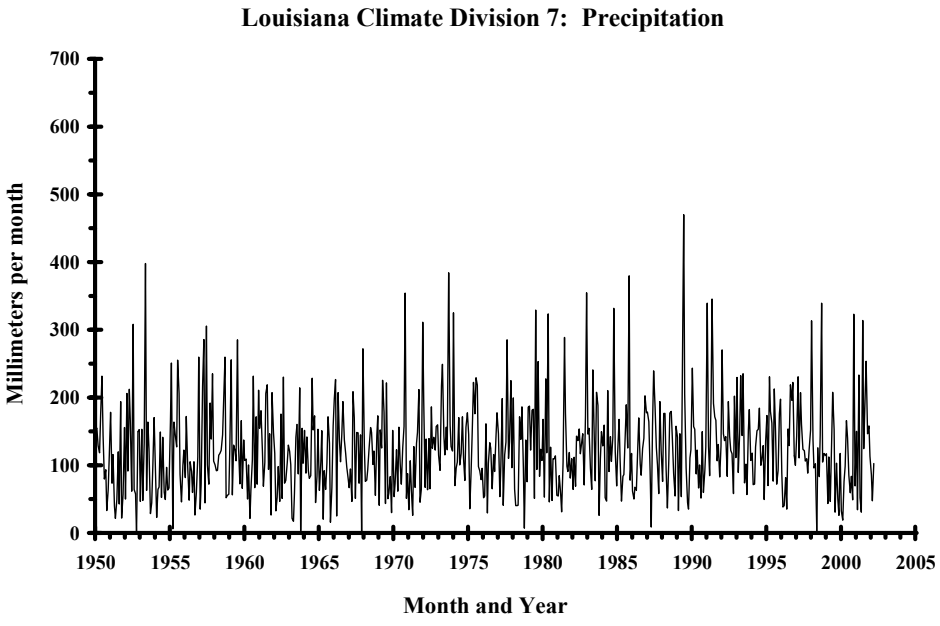

Figure F-6. Plot of monthly total precipitation (millimeters) for Louisiana Climate Division 7. Data is from the National Climatic Data Center.

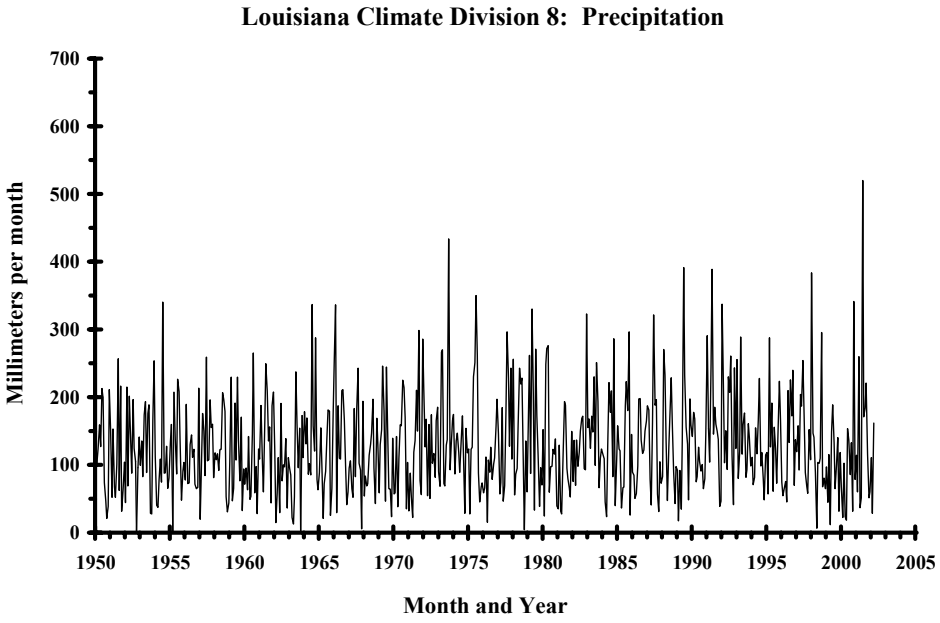

Figure F-7. Plot of monthly total precipitation (millimeters) for Louisiana Climate Division 8. Data is from the National Climatic Data Center.

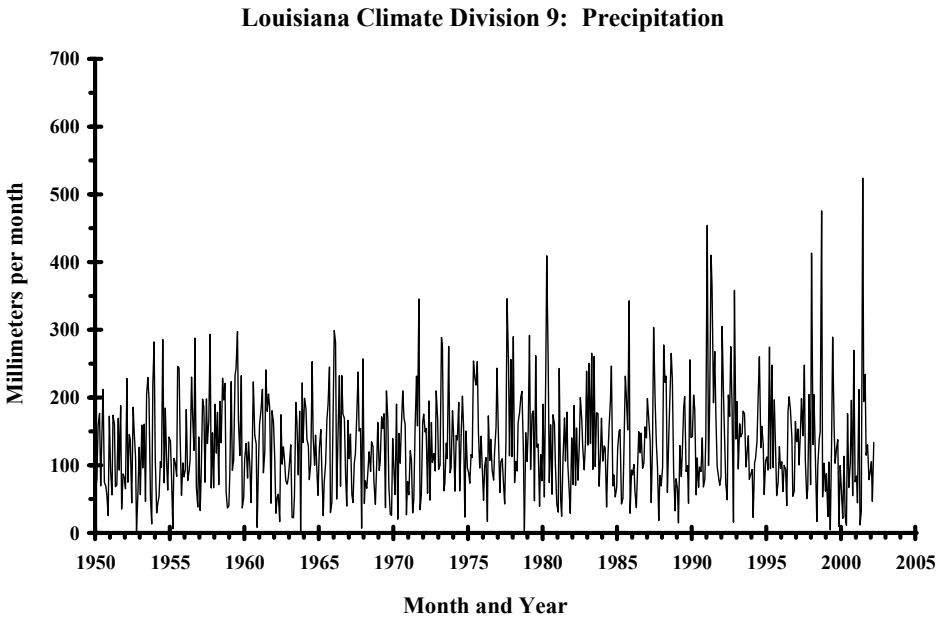

Figure F-8. Plot of monthly total precipitation (millimeters) for Louisiana Climate Division 9. Data is from the National Climatic Data Center.

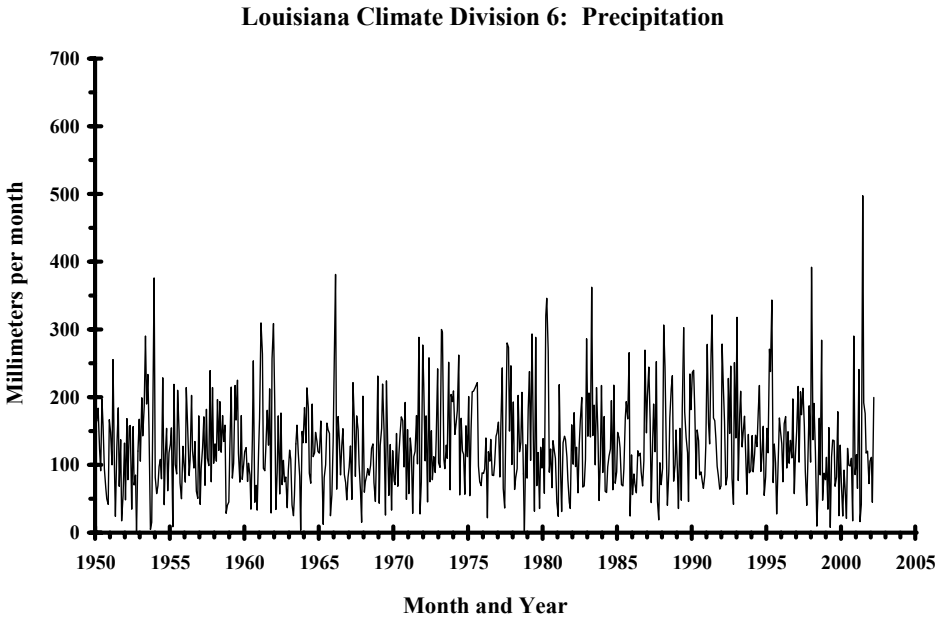

Figure F-9. Plot of monthly total precipitation (millimeters) for Louisiana Climate Division 6. Data is from the National Climatic Data Center.

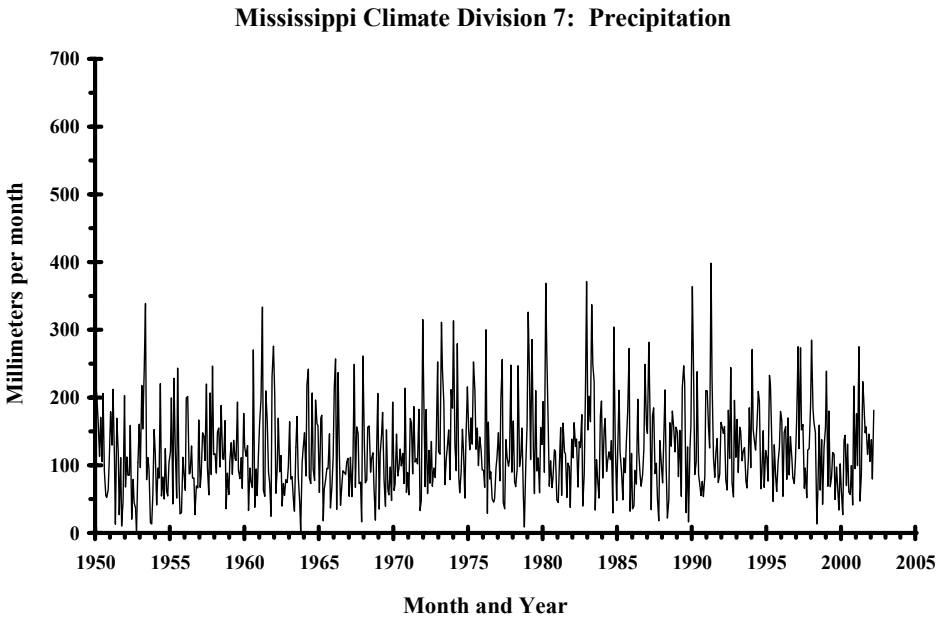

Figure F-10. Plot of monthly total precipitation (millimeters) for Mississippi Climate Division 7. Data is from the National Climatic Data Center.

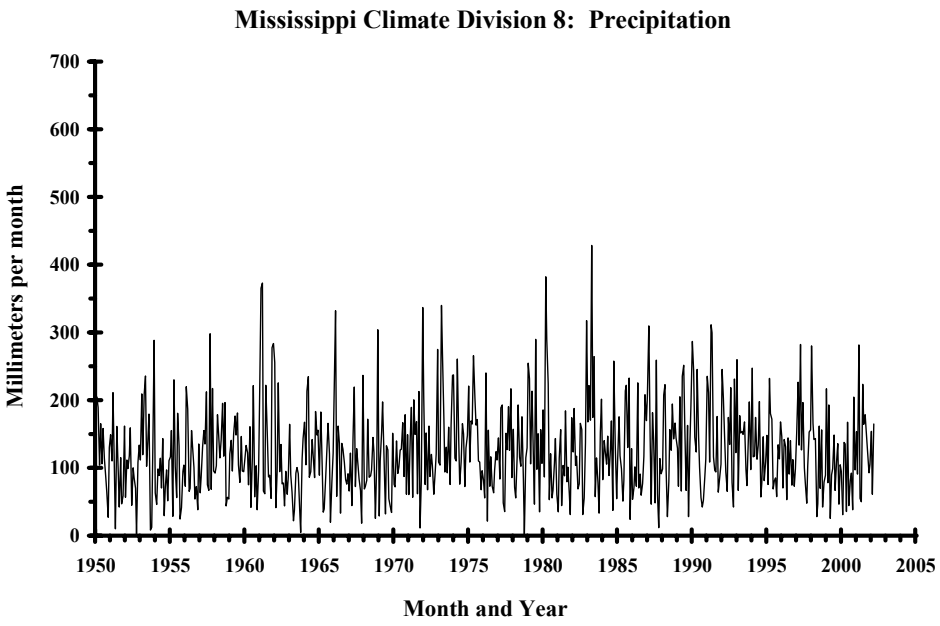

Figure F-11. Plot of monthly total precipitation (millimeters) for Mississippi Climate Division 8. Data is from the National Climatic Data Center.

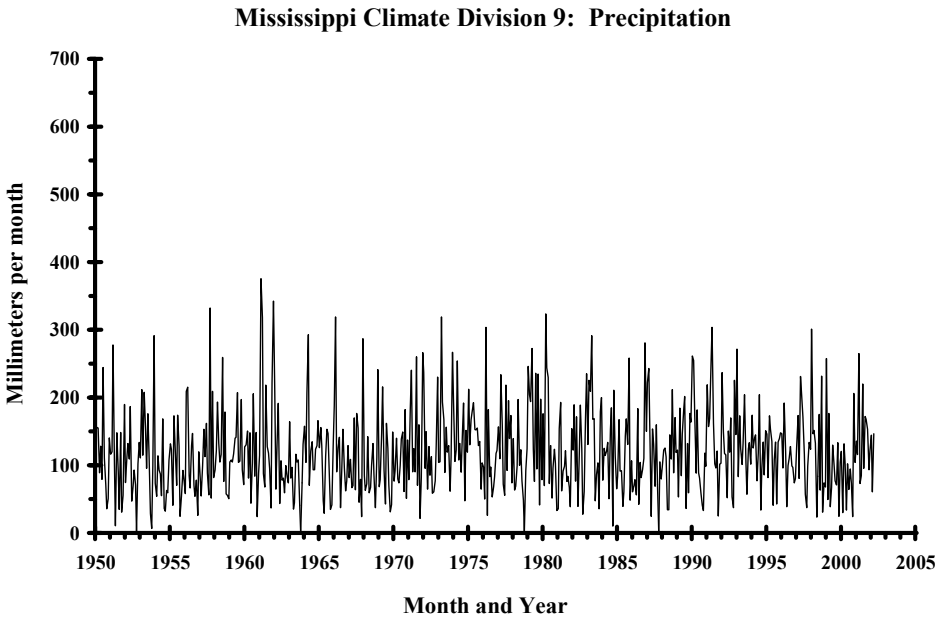

Figure F-12. Plot of monthly total precipitation (millimeters) for Mississippi Climate Division 9. Data is from the National Climatic Data Center.

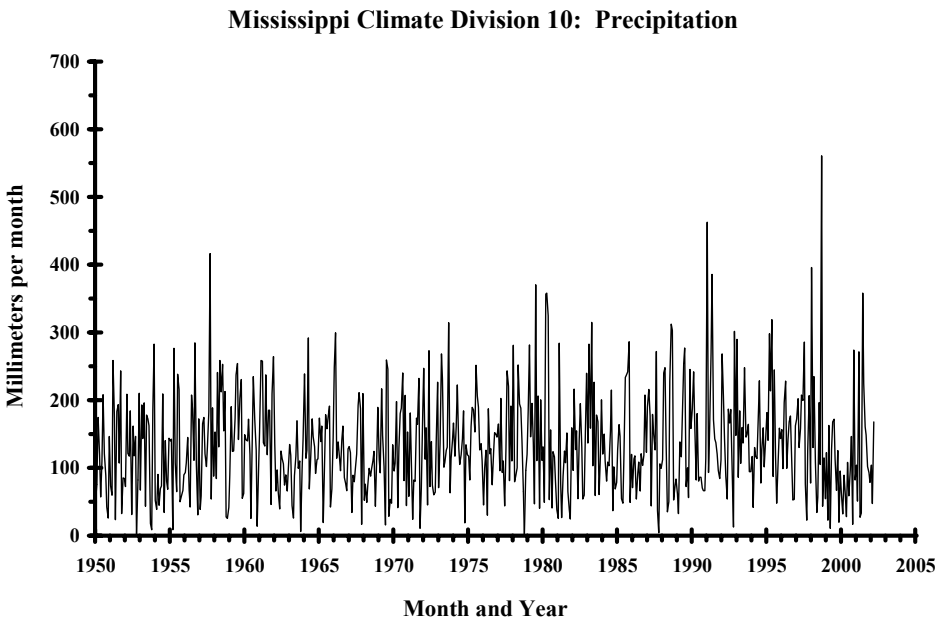

Figure F-13. Plot of monthly total precipitation (millimeters) for Mississippi Climate Division 10. Data is from the National Climatic Data Center.

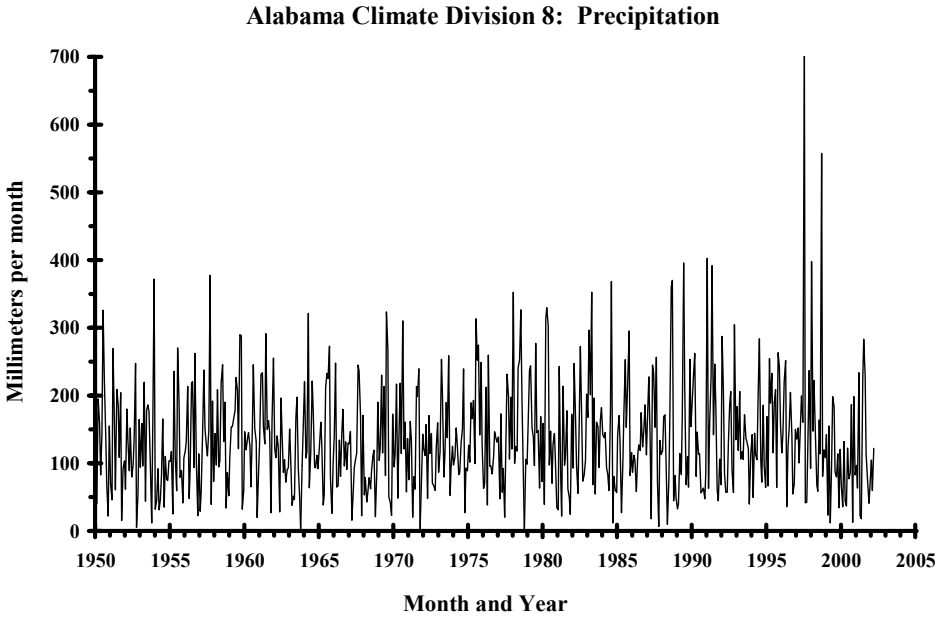

Figure F-14. Plot of monthly total precipitation (millimeters) for Alabama Climate Division 8. Data is from the National Climatic Data Center.

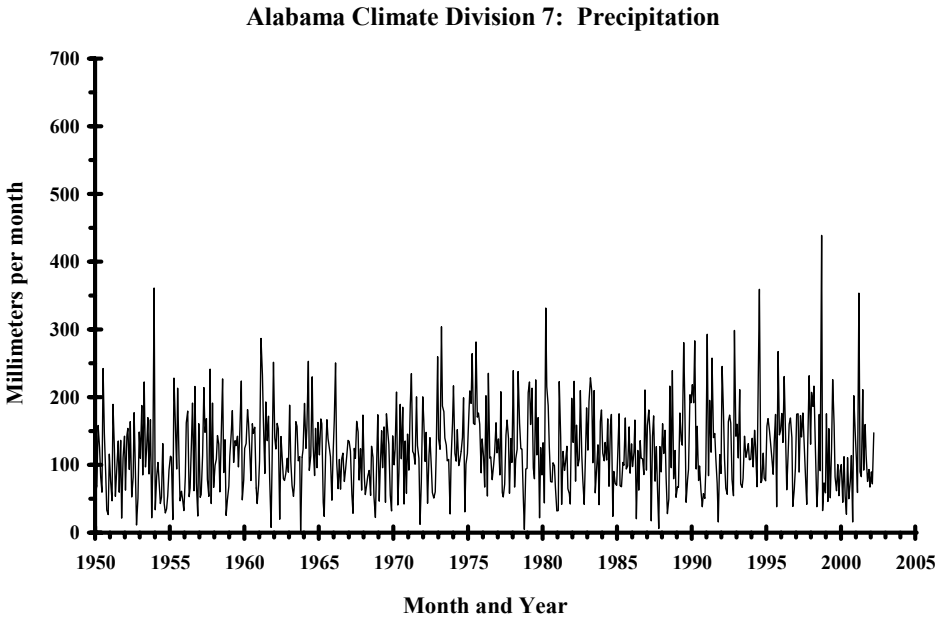

Figure F-15. Plot of monthly total precipitation (millimeters) for Alabama Climate Division 7. Data is from the National Climatic Data Center.

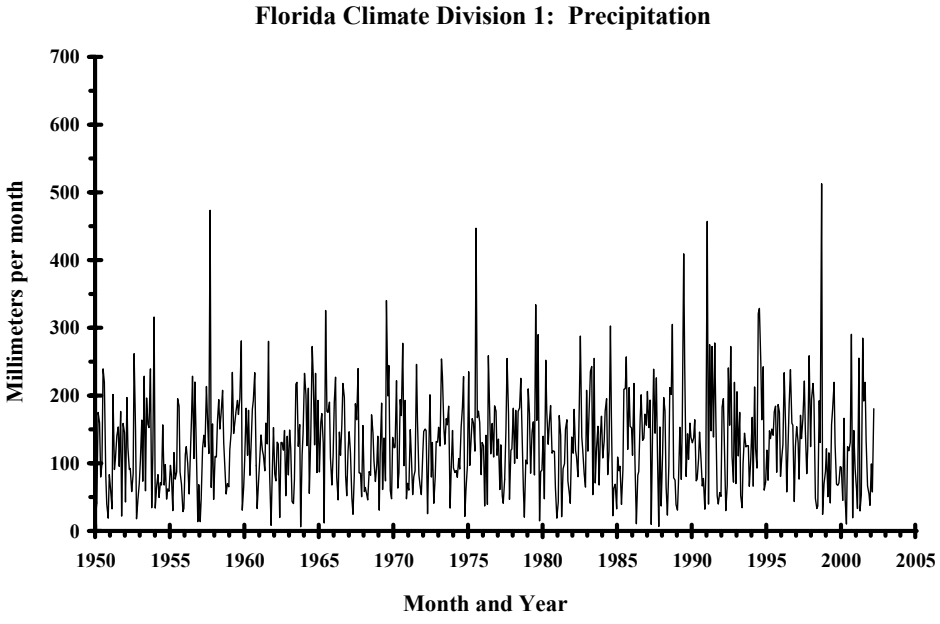

Figure F-16. Plot of monthly total precipitation (millimeters) for Florida Climate Division 1. Data is from the National Climatic Data Center.

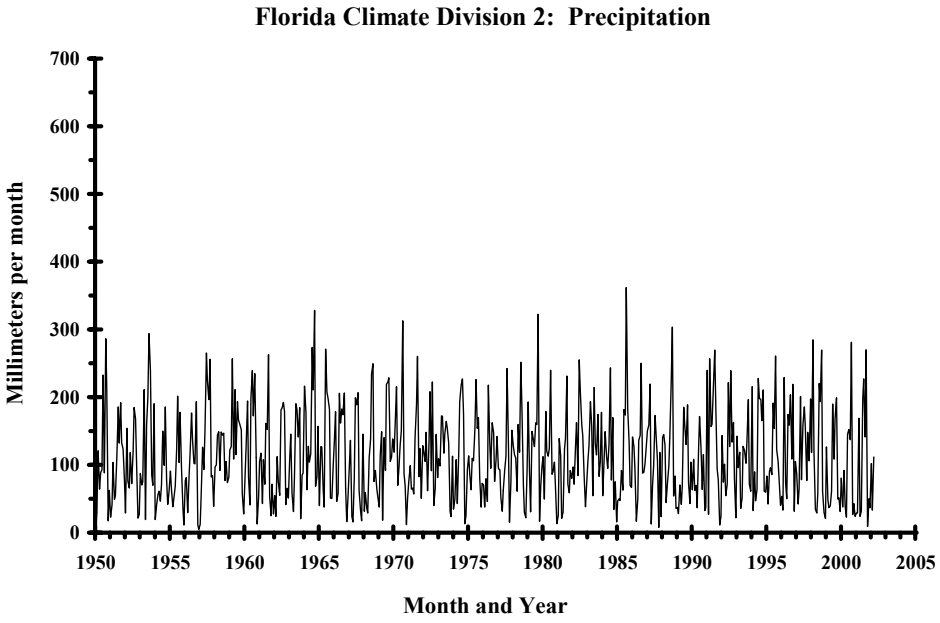

Figure F-17. Plot of monthly total precipitation (millimeters) for Florida Climate Division 2. Data is from the National Climatic Data Center.

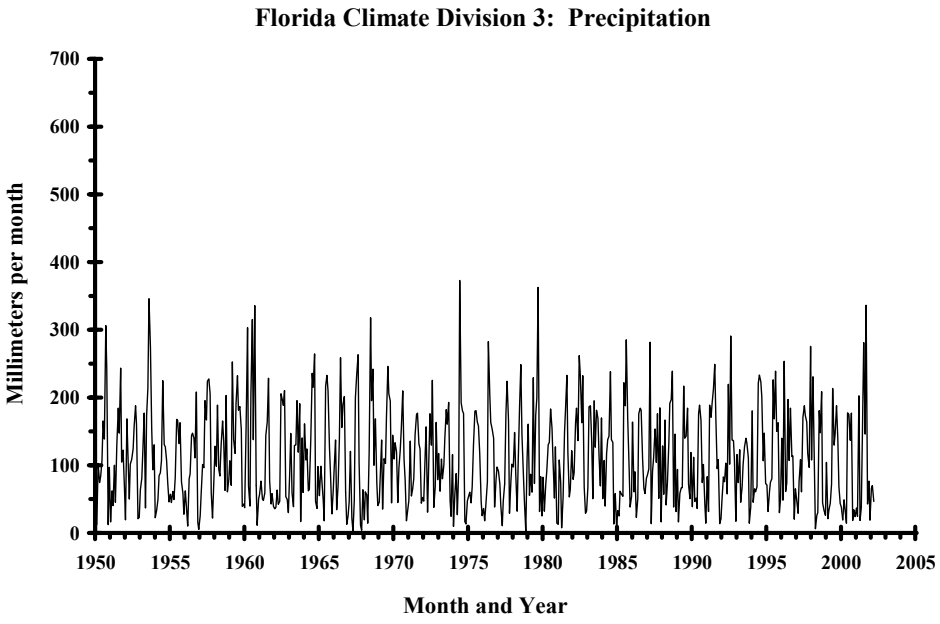

Figure F-18. Plot of monthly total precipitation (millimeters) for Florida Climate Division 3. Data is from the National Climatic Data Center.

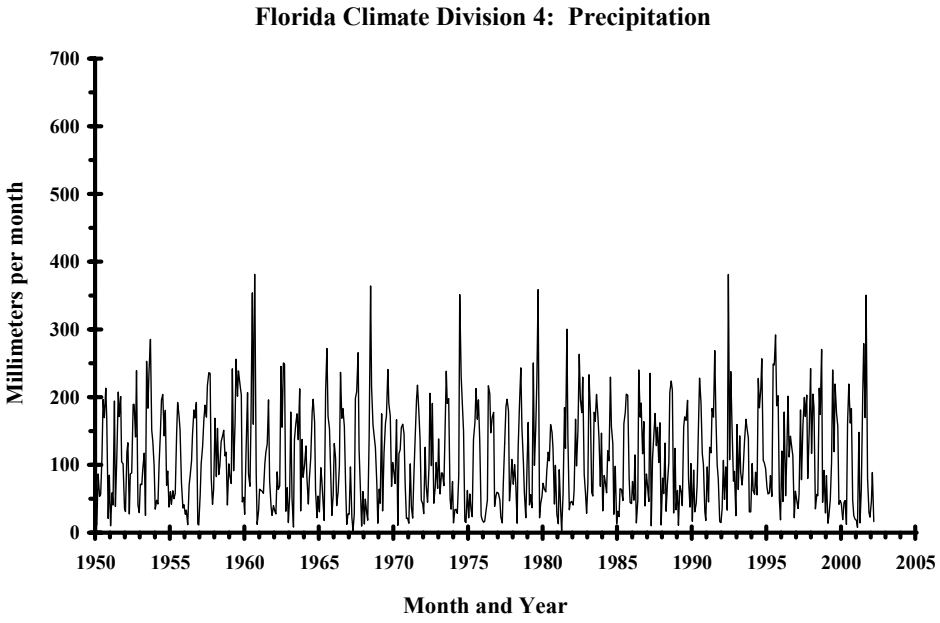

Figure F-19. Plot of monthly total precipitation (millimeters) for Florida Climate Division 4. Data is from the National Climatic Data Center.

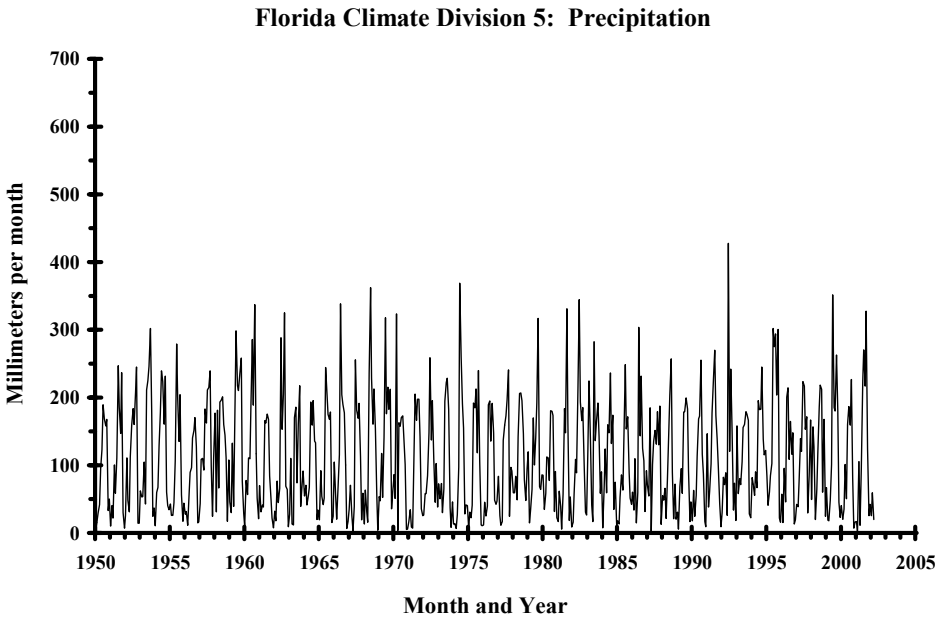

Figure F-20. Plot of monthly total precipitation (millimeters) for Florida Climate Division 5. Data is from the National Climatic Data Center.

Appendix G: Temperature data plots.

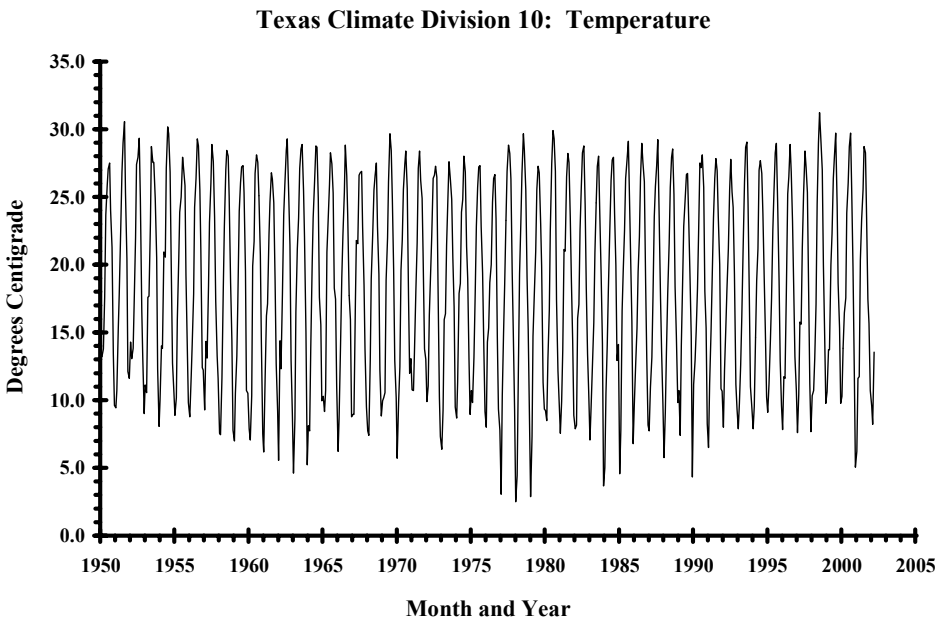

Figure G-1. Plot of monthly average temperature (degrees celsius) for Texas Climate Division 10. Data is from the National Climatic Data Center.

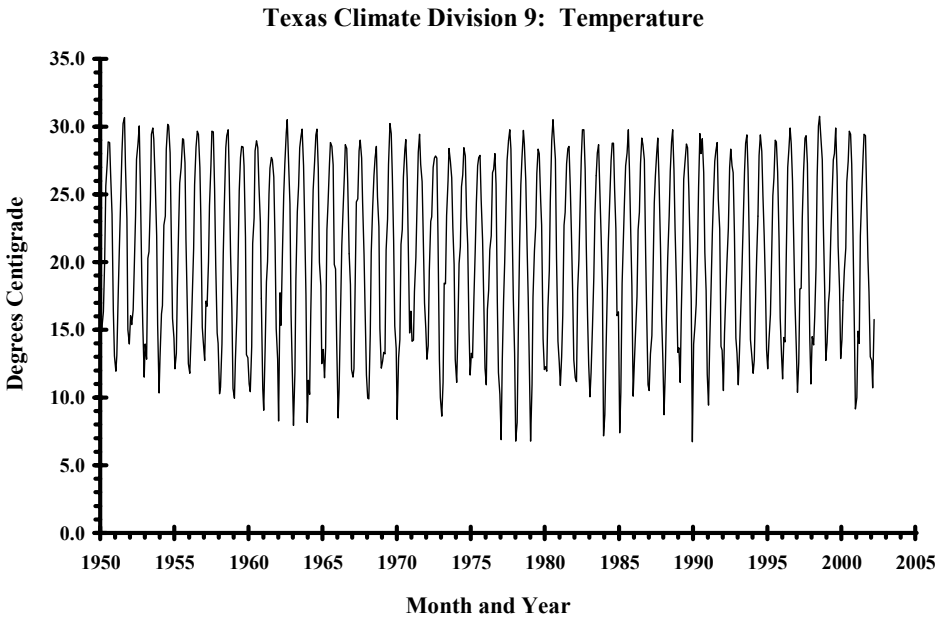

Figure G-2. Plot of monthly average temperature (degrees celsius) for Texas Climate Division 9. Data is from the National Climatic Data Center.

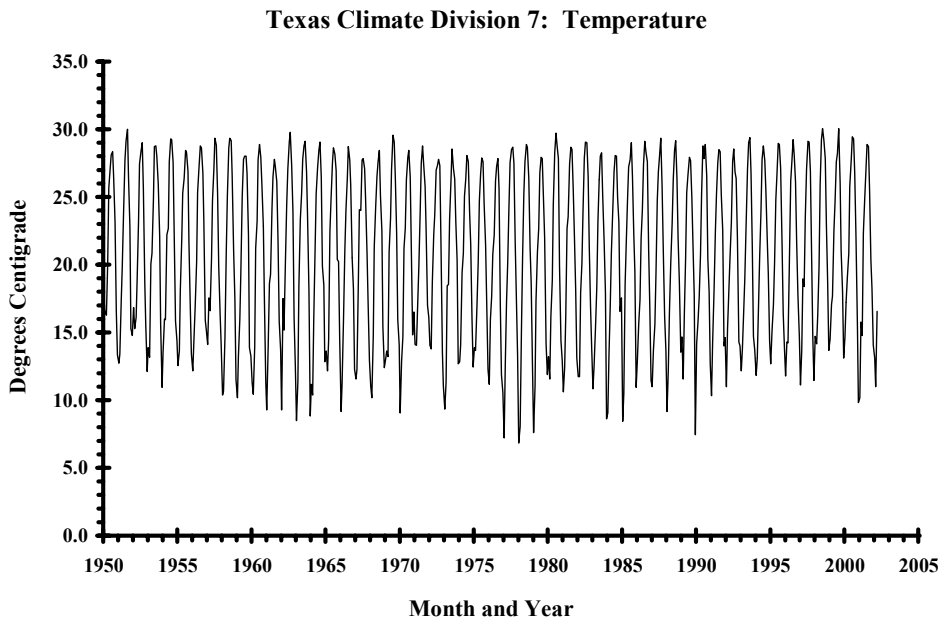

Figure G-3. Plot of monthly average temperature (degrees celsius) for Texas Climate Division 7. Data is from the National Climatic Data Center.

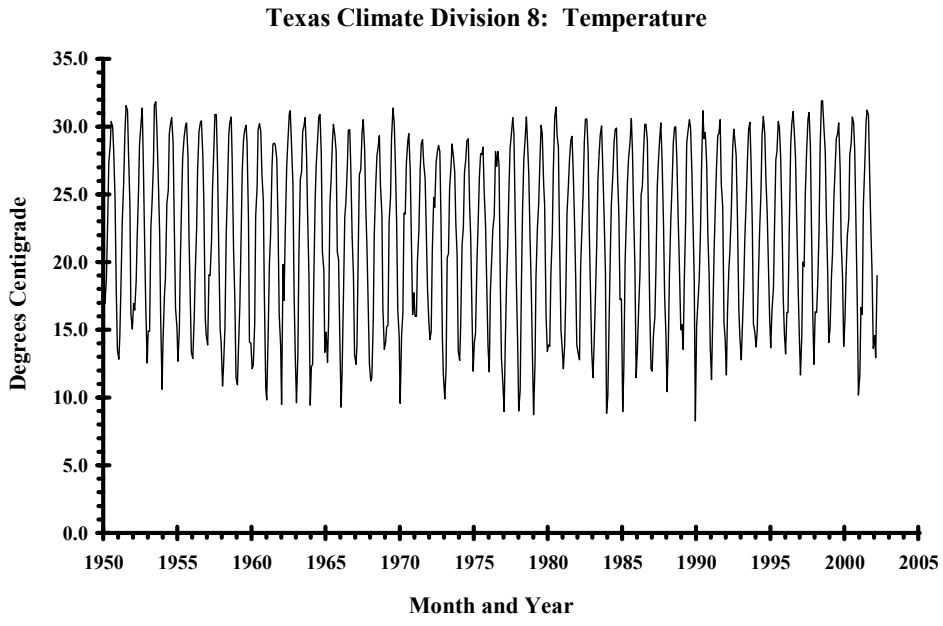

Figure G-4. Plot of monthly average temperature (degrees celsius) for Texas Climate Division 8. Data is from the National Climatic Data Center.

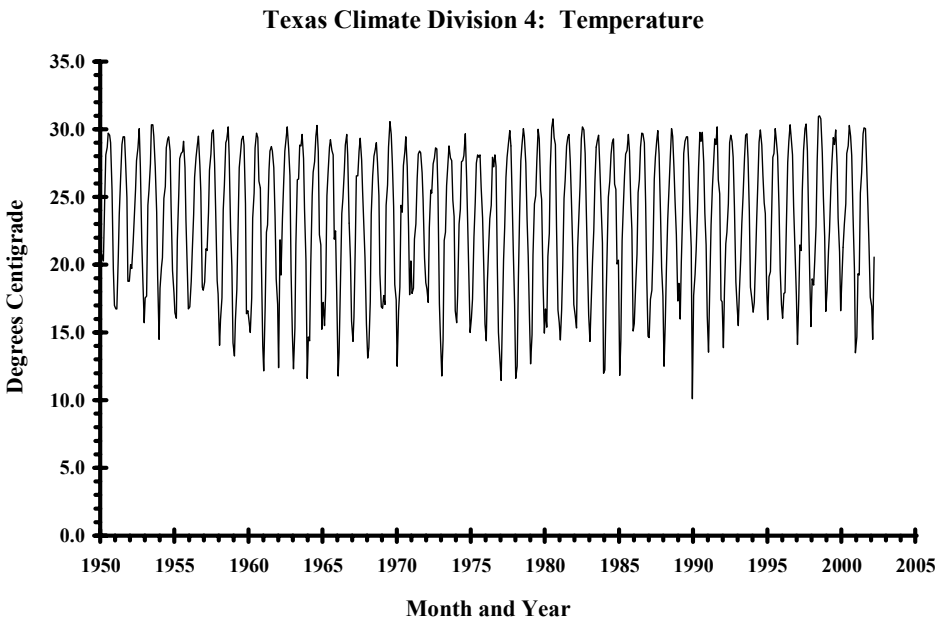

Figure G-5. Plot of monthly average temperature (degrees celsius) for Texas Climate Division 4. Data is from the National Climatic Data Center.

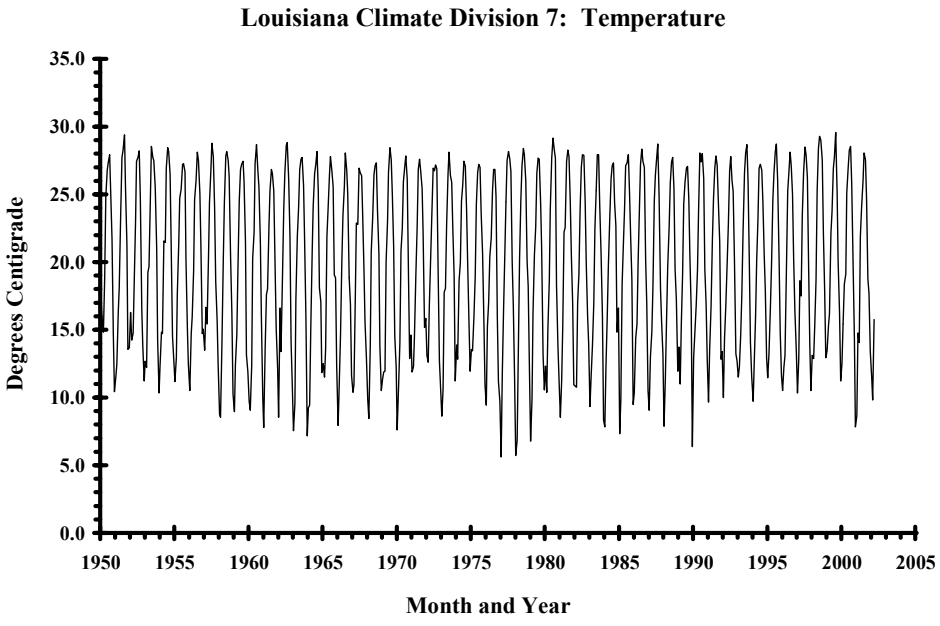

Figure G-6. Plot of monthly average temperature (degrees celsius) for Louisiana Climate Division 7. Data is from the National Climatic Data Center.

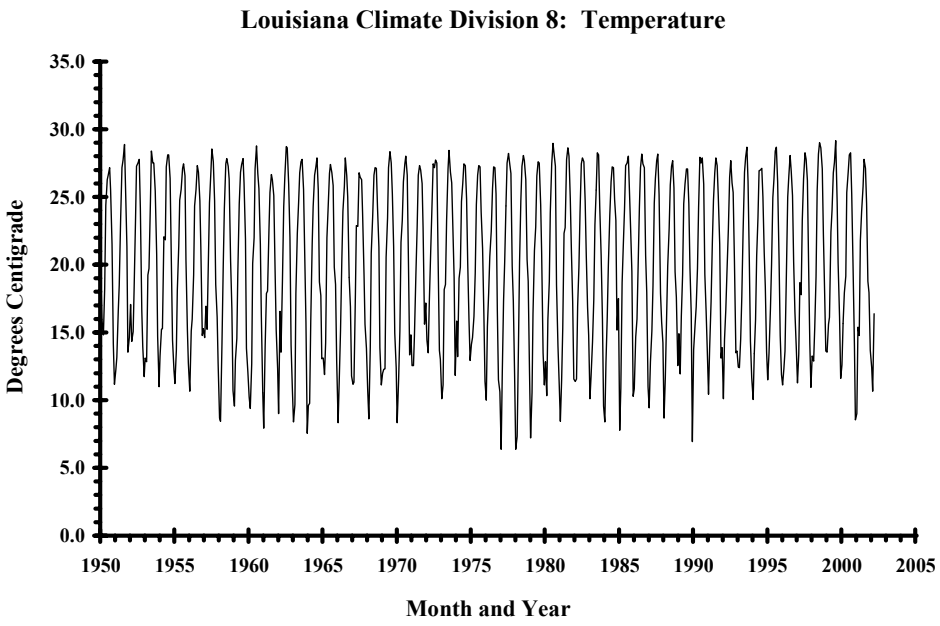

Figure G-7. Plot of monthly average temperature (degrees celsius) for Louisiana Climate Division 8. Data is from the National Climatic Data Center.

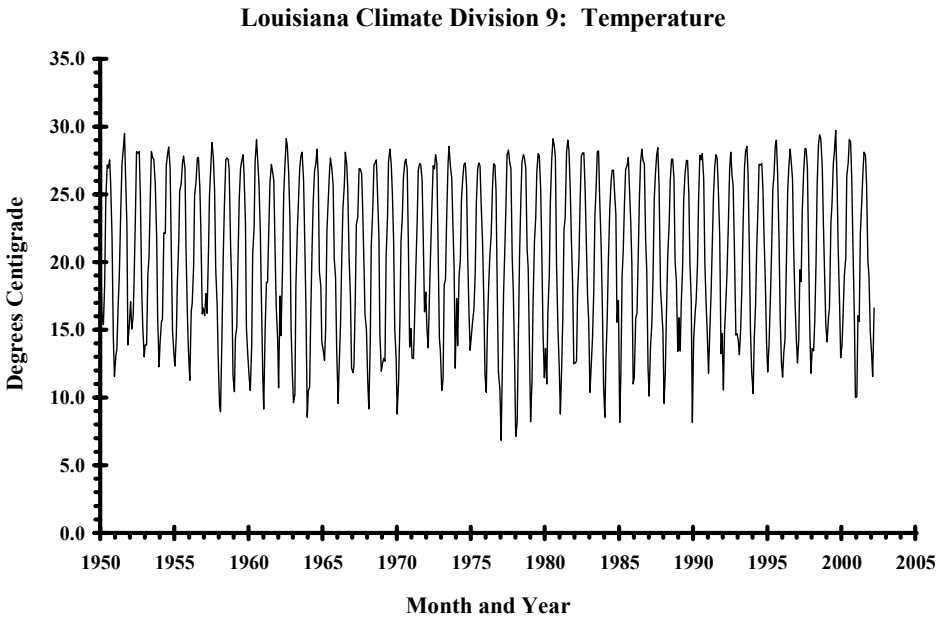

Figure G-8. Plot of monthly average temperature (degrees celsius) for Louisiana Climate Division 9. Data is from the National Climatic Data Center.

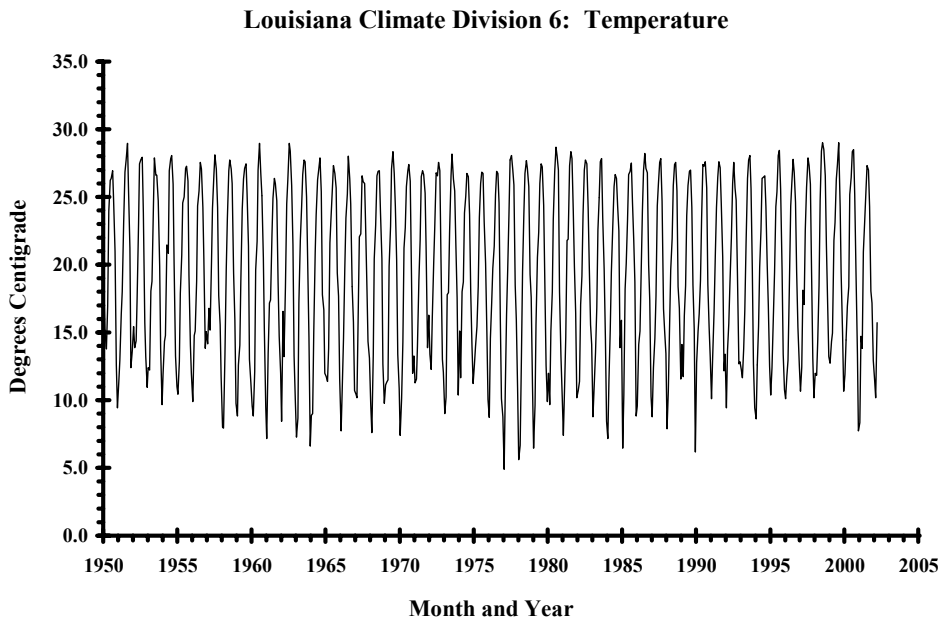

Figure G-9. Plot of monthly average temperature (degrees celsius) for Louisiana Climate Division 6. Data is from the National Climatic Data Center.

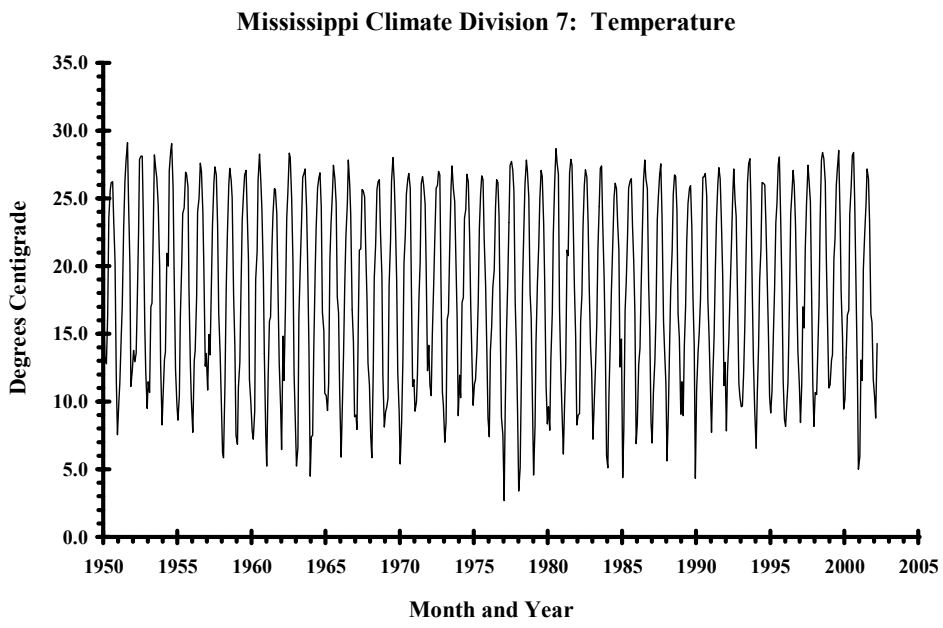

Figure G-10. Plot of monthly average temperature (degrees celsius) for Mississippi Climate Division 7. Data is from the National Climatic Data Center.

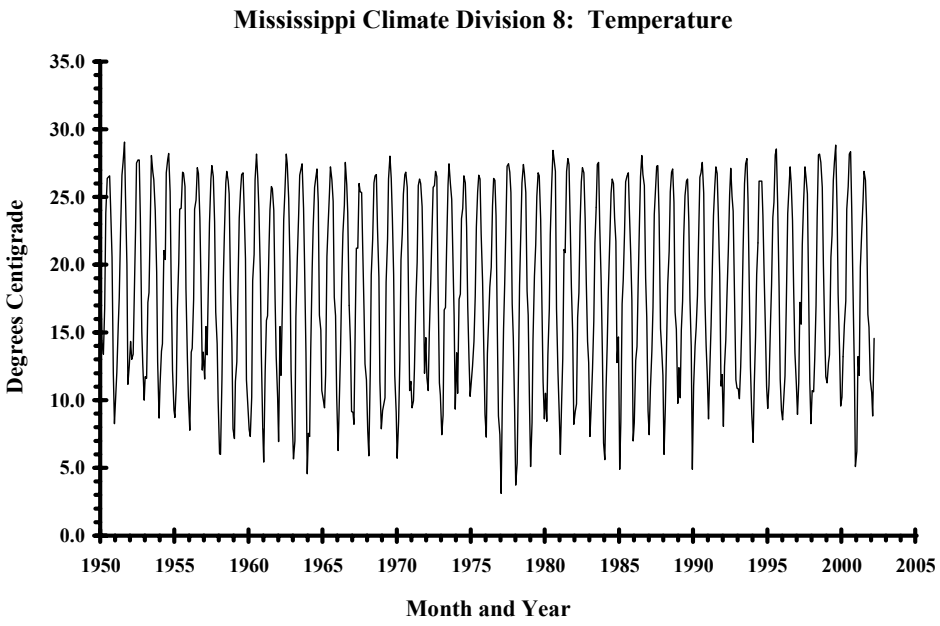

Figure G-11. Plot of monthly average temperature (degrees celsius) for Mississippi Climate Division 8. Data is from the National Climatic Data Center.

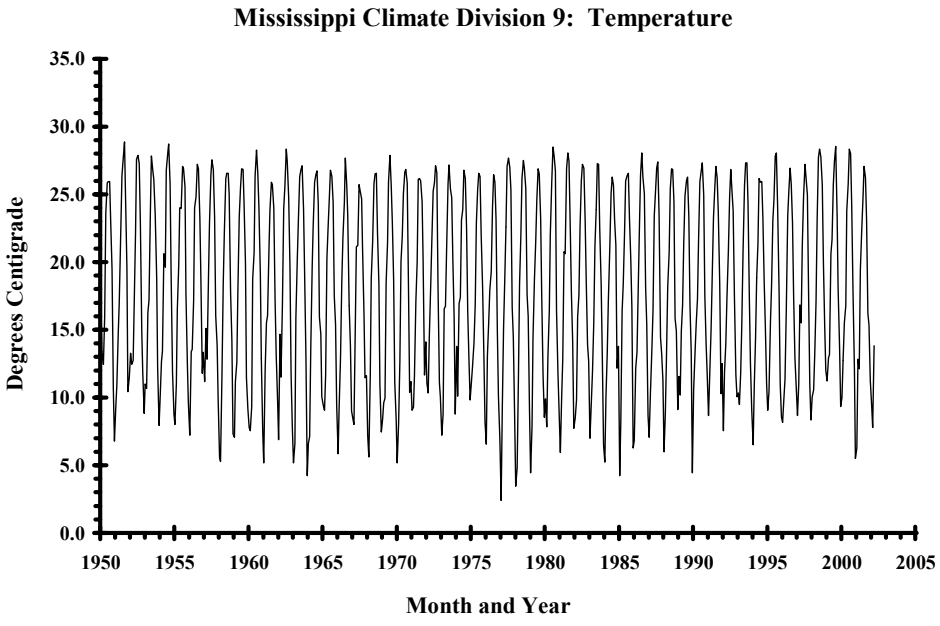

Figure G-12. Plot of monthly average temperature (degrees celsius) for Mississippi Climate Division 9. Data is from the National Climatic Data Center.

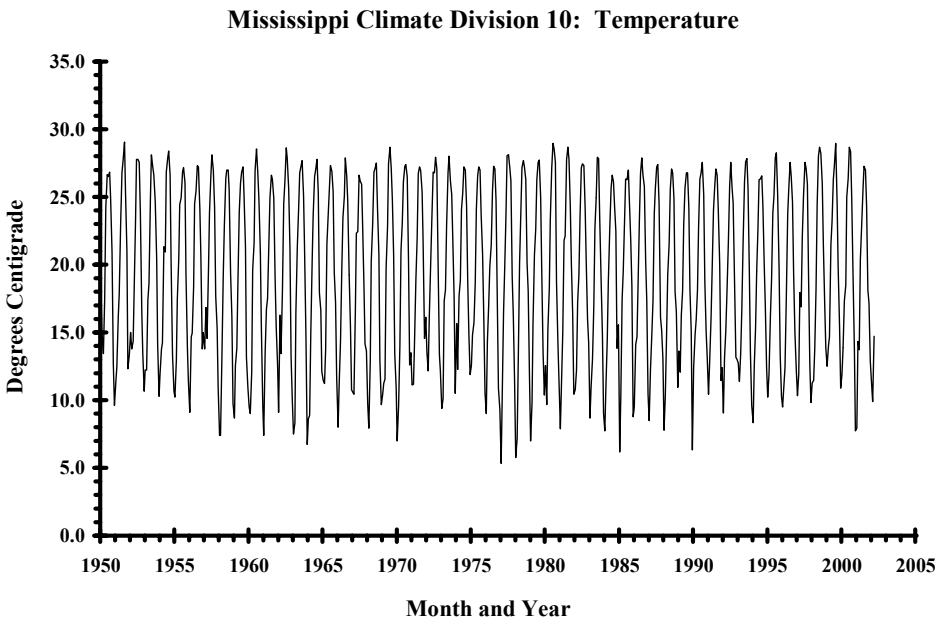

Figure G-13. Plot of monthly average temperature (degrees celsius) for Mississippi Climate Division 10. Data is from the National Climatic Data Center.

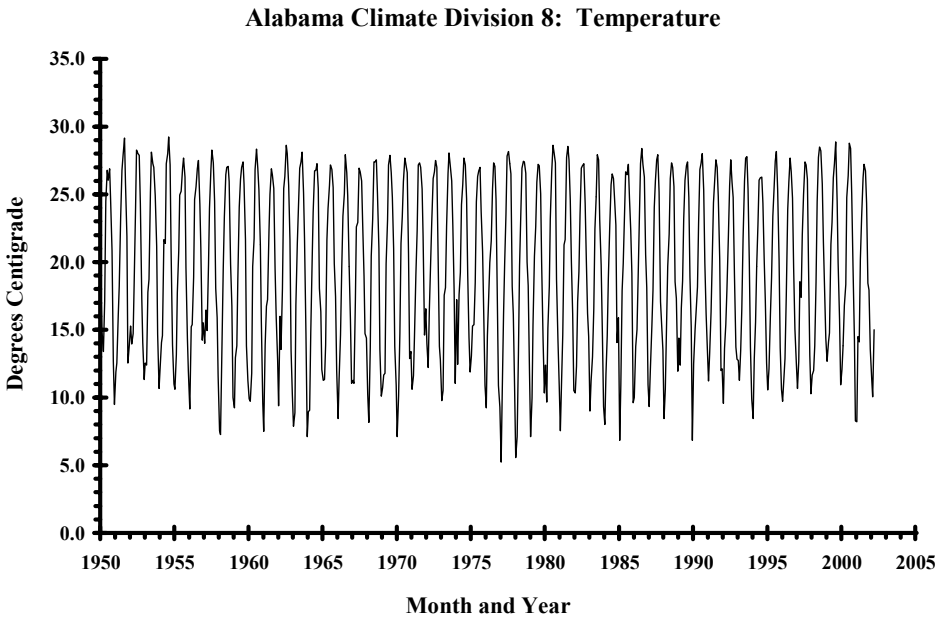

Figure G-14. Plot of monthly average temperature (degrees celsius) for Alabama Climate Division 8. Data is from the National Climatic Data Center.

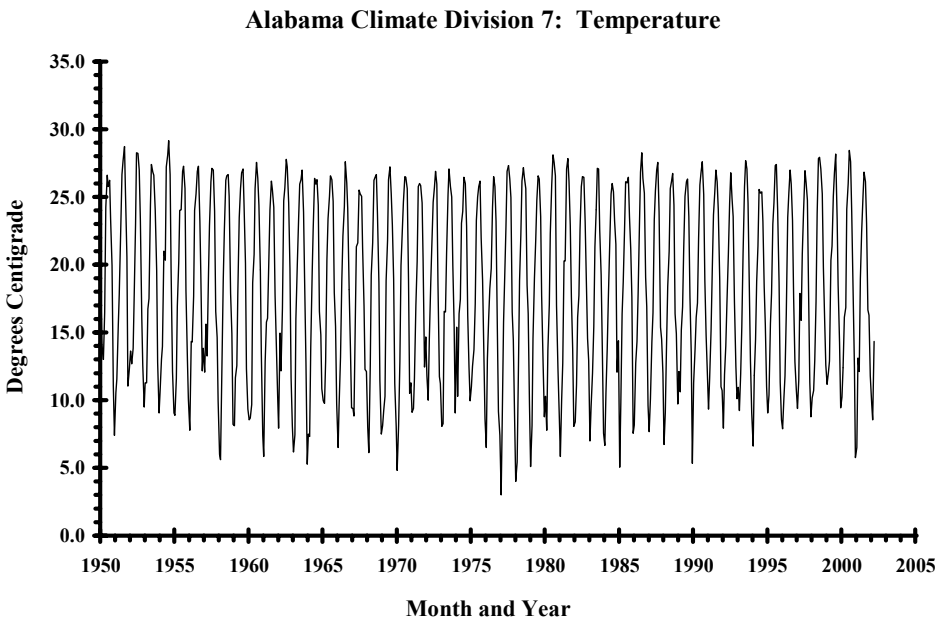

Figure G-15. Plot of monthly average temperature (degrees celsius) for Alabama Climate Division 7. Data is from the National Climatic Data Center.

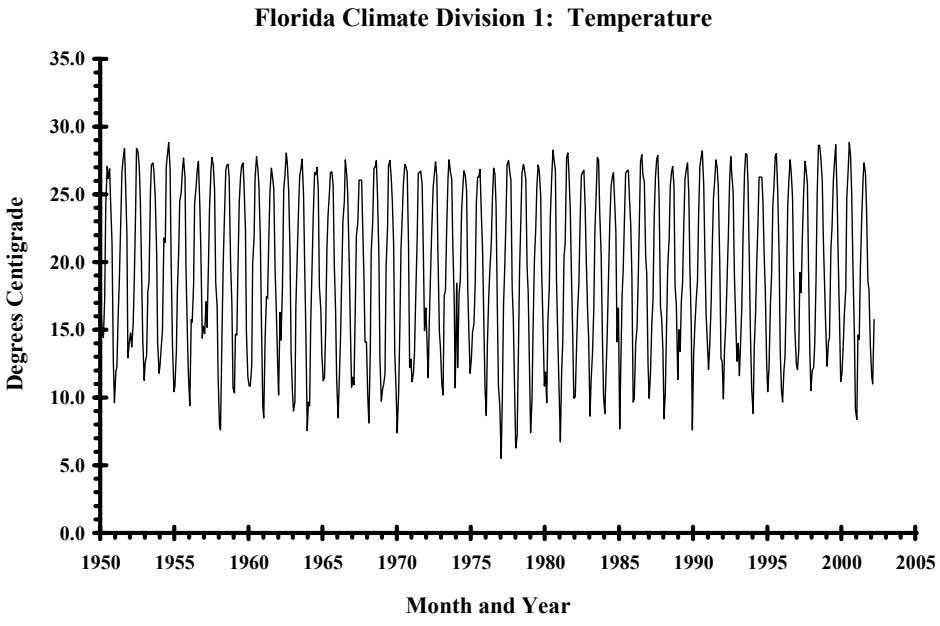

Figure G-16. Plot of monthly average temperature (degrees celsius) for Florida Climate Division 1. Data is from the National Climatic Data Center.

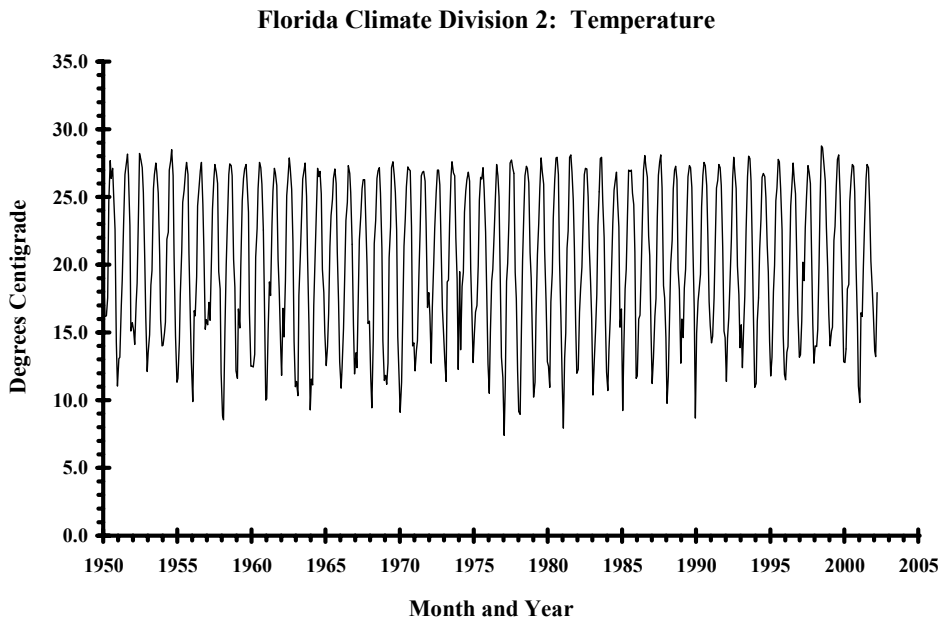

Figure G-17. Plot of monthly average temperature (degrees celsius) for Florida Climate Division 2. Data is from the National Climatic Data Center.

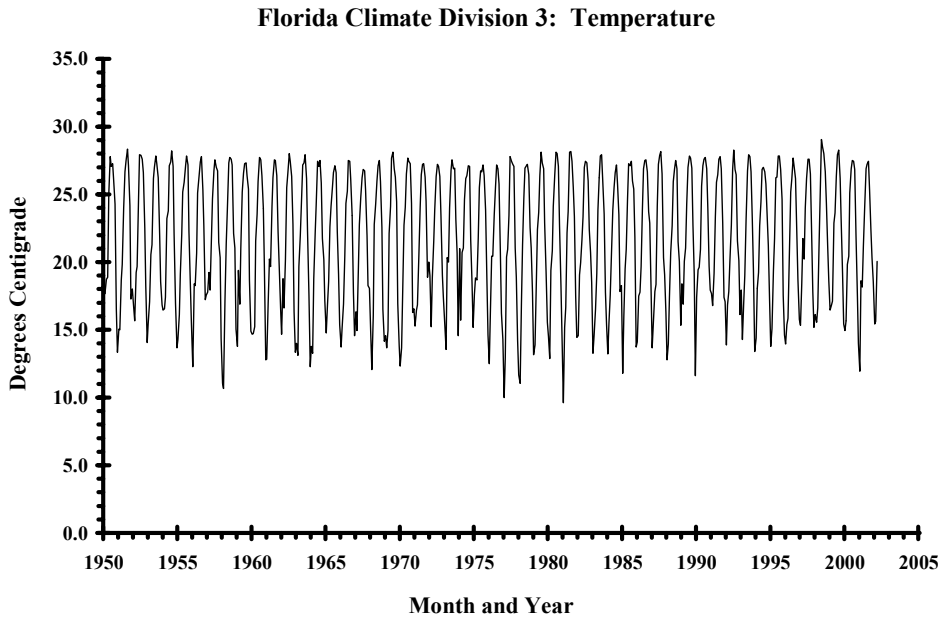

Figure G-18. Plot of monthly average temperature (degrees celsius) for Florida Climate Division 3. Data is from the National Climatic Data Center.

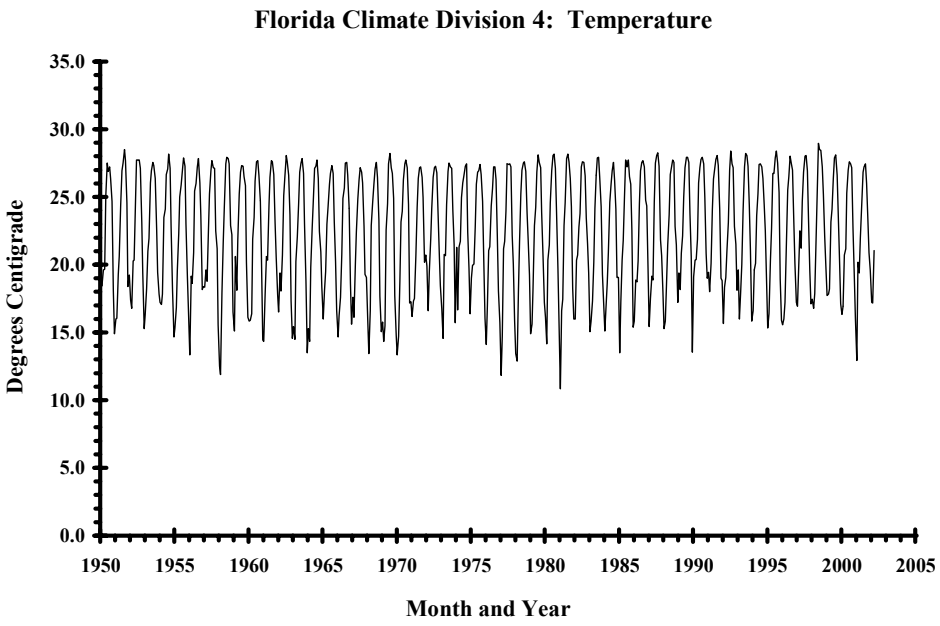

Figure G-19. Plot of monthly average temperature (degrees celsius) for Florida Climate Division 4. Data is from the National Climatic Data Center.

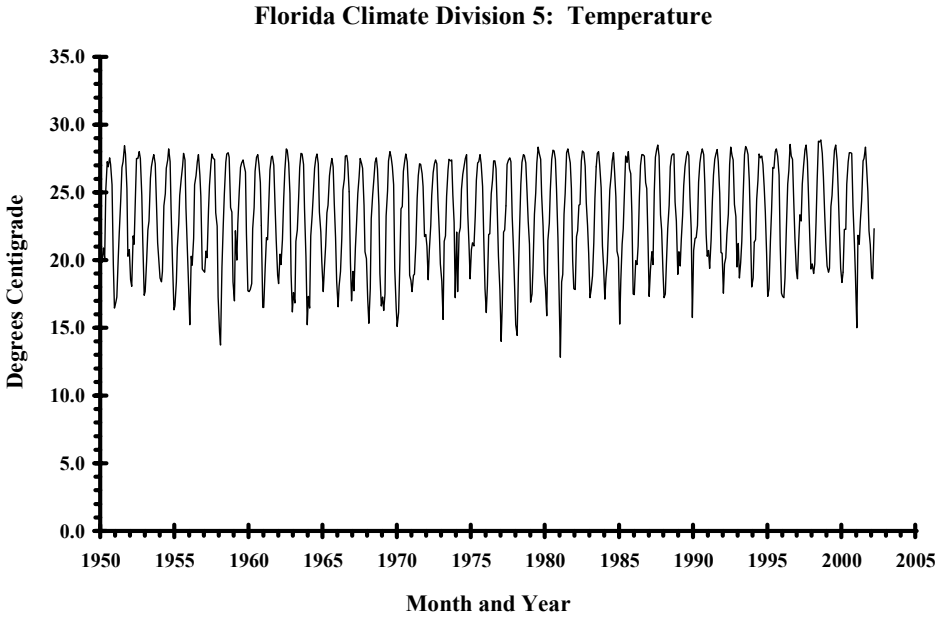

Figure G-20. Plot of monthly average temperature (degrees celsius) for Florida Climate Division 5. Data is from the National Climatic Data Center.

Appendix H: Potential Evaporation (PE) data plots.

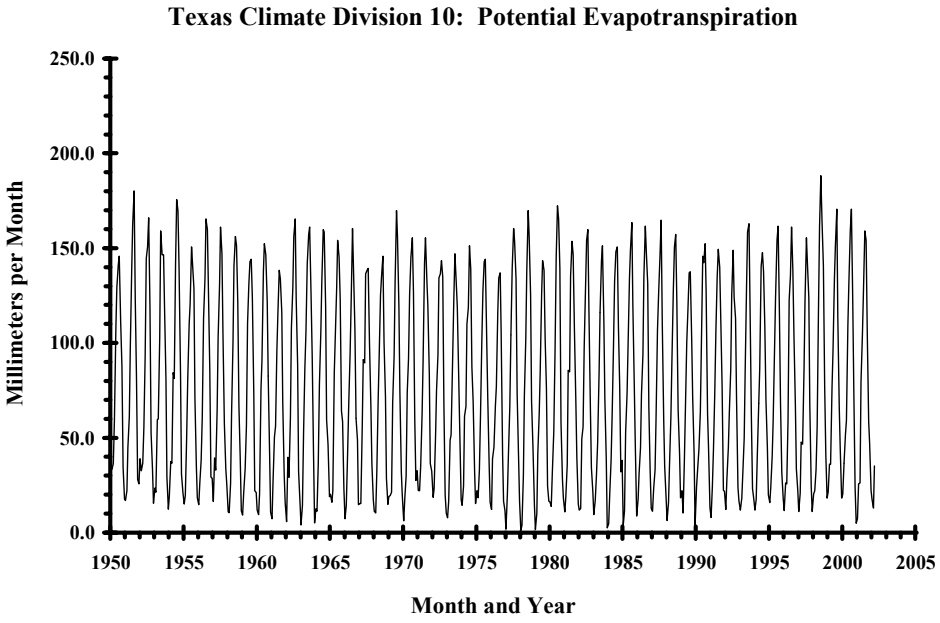

Figure H-1. Plot of monthly total potential evapotranspiration (millimeters) for Texas Climate Division 10. Data is from the National Climatic Data Center.

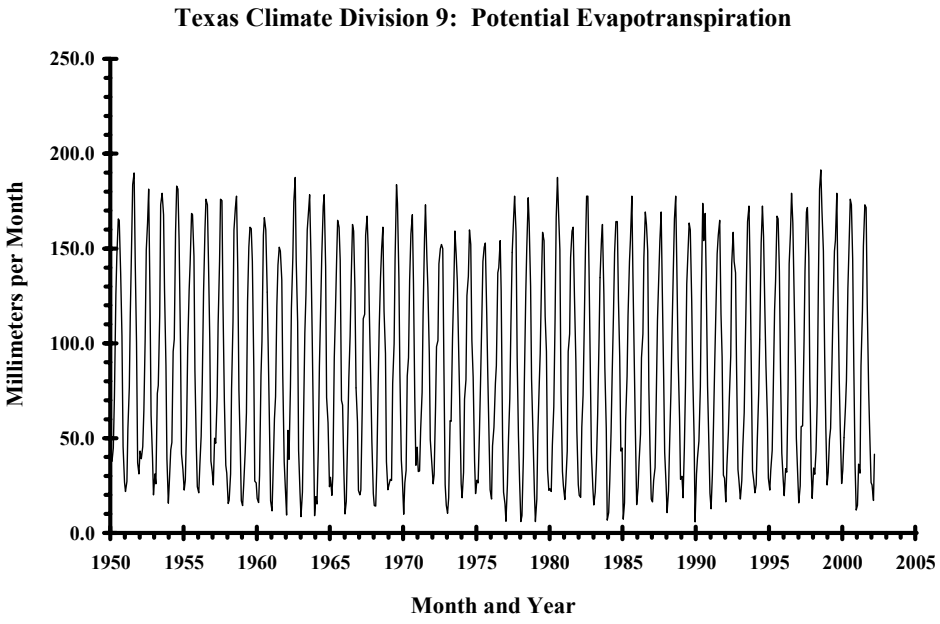

Figure H-2. Plot of monthly total potential evapotranspiration (millimeters) for Texas Climate Division 9. Data is from the National Climatic Data Center.

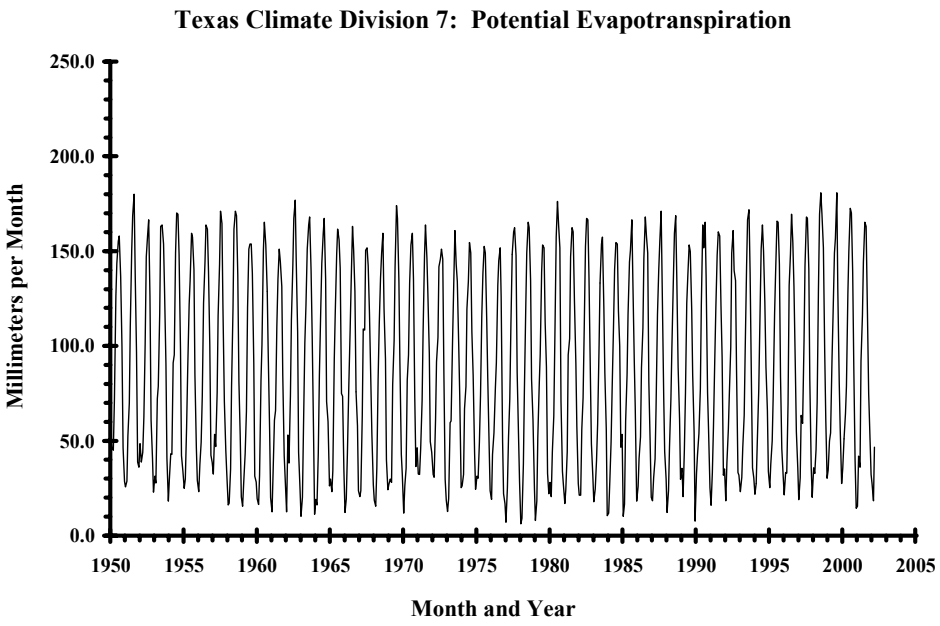

Figure H-3. Plot of monthly total potential evapotranspiration (millimeters) for Texas Climate Division 7. Data is from the National Climatic Data Center.

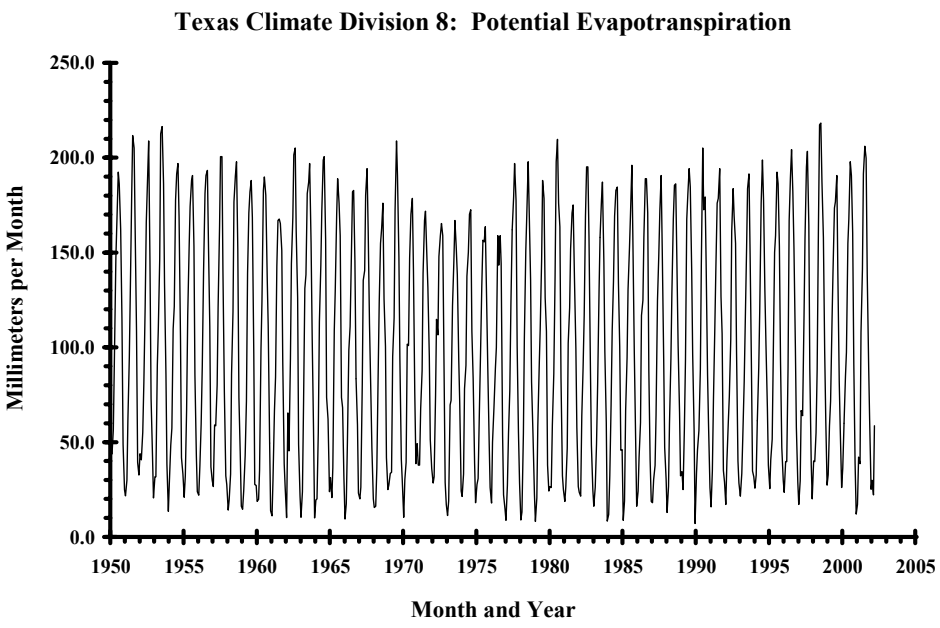

Figure H-4. Plot of monthly total potential evapotranspiration (millimeters) for Texas Climate Division 8. Data is from the National Climatic Data Center.

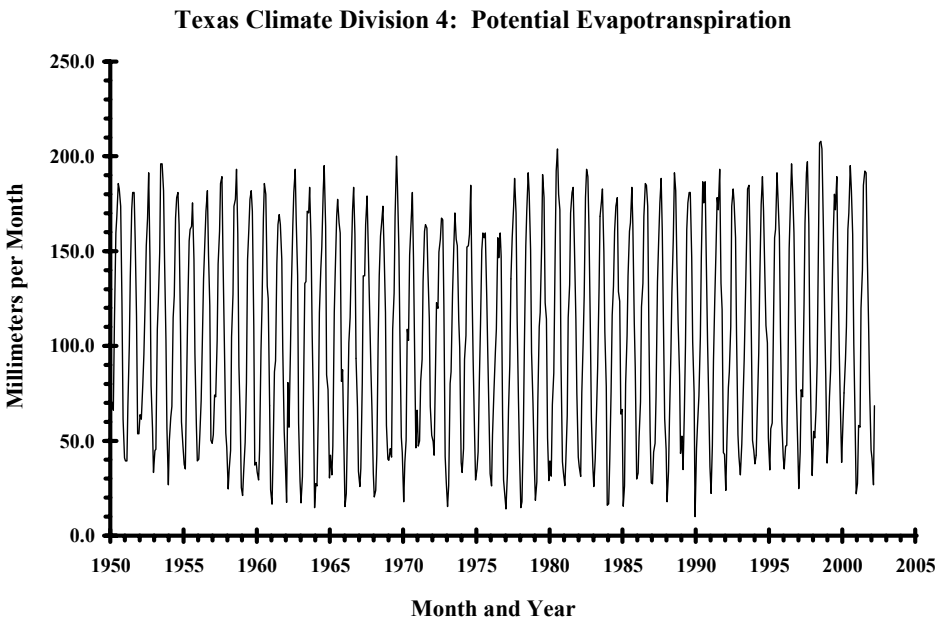

Figure H-5. Plot of monthly total potential evapotranspiration (millimeters) for Texas Climate Division 4. Data is from the National Climatic Data Center.

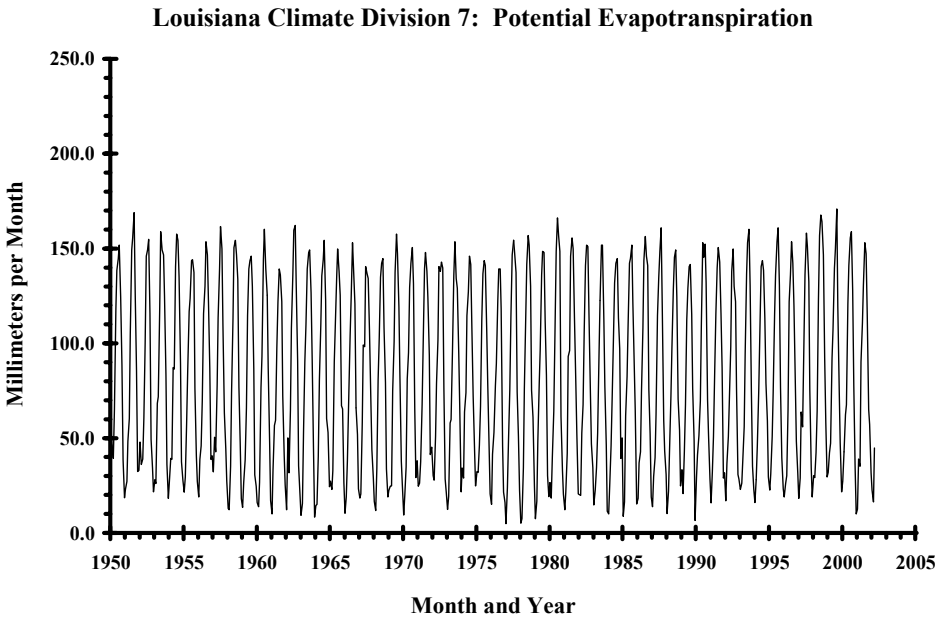

Figure H-6. Plot of monthly total potential evapotranspiration (millimeters) for Louisiana Climate Division 7. Data is from the National Climatic Data Center.

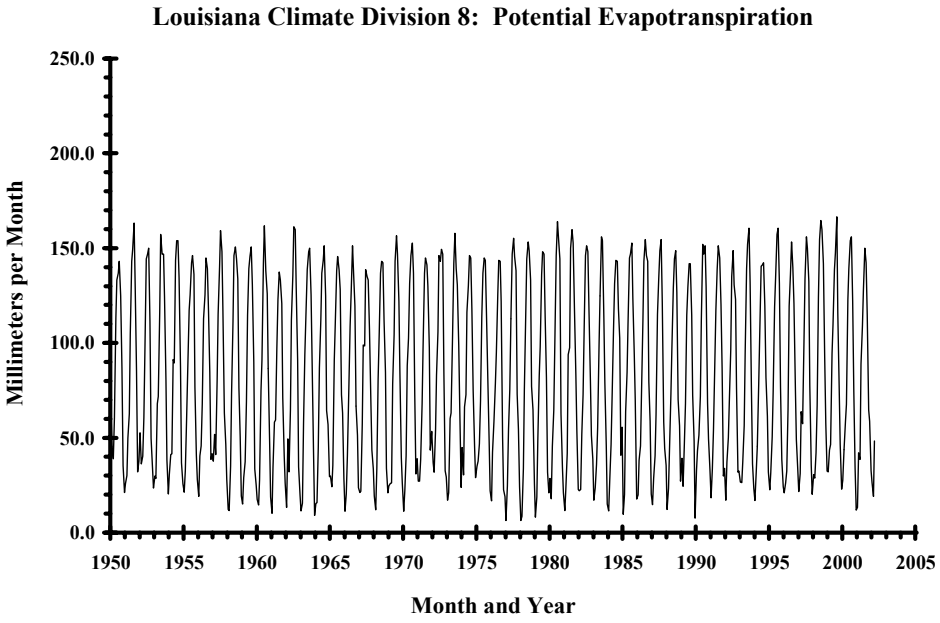

Figure H-7. Plot of monthly total potential evapotranspiration (millimeters) for Louisiana Climate Division 8. Data is from the National Climatic Data Center.

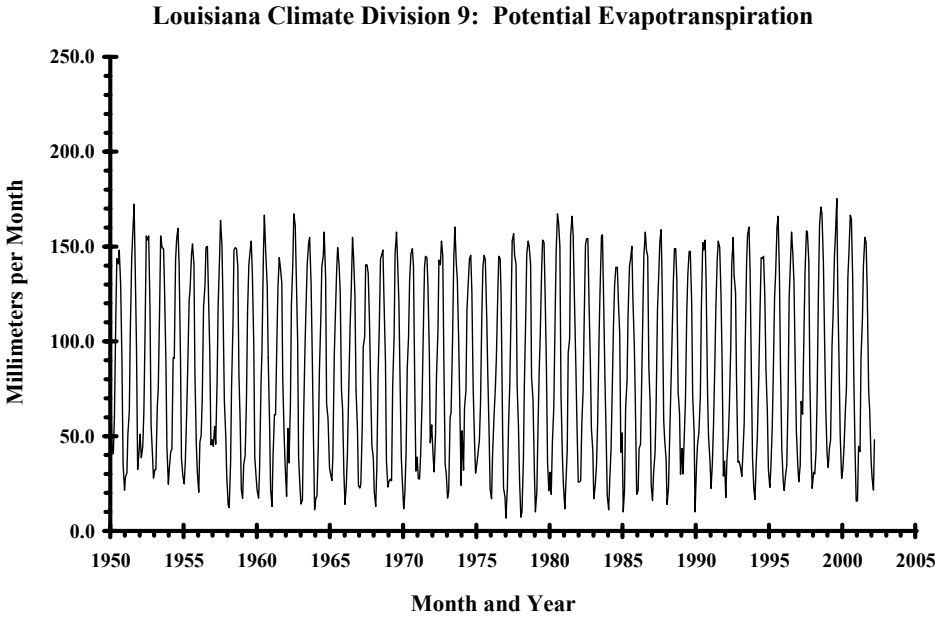

Figure H-8. Plot of monthly total potential evapotranspiration (millimeters) for Louisiana Climate Division 9. Data is from the National Climatic Data Center.

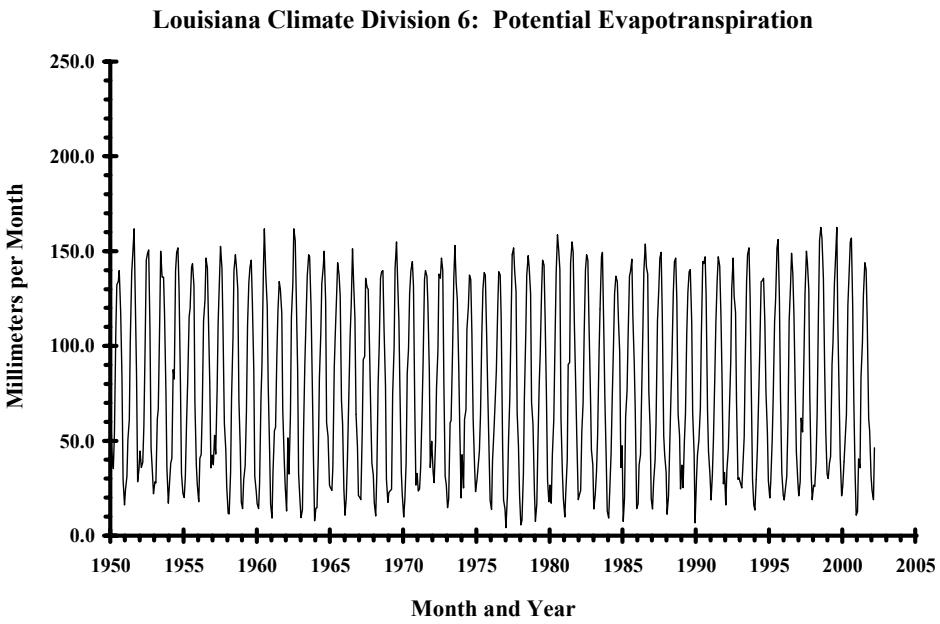

Figure H-9. Plot of monthly total potential evapotranspiration (millimeters) for Louisiana Climate Division 6. Data is from the National Climatic Data Center.

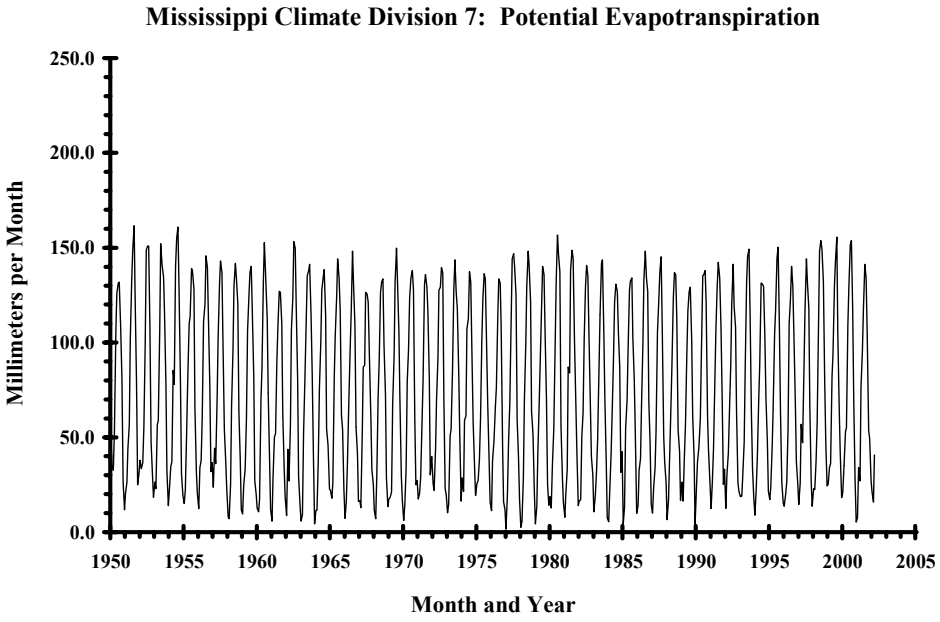

Figure H-10. Plot of monthly total potential evapotranspiration (millimeters) for Mississippi Climate Division 7. Data is from the National Climatic Data Center.

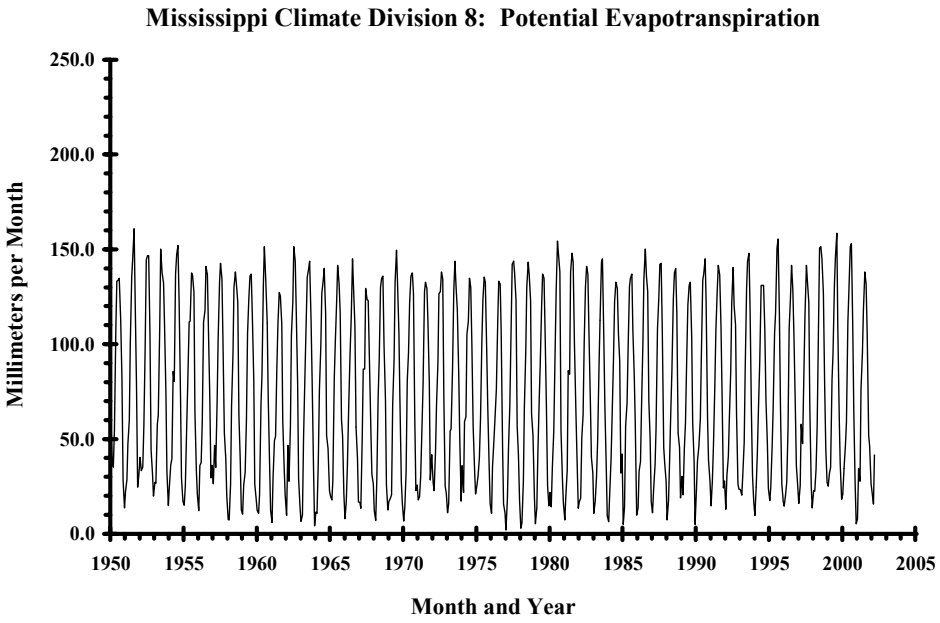

Figure H-11. Plot of monthly total potential evapotranspiration (millimeters) for Mississippi Climate Division 8. Data is from the National Climatic Data Center.

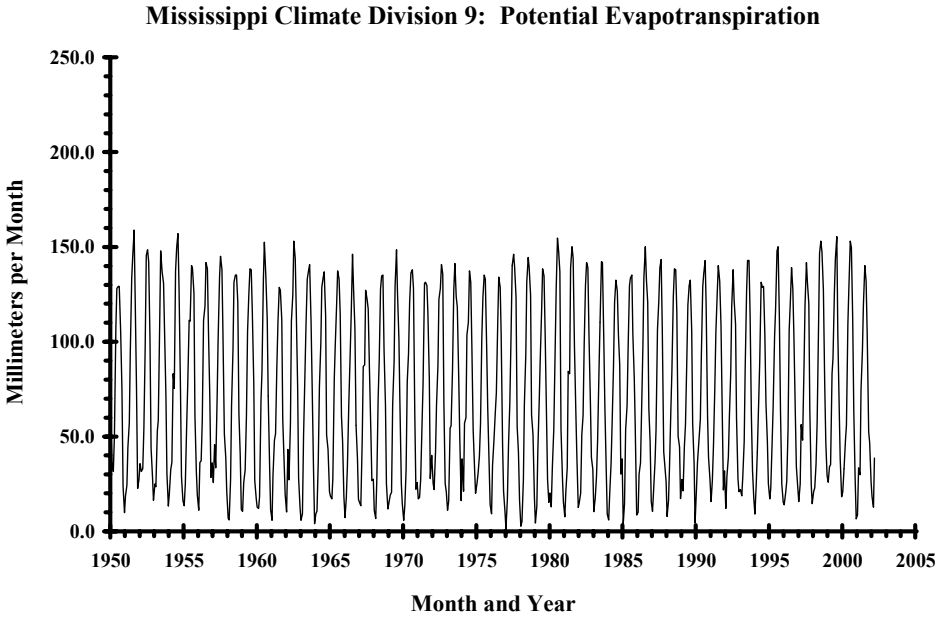

Figure H-12. Plot of monthly total potential evapotranspiration (millimeters) for Mississippi Climate Division 9. Data is from the National Climatic Data Center.

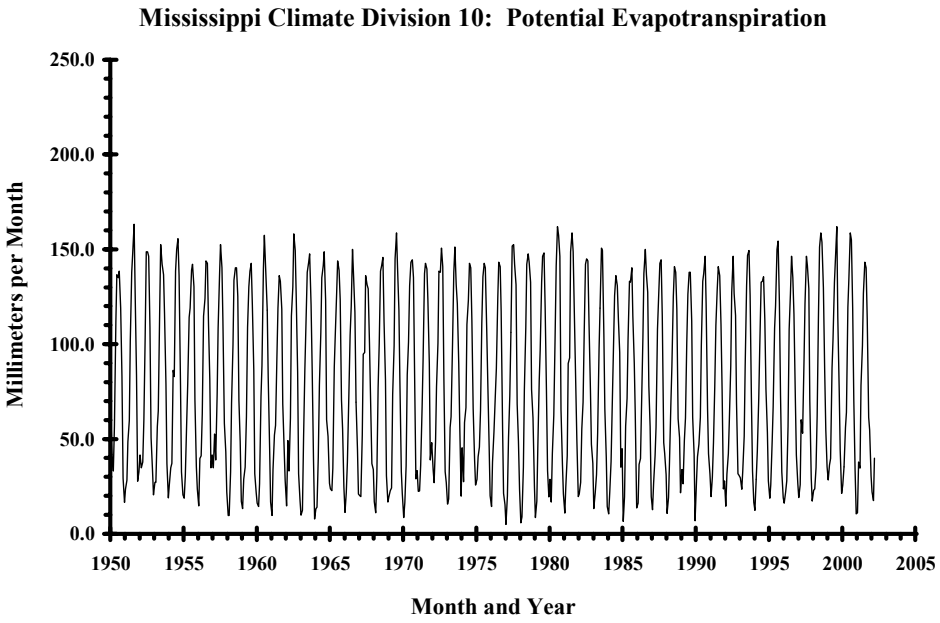

Figure H-13. Plot of monthly total potential evapotranspiration (millimeters) for Mississippi Climate Division 10. Data is from the National Climatic Data Center.

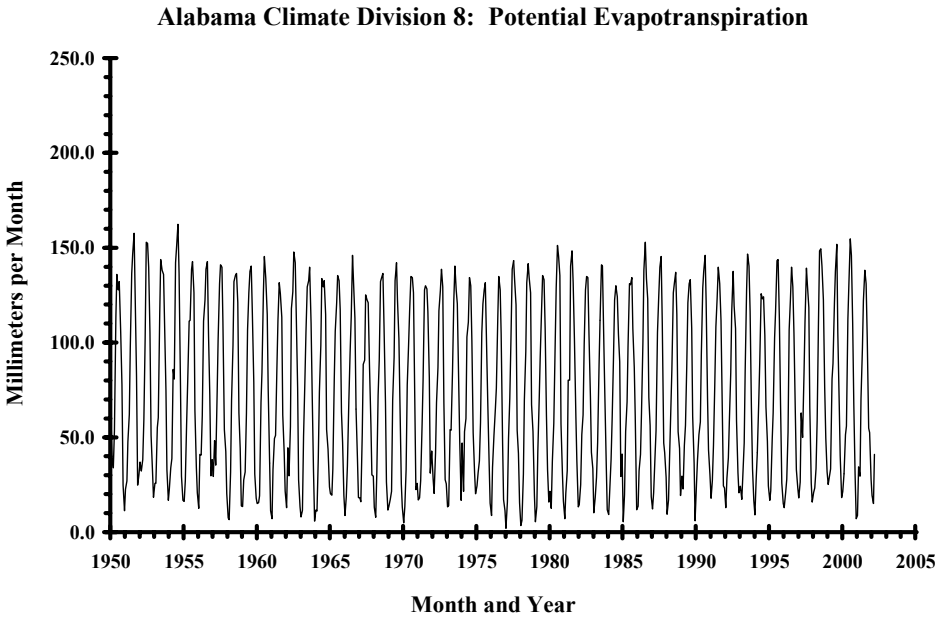

Figure H-14. Plot of monthly total potential evapotranspiration (millimeters) for Alabama Climate Division 8. Data is from the National Climatic Data Center.

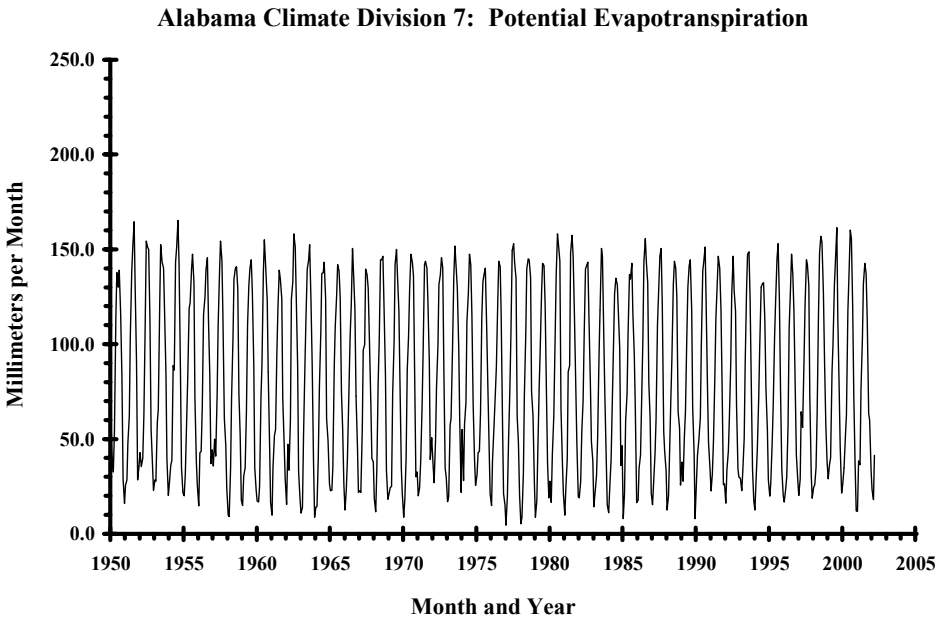

Figure H-15. Plot of monthly total potential evapotranspiration (millimeters) for Alabama Climate Division 7. Data is from the National Climatic Data Center.

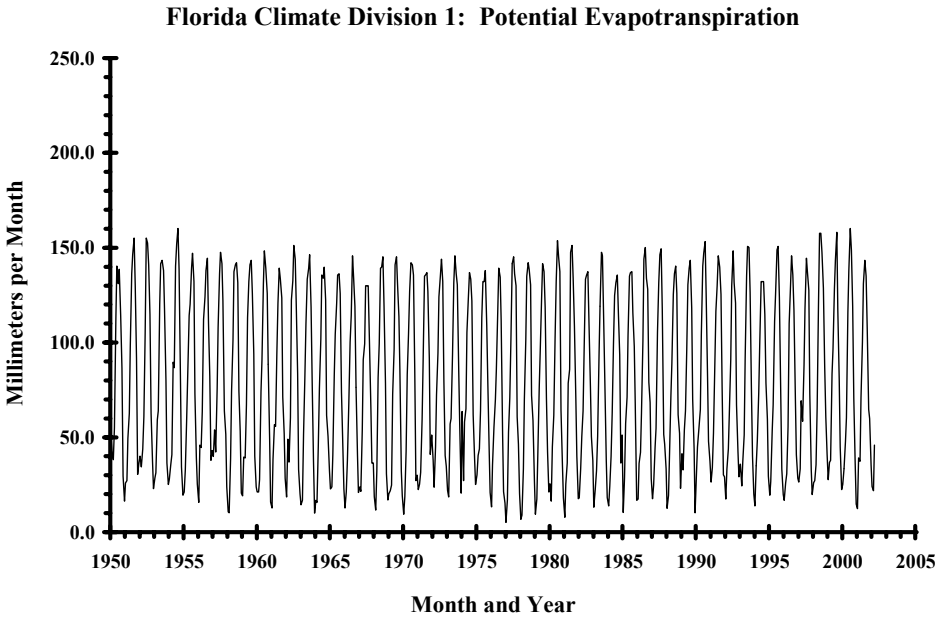

Figure H-16. Plot of monthly total potential evapotranspiration (millimeters) for Florida Climate Division 1. Data is from the National Climatic Data Center.

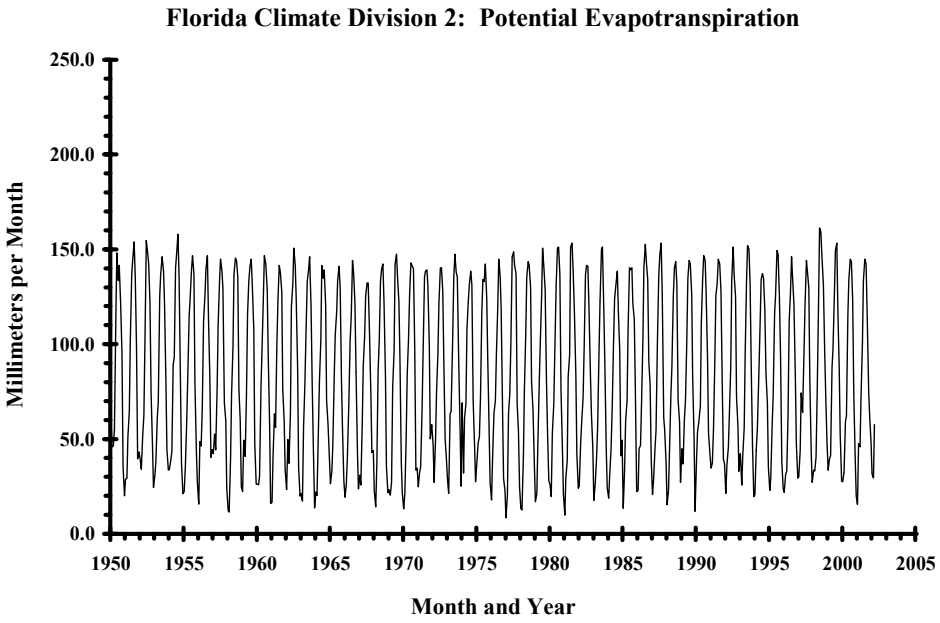

Figure H-17. Plot of monthly total potential evapotranspiration (millimeters) for Florida Climate Division 2. Data is from the National Climatic Data Center.

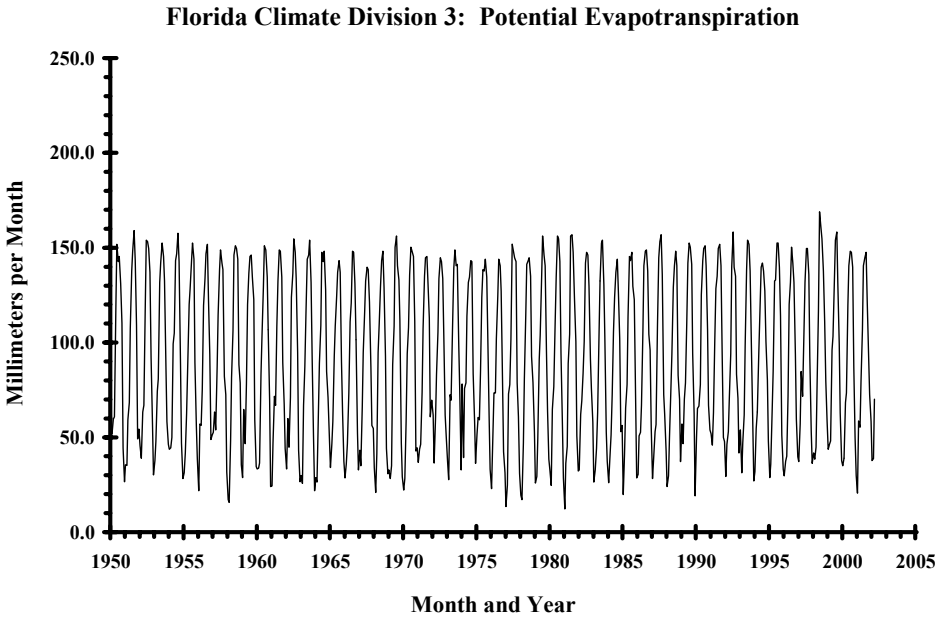

Figure H-18. Plot of monthly total potential evapotranspiration (millimeters) for Florida Climate Division 3. Data is from the National Climatic Data Center.

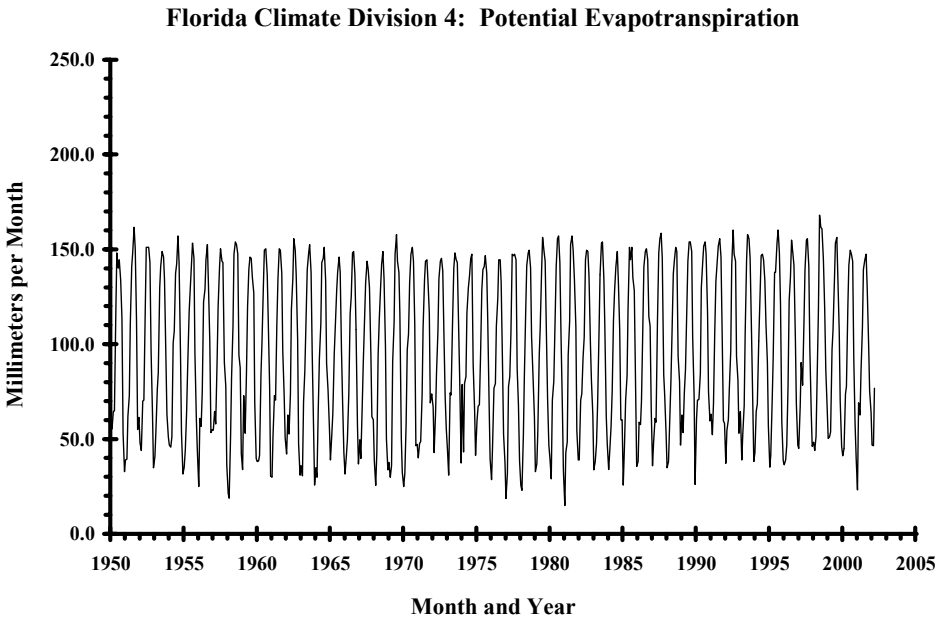

Figure H-19. Plot of monthly total potential evapotranspiration (millimeters) for Florida Climate Division 4. Data is from the National Climatic Data Center.

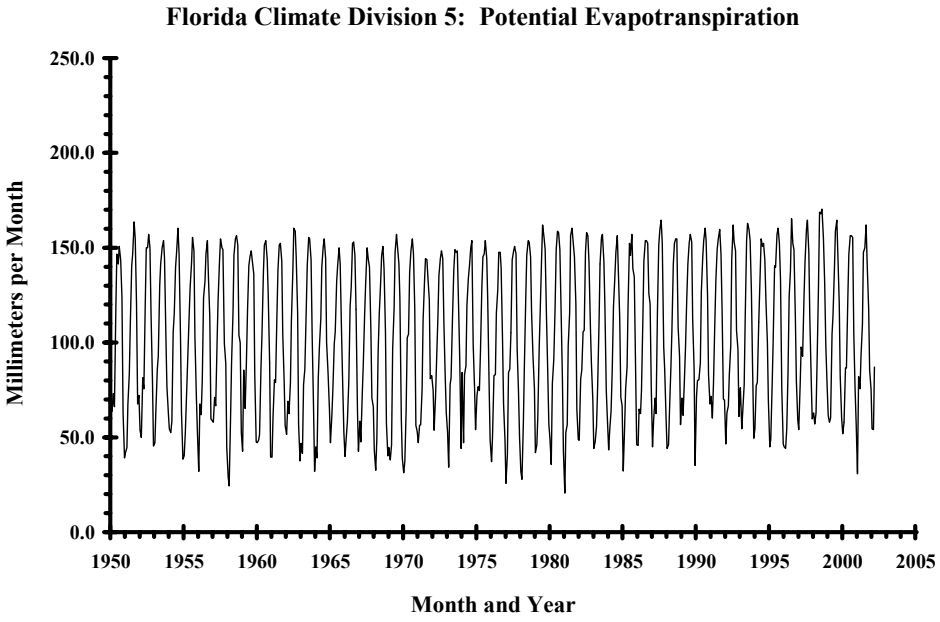

Figure H-20. Plot of monthly total potential evapotranspiration (millimeters) for Florida Climate Division 5. Data is from the National Climatic Data Center.

Appendix I: Precipitation surplus data plots.

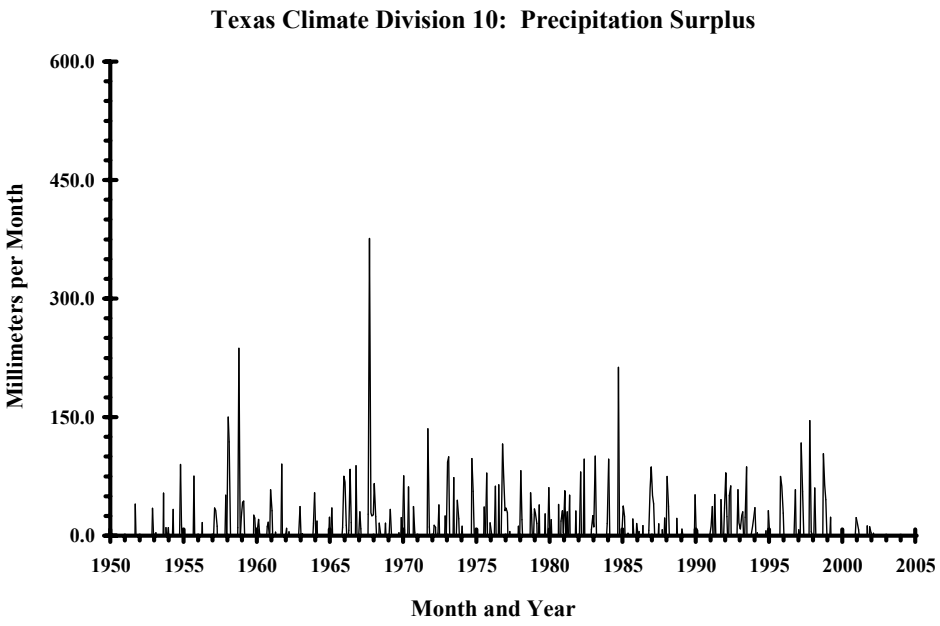

Figure I-1. Plot of monthly total precipitation surplus (millimeters) for Texas Climate Division 10. Data is from the National Climatic Data Center.

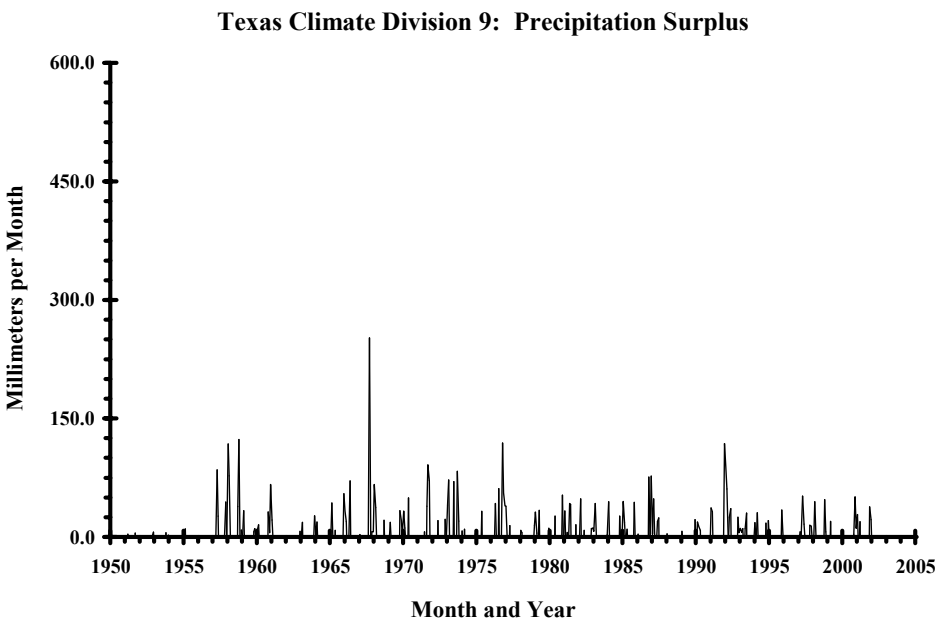

Figure I-2. Plot of monthly total precipitation surplus (millimeters) for Texas Climate Division 9. Data is from the National Climatic Data Center.

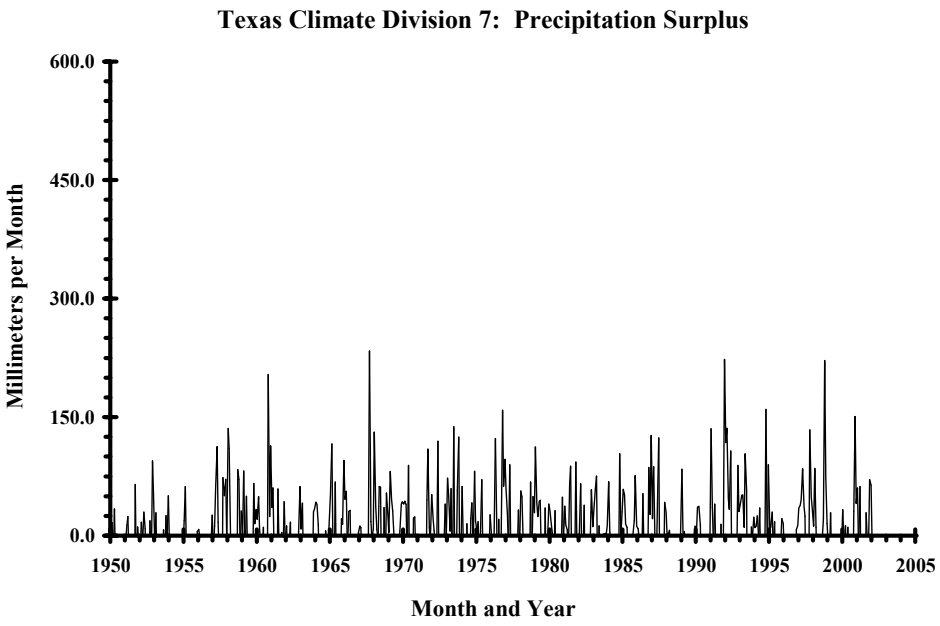

Figure I-3. Plot of monthly total precipitation surplus (millimeters) for Texas Climate Division 7. Data is from the National Climatic Data Center.

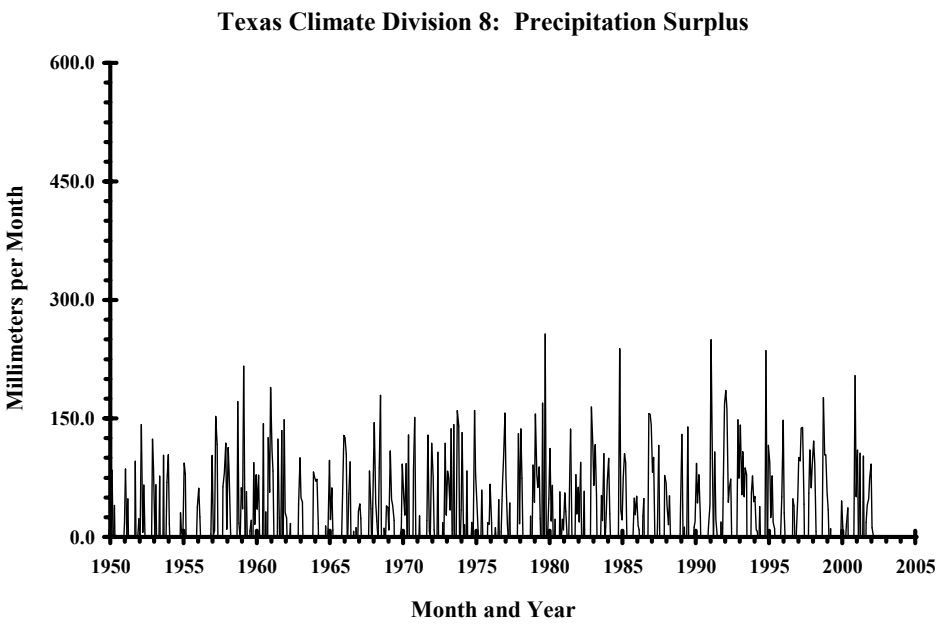

Figure I-4. Plot of monthly total precipitation surplus (millimeters) for Texas Climate Division 8. Data is from the National Climatic Data Center.

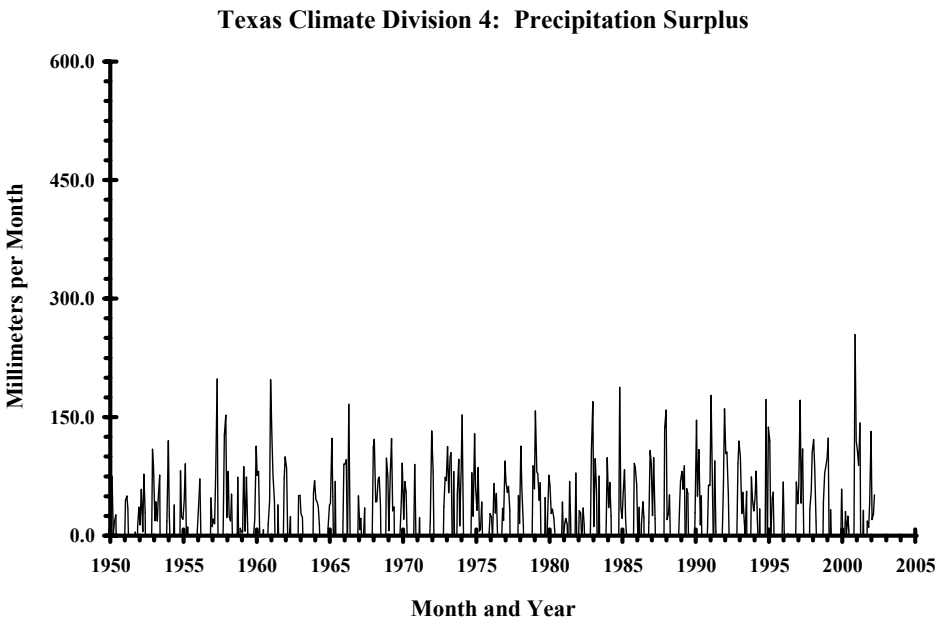

Figure I-5. Plot of monthly total precipitation surplus (millimeters) for Texas Climate Division 4. Data is from the National Climatic Data Center.

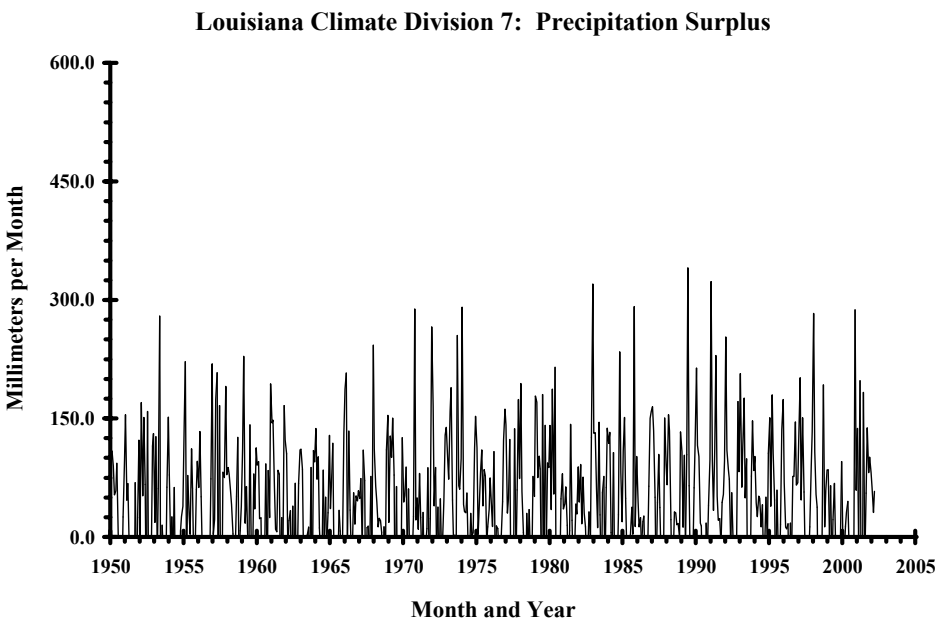

Figure I-6. Plot of monthly total precipitation surplus (millimeters) for Louisiana Climate Division 7. Data is from the National Climatic Data Center.

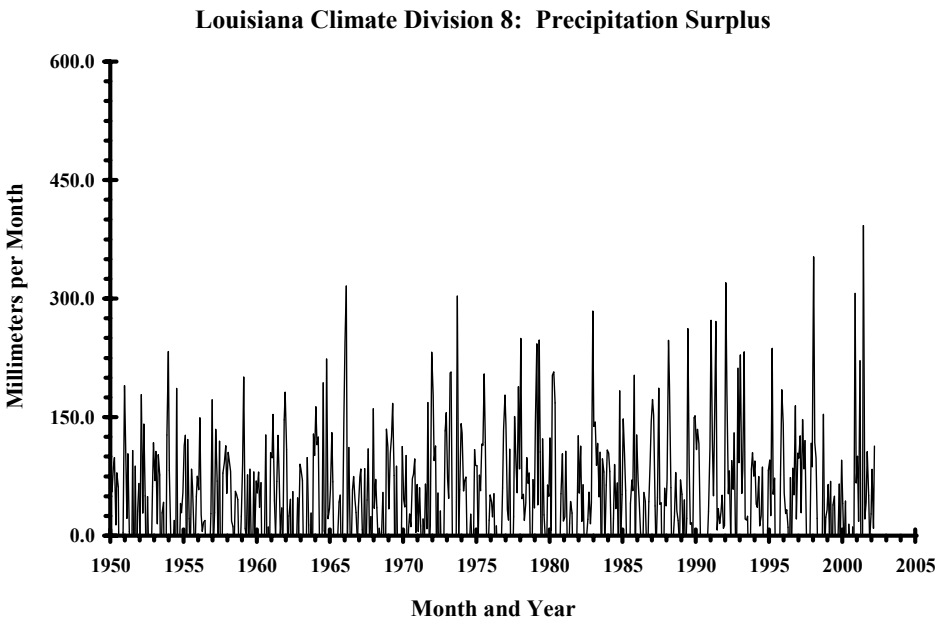

Figure I-7. Plot of monthly total precipitation surplus (millimeters) for Louisiana Climate Division 8. Data is from the National Climatic Data Center.

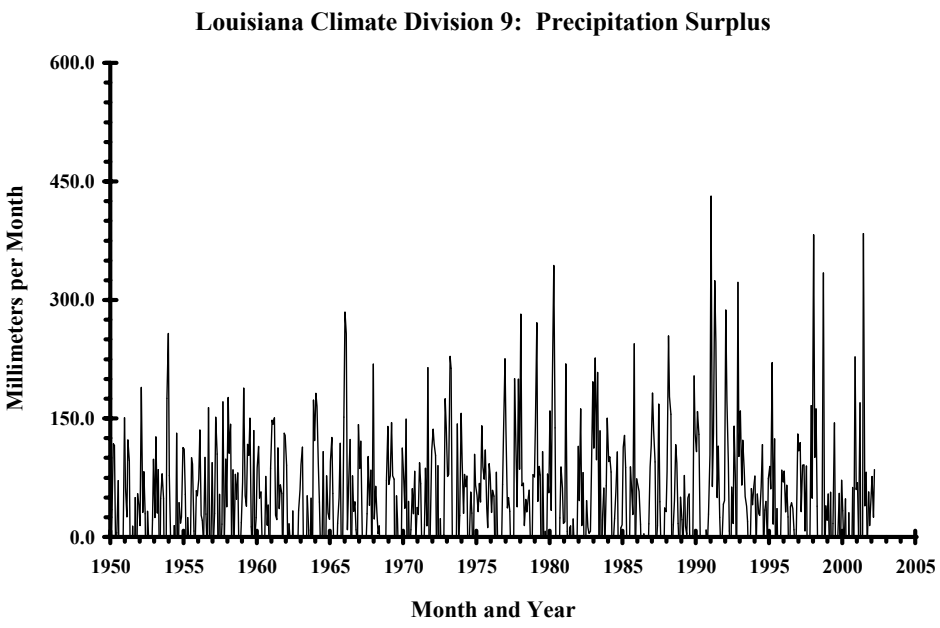

Figure I-8. Plot of monthly total precipitation surplus (millimeters) for Louisiana Climate Division 9. Data is from the National Climatic Data Center.

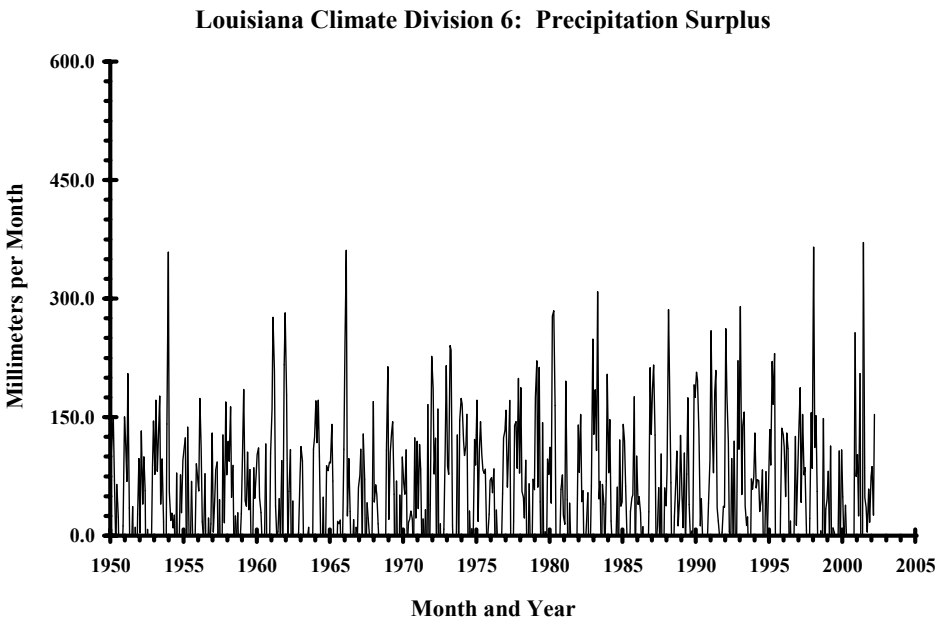

Figure I-9. Plot of monthly total precipitation surplus (millimeters) for Louisiana Climate Division 6. Data is from the National Climatic Data Center.

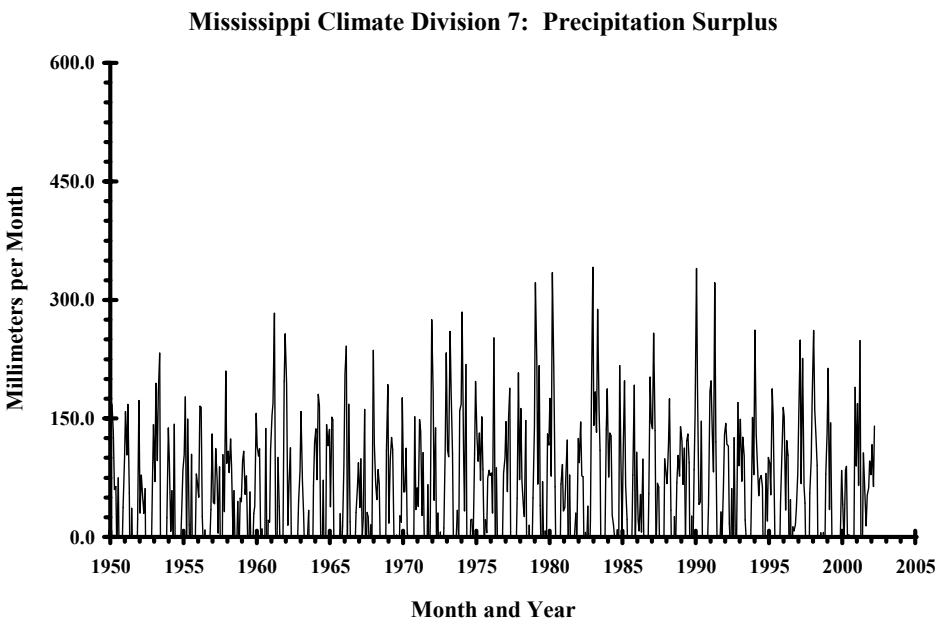

Figure I-10. Plot of monthly total precipitation surplus (millimeters) for Mississippi Climate Division 7. Data is from the National Climatic Data Center.

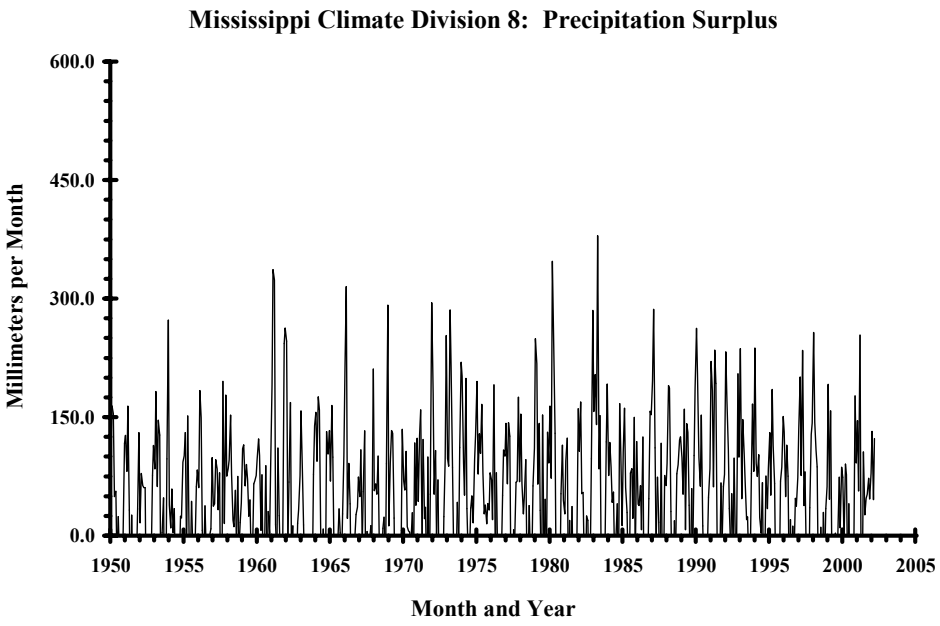

Figure I-11. Plot of monthly total precipitation surplus (millimeters) for Mississippi Climate Division 8. Data is from the National Climatic Data Center.

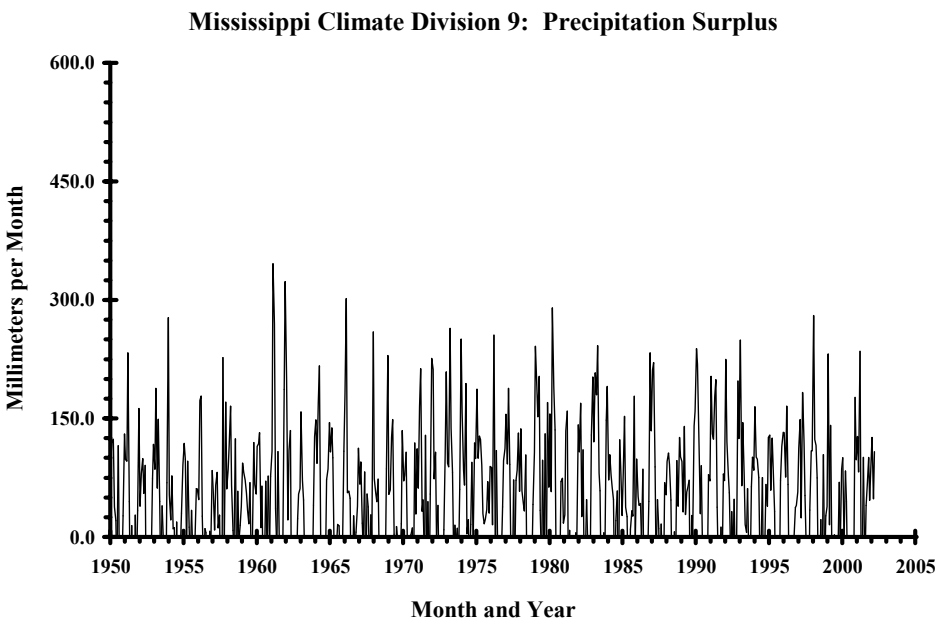

Figure I-12. Plot of monthly total precipitation surplus (millimeters) for Mississippi Climate Division 9. Data is from the National Climatic Data Center.

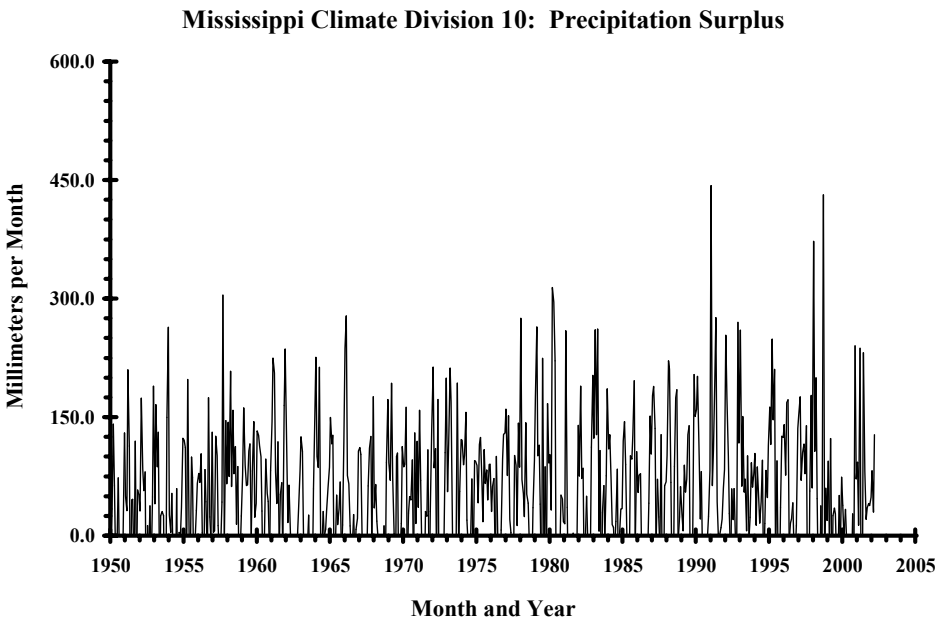

Figure I-13. Plot of monthly total precipitation surplus (millimeters) for Mississippi Climate Division 10. Data is from the National Climatic Data Center.

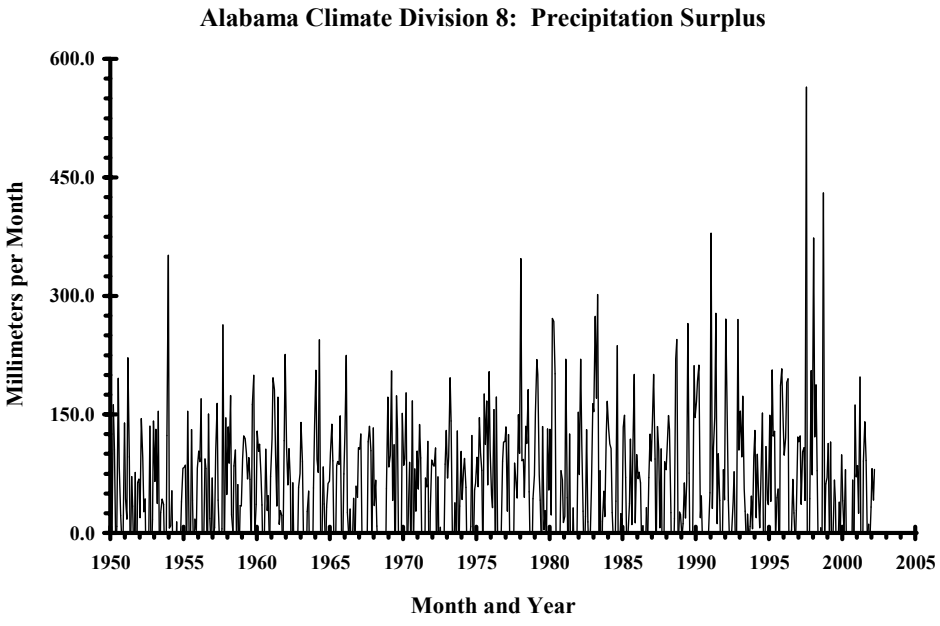

Figure I-14. Plot of monthly total precipitation surplus (millimeters) for Alabama Climate Division 8. Data is from the National Climatic Data Center.

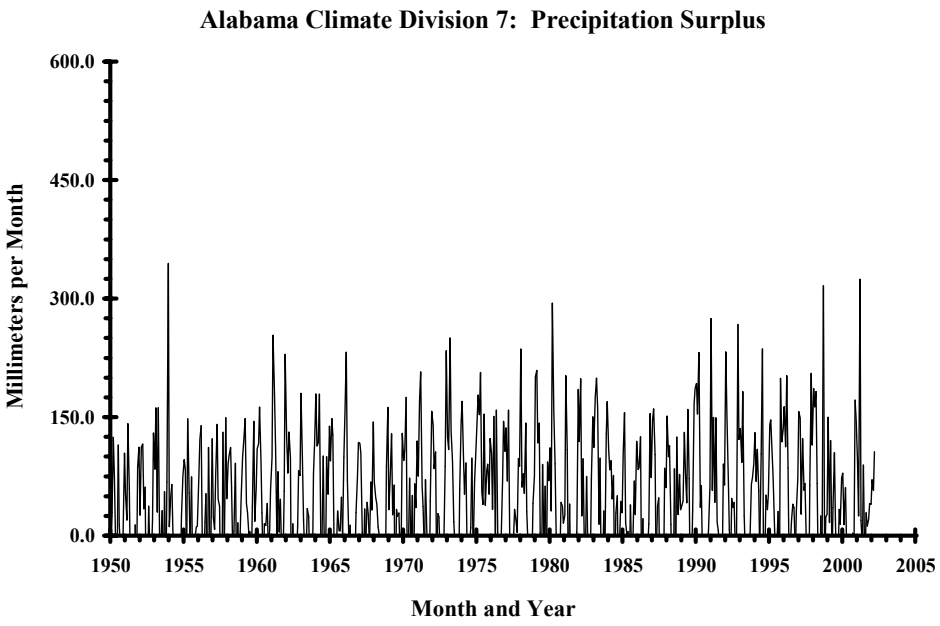

Figure I-15. Plot of monthly total precipitation surplus (millimeters) for Alabama Climate Division 7. Data is from the National Climatic Data Center.

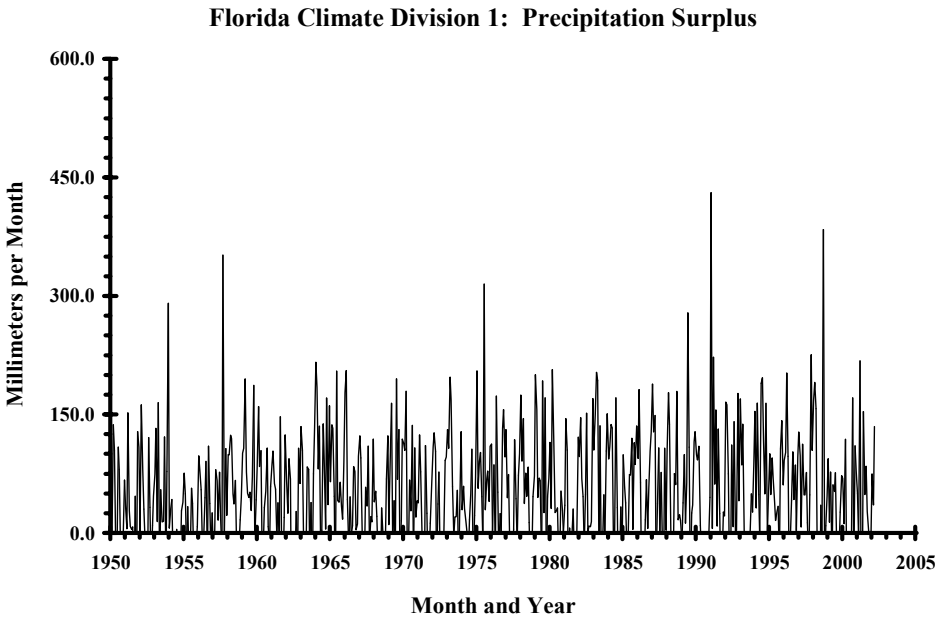

Figure I-16. Plot of monthly total precipitation surplus (millimeters) for Florida Climate Division 1. Data is from the National Climatic Data Center.

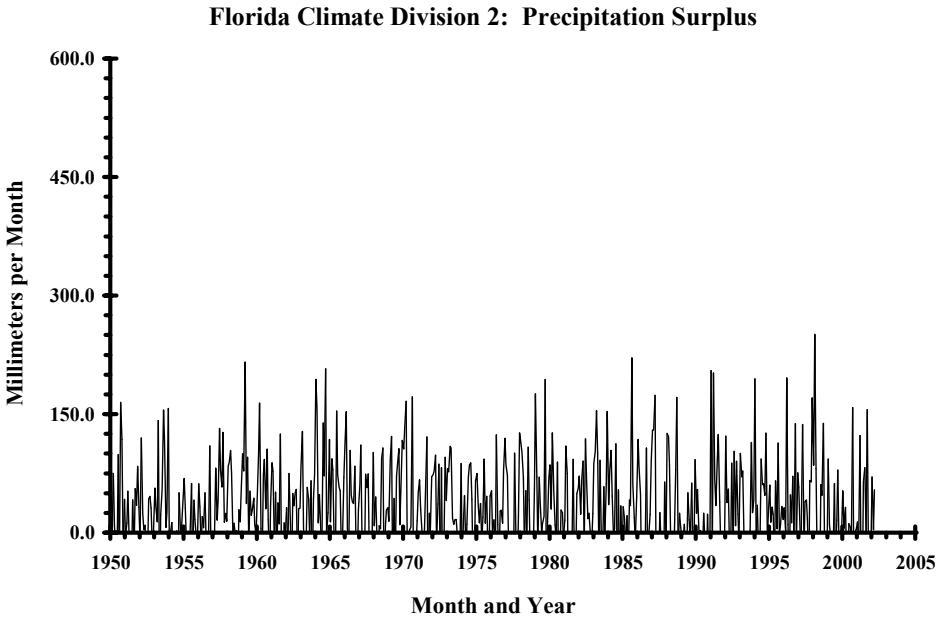

Figure I-17. Plot of monthly total precipitation surplus (millimeters) for Florida Climate Division 2. Data is from the National Climatic Data Center.

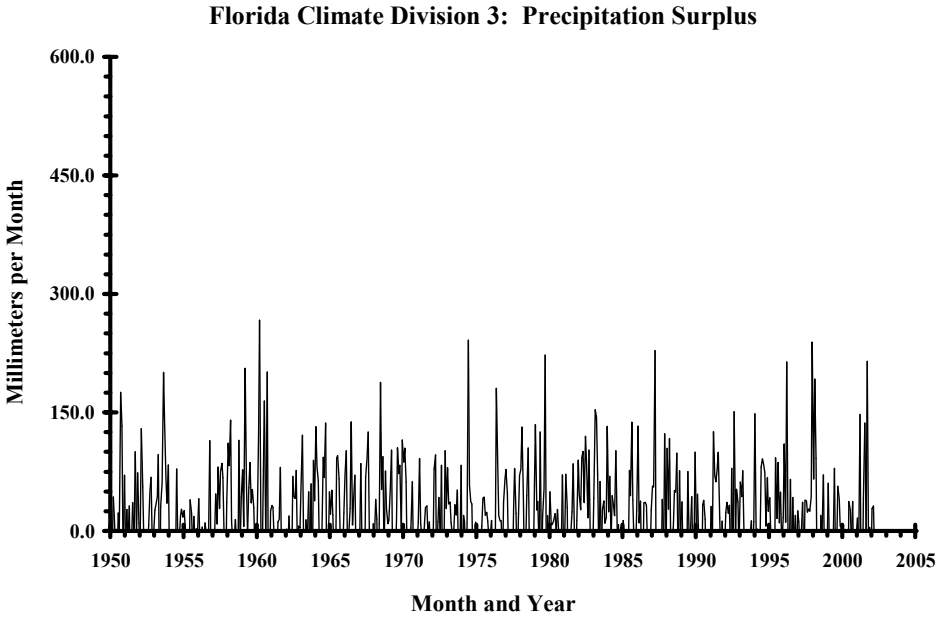

Figure I-18. Plot of monthly total precipitation surplus (millimeters) for Florida Climate Division 3. Data is from the National Climatic Data Center.

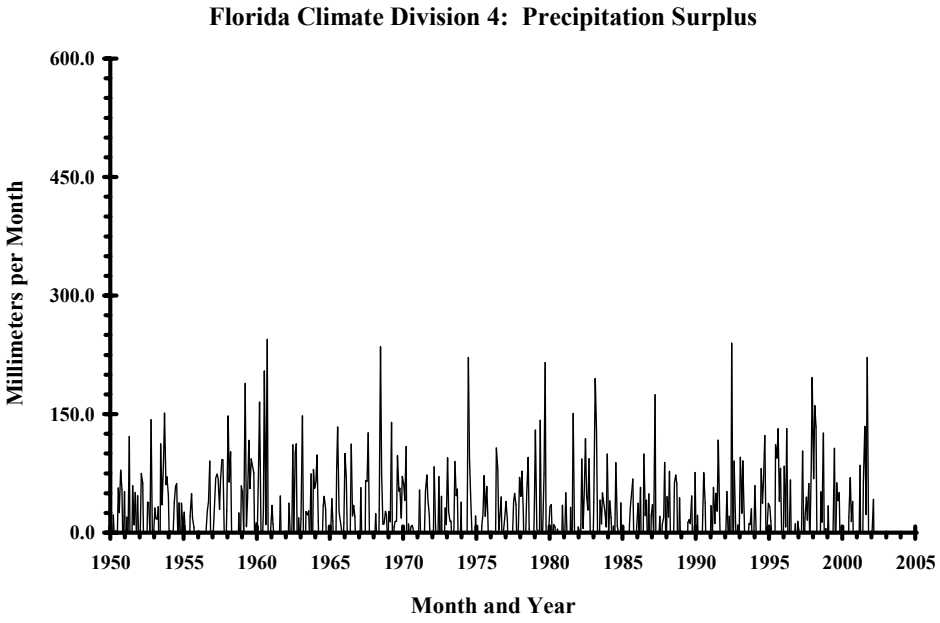

Figure I-19. Plot of monthly total precipitation surplus (millimeters) for Florida Climate Division 4. Data is from the National Climatic Data Center.

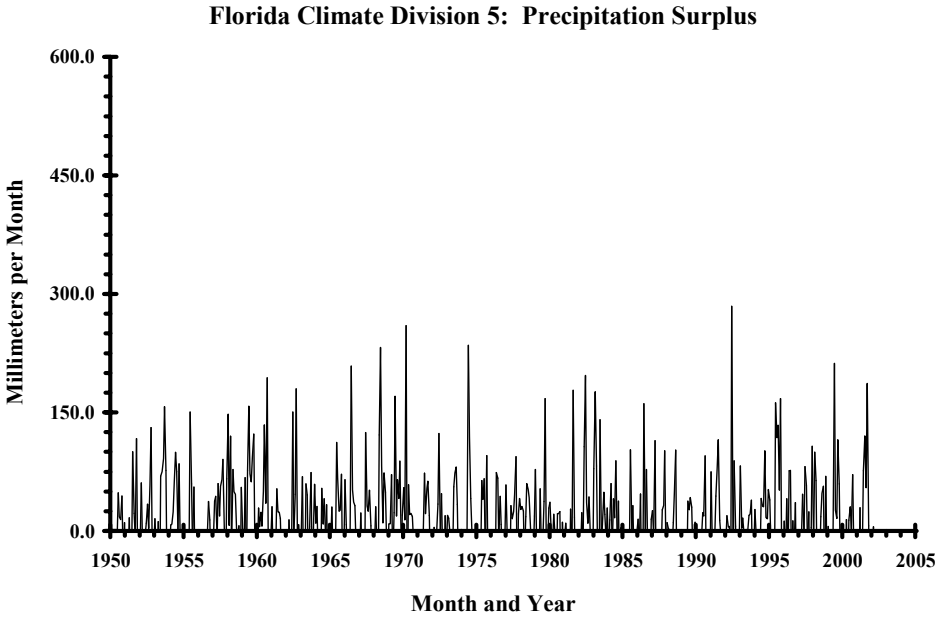

Figure I-20. Plot of monthly total precipitation surplus (millimeters) for Florida Climate Division 5. Data is from the National Climatic Data Center.

Appendix J: Coastal Winds data plots.

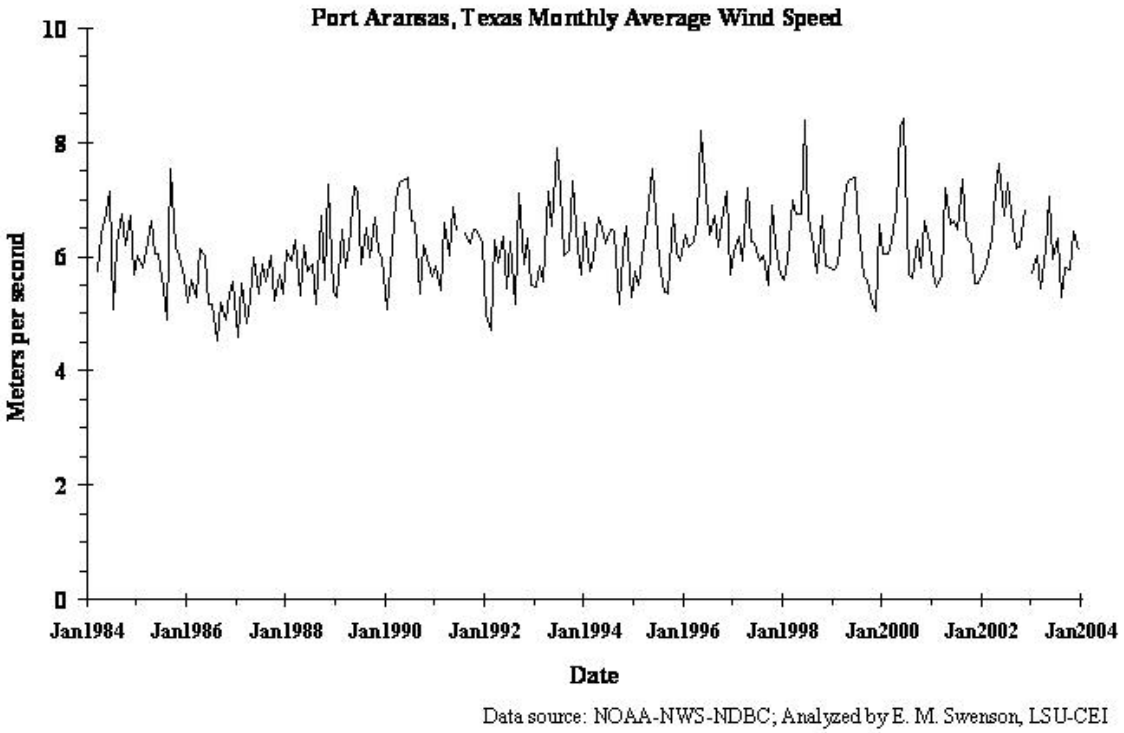

Figure J-1. Plot of monthly average wind speed for Port Anansas, Texas. Data is from the National Data Data Center.

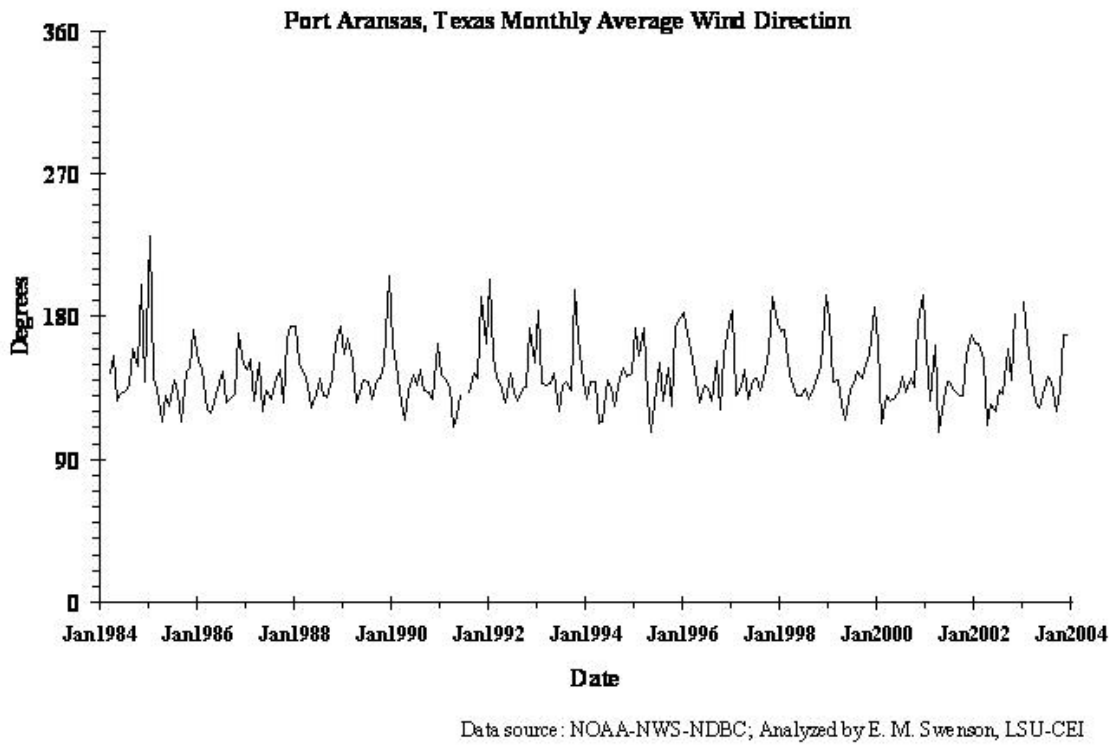

Figure J-2. Plot of monthly average wind direction for Port Aransas, Texas. Data is from the National Data Data Center.

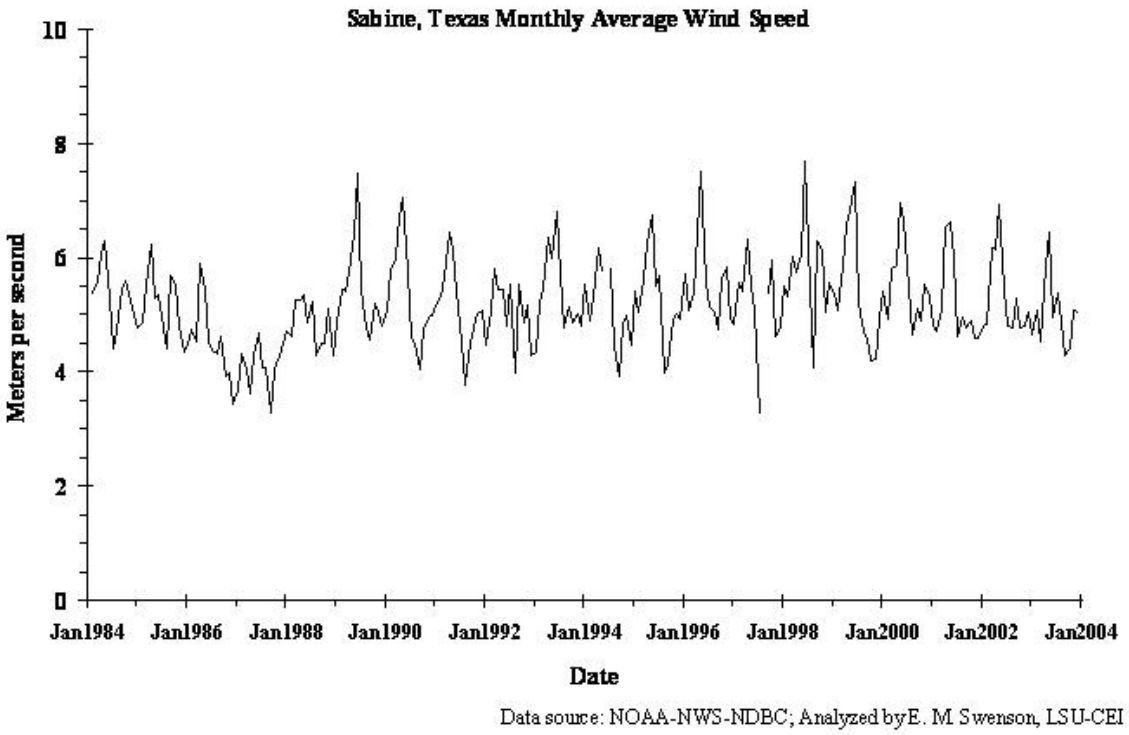

Figure J-3. Plot of monthly average wind speed for Sabine, Texas. Data is from the National Data Data Center.

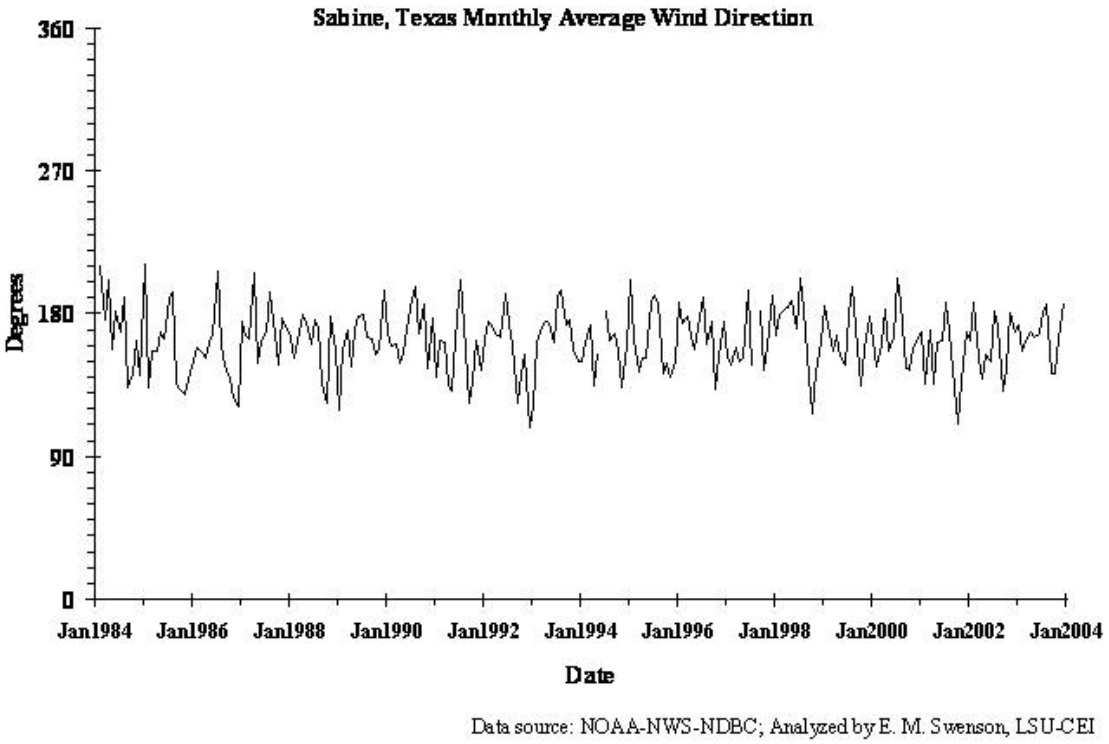

Figure J-4. Plot of monthly average wind direction for Sabine, Texas. Data is from the National Data Data Center.

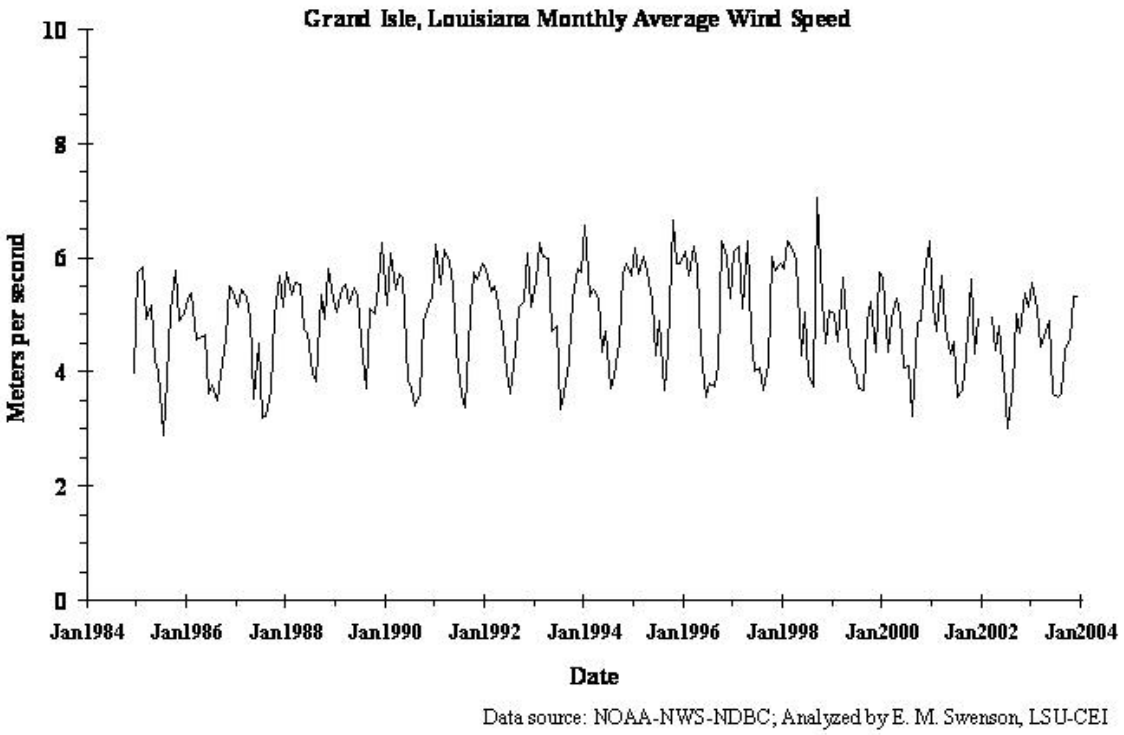

Figure J-5. Plot of monthly average wind speed for Grand Isle, Louisiana. Data is from the National Data Data Center.

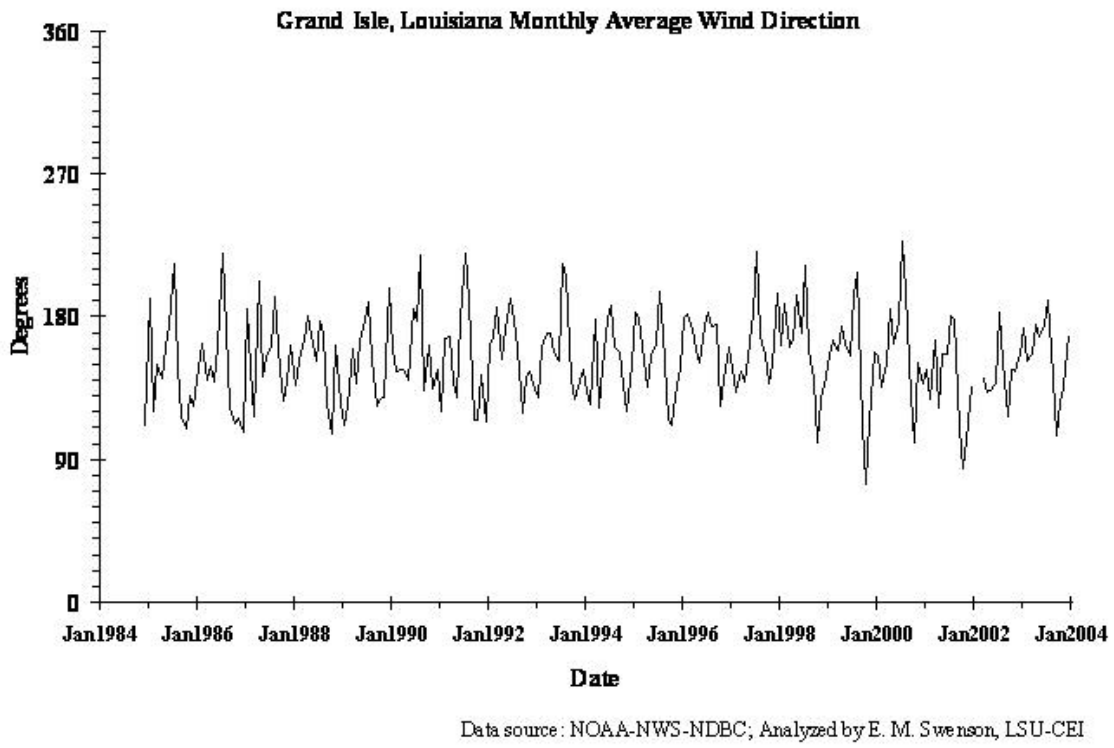

Figure J-6. Plot of monthly average wind direction for Grand Isle, Louisina. Data is from the National Data Data Center.

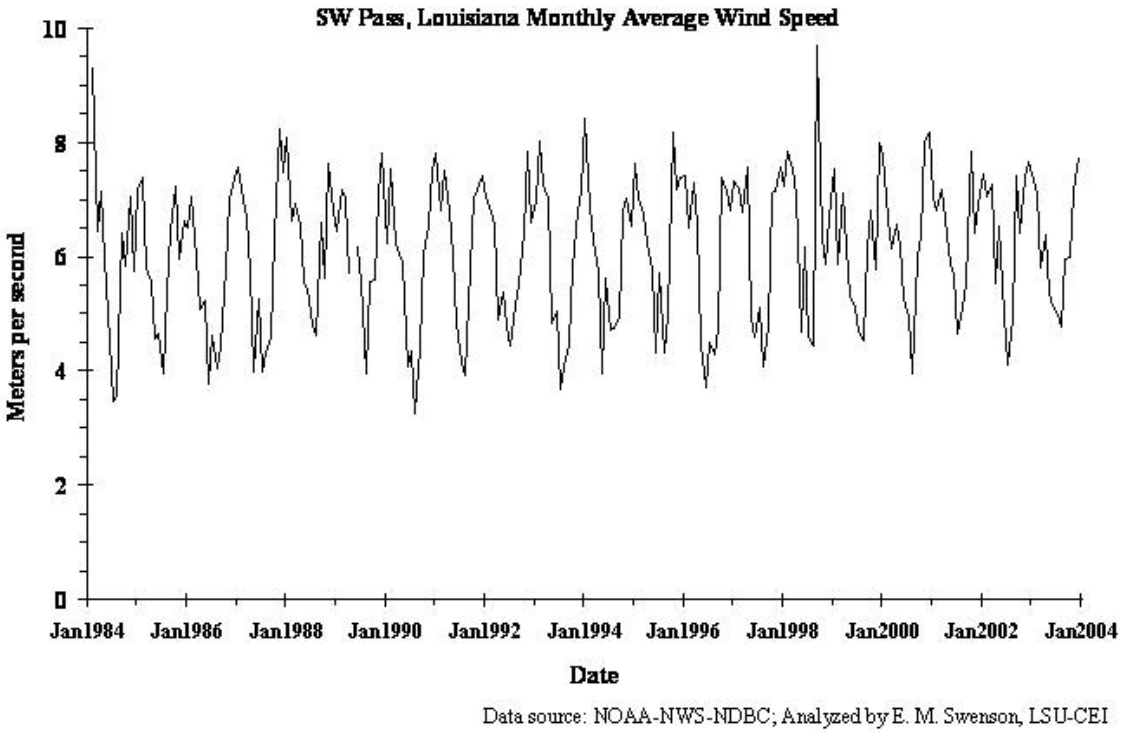

Figure J-7. Plot of monthly average wind speed for Southwest Pass, Louisiana. Data is from the National Data Data Center.

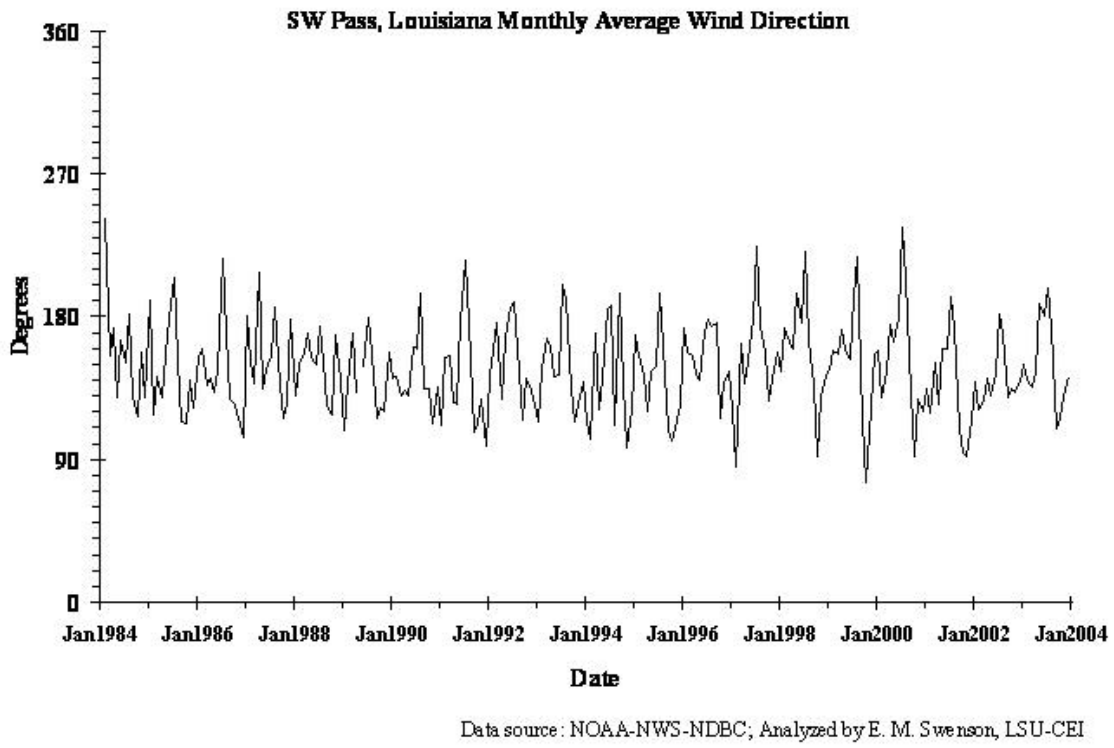

Figure J-8. Plot of monthly average wind direction for Southwest Pass, Louisina. Data is from the National Data Data Center.

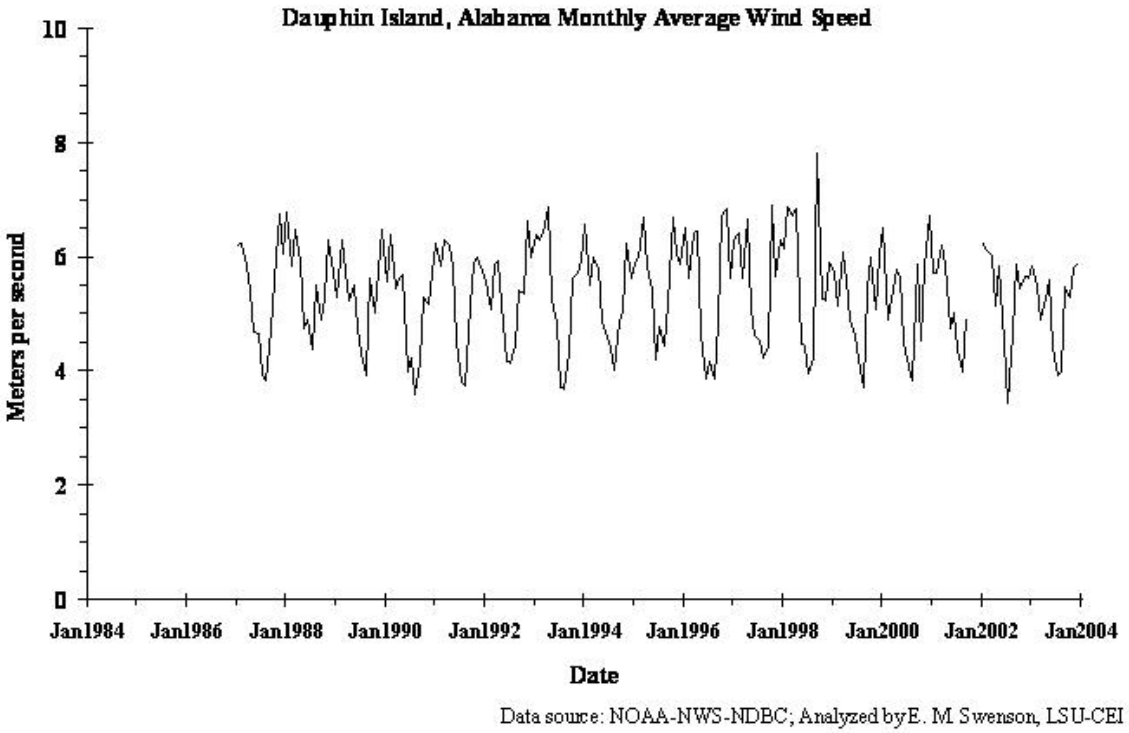

Figure J-9. Plot of monthly average wind speed for Dauphin Island, Alabama. Data is from the National Data Data Center.

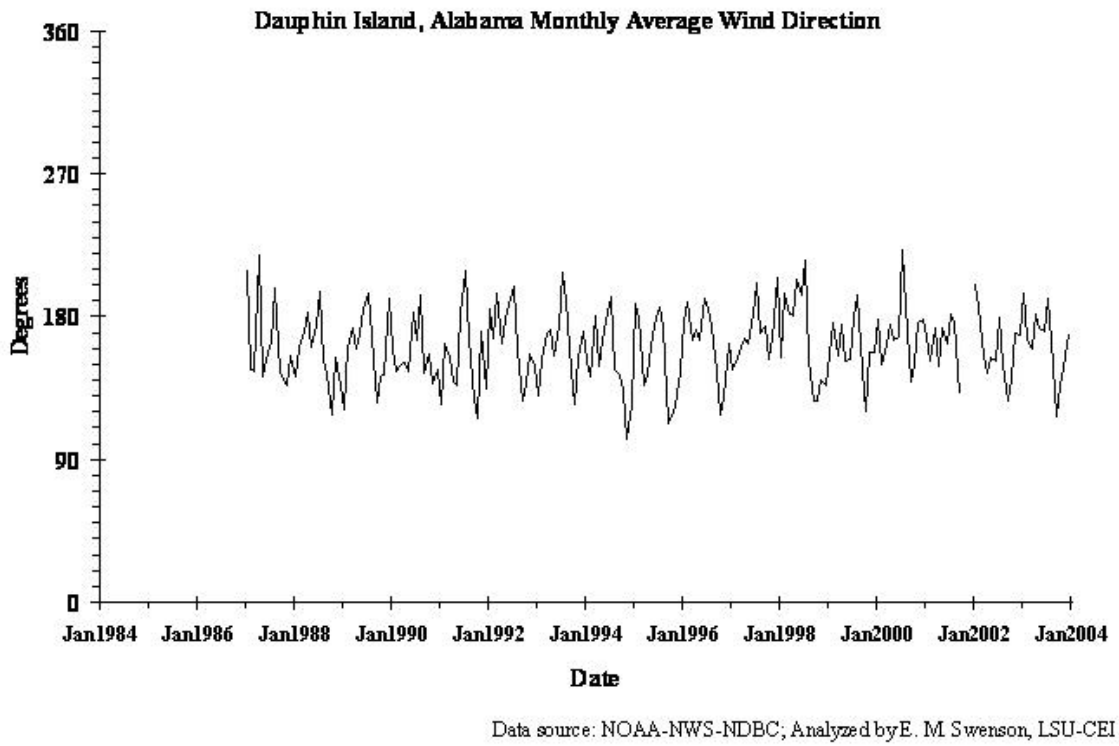

Figure J-10. Plot of monthly average wind direction for Dauphin Island, Alabama. Data is from the National Data Data Center.

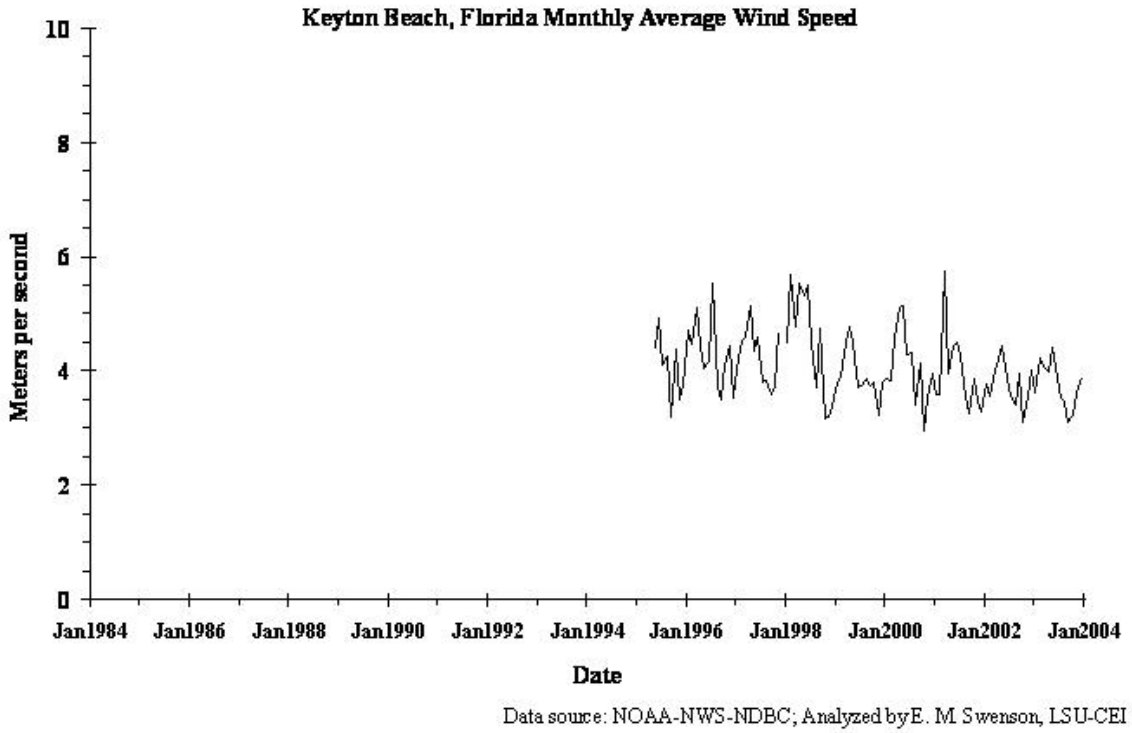

Figure J-11. Plot of monthly average wind speed for Keyton Beach, Florida. Data is from the National Data Data Center.

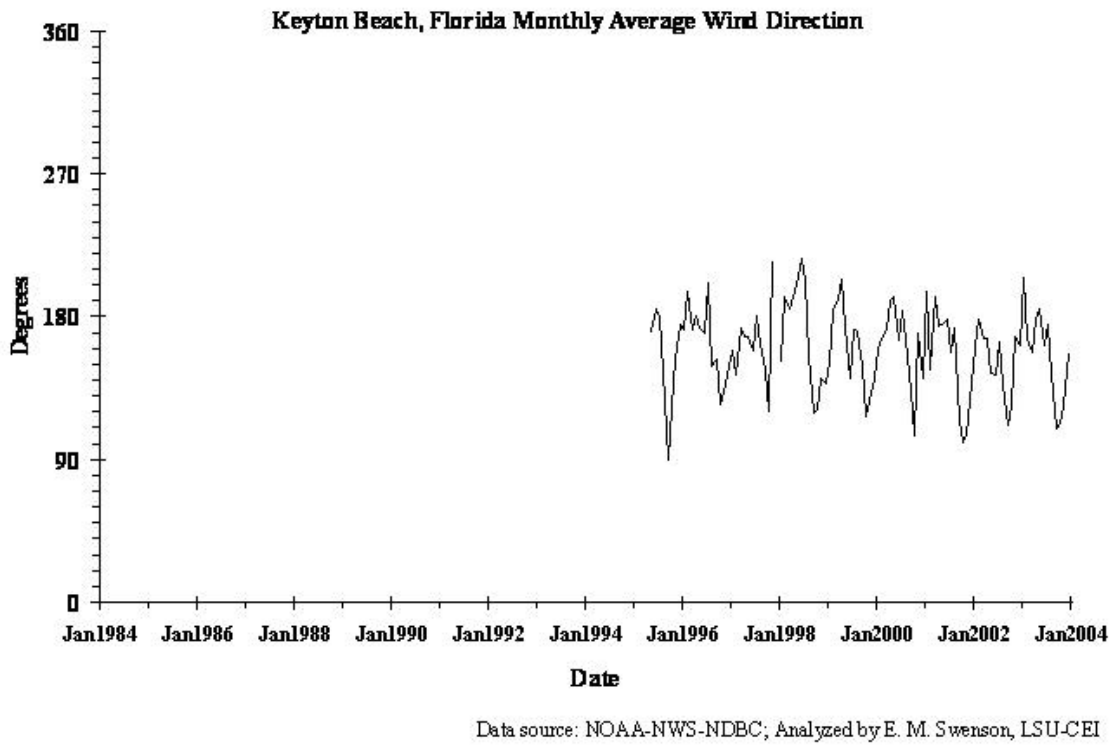

Figure J-12. Plot of monthly average wind direction for Keyton Beach, Florida. Data is from the National Data Data Center.

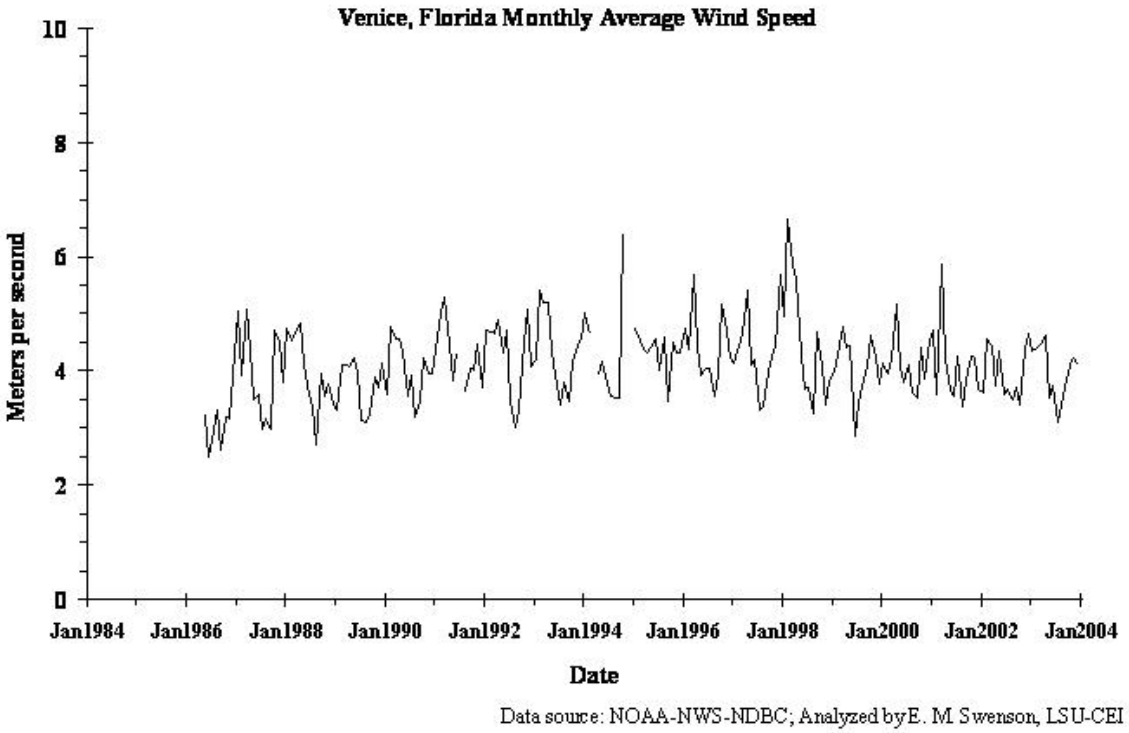

Figure J-13. Plot of monthly average wind speed for Venice, Florida. Data is from the National Data Data Center.

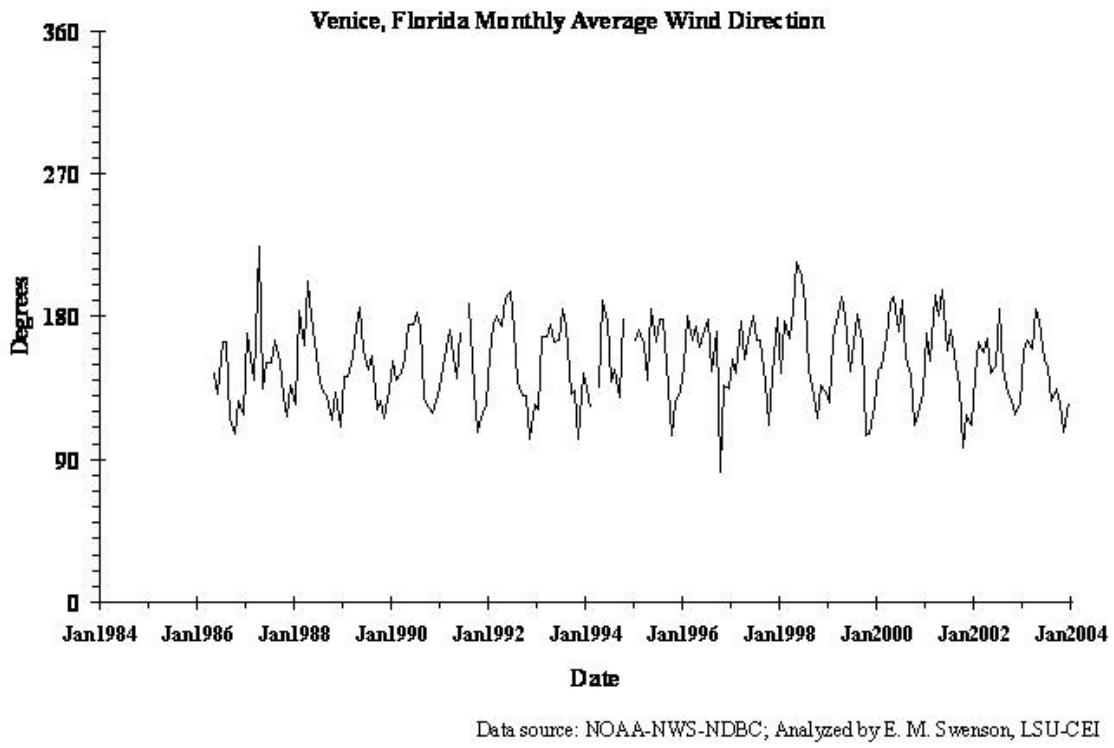

Figure J-14. Plot of monthly average wind direction for Venice, Florida. Data is from the National Data Data Center.